Geological Survey of Finland

Bulletin 374

Hydrothermal alteration in volcano-sedimentary rocks in the Central Lapland greenstone belt, Finland

by Pasi Eilu

Geologian tutkimuskeskus
Espoo 1994

Geological Survey of Finland, Bulletin 374

HYDROTHERMAL ALTERATION IN VOLCANO-SEDIMENTARY ROCKS IN THE CENTRAL LAPLAND GREENSTONE BELT, FINLAND

by

PASI EILU

with 62 figures, 37 tables and 3 appendices

GEOLOGIAN TUTKIMUSKESKUS
ESPOO 1994

Vammala 1994 Vammalan Kirjapaino Oy

Eilu, Pasi 1994. Hydrothermal alteration in volcano-sedimentary rocks in the Central Lapland greenstone belt, Finland. *Geological Survey of Finland, Bulletin 374*, 145 pages, 62 figures, 37 tables and 3 appendices.

Hydrothermally altered rocks showing various types of alteration are widespread in the intra-cratonic rift-related Central Lapland greenstone belt (CLGB). Seven areas in the central part of the CLGB were selected for detailed study in order to deduce the effect of hydrothermal alteration on the mineralogical and chemical composition of the sequence.

The Middle Lapponian sediments were deposited in a Palaeoproterozoic rift zone in the central part of the CLGB. They were soon albitized in diagenetic conditions (T = 60-150°C) under the high heat flow regime of the rift zone. The provenance information carried by the clastic feldspars was completely lost during the albitization. Upper Lapponian igneous activity probably began with small-volume lamprophyric magmatism and was followed by a voluminous tholeiitic phase ca. 2.2 Ga ago. Small-scale hydrothermal systems may have been generated by the lamprophyres. Large-scale hydrothermal activity causing pervasive and widespread alteration was evidently generated by the tholeiitic magmatism 2.2 Ga ago, when the main heat sources were the mafic dykes and sills.

Temperature zonation of the hydrothermal systems related to the intrusions was weakly developed as most of the alterations took place in the same temperature range, but the chemical zonation was more complex. The prevailing pressure was low (≤0.5 kb). The prevailing temperature varied from 260 to 430°C between the areas studied, but within an area the temperature variation was within 20-60°. The igneous rocks were spilitized into mineral assemblages dominated by amphibole (low water/rock regime) and chlorite (high water/rock regime) by sea water-derived, low pH, reducing, very low f_{CO2} and high a_{Na+}/a_{K+} and a_{Na+}/a_{Ca2+} fluid. Simultaneously, their wall rocks were albitized and carbonated by near-neutral, predominantly oxidizing, high f_{CO2}, a_{Ca2+} and a_{Na+}/a_{K+} fluid. Biotitization caused by element exchange between the spilitizing and carbonating zones took place in the margins of the igneous bodies in low a_{Na+}/a_{K+} and a_{Ca2+}/a_{K+}, near-neutral, weakly reducing conditions. During the evolution of the hydrothermal system, the carbonation process expanded, covering even the most brecciated zones and the marginal zones of the igneous rocks.

Since the reactions of carbonation and albitization caused H^+ release into the fluid and Na depletion in the fluid, pH, the a_{Na+}/a_{K+} and a_{Ca2+}/a_{K+} of the hydrothermal fluid decreased, and carbonation was followed and overprinted by sericitization. Weak chloritization and talc formation took place locally during the sericitization stage because of somewhat higher pH and significantly higher a_{Mg2+} than in the sericitizing fluid. This local enrichment of Mg suggests that the evolved hydrothermal fluid was mixed with fresh sea water in upflow zones of the hydrothermal system.

Felsic magmatism, manifested by dykes in the Sivakkavaara area, generated local small-scale hydrothermal systems causing carbonation + albitization and sericitization after the cessation of the diabase-related hydrothermal systems. The alterations indicate P-T and chemical conditions similar to those related to

carbonation + albitization and sericitization combined with the diabase related hydrothermal systems.

During the Svecokarelian orogeny, carbonation and intensive albitization related to fracture zones took place locally in the CLGB as displayed in the sediments of the Isolaki area. The origin of the metasomatic fluid remains unresolved, as roughly all fluid sources and their combinations are possible. The fluid was alkaline or near-neutral, had a high a_{Na+}/a_{K+}, and moderate or high a_{Ca2+} and f_{CO2}. The alteration probably took place during the Svecokarelian orogeny 1.9-1.8 Ga ago, when the synorogenic plutonism formed the heat source for the hydrothermal system. No signs of metamorphic or post-metamorphic alterations were found in the other areas studied here.

Mass balance calculations indicate substantial changes in chemical composition and rock volume during the alteration processes, the relative volume changes ranging from -30% to >+50%. Only Ti, Al and Zr remained immobile during all stages of alteration. Most of the chemical changes are easily explained by the mineral reactions and replacement related to the various stages of alteration.

Key words (GeoRef Thesaurus, AGI): greenstone belts, metavolcanic rocks, metasedimentary rocks, mineral composition, chemical composition, hydrothermal alteration, albitization, carbonation, geologic thermometry, geologic barometry, low-grade metamorphism, Proterozoic, Paleoproterozoic, central Lapland, Finland.

Pasi Eilu, Geological Survey of Finland, FIN-96100 ROVANIEMI, FINLAND

ISBN 951-690-537-4
ISSN 0367-522X

CONTENTS

INTRODUCTION

Preface

"Desperation rock" wrote an anonymous geologist in a drill-core report in the early 1970's, referring to a pale grey, irregularly banded, biotite-bearing albite-carbonate rock. This was not the first nor the last time that someone has been puzzled by the widespread Na-rich, low-grade rocks of the Palaeoproterozoic greenstone belts of the northern Fennoscandian Shield. They have been called adinoles, albitites, albitolites, carbonate albitites, carbonate-albite rocks, albite felses, keratophyres, etc. (e.g., Amstutz 1974). It has been difficult to understand the formation of these pale rocks and their obscure structures. How, for example, can a rock with totally unaltered magmatic texture have a mineral assemblage of albite, chlorite and magnetite? How was a fine-grained, granoblastic, massive rock consisting only of albite formed? And what are the fine and medium-grained carbonate-albite rocks with a massive, magmatic or layered texture? No wonder the rocks were given strange and occasionally misleading names in the field and even in some research reports.

Interest in albitized and carbonated rocks has increased significantly during the last ten years, as a number of gold deposits (e.g., the Bidjovagge mine in Norway and the Saattopora mine and several occurrences in the Kuusamo district in Finland) and base metal deposits (e.g., Saattopora and Riikonkoski in Finland) occur partly or completely in the rocks termed albite felses, i.e., fine-grained, intensively albitized and variably carbonated metasediments (Lång et al. 1984, Björlykke et al. 1991, Korvuo 1991, Nurmi et al. 1991, Pankka 1992).

Researchers have usually considered the formation of the Na-rich rocks to be related in one way or another to the formation of the albite diabases and mafic spilites of the greenstone belts (e.g., Eskola 1925, Piispanen 1972, Amstutz 1974, Kerrich 1983). Before the 1970's, magmatic differentiation and the spilitic magma hypothesis were favoured as explanations for the formation of albite-chlorite, albite-actinolite, albite and carbonate-albite rocks with magmatic textures (Ödman 1939, Gjelsvik 1958, Meriläinen 1961, Piispanen 1972, Lehmann 1974, Piirainen and Rouhunkoski 1974), and regional metasomatism, metamorphism or regional sodium metasomatism related to plutonic magmatism were sometimes invoked to explain the Na-rich rocks of the greenstone belts (e.g., Coombs 1974, Eriksson and Hallgren 1975). As early as 1925, however, Eskola was of the opinion that spilites, albite diabases and albite rocks cannot be produced by magmatic differentiation, nor did he believe in regional sodium metasomatism. Later research has clearly indicated that spilites, albite diabases and albite rocks with magmatic textures have developed to their present state as a consequence of synmagmatic hydrothermal processes (Vallance 1974, Kerrich 1983, Reed 1983, Lesher et al. 1986, Shau and Peacor 1992). The formation of albite rocks with obvious sedimentary textures and structures has practically always been explained by means of metasomatic processes (Eskola 1925, Agrell 1939, Mikkola 1941, Holmsen et al. 1957, Piis-

panen 1972, Piirainen and Rouhunkoski 1974, Behr et al. 1983, Kalsbeek 1992, Pankka 1992).

Most of the research into hydrothermal alteration has been related to surveys of mineral deposits (e.g., Kerrich 1983, Colvine et al. 1988) and to regions of modern hydrothermal systems (e.g., Browne 1978, Cole 1986, Fournier 1989, Edmond 1992), and only a few reports have dealt with old altered bedrock without significant indications of mineralizations. Those engaged in exploration often face the problem of how to distinguish between alterations related and unrelated to mineralization as these typically overlap. It is therefore important that various types of alteration should be studied in regions of barren rock, too. In addition, it is essential for research into the general history of the bedrock to identify all signs of secondary alteration in order to find the least altered rocks and the least mobile elements. For this purpose, the altered rocks of the Central Lapland greenstone belt (CLGB) and their less altered environments are good objects of research, as their alteration grades and types are varied, covering several rock types with and without mineralizations.

The predominantly Palaeoproterozoic greenstone belts of northern Finland (Fig. 1) have been targets of geological investigations and ore exploration for many decades. In order to promote mineral exploration, to establish the classification of the volcanics and to determine their extrusion conditions and the development of the Earth's crust in northern Finland, "The Lapland Volcanite Project" (LVP) was started at the Geological Survey of Finland (GSF) in 1984 (Lehtonen 1989b). One of the main aims of the Volcanite Project was to determine the

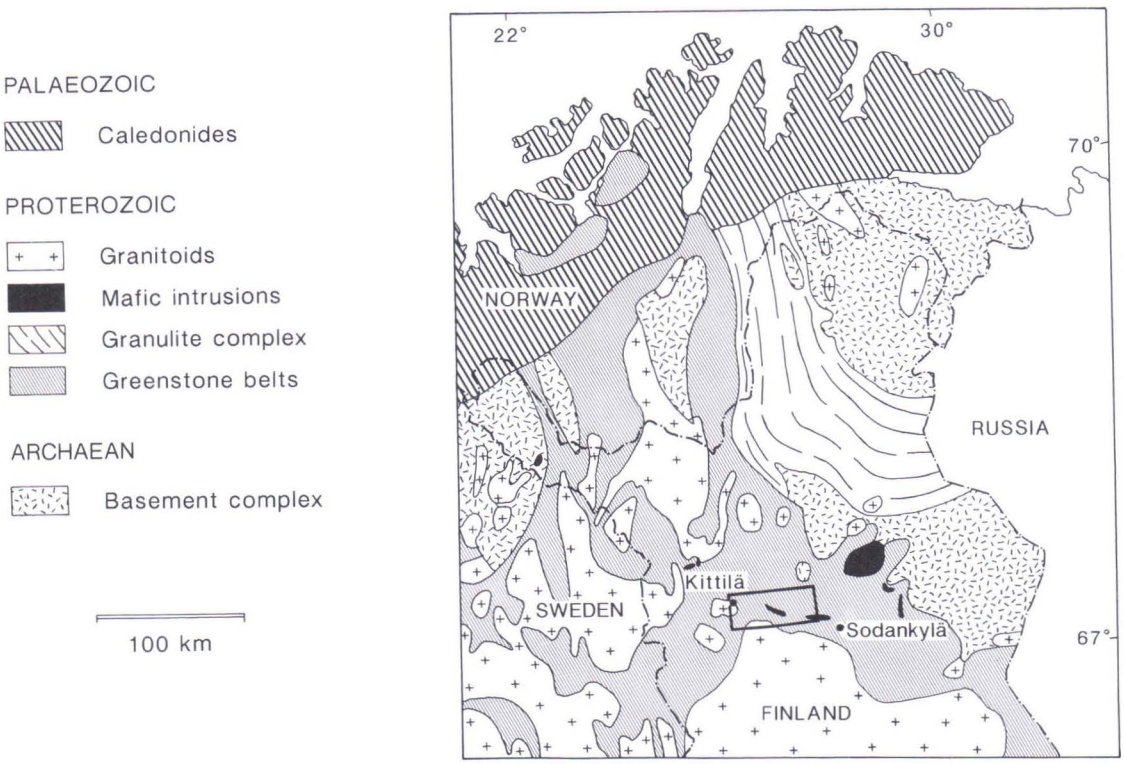

Fig. 1. Generalized geological map of the northern Fennoscandian Shield. Modified after the Metamorphic, Structural and Isotopic Age Map, Northern Fennoscandia (1988). The rectangle represents the area of Figure 2, where the sites studied here are located.

characteristics of the widespread alterations of various rock types in the CLGB. The genesis and primary nature of the pale sodium-rich rocks were considered especially important aspects. For this purpose a subproject named "Adinole Research" was set up and target areas were selected in the central part of the CLGB (Figs. 1 and 2).

Previous investigations

The Na-rich rocks of northern Fennoscandia have been described and their origins investigated by numerous geologists, including Eskola (1925), Ödman (1939), Mikkola (1941), Holmsen et al. (1957), Gjelsvik (1958), Padget (1959), Meriläinen (1961), Frietsch (1966), Paakkola (1971), Reino (1973), Piirainen and Rouhunkoski (1974), Eriksson and Hallgren (1975), Lehtonen et al. (1985), Eilu and Idman (1988), Björlykke et al. (1991), and Pankka (1992). Several occurrences of Na-rich rocks are especially well known in the CLGB, where they are most widespread and commonly occur in the Lapponian formations (Mikkola 1941, Rastas 1984, Lehtonen et al. 1984, 1985, Pihlaja and Manninen 1993) and in Kuusamo (Pankka and Vanhanen 1992), and there are abundant indications of hydrothermal alteration in barren rock areas (Meriläinen 1961, Sarapää 1980, Lehtonen et al. 1985, Tuisku 1985). In addition, alteration has been studied in connection with exploration in the CLGB, especially related to gold deposits (Härkönen and Keinänen 1989, Ward et al. 1989, Korvuo 1991, Nurmi et al. 1991, Korkiakoski 1992).

No trench excavation or drilling had been carried out at the present sites before the start of the "Adinole Research" subproject, and only two of the sites, Eksymäselkä (Reino 1973) and Isolaki (Nikula 1988), had been objects of detailed investigations. Most of the sites had been surveyed to a limited extent, however, in connection with regional surveys. Previous research had predominantly been concentrated on the stratigraphy of the greenstone belt and the determination of the general extrusion conditions and depositional environments of the volcanic rocks (Kallio 1980, Kallio et al. 1980, Kärkkäinen 1980, Sarapää 1980, Lehtonen et al. 1984, 1985, 1989, 1992, Saverikko 1988, Räsänen et al. 1989, Ward et al. 1989), description of the regional structure of the Earth's crust (Lanne 1979, Elo et al. 1989), and description of the depositional environments of the sediments (Kortelainen 1986, Nikula 1988).

The present research

The present sites represent areas where hydrothermal alterations, which are typical of a number of ore deposits and their wall rocks, apparently affected the barren greenstone belt rocks. The lithological units were thoroughly altered during the early stages of their evolution, before the regional metamorphism. The main aims of the research were to elucidate the progression and conditions of the alteration, to find differences in alteration processes between the sites, to identify the effects of the regional metamorphism and, if possible, to connect the alteration processes with the general geological history of the CLGB.

The research methods employed were detailed outcrop mapping, geophysical ground surveys, microscopic petrographic investigations, establishment of the primary nature of the rocks by mineralogical and chemical correlations, determination of the alteration temperatures and pressures by geobarometry and geothermometry, and interpretation of the whole

rock chemical data including mass balance calculations. The mineralogical and chemical composition and texture of the rocks in the areas concerned were compared with the results of experimental and theoretical alteration research carried out in bedrock areas that are known to be hydrothermally altered and areas that are hydrothermally active.

Several attempts were made to date the carbonation processes by the U-Pb and Pb-Pb methods. The only potentially radioactive mineral formed during this alteration stage and occurring in sufficient amounts for separation is rutile, however, and its radioactivity, in the samples studied, was found to be too low for reliable dating (H. Huhma, oral comm. 1993).

The sites were selected and most of the detailed fieldwork was carried out by Matti I. Lehtonen (GSF), except for the Palovaara area where Pentti Rastas (GSF) chose the sites, did the fieldwork and planning and supervised the diamond drilling and preliminary research. Most of the fieldwork was carried out in 1985-1987 and involved geological outcrop mapping, trenching and geophysical ground surveys. Diamond drilling was performed only in the Palovaara area. The geophysical methods used were magnetic, AMT, VLF-R and gravimetric measurements (Lehtonen 1989b). The present author performed complementary fieldwork at Eksymäselkä, Myllyvaara and Sivakkavaara in 1987, reviewed all the areas in 1991-1992, studied the thin sections, and processed the chemical data and calculated the mass balances and the mineral formulae.

Preliminary results of the subproject have been published in Finnish by Lehtonen (1987, 1988, 1989a), Lehtonen and Manninen (1986), Lehtonen and Rastas (1987, 1988), Lehtonen et al. (1989) and Eilu (1990) and in English by Eilu (1992, 1993) and Lehtonen et al. (1992). The present paper is the final report of the subproject.

Terminology

Adinole

According to Rosenbusch (1923), *adinole* is a country rock that has undergone metasomatic alteration under the effect of the intrusion of a dyke (commonly albite diabase). In spite of this definition, the term has repeatedly been used as a general name for albite-rich rocks of various or unknown origin, e.g., for altered dykes themselves or rocks not in contact with any dyke. Examples of this kind of *sensu lato* and partly inaccurate use are abundant in unpublished field reports and drill-log reports describing the rocks of the CLGB, and also occur in some publications (e.g., Lehtonen et al. 1984 and 1985, Pihlaja and Manninen 1993). The adinoles *sensu stricto* only constitute a small part of the altered rocks at the present sites. The use of the term adinole is thus kept to a minimum here and it is not used as the name of a lithological unit.

The prefix meta-

The lithological units described here have undergone metamorphism and, with a few exceptions, also hydrothermal alteration to varying degrees. All the rock names should therefore carry the prefix *meta-*. For simplicity and in order to avoid tautophony this prefix is not used, however. Thus, the terms sediments and volcanics, for example, as used in this paper refer to *meta*sedimentary and *meta*volcanic rocks.

Orthospilite and hyalospilite

Spilite is an altered basalt, in which albite together with chlorite, actinolite and epidote or other low-temperature hydrous minerals has replaced its primary magmatic minerals, and is typically enriched in Na and H_2O and depleted in Ca as compared to unaltered basalts (Fiala

1974, Vallance 1974, Reed 1983, Bates and Jackson 1987). Cann (1969) classifies spilites into two categories: *orthospilites*, altered low-grade basalts in which tremolite-actinolite has replaced the primary Fe-Mg silicates, and *hyalospilites*, in which they have been replaced by chlorite. Small amounts of chlorite may occur in orthospilite and small amounts of amphibole in hyalospilite. The primary feldspar is replaced by albite and the primary Ti-bearing magnetite by sphene ± Ti-poor magnetite in both types.

MATERIAL AND ANALYTICAL TECHNIQUES

A total of 1095 samples were selected from the varoius lithological units and alteration type units in the target areas (Table 1). The samples were taken from outcrops and trenches by a mini-drill, except for those from Palovaara which were selected from diamond drill cores. 780 samples were selected for preparation of thin sections (mostly polished) and 557 for whole rock analyses (Table 1). Density, magnetic susceptibility and remanence were measured in each sample. Matti I. Lehtonen (GSF) selected most of the samples, and Pentti Rastas (GSF) selected those from Palovaara. The author of the present study selected complementary samples for whole rock chemical analyses and thin sections, and samples for mineral analyses and U-Pb dating. The thin sections were prepared in the laboratory of GSF at Rovaniemi and the Department of Geology at Oulu University.

The whole rock analyses were carried out in several sets in 1985-1988. All major and some trace elements (S, Cu, V, Zr) of the whole rock samples were analysed by the XRF method at the Raahe research laboratories of the Rautaruukki Company. In addition, Br, Sb, As, W, Mo, Cs, Rb, Ba, Ag, Au, Zn, Co, Ni, La, Sm, Lu, Sc, Ta, Cr, Sn, U and Th were analysed using the instrumental neutron activation (INA) facilities of the State Technical Research Center (STRC) in Espoo. The reliability of the analytical results for each element analysed in each sample was determined at STRC. The detection limits for each element differed from sample to sample as a result of interference from other elements, and are thus difficult to specify. A number of duplicate samples were analysed and the relative precision was generally 2-5% for the main components (0.5-3% for SiO_2) and 5-30% for the trace elements. The contents of Mo, Ag, Au, Zn, Lu and Sn were in most cases found to be too low for reliable analytical results and the

Table 1. Total number of samples selected, thin sections, whole rock chemical analyses and REE analyses from the sites.

Site	Samples selected	Thin sections	Whole rock analyses	REE analyses
Eksymäselkä	302	231	143	48
Myllyvaara	143	125	76	19
Lehtovaara	173	67	67	0
Sivakkavaara	141	87	72	8
Honkavaara	139	83	71	7
Isolaki	34	24	18	2
Palovaara	163	163	110	45
Total	1095	780	557	129

data of these trace elements were therefore not used in the present study. 129 whole rock REE analyses (La, Ce, Nd, Sm, Eu, Tb, Yb, Lu) were carried out at STRC using the INA method (Lehtonen 1989b).

Mineral analyses of 65 samples were carried out with the Jeol JXA-733 Superprobe instrument at GSF in Espoo. The analytical conditions for silicate minerals were an accelerating current of 15 kV, a sample current of 25 nA (for silicates) or 20 nA (for carbonates) and a beam diametre of 10 m. Natural silicates and carbonates were employed as standards. The formulae of amphiboles and chlorites were calculated by the RECALC program of Powell and Holland (1988).

REGIONAL GEOLOGICAL SETTING

Geological investigations of the CLGB have been carried out since the beginning of this century (Mikkola 1937, 1941, and references therein). The first regional descriptions were given by Hackman (1925, 1927) and Mikkola (1941). The bedrock of northern Finland is composed of a few main units (Fig. 1): (1) the Archaean Basement Complex (3.1-2.5 Ga) consisting of granitoids, migmatitic gneisses and minor greenstone belts, (2) the Palaeoproterozoic greenstone belts (2.5-1.8 Ga), (3) mafic intrusions (2.4-2.0 Ga), (4) the Palaeoproterozoic granulite belt (ca. 1.9 Ga), and (5) Svecokarelidic orogenic granitoids (1.9-1.8 Ga) (Tyrväinen 1983, Silvennoinen 1985, Skiöld 1987, Räsänen et al. 1989, Ward et al. 1989, Huhma and Meriläinen 1991, Manninen 1991, Lehtonen et al. 1992). The CLGB is one of the most extensive units in the Palaeoproterozoic greenstone belt domain.

The CLGB is roughly 150 km long and 50-80 km wide, and it reaches to a depth of 5-6 km (Lanne 1979). It comprises a texturally well-preserved volcano-sedimentary rock sequence, which was emplaced in the rifted Archaean basement approx. 2.5-1.8 Ga ago. It is part of a linear, NW-SE trending zone of separated metavolcanite basins extending from Lake Onega, Russia, to Finnmark, northern Norway (Fig. 1) (Elo et al. 1989, Manninen 1991, Lehtonen et al. 1992). According to Lehtonen et al. (1992) the rocks of the CLGB can be divided as follows in five major units, the Lower, Middle and Upper Lapponian, the Lainio, and the Kumpu units (Fig. 2):

1. The Lower Lapponian unit consisting of komatiitic and tholeiitic basaltic, andesitic and dacitic volcanics rests unconformably on the Archaean basement. A U-Pb zircon age of 2526 ± 46 Ma from a dacite has been regarded as the age of the felsic volcanism and the minimum age of 2.44 Ga for the Lower Lapponian rocks is given by the Koitelainen layered igneous complex, which has intruded into the unit.

2. The Middle Lapponian unit consisting of sediments - quartzites, siltstones, phyllites and carbonate rocks - overlies the Lower Lapponian rocks. The sedimentation environments were dominantly shallow marine. The time of the sedimentation can be confined between the limits of 2.44 Ga (Koitelainen igneous complex) and approx. 2.2 Ga (albite diabases intruding the sediments).

3. The Upper Lapponian rocks are predominantly volcanics, but sediments are found in places. Locally the contacts with the Middle Lapponian rocks are gradational. The lowermost part of the Upper Lapponian unit consists of komatiites and picrites. Locally, however, there are lamprophyres in low stratigraphic positions cutting the Middle Lapponian sediments. It is possible that the Upper Lapponian magmatism was in fact started by a non-voluminous alkaline phase manifested by the lam-

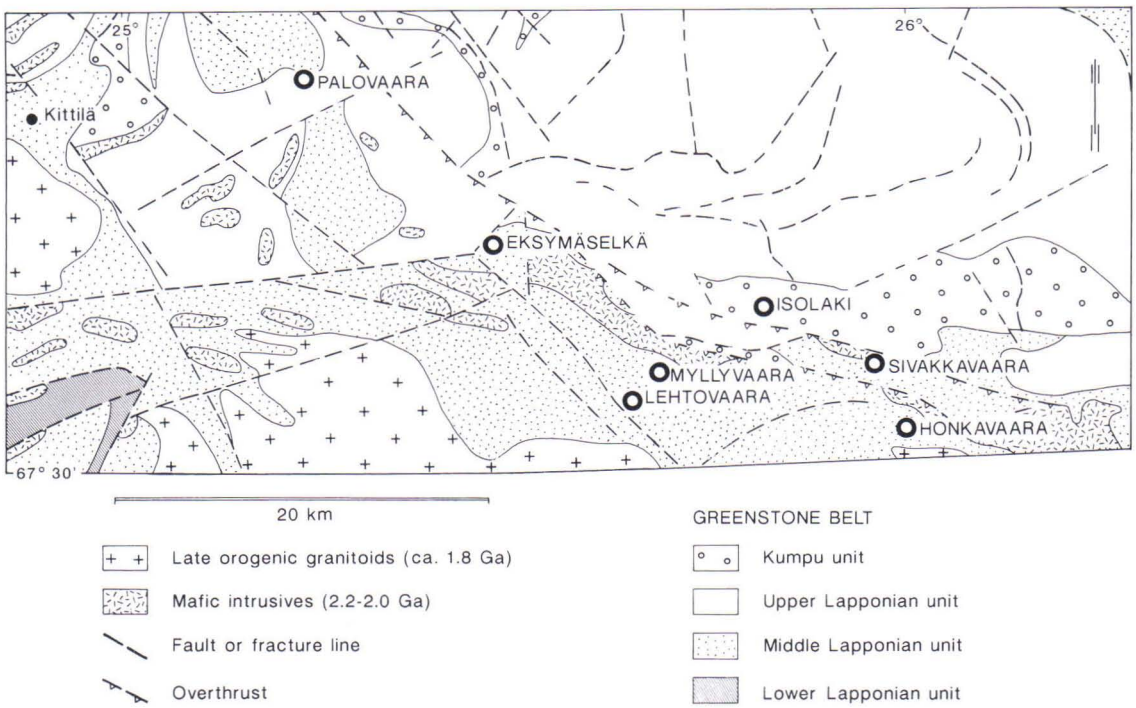

Fig. 2. Central part of the Central Lapland greenstone belt. The study sites are indicated by open circles. Modified after Lehtonen et al. (1992).

prophyres. The komatiites and picrites are overlain by iron tholeiites, which are in turn overlain by banded iron formations. The Fe tholeiites and iron formations are followed by Mg tholeiites. There are no reliable radiometric datings of the lamprophyres, nor of the mafic and ultramafic volcanics. Intensive diabase magmatism, chemically very similar to that of the Fe tholeiites, took place approx. 2200 Ma ago (zircon and sphene ages). The U-Pb zircon age of 2012 ± 3 Ma of a felsic magmatism gives the minimum age for the upper part of the Upper Lapponian unit. The mafic volcanics are cut by approx. 2060-2010 Ma old diabases (zircon ages) and all the Lapponian successions are cut by approx. 1920 Ma old (zircon ages) felsic porphyries.

4. The rocks of the Lainio unit were deposited discordantly on the Upper Lapponian volcanics in the western part of the CLGB (west of the area covered by Fig. 2). The unit is composed of fluvial sediments and K-rich volcanics. The age of the volcanics is 1883 ± 5 Ma, and thus they erupted during the synorogenic stage of the Svecokarelidic igneous activity.

5. Fluvial and alluvial sediments, mainly conglomerates and sandstones of the Kumpu unit, were deposited discordantly on the older units. Datings of zircons deposited in the Kumpu sediments show Pb-Pb ages of 2066-1913 Ma.

A rift-related origin has been proposed for the mafic and ultramafic volcanics and for the terrestrial sediments of the intracratonic CLGB (Räsänen et al. 1989, Ward et al. 1989, Gaál 1990, Manninen 1991, Lehtonen et al. 1992, Pankka 1992). The belt never developed to the point where new ocean crust formed, at least not in notable amounts, although pillow lavas indicate widespread subaqueous and tidal sediments indicate marine conditions (Räsänen et

al. 1989, Lehtonen et al. 1985, 1989, Nikula 1988). The extensional phase of the rift, with alkaline, komatiitic and tholeiitic magmatism lasted from approx. 2.5 Ga to 2.0 Ga before present (Ward et al. 1989, Korja et al. 1993).

As shown later on in this study, diagenetic albitization of the primary feldspars destroyed the provenance information of the Middle Lapponian sediments. Synmagmatic hydrothermal alteration occurred during magmatic episodes 2.5-2.0 Ga ago (Ward et al. 1989), but in the central part of the CLGB it was most extensive during the Upper Lapponian magmatism 2.2 Ga ago, resulting in spilitic mineral associations in igneous rocks and carbonation and intensive, overprinting albitization in their wall rocks. These alterations were soon followed and further overprinted by sericitization. A few Cu and Cu-Co deposits, like Pahtavuoma in Kittilä (Inkinen 1979), were formed during the synmagmatic hydrothermal alteration stage.

Collision during the Svecokarelian orogeny resulted in rift closure and regional metamorphism about 2.0-1.8 Ga ago. Gold mineralization and potassium enrichment due to metamorphic fluid circulation resulting in sericite-biotite alteration assemblages took place during and after the deformation peak (Härkönen and Keinänen 1989, Ward et al. 1989, Nurmi et al. 1991, Korkiakoski 1992, Pankka 1992). Brittle deformation, concentrated in some fracture zones possibly related to the postorogenic granites 1.77 Ga ago, was the final phase in the development of the greenstone belt (Ward et al. 1989).

Seven areas were selected for detailed study of the alteration phenomena. The main basis for the selection was the fact that the albitized and carbonated rocks of the CLGB are dominantly found in the transitional zone from Middle to Upper Lapponium, but little was actually known about the detailed geology of the sites. Most of them (Fig. 2) represent analogous stratigraphic positions: 2.2 Ga old albite diabases cut Middle Lapponian sediments, which at some sites are covered by Upper Lapponian volcanics. The sediments are also cut by lamprophyres, probably of Upper Lapponian age. The Isolaki site represents a different stratigraphic position with an albite diabase partly covered by sediments of the Kumpu unit. These seven areas were selected for the following additional reasons:

1. **Eksymäselkä**: Exploration drilling had shown an occurrence of albite rocks nearby. In the area, albite diabases and "albitites" were known to occur in outcrops (Reino 1973) and brecciated albite-carbonate rocks of unknown origin were found as boulders (Lehtonen and Manninen 1986).

2. **Myllyvaara**: Brecciated albite-carbonate rocks, similar to those at Eksymäselkä, as boulder fields, and biotite-bearing, reddish "diabases" (actually lamprophyres), also as boulder fields, were found in the area (Lehtonen and Manninen 1986).

3. **Lehtovaara**: An albite diabase has intruded Middle Lapponian quartzites. Alteration could not be observed by macroscopic investigation (Lehtonen and Manninen 1986), but was supposed to be found by thin section and geochemical investigation.

4. **Sivakkavaara**: The Middle Lapponian quartzite has been thoroughly and widely albitized, but the total volume of known albite diabases was relatively small in comparison with the other study sites (Lehtonen 1987).

5. **Honkavaara**: The albite diabases cut both Middle Lapponian and Archaean (2.7 Ga) rocks. Brecciated albite-carbonate rocks and pale albite rocks of volcanic origin occur widely in outcrops and boulders, but their relations to the 2.2 Ga albite diabases and the 2.7 Ga altered felsic volcanics was unknown (Lehtonen 1987).

6. **Isolaki**: The stratigraphic position differs from that of the other study sites: The 2.2. Ga albite diabase is in contact with the Kumpu sediments. The albite diabase was believed to have intruded in the sediments and albitized fragments were found in the Kumpu conglomerate. Albitization thus seemed to have taken

place before the intrusion and was unrelated to the diabase (Lehtonen 1987). The radiometric age determinations from sediment clasts were not available at the time.

7. **Palovaara**: A sequence from Middle Lapponian sediments to Upper Lapponian volcanic rocks exists in the area (Lehtonen et al. 1984). Au showings and albitized and carbonated rocks were found in surrounding areas (Härkönen and Keinänen 1989).

DESCRIPTION OF THE AREAS STUDIED

The stratigraphic position of the areas studied is roughly similar and they have several lithological features in common. All intrusive bodies are dykes, mostly albite diabase. At all study sites, there are sedimentary units, both quartzites and siltstones. Mafic lava, lamprophyre, phyllite, sedimentary carbonate rock, and conglomerate occur only at some of the study sites, but all these rock types are found within a few kilometres from each area.

Thin section investigations show that the textures and mineral associations formed during the secondary alterations are similar at all study sites. The mineral assemblages of even the least altered rocks were formed by alteration processes and were partially recrystallized during greenschist facies regional metamorphism. The alteration types are classified on the basis of their diagnostic minerals. This method facilitates comparison of the areas studied, and comparison with other altered areas and with experimental research. The common alteration types found are formation of amphibole zones, chloritization, biotitization, albitization, carbonation, and sericitization, which are all common in numerous hydrothermally altered areas and ore deposit environments (e.g., Cann 1969, Fyon and Costa et al. 1983, Reed 1983, Colvine et al. 1988, Kalsbeek 1992). Figure 3 shows photomicrographs of the dominant alteration types.

The width of alteration zones varies from millimetres to hundreds of metres. Up to 20 cm wide alteration haloes occur around single filled fractures. In places, wider zones are connected to filled fracture frameworks. Zones formed at different stages frequently overlap each other, but except for the thorough albitization of sediments they mostly follow the strike of the dykes. The boundaries of the alteration zones are nearly always gradual.

Polyphasic brittle deformation is connected with the early evolution of the areas studied. Early brecciation predates all secondary alteration, but fracturing and brecciation also took place during the alteration stages. Ductile deformation took place after the secondary alterations in all areas. This is indicated by the formation of schistosity in the fracture fillings and in the alteration zones of all alteration stages. Only at Palovaara the ductile deformation had major effect on rock textures, but weak signs of it were also recognized at Eksymäselkä and Lehtovaara. Regional metamorphic greenschist facies recrystallization took place in all areas except Isolaki, but the recrystallization grade was in most cases so low that significant destruction of the alteration textures and mineral assemblages did not take place. No signs of metamorphic or post-metamorphic alterations, like rearrangement or formation of new alteration zones, were found. The tiny and scarce calcite-filled fractures are the only evidence of brittle deformation following the ductile phase.

In order to understand the alteration processes, it is necessary to establish the chemical composition of the altered rocks prior to their alteration. Several common discrimination diagrams, like the AFM diagram of Irvine and Baragar (1971) or the TAS diagram of Le Bas et al. (1986), are essentially based on elements - like the alkaline metals - which are highly

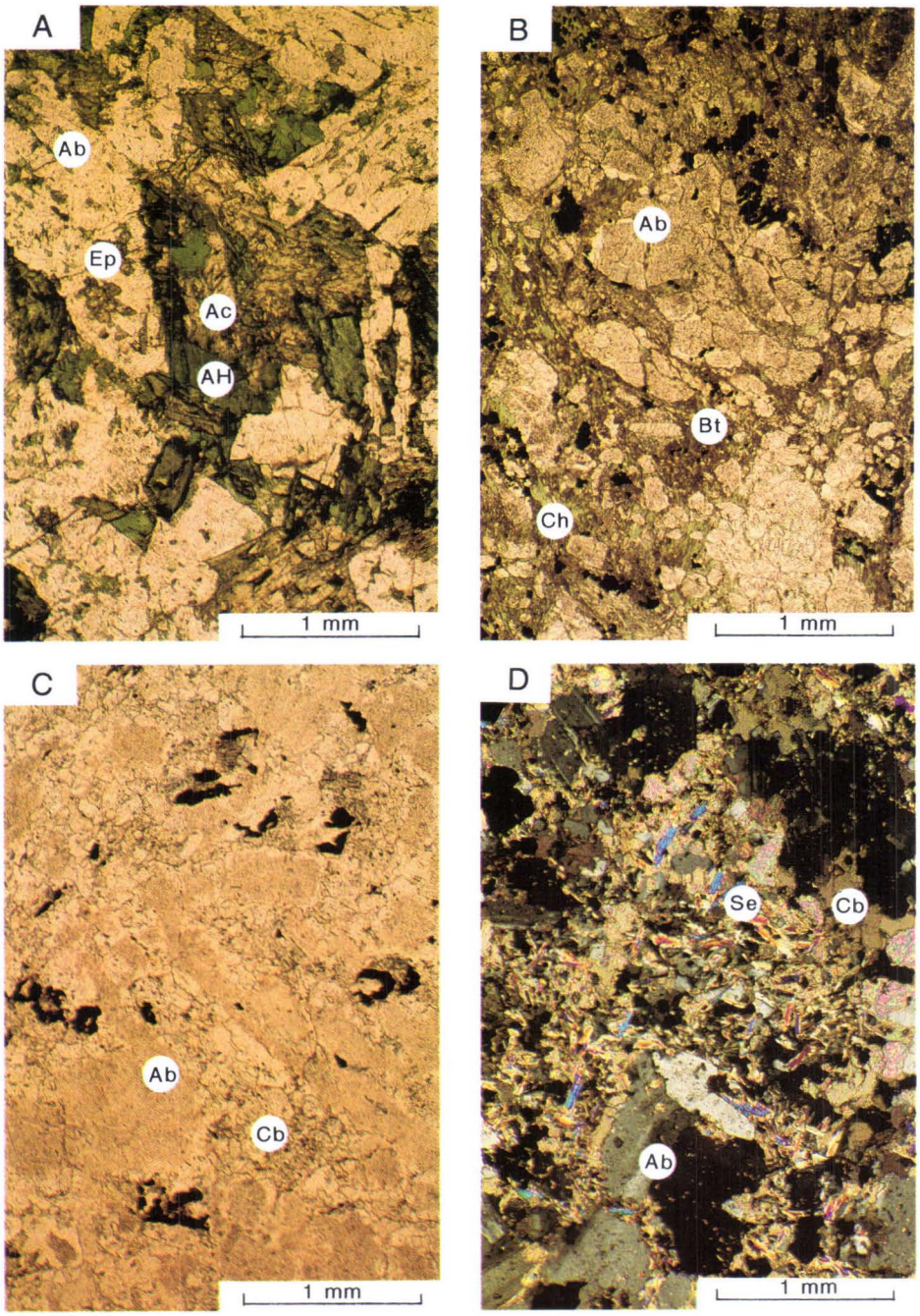

Fig. 3. Photomicrographs of the dominant alteration types at the study sites. Abbreviations: Ab = albite, Ac = actinolite, AH = actinolitic hornblende , Bt = biotite, Cb = carbonate, Ch = chlorite, Ep = epidote, Qz = quartz, Py = pyrite, Rt = rutile, Se = sericite, Tc = talc. **A**: Amphibole zone in weakly fractured albite diabase, Eksymäselkä. Plane-polarized light. **B**: Chloritization and biotitization. All opaque grains are magnetite. Moderately fractured albite diabase, Eksymäselkä. Plane-polarized light. **C**: Carbonation and albitization. All opaque grains are rutile. Moderately fractured albite diabase, Eksymäselkä. Plane-polarized light. **D**: Sericite replacing carbonate in moderately fractured albite diabase. Eksymäselkä. Crossed polarizers.

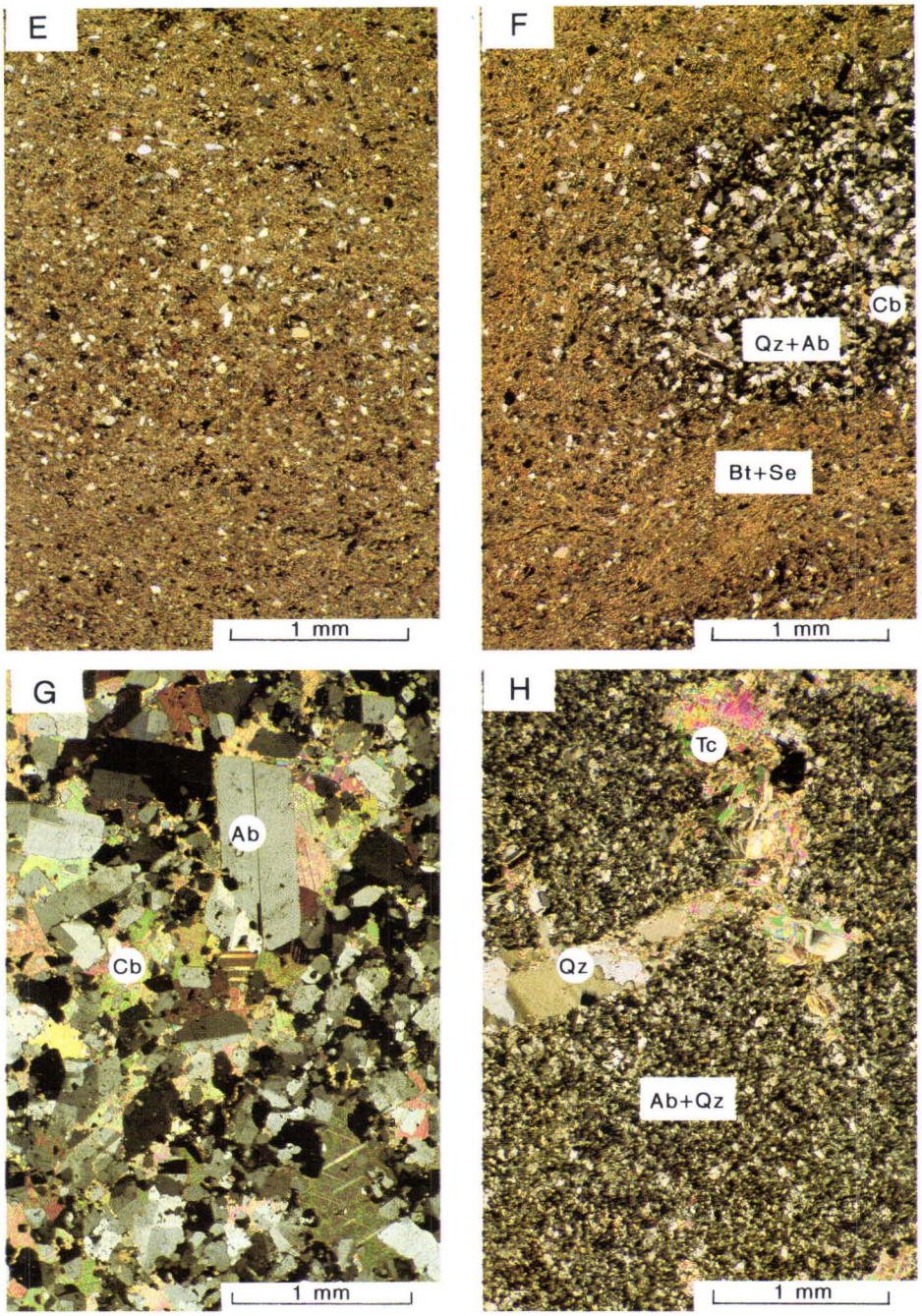

Fig. 3. Continued. **E**: Least altered siltstone; quartz clasts in biotite-sericite matrix. Biotite-sericite zone, Myllyvaara. Crossed polarizers. **F**: Weakly albitized and carbonated siltstone. A bleached spot of quartz-albite-carbonate in the least altered rock, Myllyvaara. Crossed polarizers. **G**: Intensively albitized and carbonated siltstone consisting of only albite and Fe dolomite, Myllyvaara. Crossed polarizers. **H**: Intensively albitized siltstone with talc and quartz in fractures. Myllyvaara. Crossed polarizers.

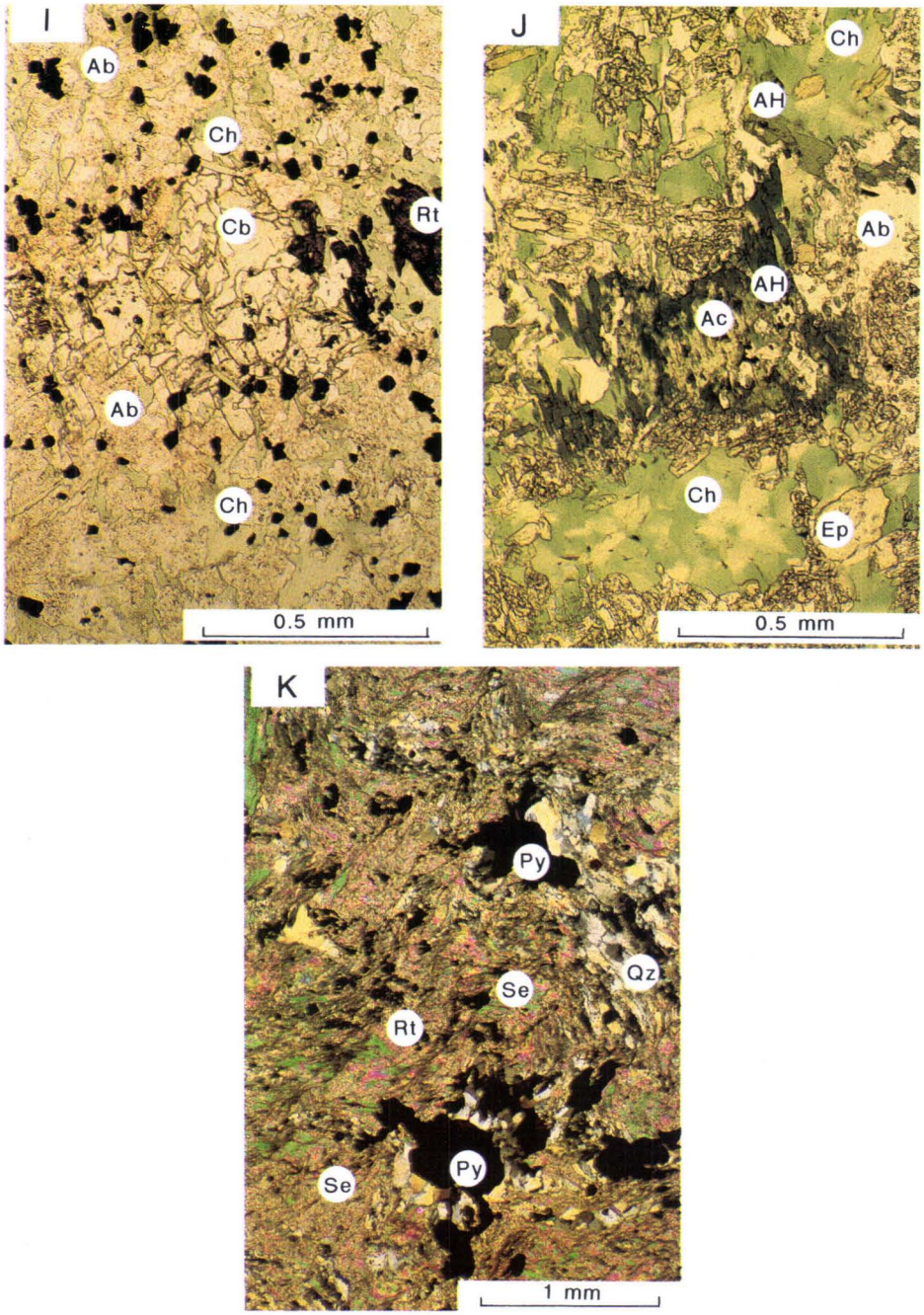

Fig. 3. Continued. **I**: Chloritized lamprophyre where chlorite has partially replaced carbonate, Myllyvaara. Plane-polarized light. **J**: Replacement of hydrothermal actinolite and chlorite by epidote and actinolitic hornblende formed in regional metamorphism. Amphibole zone, weakly fractured albite diabase, Lehtovaara. Plane-polarized light. **K**: Intensively sericitized and moderately pyritized metasediment where most of the pyrite and quartz occur in fractures. Very fine-grained rutile clusters occur in sericite. Palovaara. Crossed polarizers.

mobile in alteration processes. Because completely unaltered rocks are exceedingly rare in the areas of the present study, the igneous rocks were classified by using diagrams based on the least mobile elements. In addition, the use of the least altered samples allowed use of elements that were obviously mobile during intensive stages of alteration.

Eksymäselkä

General structure

The bedrock of the site is composed of Middle Lapponian sediments and tuffites, of Upper Lapponian albite diabase that has intruded in the sediments and tuffites, and of Upper Lapponian mafic lavas (Fig. 4). The zircon age of the albite diabase is 2.214 ± 2 Ga (U-Pb method, Kallio 1980). The lava units of the western and northern parts of the study site (the Fe-Ti tholeiites) are assumed to be comagmatic with and of the same age as the albite diabase because the chemical data (Figs. 5 and 6, Table 3, p. 57) indicate strong similarity between them.

The primary sedimentary textures are badly damaged by brittle deformation and alteration.

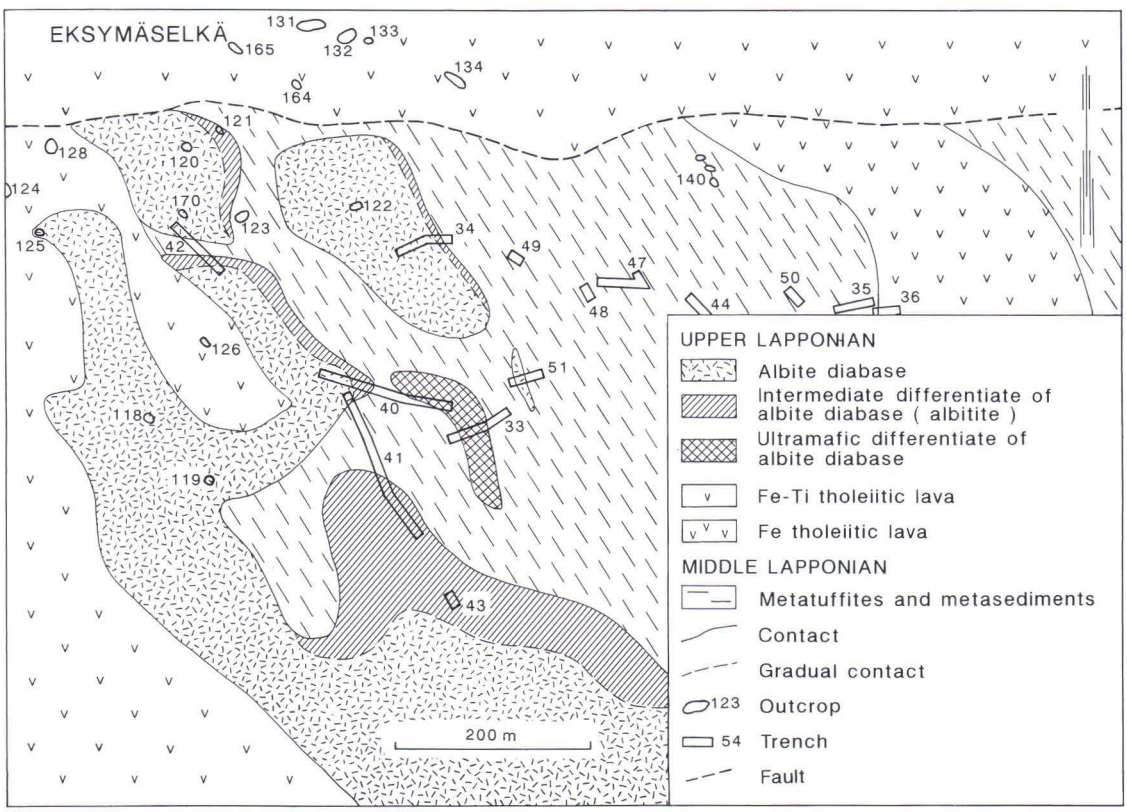

Fig. 4. Geology of the Eksymäselkä site with outcrop and trench numbers. Natural outcrops occur only at the western and northern margins of the area. The geological map is therefore chiefly based on excavated trenches and geophysical surveys. Previous studies of the area by Reino (1973), Lehtonen and Manninen (1986), Lehtonen (1988, 1989a), and Eilu (1990, 1992).

The strike of the sediments is roughly N-S, but the dip is obscure. In the closest vicinity of the albite diabase, the layered structure is extremely confused because of the intrusion of the diabase into the sediment sequence. The most felsic types of the diabase - the albitites - occur without an exception on the eastern side of the intrusive (Fig. 4), hence, the stratigraphic top was to the east when the diabase magma intruded to its present surroundings. According to the geophysical surveys, the dip of the intrusive is steeply to the west.

Brittle deformation dominates in the whole area studied; each lithological unit is variably brecciated, both on a large and a small scale. A weak ductile phase followed the brittle deformation stages. It is possible to see ductile deformation only locally in strongly altered parts of the mafic lavas at the northern margin of the area and in the ultramafic cumulate of the albite diabase where sheet silicates have partially recrystallized, forming a weak schistosity.

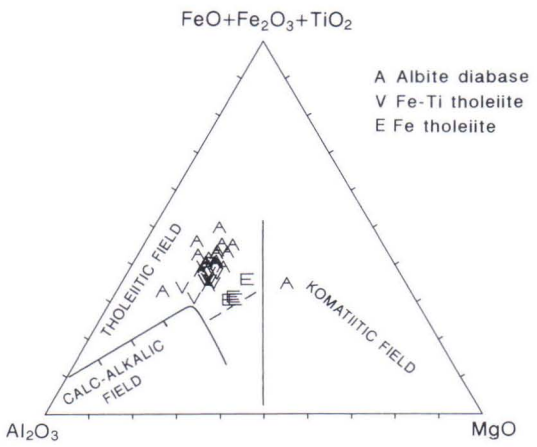

Fig. 5. Albite diabase and tholeiitic lavas from Eksymäselkä on the Jensen cation plot diagram (Jensen 1976).

Mafic lavas and albite diabase

The mafic lava units can be divided in two chemically distinct tholeiite groups (Table 3, p. 57). High Ti and Fe concentrations are characteristic of the lava of the northern and western part of the area studied. In the lava of the eastern part, the Fe and Ti concentrations are lower, but, according to the Jensen cation plot diagram (Fig. 5), this unit is also a Fe tholeiite. Consequently, the lava units of the northern and western part are called Fe-Ti tholeiites and the eastern lava unit Fe tholeiite (Fig. 4, Table 3). In the SiO_2 vs. Zr/TiO_2 diagram (Fig. 6) the lava and albite diabase samples are in the subalkaline field.

Albite diabase is the sole intrusive rock at Eksymäselkä. Ultramafic and intermediate cumulates, originally olivine-dominated ultramafic and plagioclase-dominated intermediate types, are related to the mafic albite diabase intrusive (Fig. 4).

The primary texture of the Fe-Ti tholeiites is massive and porphyritic; the phenocrysts were originally plagioclase and clinopyroxene. The texture of coarser-grained Fe-Ti tholeiites highly resemble that of albite diabase shown in Figure 3A. The texture is intergranular and phenocrysts can no longer be found in the Fe tholeiite. Macroscopically, the Fe-Ti tholeiites are massive or pillowed and the Fe tholeiites massive. The texture of the least altered types of albite diabase (Fig. 3A) is intergranular or subophitic (terminology of igneous textures after MacKenzie et al. 1982). These primary textures are best preserved in the mafic types and moderately well in the intermediate cumulates. The primary texture of the ultramafic cumulate has been totally altered: it is now lepidoblastic-granoblastic and weakly foliated. The mineral associations of the least altered lava and albite diabase types are:

Fe-Ti tholeiite: albite + tremolite-actinolite + epidote + magnetite + sphene

Fe tholeiite: albite + chlorite + magnetite

Albite diabase (mafic type): albite + tremolite-actinolite + epidote + magnetite + ilmenite

Intermediate cumulate of albite diabase: albite + chlorite + magnetite ± quartz

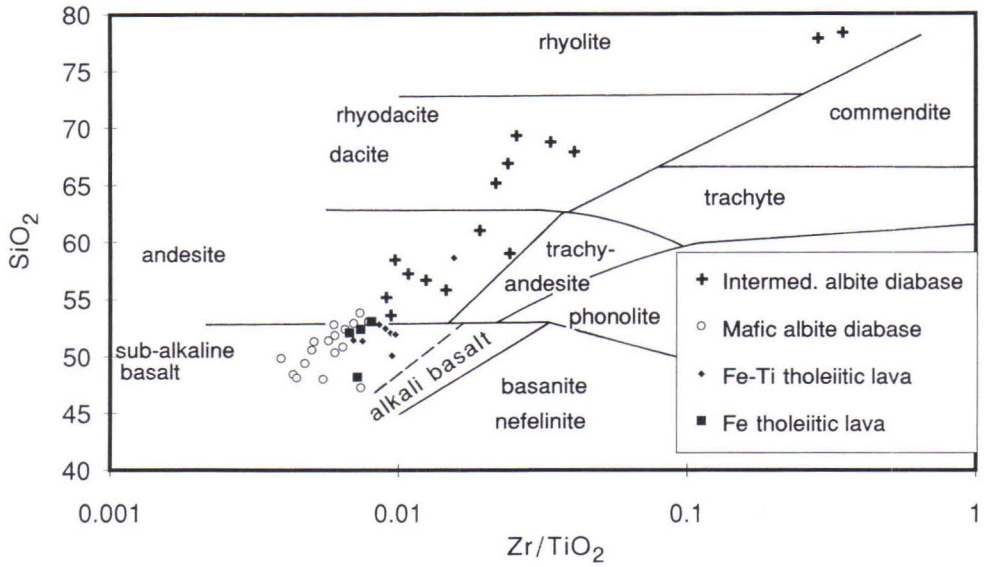

Fig. 6. SiO_2-Zr/TiO_2 diagram for albite diabase and tholeiitic lavas form Eksymäselkä. Fields after Winchester and Floyd (1977). SiO_2 was recalculated on volatile-free basis.

Ultramafic cumulate of albite diabase: talc + chlorite + Fe dolomite + magnetite ± calcite.

Sediments and pyroclastites

The sediments and tuffites are variably altered and occur in the vicinity of the albite diabase as highly altered beds, which only indirectly show their primary nature. In the central parts of the area studied, the alteration intensity is lower and there one can see that these rocks are dominantly sediments, locally including volcanic material. The texture of the least altered sediments is blastoclastic and banded. Their dominant mineral associations reflect thorough albitization:

Quartzite: quartz + albite ± sericite
Siltstone: quartz + albite + biotite ± sericite
Tuffite: quartz + albite + chlorite ± biotite.

Alteration types

Five alteration types can be distinguished on the basis of the occurrence and replacement relationships of secondary minerals (Figs. 3A-3D). In the albite diabase and mafic lava these are amphibole, chlorite-biotite, carbonate, and sericite alteration and in sediments and tuffites chlorite-biotite, intensive albite, carbonate, and sericite alteration (Fig. 7). The chemical compositions of the lithological units in different alteration zones and alteration zone combinations are presented in Tables 3-5 (pp. 57-59).

1. The **amphibole zones** (Fig. 3A) represent the least altered diabase and lava. Their mineral association is equal to the typical greenschist facies orthospilite association (Cann 1969) and was formed when tremolite-actinolite replaced primary Mg-Fe silicates (olivine and pyroxene) and albite ± epidote replaced primary plagioclase. Primary magmatic textures are unaltered, rocks are only weakly brecciated. Fractures are filled with epidote and albite.

Amphibolization as such is rare: amphibole only occurs in the inner parts of the albite diabase and Fe-Ti tholeiite units, and even there it is overlapped by weak chloritization and bioti-

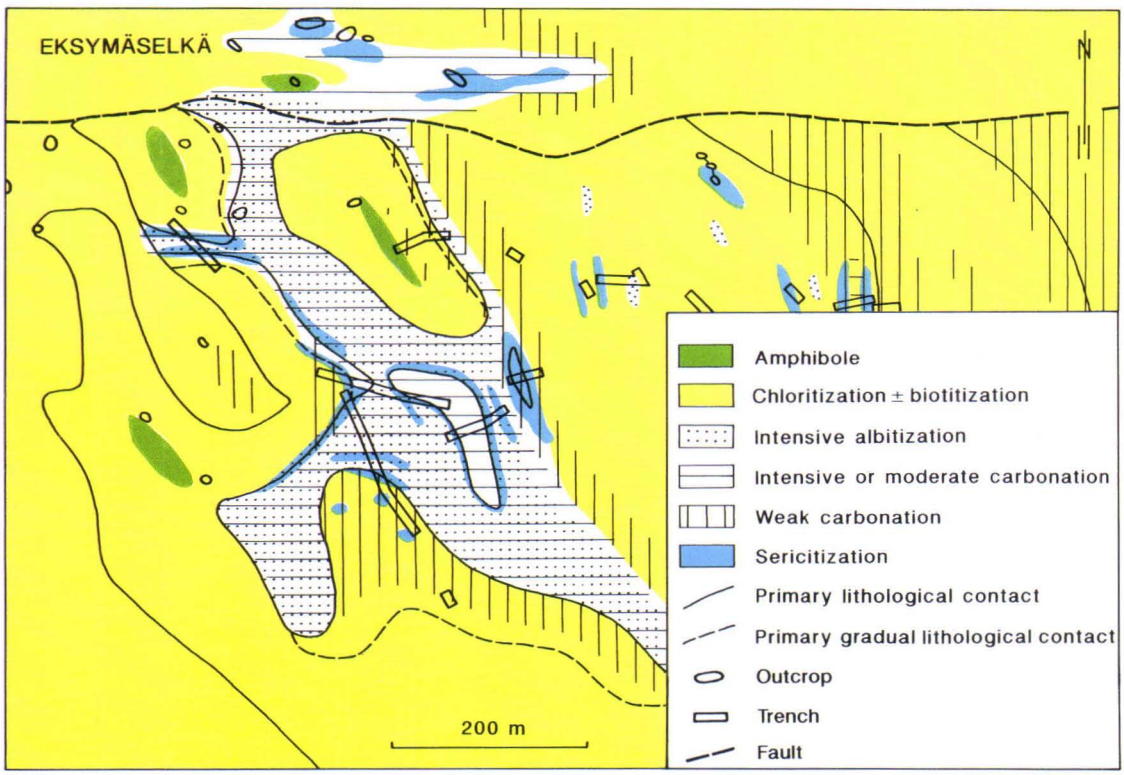

Fig. 7. Alteration types at Eksymäselkä.

tization. The typical mineral association in the amphibole zones is:

albite + tremolite-actinolite + epidote + magnetite + chlorite ± biotite.

2. The **chlorite-biotite zones** (Fig. 3B) cover most of the area studied (Fig. 7). Within these zones, chlorite has replaced the primary Mg-Fe silicates (olivine and pyroxene), secondary amphibole and epidote, and albite have replaced plagioclase and K feldspar and, after that, biotite has partially replaced chlorite. Amphibole completely disappears from the mineral association at the margin of the amphibole zones. Epidote disappears gradually after amphibole, with increasing intensity of chloritization. In the most fractured, <0.5 m wide zones, chlorite and quartz have nearly completely replaced albite. White K mica with a composition similar to that of the diagnostic mica of the sericitized zones occurs in quartzites and siltstones. In contrast to the sericitized zones, the K mica of the chlorite-biotite zones does not occur as fracture fill nor replacing other silicates or carbonates, but forms part of the matrix, and is most probably related to the diagenesis of the sediments.

The mineral association and texture of the most chloritized lava closely resemble that of the hyalospilite of Cann (1969). The textures of sediments and tuffites are blastoclastic and layered (as in Fig. 3E). The typical mineral associations in the chlorite-biotite zones are:

Albite diabase and Fe-Ti tholeiite: albite + chlorite + magnetite + ilmenite ± biotite ± quartz

Fe tholeiite: albite + chlorite + magnetite

Tuffites: albite + chlorite + quartz ± biotite

Quartzite: quartz + albite + muscovite

Siltstone: quartz + albite + biotite ± muscovite.

The brecciation is clearly more intensive in the chlorite-biotite zones than in the amphibole zones (cf. Figs. 3A and 3B). The textures are variably fractured and the larger (>0.5 mm) albite crystals have a chessboard texture or are replaced by aggregates of tiny albite crystals. The primary magmatic texture is, however, still recognizable in most cases. Fractures are filled with chlorite + biotite and quartz ± albite ± pyrite ± chalcopyrite. Weak brecciation with quartz-filled fractures occurs throughout the sediments and tuffites.

3-4. In **the carbonated zones** (Fig. 3C), Fe-bearing dolomite and calcite replace all the other minerals except quartz and zircon, and dolomite is the dominating carbonate. If any epidote or sphene was present in the rocks, these minerals were totally altered during the first stages of carbonation. Chlorite, biotite and magnetite, in this order, were replaced next. In addition, the rocks were **albitized**, the igneous ones weakly and the sediments and tuffites intensively (as in Figs. 3F-3H). SiO_2 was released and crystallized as quartz in the fractures. The mineral associations and textures of the chlorite-biotite zones are observable only in the weakly carbonated zones. The mineral associations of the most carbonated zones are:

Albite diabase, its intermediate cumulate, tholeiites: albite + carbonate + quartz + rutile

Ultramafic cumulate of the diabase: carbonate + talc + magnetite ± rutile

Sediments and tuffites: albite + quartz + dolomite + magnetite or haematite ± rutile ± calcite.

The primary textures were gradually destroyed, replaced by granoblastic textures and brecciated during carbonation and albitization. Alteration is concentrated in zones brecciated before the carbonation. Therefore, there are always both fractures filled with chlorite, biotite and quartz, related to pre-carbonation brecciations and fractures related to albitization and carbonation and filled with quartz ± albite and carbonate ± quartz. Some fractures related to albitization + carbonation also include small amounts of pyrite and chalcopyrite.

5. Fine-grained K mica has replaced albite, biotite, chlorite and carbonates, especially Fe dolomite, in the **sericitized zones**. The alteration grade is weak and all pre-sericitization features are identifiable. Sericitization and carbonation commonly overlap (Fig. 3D); the chlorite-biotite zone rocks have been sericitized without a carbonation inter-stage in only a few localities. The mineral associations of the sericitized zones always contain, in addition to sericite, minerals of other alteration zones. Weak chloritization is related to the sericitization: in places chlorite replaces carbonate instead of sericite. Weak brecciation with sericite-filled fractures with is related to the alteration stage.

Regional metamorphic recrystallization

The regional metamorphic, isochemical recrystallization has affected the Eksymäselkä area in places. Actinolitic hornblende has partially replaced tremolite-actinolite (Fig. 3A), epidote, biotite and chlorite (as in Fig. 3J) in the albite diabase. Biotite has partially replaced carbonates, chlorite and early biotite in diabase, sediments and tuffites. Metamorphic biotite and amphibole have, however, formed only where biotite and amphibole existed before, indicating that the hydrothermal zonation did not change during the regional metamorphism.

Myllyvaara

General structure

The structure of the Myllyvaara area is simple (Fig. 8). Middle Lapponian sediments, mostly siltstone, form the bulk of it and lamprophyre dykes the remaining parts. The southern margin is composed of quartzite, and several 0.1-1 m thick quartzite layers occur among the sediments, too. Two interlayers of polymictic conglomerate were found in siltstone in the northern part of the area. Lamprophyre dykes, 10 cm to 10 m in width, occur throughout the area nearly conformably among the sediments and locally include siltstone xenoliths with a size of 0.1-1 m. The age relationship between the lamprophyre dykes and the closest albite diabase dykes, 1-2 km away from Myllyvaara, is unknown: the contacts between them have not been found. Nevertheless, the sediments were already consolidated when the lamprophyres intruded them. This is indicated by brecciation in the sediment-lamprophyre contacts and by the lack of plastic deformation, which would be typical of interaction between magma and unconsolidated sediments. The strike of the bedding is E-W and the dip is steeply to the north. On the basis of grading of silt layers, the stratigraphic top is to the north.

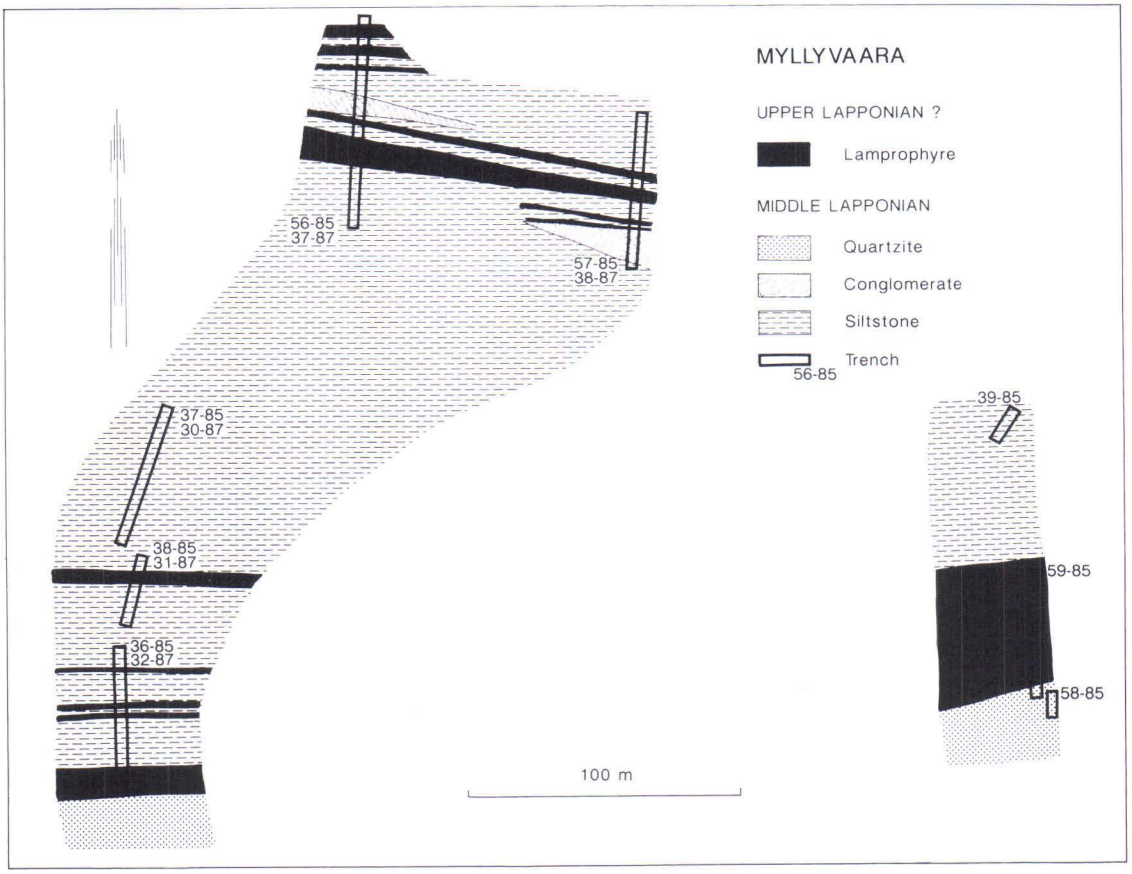

Fig. 8. Geology of the Myllyvaara study site with trench numbers. The map is based on excavated trenches and geophysical surveys because natural outcrops are lacking. The Myllyvaara area and its vicinity have previously been described by Kallio et al. (1980), Kärkkäinen (1980), Lehtonen and Manninen (1986), Lehtonen (1988, 1989a), and Eilu (1990, 1992).

The area of study belongs to a region where open folding dominates (Lehtonen et al. 1984), but no indications of ductile deformation were found, only brittle deformation. Fracturing is thorough in the whole area, being most intensive in the most altered zones.

Lamprophyres

Two types of lamprophyres occur at Myllyvaara: according to the Sc/Ta vs. Cr/V diagram (Fig. 9) alkaline and calc-alkaline lamprophyre. These differ clearly from the albite diabases on the SiO_2 vs. Zr/TiO_2 diagram (Fig. 10). Both alkaline and calc-alkaline lamprophyres are found in the whole Myllyvaara area, their altered types are petrographically similar, and they do not intersect nor show other indications of age differences.

The textures of the least altered lamprophyres are primary magmatic: narrow dykes and margins of wider dykes are biotite-phyric and trachytoidal; idiomorphic biotite phenocrysts (size 0.5-5 mm) are bent and contain abundant sphene, zircon and opaque inclusions. The ground mass consists of feldspar, biotite and magnetite. The inner parts of the wider dykes are either hypidiomorphic or intergranular in textute. In two wide dykes, tremolite-actinolite is a chief constituent in addition to plagioclase and biotite. Quartz-filled amygdales (size approx. 1 mm) were found in a sin-

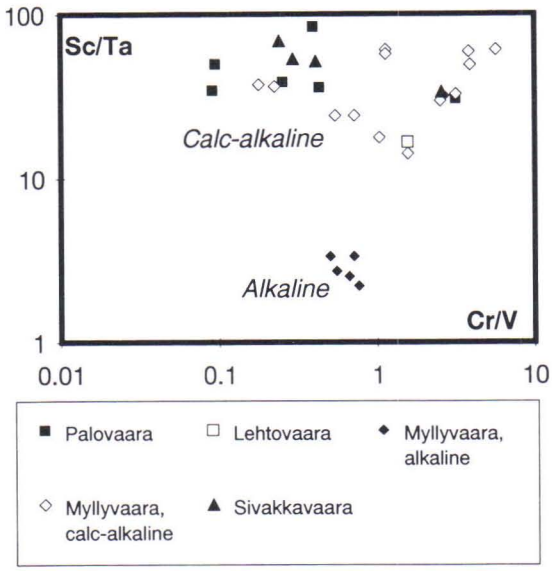

Fig. 9. Lamprophyres from Myllyvaara, Lehtovaara, Sivakkavaara and Palovaara on a Sc/Ta vs. Cr/V diagram. Discrimination is based on the data of Rock (1991).

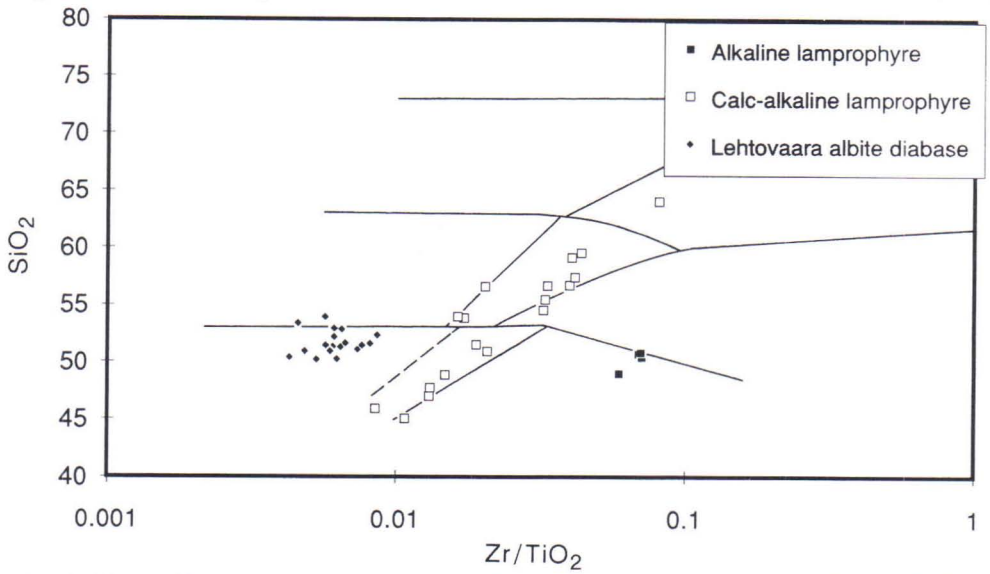

Fig. 10. SiO_2-Zr/TiO_2 diagram for lamprophyres from Myllyvaara and typical albite diabase of the CLGB from Lehtovaara. Fields as in Figure 6, after Winchester and Floyd (1977). SiO_2 was recalculated on volatile-free basis.

gle dyke. The mineral associations of the least altered lamprophyres are:

K feldspar + albite + tremolite-actinolite + biotite + epidote + sphene + magnetite + apatite

albite + tremolite-actinolite + biotite + epidote + magnetite + sphene + apatite

albite + biotite + magnetite + apatite ± quartz.

Sediments

The texture of the least altered sediments is blastoclastic and layered, but not foliated (Fig. 3E). The siltstone is locally graded and the quartzite is cross-bedded. There are no obvious indications of volcanic or plutonic sources in the sediments. The clasts are mainly quartz, however, 1-10 vol. % of albite clasts are present. The matrix of the quartzite consists of albite and sericite; the matrix of the siltstone consists of albite, sericite and biotite. The dominant mineral associations of the least altered sediments are:

Quartzite: quartz + albite + muscovite

Siltstone: quartz + albite + biotite + muscovite.

The conglomerate is strongly altered, and thus the origin of all its angular fragments is not evident. Some of the fragments are obviously albite diabase, but most of them are probably quartzite and siltstone. The matrix of the conglomerate consists of albite, quartz, dolomite and talc.

Alteration types

The following alteration types were observed at Myllyvaara: amphibole, biotite-sericite, weak albite-carbonate, intensive albite, moderate and intensive carbonate, and chlorite-talc alteration (Figs. 3E-3I). The most important alteration zones are shown in Figure 11. The chemical composition of the lithological units in different alteration zones and alteration zone combinations is presented in Tables 7-9 (pp. 63-65).

1. The **amphibole zones** are represented by the least altered lamprophyres. The brecciation is weak and primary magmatic textures are well preserved. The textures and mineral associations were described in the general description of the lamprophyres. The amphibole is secondary; it has completely replaced the primary clinopyroxene and hornblende crystals, which can be distinguished only as pseudomorphs. Some of the biotite crystals may be primary, but part of them are secondary, formed by replacement of primary biotite and clinopyroxene or hornblende.

2. **Biotite-sericite zones** (Fig. 3E) cover the least altered sediments. The textures are well preserved, the rocks are very weakly or not at all brecciated. The fractures are filled with quartz and sericite. The biotite seems to belong to the primary mineral association: there are no indications that it has replaced, e.g., chlorite. On the contrary, sericite is clearly a secondary mineral although it is in equilibrium with albite: it has only replaced biotite. The sediments contain no calcic plagioclase or K feldspar; if they did originally, albite has replaced it.

3. **Weak albitization and carbonation** (Fig. 3F) comprises frameworks of 1-20 cm wide bleached haloes around fractures filled with quartz + carbonate + biotite ± albite ± haematite. Biotite, sericite and magnetite have been replaced by albite and carbonate (chiefly Fe dolomite) in the siltstones, and biotite and K feldspar have been replaced by albite, muscovite, quartz and carbonate in the lamprophyres. Granoblastic texture has partly replaced primary sedimentary and igneous textures. The diagnostic mineral associations are:

Siltstone: albite + quartz + dolomite + rutile ± calcite ± biotite

Lamprophyre: albite + quartz + muscovite + dolomite + rutile + apatite ± biotite.

4-5. **Intensively albitized** and **moderately** or **intensively carbonated zones** roughly overlap each other. The alteration has advanced further in these zones as compared to weakly albitized and carbonated zones: albite, quartz and carbonate replaced all other minerals ex-

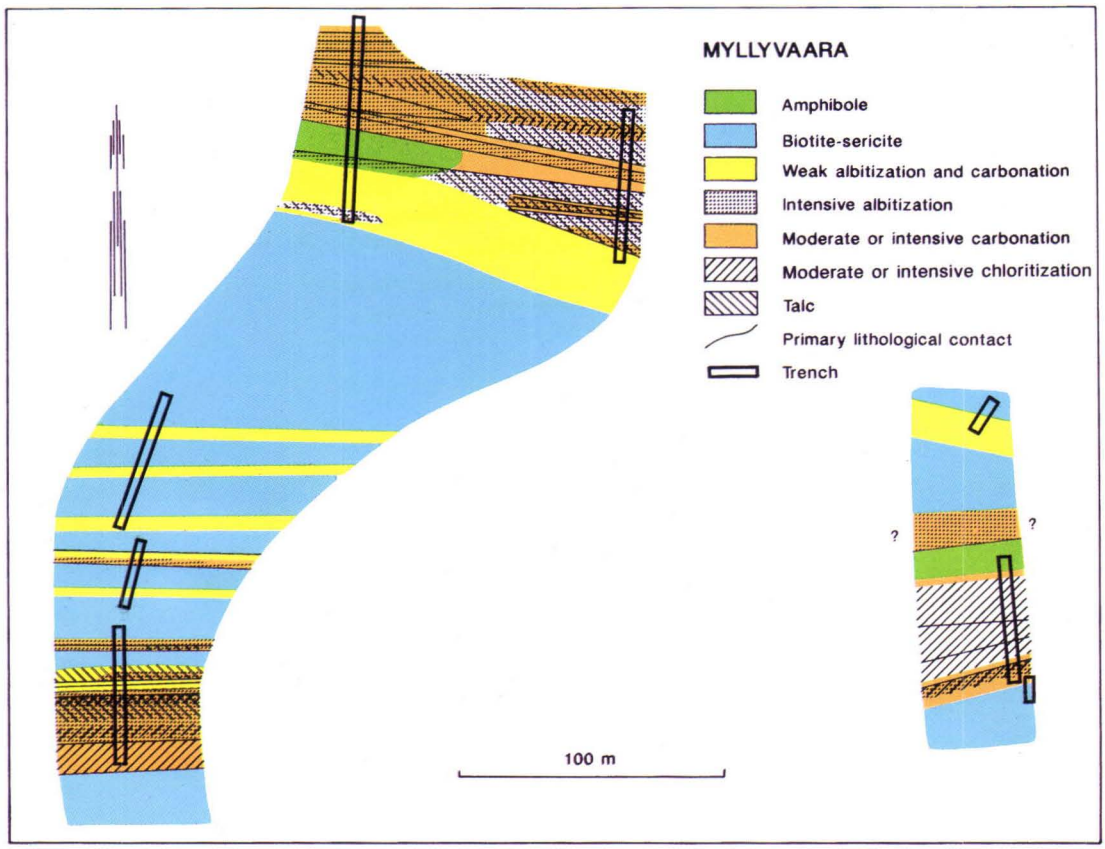

Fig. 11. Alteration types at Myllyvaara.

cept rutile and zircon (Figs. 3G and 3H). The brecciation was intensive. The fractures are filled with quartz, carbonate and albite. In the most intensively altered zones (in siltstone and conglomerate), albite formed idioblastic crystals (Fig. 3G) and the SiO_2 release from carbonated silicates was so intensive that quartz occurs, both in fractures and as 5-10 mm wide poikiloblasts. The textures have completely turned granoblastic; in lamprophyres, the Ti-rich inclusions, which have been altered to rutile, are the only traces left of biotite phenocrysts, still showing the form of the primary phenocrysts. Regardless of the original rock type, igneous or sedimentary, the dominating mineral association is:

albite + dolomite + quartz + rutile.

6. **Chloritization** (Fig. 3I) and **talc formation** (Fig. 3H) were contemporaneous during the latest alteration stage at Myllyvaara. Late chloritization took place in most of the lithological units, but talc formation only in the most albitized and carbonated zones of siltstones and conglomerates. In both cases, carbonate was replaced in an equal manner: as crystals of equal size and beginning from the crystal boundaries of carbonate. Chlorite also replaced amphibole, biotite, sericite and amphibole; and talc also replaced albite. In some lamprophyre dykes chlorite replaced all the other Fe-Mg silicates (Fig. 3I). Weak brecciation is related to the alteration stage and frac-

tures were filled with either chlorite or talc (Fig. 3H).The mineral associations related to chloritization and talc formation are:

Lamprophyre: albite + chlorite + magnetite + rutile + apatite

Sediments: albite + chlorite + dolomite + quartz + rutile, and albite + talc + dolomite + quartz + rutile.

Regional metamorphic recrystallization

Regional metamorphic recrystallization is uncommon at Myllyvaara. Metamorphic biotite locally replaced chlorite and early biotite in lamprophyres; nematoblastic actinolite (a very rare case) replaced both early and metamorphic biotite and chlorite in lamprophyres.

Lehtovaara

General structure

The bedrock of the Lehtovaara area consists of Middle Lapponian quartzite and albite diabase (Fig. 12). The radiometric age determinations of the diabase have failed to give accurate results, although they point to an age of approx. 2.2 Ga (Kallio 1980). The texture and the chemical composition of the albite diabase also highly resemble those albite diabases that occur in adjacent areas and have a U-Pb zircon age of 2.2 Ga (Lehtonen et al. 1992). During the field survey, a zone of altered mafic rock was found in an excavated trench. The rock was not immediately identified as a lamprophyre dyke and the trench was refilled before the thin section and chemical identification were made. For this reason, the unexposed diabase-lamprophyre contact was not searched for, and the age relationship between diabase and lamprophyre

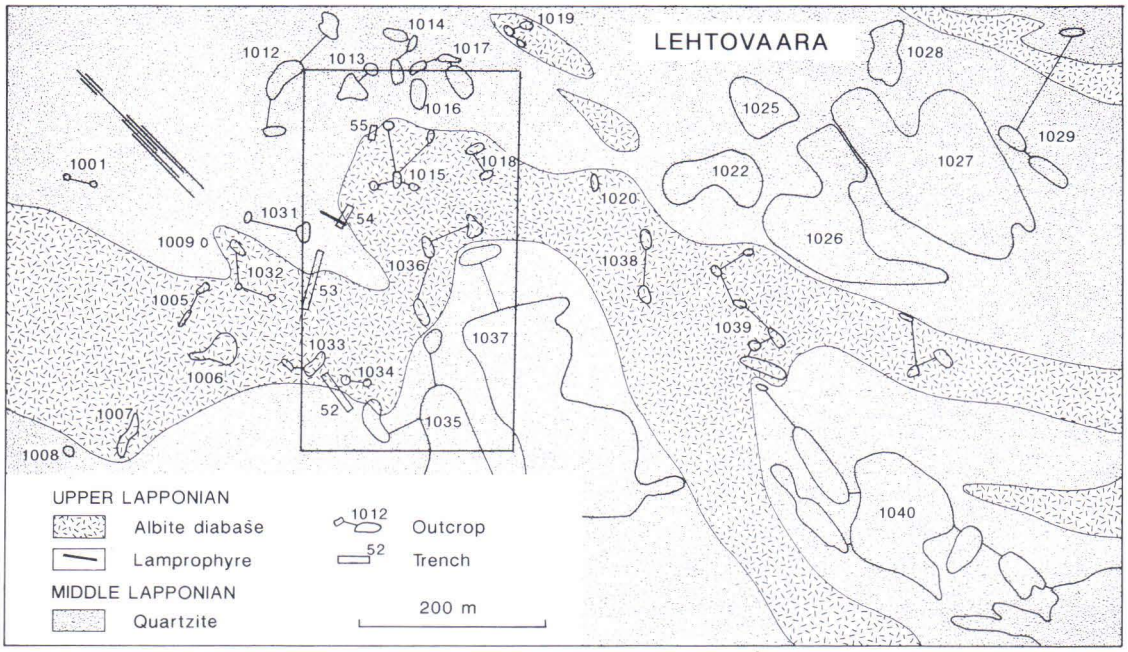

Fig. 12. Geology of the Lehtovaara site, chiefly based on outcrops and geophysical surveys. Only a few short trenches were excavated. Also the outrop and trench numbers are shown. The area has previously been described by Lehtonen and Manninen (1986) and Lehtonen (1987). The central part of the site shown in Figure 15, is outlined.

is yet to be solved.

The quartzite is layered, but no cross bedding or any other textures indicating the stratigraphic top were found. The regional structure indicates that the stratigraphic top is to the north or north-east (Lehtonen et al. 1984).

Brittle deformation dominates at Lehtovaara, but the brecciation is not intense. The rocks are mostly unfractured and the fracturing is intense only in the narrow contact zone between quartzite and diabase. No faults were found. After the brittle phases, weak ductile deformation has taken place, indicated by granoblastic texture and weak foliation in quartzite.

Albite diabase

Chemically, the albite diabase of Lehtovaara is a subalkaline Fe tholeiite (Figs. 13 and 14) and analogously to the Eksymäselkä diabase (Fig. 3A) the texture is dominantly intergranular. At Lehtovaara, the dominant mineral association is amphibole-bearing, which is the most significant difference as compared to Eksymäselkä. The following mineral association is typical of the least altered albite diabase of Lehtovaara:

albite + tremolite-actinolite + epidote + magnetite ± sphene.

Lamprophyre

The width of the dyke is 2 m, but the length is unknown. Petrographically and chemically the rock resembles the calc-alkaline lamprophyres of Myllyvaara (Fig. 9, p 27) and differs

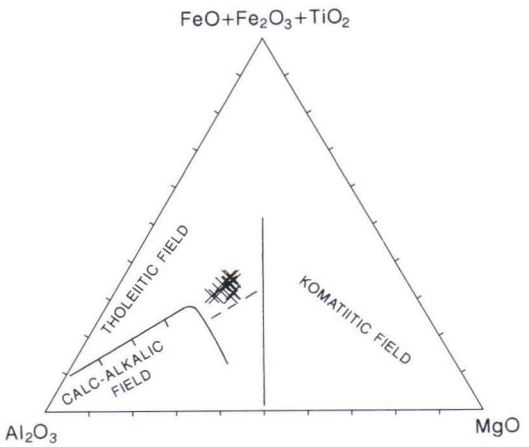

Fig. 13. Albite diabase from Lehtovaara on the Jensen cation plot diagram (Jensen 1976).

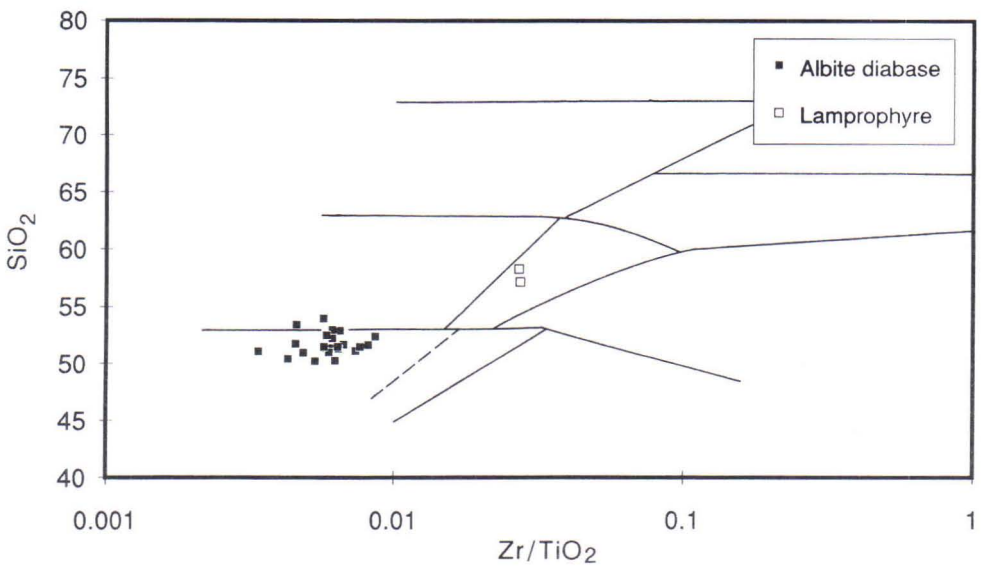

Fig. 14. SiO_2-Zr/TiO_2 diagram for albite diabase and lamprophyre from Lehtovaara. Fields as in Figure 6, after Winchester and Floyd (1977). SiO_2 was recalculated on volatile-free basis.

from the tholeiitic albite diabase (Fig. 14). Its texture is biotite-phyric, trachytoidal and amygdaloidal with quartz amygdales of 3-5 mm in size. The size of the phenocrysts is 0.5-1 mm. Because the dyke is in a carbonated zone, the mineral association is the following, even in its least altered parts:

albite + biotite + chlorite + carbonate + rutile + apatite.

Quartzite

The texture of the quartzite is mainly granoblastic, layered and locally foliated. However, a blastoclastic texture with recrystallized clasts can still be identified. The clasts are dominantly quartz, but albite account for 0-10 vol. % and clasts of K feldspar for 0-3 vol. %. The matrix is completely recrystallized, consisting of albite, quartz and sericite, locally also of biotite. Some beds do not contain feldspar, and the rock is then a pure sericite quartzite.

Alteration types

On the basis of the occurrence and replacement relationships of secondary minerals, seven alteration types can be distinguished (Fig. 15). In the albite diabase these types are amphibole, chlorite, biotite, carbonate and sericite alteration. In the quartzite, only moderate albitization and intensive albitization + carbonation were identified. The lamprophyre is completely in a carbonated area. The chemical composition of the lithological units in different alteration zones and alteration zone combinations is presented in Tables 10-12 (pp. 68-70).

1. **Moderate albitization** of quartzite is probably the earliest alteration at Lehtovaara. It covers the whole quartzite area except the rare non-feldspathic layers, and thus it is not hatched in Figure 15. Albite has completely replaced primary plagioclase and nearly completely replaced K feldspar in the matrix and in the clasts. Some partially albitized K-feldspar clasts are left at the eastern flank of the area studied. Most of the completely albitized clasts consist of one crystal, but clasts consisting of aggregates of very fine-grained albite crystals are not uncommon. Irregular, very weak carbonation (≤0.2 vol. % carbonate) is related to the moderate albitization.

2. **Intensively albitized** and **weakly carbonated** quartzite occurs in three <3 m wide zones at Lehtovaara. Two of the zones form the contact with the albite diabase and the third one

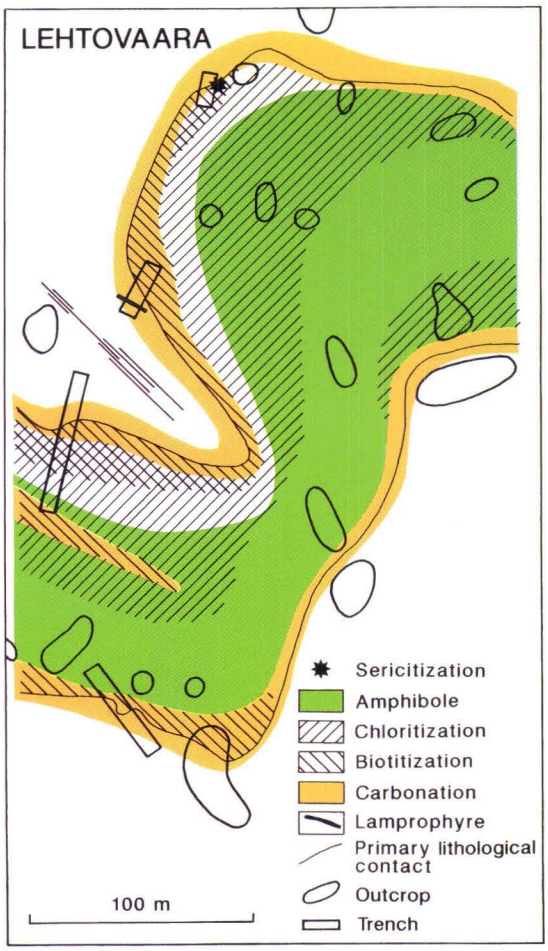

Fig. 15. Alteration types in the central part of the Lehtovaara site. The unhatched areas consist of moderately albitized quartzite.

(outside the area shown in Fig. 15) roughly follows the strike of the contact. Within these zones, albite has completely replaced the primary sericite. The rock texture does not, however, differ from that of the moderately albitized type.

3. The **amphibole zone** forms the least altered, inner part of the albite diabase. The texture and mineral association of this zone are described above, in the general description of the albite diabase. The mineral assemblage was formed when tremolite-actinolite replaced primary Mg-Fe silicates and albite + epidote replaced the primary plagioclase. The primary texture is unaltered, only weakly brecciated. The fractures are filled with epidote and quartz.

4. The amphibole zone gradually changes into a **chlorite zone** as chlorite replaces amphibole and primary Mg-Fe silicates. In places, chlorite has also replaced epidote. During chloritization, weak silicification took place. The mineral association resembles the hyalospilite of Cann (1969) only in the most chloritized zones. The dominating mineral association in the chloritized zones is:

albite + chlorite + epidote + magnetite + sphene + quartz.

The rock is brecciated, but the primary igneous textures are, however, identifiable in most places. Only where the rock is intensively brecciated, the texture is granoblastic. The fractures are mostly filled with chlorite and quartz, but locally also with pyrite.

5. **Biotite** has gradually replaced all chlorite and epidote in the diabase margins and in one fracture zone in the diabase interior. Brecciation is intensive and fractures are filled with biotite, quartz and magnetite. The dominating mineral association is:

albite + biotite + quartz + magnetite.

6. Significant **carbonation** (>2 vol. % carbonate) has only taken place near the quartzite-diabase contact, where carbonate has completely replaced epidote, sphene and chlorite and partially biotite and albite in the diabase. The intensively carbonated diabase has a granoblastic, moderately brecciated texture. The fractures are filled with carbonate, biotite and pyrite. The typical mineral association of carbonated diabase is:

albite + carbonate + biotite + quartz + rutile.

The lamprophyre is completely in a carbonated zone. With proceeding carbonation its mineral association was altered to: albite + quartz + carbonate + rutile. The trachytoidal texture was altered to granoblastic, but the porphyritic texture is left because the biotite phenocrysts were altered to pseudomorphic carbonate-quartz-rutile aggregates.

7. **Sericitization** was the latest alteration stage. It has been found at one site only (Fig. 15), in highly carbonated diabase. In some cases, weak chloritization of carbonates has taken place instead of sericitization. No fracturing is related to this alteration type. Sericite has replaced biotite, albite and carbonate, forming the mineral association:

albite + sericite + carbonate + quartz + rutile ± biotite.

Regional metamorphic recrystallization

Regional metamorphic recrystallization has affected the whole area studied. Actinolitic hornblende has partially replaced tremolite-actinolite and chlorite in the amphibole zone (Fig. 3J), epidote and biotite have replaced chlorite in the chlorite zones and metamorphic biotite replaced carbonate and early biotite in the carbonate and biotite zones in albite diabase. Porphyroblastic muscovite and biotite have replaced recrystallized matrix sericite in quartzite.

Sivakkavaara

General structure

The study site (Fig. 16), previously described by Lehtonen (1987), is a cross section of a 200-300 m wide zone of Middle Lapponian sediments and pyroclastites bordered by albite diabase dykes. Several felsic dykes cut the sediments and diabase dykes; the sediments are also cut by a lamprophyre dyke. The age of the albite diabase is 2.214 ± 6 Ga (0.5 km north of the site, zircon age, U-Pb method, Kallio 1980). The age relationship between the lamprophyre and the other dykes is unknown, because their mutual contacts are unexposed; apparently lamprophyre cuts only quartzite on the present level of erosion (Fig. 16).

No textures indicating the top during the intrusion of magmas were found. The sedimentary textures are rather well-preserved: the strike of the bedding is NW-SE and the dip and the stratigraphic top to NE. Hence, the sequence of the sediment-pyroclastite pile is: carbonate rock (oldest), quartzite, tuffite and tuff (youngest).

The deformation was brittle, but the brecciation is predominantly weak. Intensive brecciation is found only within 2 m from the dyke contacts and within a few zones 1-2 m wide in quartzite and albite diabase dykes.

Albite diabase

The albite diabase dykes at Sivakkavaara are transitional between Fe and Mg tholeiites (Fig. 17) and subalkaline (Fig. 18). Their primary texture is intergranular. The characteristic min-

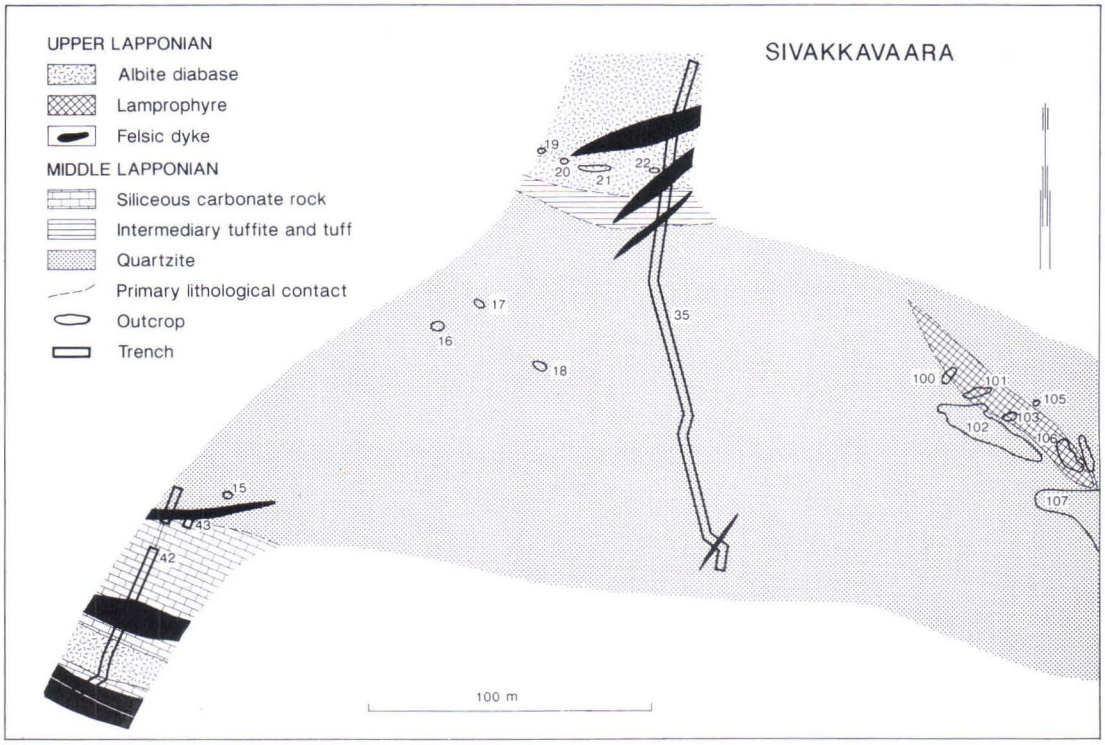

Fig. 16. Geology of the Sivakkavaara site based on outcrops, excavated trenches and geophysical surveys. Also the outrop and trench numbers are shown.

eral association of the least altered albite diabase dykes closely resembles the amphibole zones of the albite diabases at Eksymäselkä and Lehtovaara:

albite + tremolite-actinolite + chlorite + epidote + magnetite ± biotite.

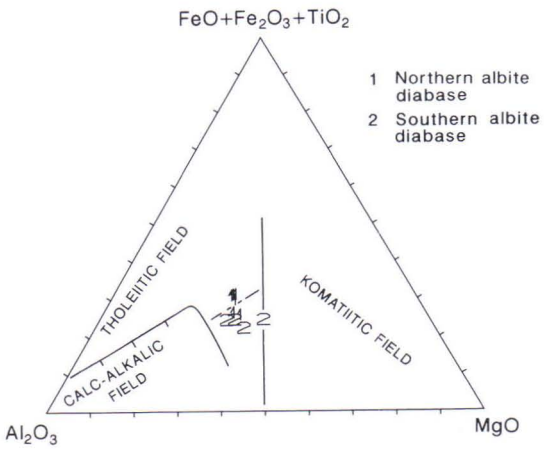

Fig. 17. Albite diabases from the Sivakkavaara area on the Jensen cation plot diagram (Jensen 1976).

Lamprophyre

The Sivakkavaara lamprophyre differs from the lamprophyres of both Myllyvaara and Lehtovaara. According to the Sc/Ta vs. Cr/V diagram, it is calc-alkaline (Fig. 9, p. 27), but clearly more mafic than the Lehtovaara lamprophyre, and on the SiO_2 vs. Zr/TiO_2 diagram (Fig. 19) it falls between the calc-alkaline and

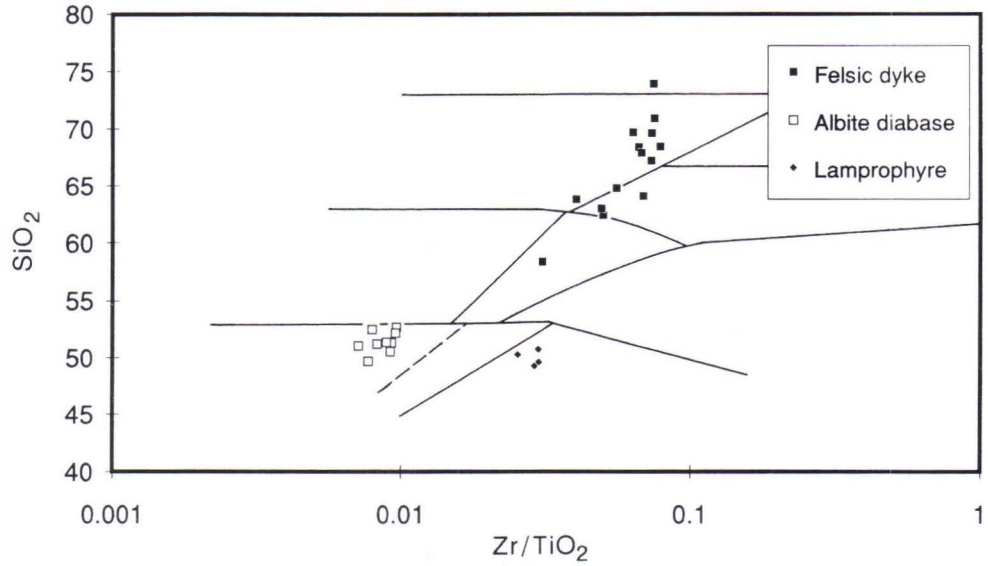

Fig. 18. SiO_2-Zr/TiO_2 diagram for albite diabase, felsic dykes and lamprophyre from Sivakkavaara. Fields as in Figure 6, after Winchester and Floyd (1977). SiO_2 was recalculated on volatile-free basis.

alkaline groups of the Myllyvaara lamprophyres. Petrographically it resembles the Myllyvaara lamprophyres: the primary texture is intergranular or subophitic in the inner parts of the dyke and biotite-phyric and trachytoidal in the dyke margins. The mineral association of the least altered type is:

albite + tremolite-actinolite + biotite + epidote + sphene + apatite.

Felsic dykes

The alteration has been extremely weak in the inner parts of most of the felsic dykes. Among other facts, the good preservation of the

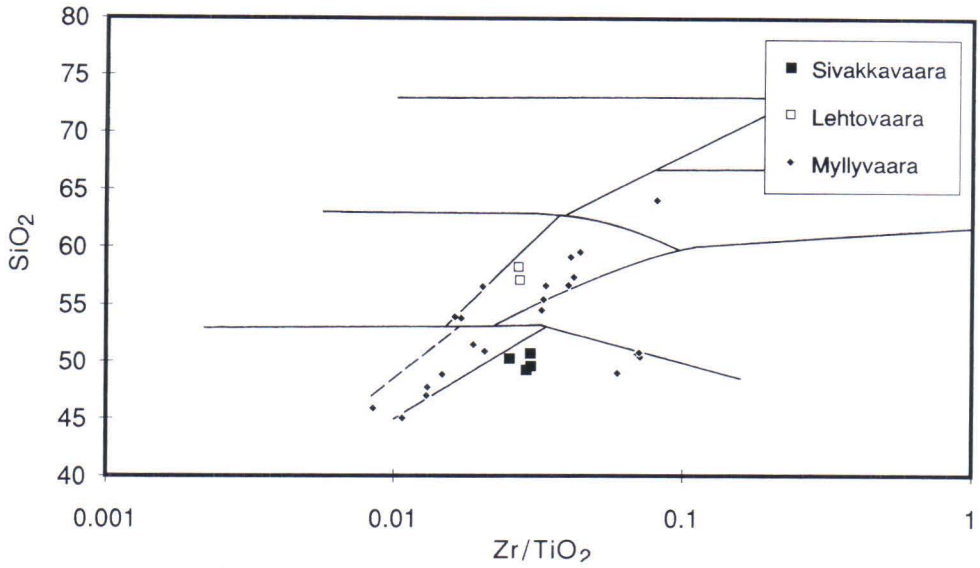

Fig. 19. SiO_2-Zr/TiO_2 diagram for lamprophyres from Sivakkavaara, Myllyvaara and Lehtovaara. Fields as in Figure 6, after Winchester and Floyd (1977). SiO_2 was recalculated on volatile-free basis.

K feldspar makes the use of the R1R2 diagrams (of De la Roche et al. 1980) reliable in the classification of the felsic dykes. The dykes are, according to both the R1R2 diagram (Fig. 20) and the SiO_2 vs. Zr/TiO_2 diagram (Fig. 18), subalkaline or transitional between alkaline and subalkaline type.

The texture of the felsic dykes is porphyritic, with a phenocryst size of 1-5 mm. Phenocrysts in rhyolites and quartz-latites consist of quartz, K feldspar, plagioclase and biotite; in quartz-trachytes of K feldspar and plagioclase; and in trachytes and lati-andesites of K feldspar, plagioclase and biotite. The rhyolites and lati-andesites also contain quartz amygdales with a size of of 1-5 mm. The groundmass, which chiefly consists of feldspars and quartz, is non-oriented and in places its texture is granoblastic. Any primary amphibole or pyroxene has been completely replaced by biotite with epidote, magnetite or sphene.

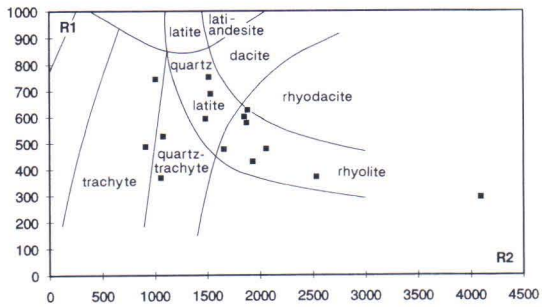

Fig. 20. Felsic dykes from Sivakkavaara on the R1R2 diagram of De la Roche et al. (1980).

Quartzite

The quartzite is blastoclastic, layered and in places cross-bedded. The clasts consist of quartz and albite. The matrix is chiefly albite, but some biotite and sericite is present in equilibrium with albite. No K feldspar was found. Part of the quartz and albite clasts are recrystallized, but the rock is not foliated.

Impure carbonate rock

A zone of banded, dark green rock, some tens of metres wide, probably an impure, sedimen-

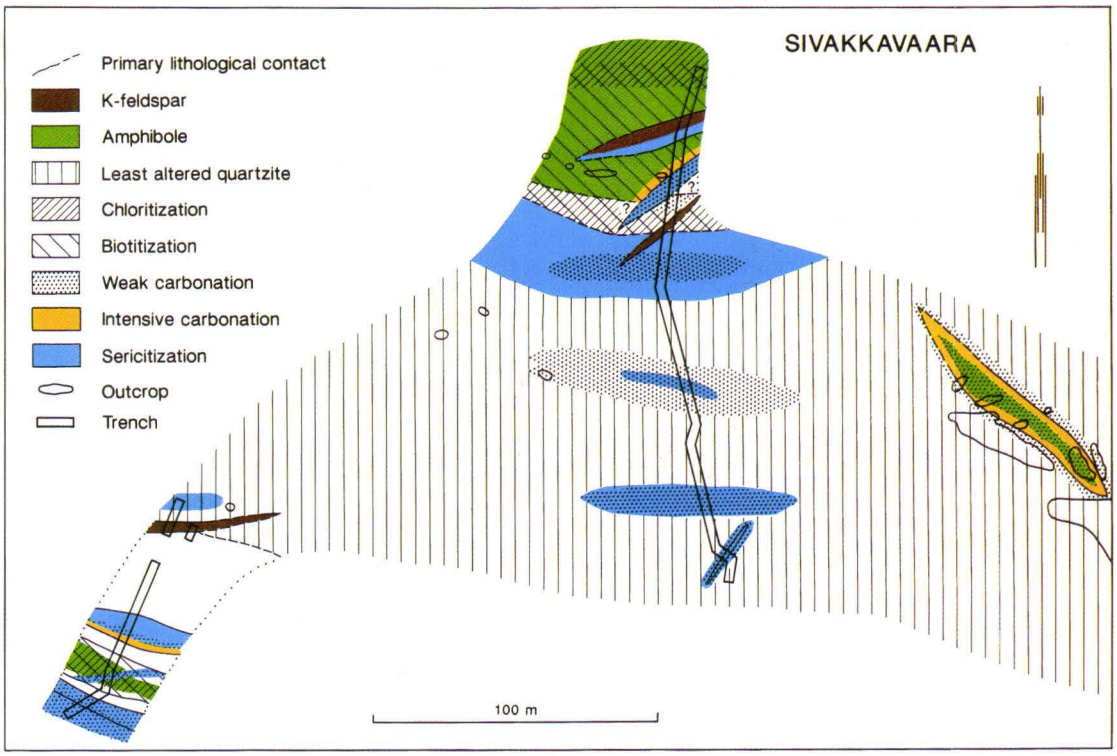

Fig. 21. Alteration types at the Sivakkavaara site. Areas with carbonate rocks are unhatched.

tary carbonate rock, underlies the quartzite in the southern part of the area. According to the regional structural interpretation (M.I. Lehtonen, oral comm. 1992), this rock is the western continuation of a dolomite dominated sedimentary horizon. The main minerals are tremolite (40-80%), calcite (5-20%), phlogopite (0-25%) and epidote (0-30%) and the texture is nematoblastic with porphyroblasts of tremolite and epidote.

Tuffs and tuffites

A bed of banded, intermediate tuff and tuffite, about 20 m in thickness, occurs between the quartzite and the northern albite diabase. The texture of the tuff is lepidoblastic-granoblastic and its main constituents are chlorite, biotite and albite. The texture of the tuffite is granoblastic and blastoclastic with albite and quartz clasts in a biotite-dominated matrix.

Alteration types

Seven alteration types were found at Sivakkavaara (Fig. 21). In the albite diabase dykes the alteration is characterized by amphibole, chlorite, biotite, carbonate and sericite; in the lamprophyre by amphibole, carbonate and sericite; in the felsic dykes by K feldspar, albite, carbonate and sericite; in the quartzite by albite, carbonate and sericite, and in the tuffs and tuffites by biotite + chlorite and albite + carbonate. Possibly due to great primary compositional variation, no obvious alteration types or zonation can be recognized in the carbonate rock. The chemical composition of the lithological units in the varous alteration

zones and alteration zone combinations at Sivakkavaara are presented in Tables 13-16 (pp. 76-79).

1. The character of the weakest alteration and its mineral association follow the lithological units: in albite diabase and lamprophyre they follow the **amphibole zones**, in felsic dykes the **K-feldspar zones**, and in pyroclastites the **chlorite-biotite zone**. The least altered quartzite is **albitized**. The rocks are unbrecciated or slightly brecciated and their primary textures are well preserved. The breccia fractures are filled with albite and quartz, and in the albite diabase also with epidote and chlorite.

2. **Biotite zones** cover most of the albite diabase dykes at Sivakkavaara, but the intensity of biotitization varies widely. It is intensive in the middle parts of the southern diabase dyke and negligible in the northern half of the northern diabase dyke. Biotite has replaced mainly chlorite, but in places also epidote and amphibole. Weak silicification is related to the biotitization of amphibole. The rocks were not fractured during biotitization, but where the degree of alteration was moderate or intensive, the textures partially changed to granoblastic. The mineral association of the thoroughly biotitized albite diabase is:

albite + biotite + quartz + magnetite.

3. Calcite and dolomite tended to replace all the minerals of the alteration zones mentioned earlier, except for quartz and zircon in the **carbonate zones**. The rocks were also weakly silicified and sericitized, and weak or moderate albitization took place in lamprophyre, felsic dykes and tuff. The albitization of the quartzite, however, took place earlier and is not related to carbonation. The carbonation is commonly weak; it is intensive only near some dyke contacts and the alteration is chiefly incomplete. Intensive brecciation is related to all kinds of carbonation. The fractures are filled with carbonate, quartz and biotite. The textures have turned granoblastic in the most intensively altered zones.

4. The latest alteration stage was **sericitization**. Sericite has commonly replaced feldspars and carbonate, in places also biotite and chlorite. In some places, chloritization of carbonates has taken place instead of sericitization. The degree of alteration varied widely, but it was generally low and the replacements partial. Brecciation is frequently related to sericitization; especially the quartzite contains abundant sericite-filled fractures.

Regional metamorphic recrystallization

The regional metamorphic recrystallization was analogous to that of Eksymäselkä and Myllyvaara. Lepidoblastic biotite replaced chlorite, sericite, carbonates and hydrothermal biotite in all rock types. In addition, actinolitic hornblende replaced chlorite and tremolite-actinolite, and epidote replaced chlorite and carbonates in albite diabase. In lamprophyre, actinolitic hornblende replaced only actinolite.

Honkavaara

General structure

The main rock units at the site consist of intermediate tuffite, felsic volcanic rock and albite diabase dykes (Fig. 22). The diabase dykes have intruded in Middle Lapponian (?) tuffites and Archaean felsic volcanic rocks. In addition, mafic lava and heterolithic volcanic breccia occur in the area studied. The U-Pb age of zircon and sphene in the albite diabase is 2.2 Ga. The U-Pb age of zircon in the felsic volcanic rocks is 2.7 Ga, but the age of sphene is 2.2 Ga (Lehtonen et al. 1989, Lehtonen et al. 1992). The results obtained by the Sm-Nd

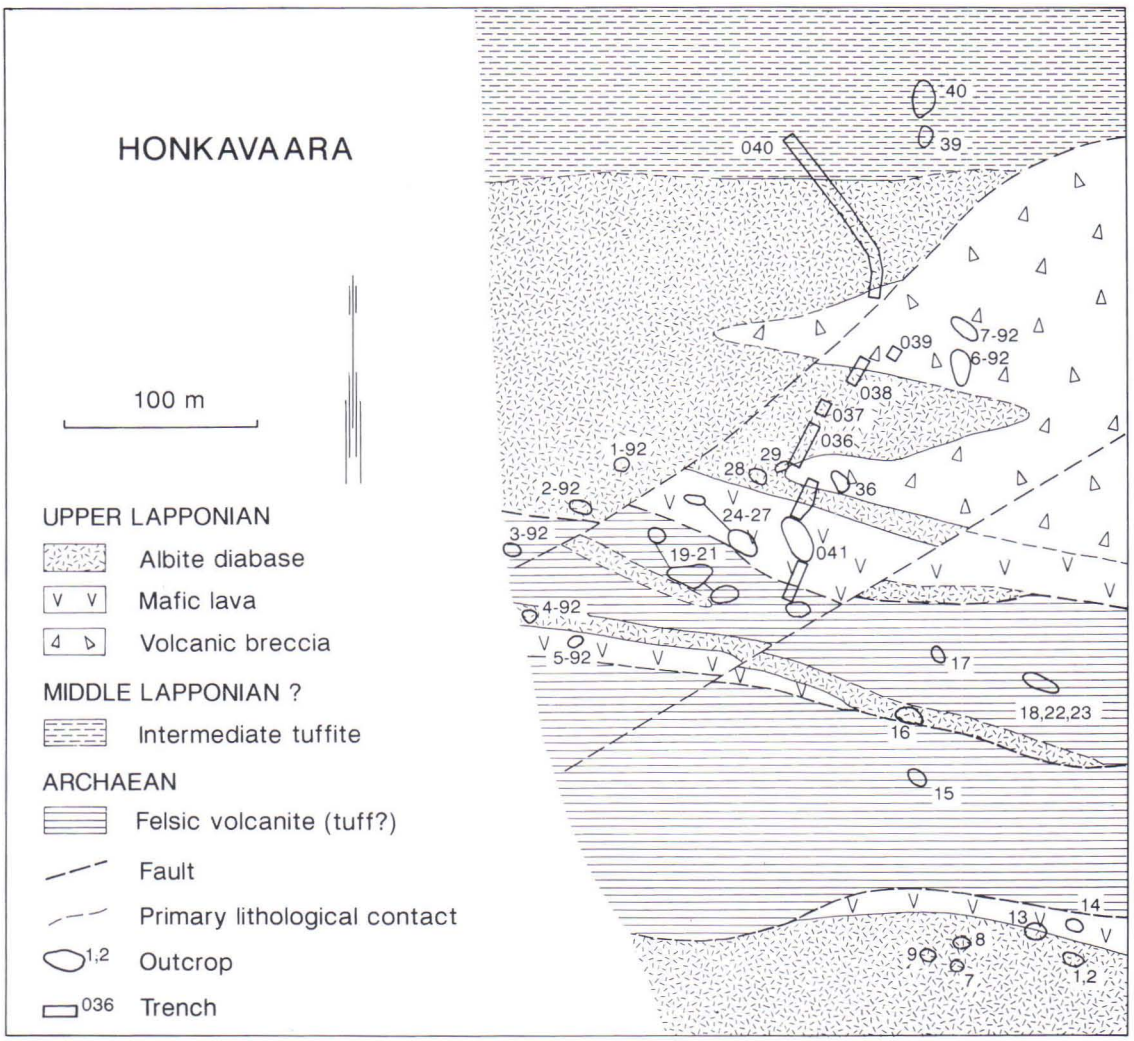

Fig. 22. The geology of the Honkavaara site, previously reviewed by Kallio et al. (1980), Lehtonen (1986) and Lehtonen et al. (1989), based on outcrops, excavated trenches and geophysical surveys. Also the outrop and trench numbers are shown.

method (H. Huhma, oral comm. 1992) support the above-mentioned age determinations. The chemical similarity between albite diabase and mafic lava (see Figs. 23 and 24, Table 17, p. 84) suggests that they may have a comagmatic origin and roughly the same age, i.e., Upper Lapponian.

In the volcanic breccia there are fragments of all rock types occurring at the site, including diabase. The breccia is thus most probably the youngest lithologic unit, although the age difference from diabase and mafic lava need not be large. The bedding of the volcanic breccia is roughly horizontal, so that its wide horizontal extent (Fig. 22) does not neccessarily indicate that the formation is thick.

The general strike of the bedding is E-W, the dip is nearly vertical and the stratigraphic top to the north. The fractionation within the diabase dykes - the most felsic types are at the

southern margins of the dykes - implies that the top was to the south when the dykes intruded in their present surroundings.

Only brittle deformation was observed and the brecciation is of variable intensity. It is most intensive near the contacts of the albite diabase dykes. In addition, 0.5-5 m wide breccia zones with strikes E-W, NW-SE and SW-NE can be found in all lithological units. According to magnetic ground surveys, two SW-NE faults intersect the area studied (Fig. 22).

Mafic lava

The mafic lava is transitional between Fe and Mg tholeiites (Fig. 23). On the SiO_2 vs. Zr/TiO_2 diagram (Fig. 24) the lava is in the subalkalic field, in the same region as the least altered albite diabase. The primary texture of the lava is massive and porphyritic. Phenocrysts, mostly albite (originally plagioclase), but in places also actinolite (originally clinopyroxene), make up 10-35 vol. %. The groundmass consists of very fine-grained albite, actinolite and chlorite. The dominant mineral association is:

albite + tremolite-actinolite + magnetite ± chlorite.

Albite diabase

The albite diabase is Fe tholeiite (Fig. 23) and is situated in the subalkalic field of the SiO_2 vs. Zr/TiO_2 diagram (Fig. 24). The field locations of fine-grained margins and cumulate types implies that all the wide albite diabase units in the geological map (Fig. 22) are actually composed of several parallel dykes.

The texture of the least altered diabase is intergranular or subophitic. The primary tex-

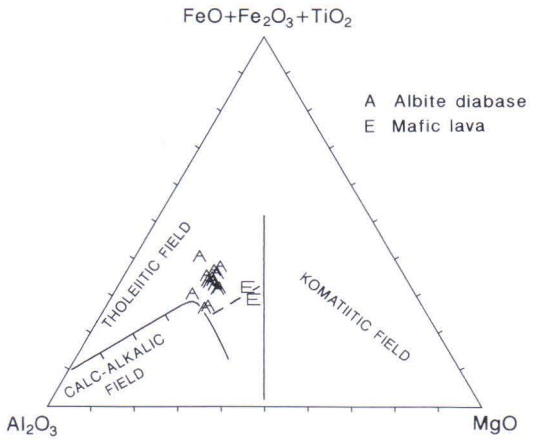

Fig. 23. Mafic lava and albite diabase from Honkavaara on the Jensen cation plot diagram (Jensen 1976).

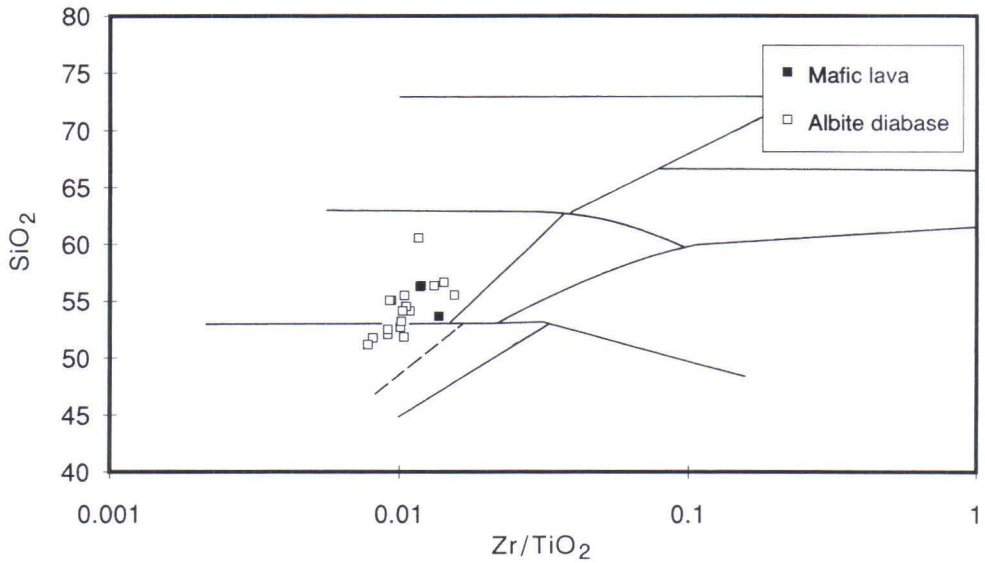

Fig. 24. SiO_2-Zr/TiO_2 diagram for mafic lava and albite diabase and from Honkavaara. Fields as in Figure 6, after Winchester and Floyd (1977). SiO_2 was recalculated on volatile-free basis.

ture is commonly well-preserved in the normal, mafic type, but only moderately preserved in the intermediate, plagioclase-rich type. The mineral association of the least altered albite diabase is:

albite + tremolite-actinolite + epidote + magnetite + sphene ± biotite.

Felsic volcanic rocks

The felsic volcanic rocks are banded and granoblastic, most probably tuff or tuffite, although indicative primary textures are rare. The grain size of the rocks is <0.05 mm. In the least altered zones the dominant mineral association is:

albite + quartz + tremolite-actinolite + magnetite + sphene.

Tuffites and sediments

The northern part of the area studied is composed of banded and granoblastic, intermediate tuffite with 1-2 m thick sediment interlayers. The main constituent of the sediment beds is a blastoclastic quartzite. The mineral associations of the least altered types are:

Tuffite: quartz + albite + haematite + rutile
Quartzite: quartz + albite.

Volcanic breccia

The structure of the volcanic breccia is chaotic. Layering and grading are rarely found in the outcrops and never in normal sample size (sample diameter <20 cm). The fragments range in size from a few millimetres to approx. 50 cm and they are always angular with a rough surface. The chaotic, matrix-supported texture and the high angularity of the fragments imply deposition after short, lahar-like transport (Lehtonen et al. 1989). Most of the fragments are bleached (albitized and carbonated) and their composition is, usually regardless of their origin, albite + quartz ± carbonate. The matrix is composed of albite, quartz and carbonate with sericite and chlorite in places.

Alteration types

Seven alteration types were observed at Honkavaara (Fig. 25). In the albite diabase dykes the alteration is characterized by amphibole, epidote, chlorite, biotite, carbonate and sericite; in the mafic lava by amphibole, chlorite and carbonate; in the felsic volcanic rocks by amphibole, carbonate and sericite; and in the tuffites by albite, chlorite, carbonate and sericite. Quartzite occurs only in the least altered, albitized zone of the tuffite-sediment area. Intensive carbonation and weak sericitization cover the whole volcanic breccia. The chemical composition of the lithological units in different alteration zones and alteration zone combinations is shown in Tables 17-19 (pp. 84-87).

1. The weakest alteration type and its mineral association follow the lithological units. In albite diabase, mafic lava and felsic volcanic rock it is represented by the **amphibole zones**. The least altered types of tuffite and quartzite are **moderately albitized**: albite has replaced all Ca plagioclase, K feldspar and sericite. In the volcanic breccia, no weakly altered zone are to be found.

Albite is the only feldspar present and actinolite has completely replaced the primary Mg-Fe silicates (olivine and pyroxene) as in Figure 3A. The rocks are unbrecciated or only weakly brecciated and the primary textures are well preserved, except in the felsic volcanic rock, which is nematoblastic-granoblastic. Fractures are commonly filled with albite and quartz, in the albite diabase also by epidote and amphibole.

2. Intensive **epidotization** has taken place in a few places in the albite diabase, within the amphibole zones. The epidotized zones are 1-2 m wide and contain epidote-dominated spots with a diameter of 1-50 cm. Within these spots, epidote has nearly completely replaced plagioclase. In addition, weak or moderate apatite formation was related to the epidotization.

3. Chlorite has replaced primary Mg-Fe silicates (olivine and pyroxene) and secondary

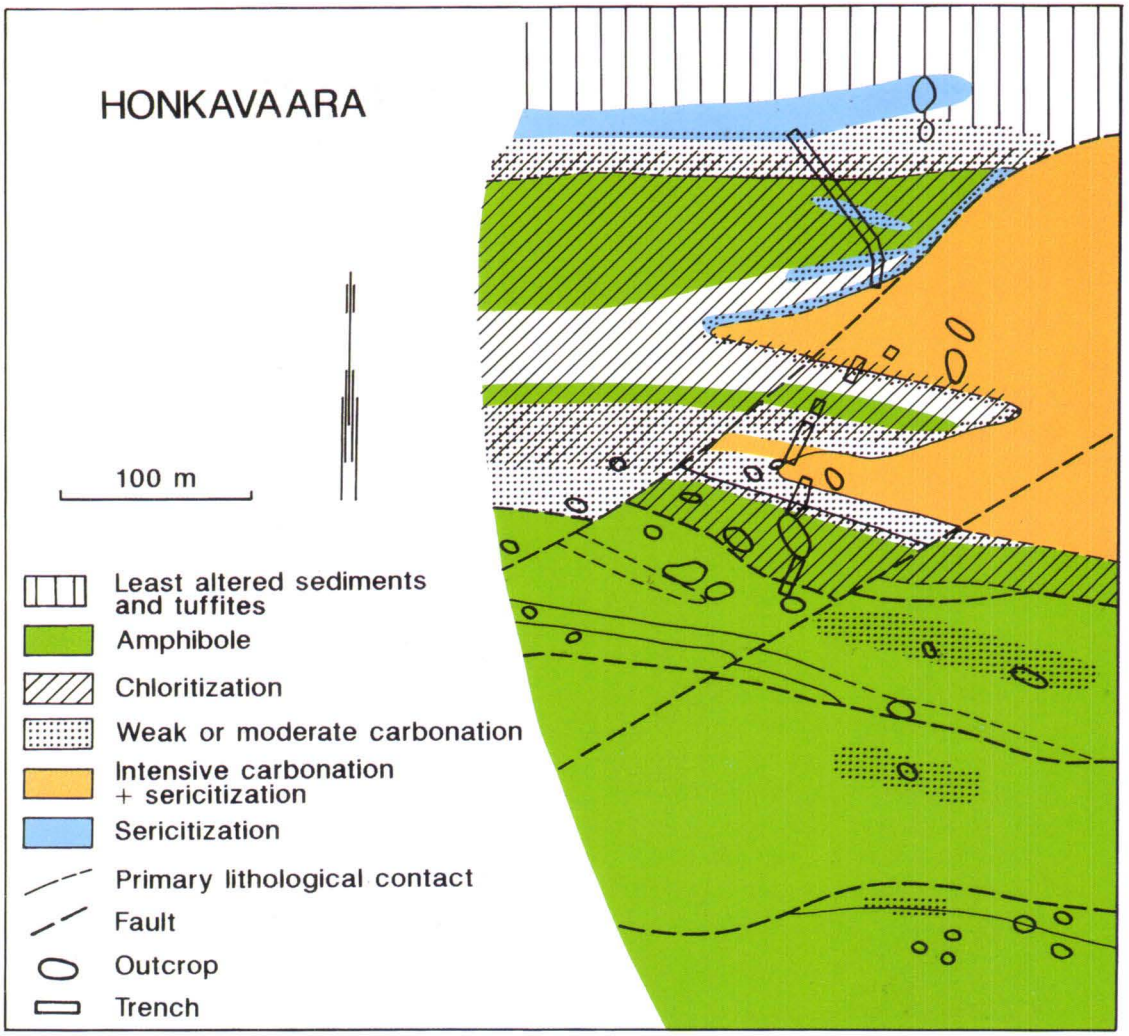

Fig. 25. Alteration types at the Honkavaara site. Amphibole, chlorite, carbonate and sericite zones wider than 5 metres are shown. Biotitization has taken place only in albite diabase and roughly covers the chloritized zones.

minerals in connection with the formation of the amphibole zone (tremolite-actinolite, epidote and albite) in the **chloritized zones**. The mineral associations of the mafic rocks are intermediate between orthospilite and hyalospilite types (Cann 1969), because they contain both amphibole and chlorite. In addition, the chloritization of diabase and tuffite is everywhere overlapped by weak biotitization and locally by weak carbonation. The typical mineral associations of the chlorite zones are:

Albite diabase: albite + chlorite + biotite + magnetite + sphene ± tremolite-actinolite ± quartz ± epidote

Mafic lava: albite + chlorite + tremolite-actinolite + magnetite

Tuffite: albite + quartz + chlorite + biotite + carbonate + magnetite.

The rock textures did not significantly change during chloritization. The degree of brecciation is slight in diabase dykes and lava units and intensive in tuffite. Fractures are filled with chlorite and small amounts of pyrite and chalcopyrite.

4. In the **biotitized zones**, biotite has replaced chiefly chlorite, and locally also epidote. The degree of alteration is generally low. Moderately or intensively biotitized zones are scarce and narrow (<1 m) with unaltered rock texture.

5. **Carbonation** has taken place in all rock types. The alteration is slight, and so only the most important zones are shown in Figure 25. Carbonates have replaced all minerals except quartz, rutile and zircon. Weak silicification was related to these replacements. The primary textures and pre-carbonation mineralogies are easily identified in weakly and moderately carbonated zones, but in intensively altered zones, i.e. in the volcanic breccia and some zones in the albite diabase dykes, the texture is granoblastic and the identification of primary textures difficult. The fractures related to carbonation are filled with quartz and carbonates. In the intensively carbonated zones, the dominating mineral association is, regardless of the original rock type:

albite + carbonate + quartz + rutile.

6. **Sericitization** was the latest alteration stage in the Honkavaara area. Sericite partially replaced albite and carbonates, in places also biotite and chlorite. In some cases, carbonate was altered to chlorite or talc instead of sericite. Weak brecciation is related to the sericitization and fractures are commonly filled with sericite, in some cases also with chlorite or talc. The degree of alteration is normally low; moderate or intensive sericitization has taken place only in albite diabase and tuffite and is indicated by the following mineral association:

albite + sericite + quartz + magnetite.

Regional metamorphic recrystallization

In the Honkavaara area, the rocks partially recrystallized during the regional metamorphism. Lepidoblastic biotite replaced chlorite, carbonates and early biotite; nematoblastic actinolitic hornblende replaced tremolite-actinolite and chlorite; and granoblastic epidote replaced chlorite. Metamorphic biotite, epidote and amphibole were, however, formed only where biotite, epidote and amphibole existed before the regional metamorphism.

Isolaki

General structure

The northern part of the Isolaki area consists of conglomerate and the southern part of quartzite. Between the conglomerate and the quartzite of the Kumpu unit of the CLGB there is a lump of albite diabase, 40 x 100 m in size (Fig. 26). The U-Pb age of zircon and sphene in the albite diabase is 2.210 Ga (Lehtonen 1987). The Pb-Pb age of detrital zircon in quartzite ranges from 1.913 to 1.99 Ga (Lehtonen 1987, Lehtonen et al., in prep.). The diabase is thus of Upper Lapponian age and is older than its country rocks. This age relationship is also supported by the occurrence of diabase fragments in the conglomerate, near its contact with the diabase.

The albite diabase can be either allochthonous, i.e., tectonically transported to its site, or an erosion remnant (like a small butte) and the sediments later deposited around and above it. Only brittle deformation has been observed at Isolaki. The diabase and its contacts are fractured, a feature that supports the tectonic hy-

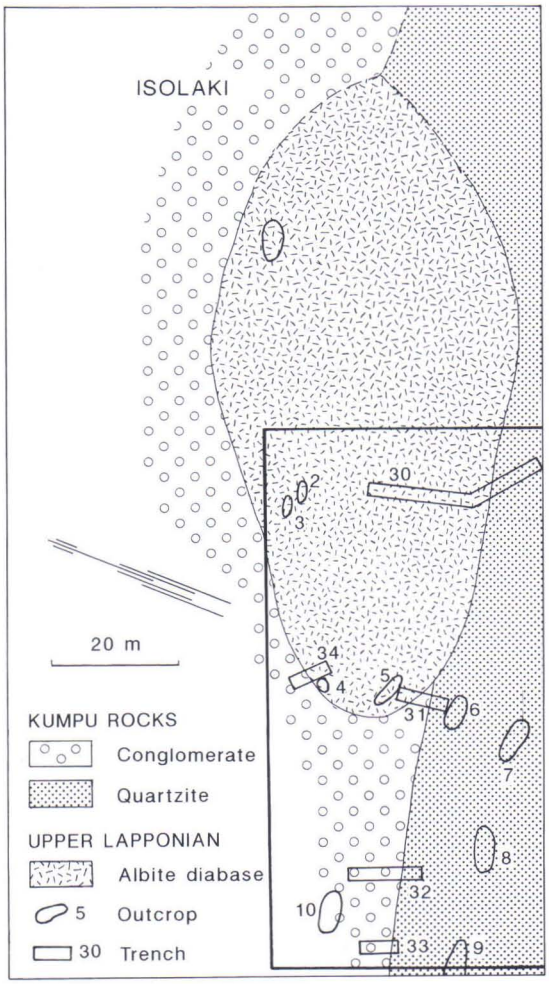

Fig. 26. Geology of the Isolaki site with outcrop and trench numbers. The map is based on outcrops, excavated trenches and geophysical surveys. The area studied and its vicinity has been described previously by Kallio et al. (1980), Lehtonen and Manninen (1986), Lehtonen (1987), and Nikula (1988). The area covered by Figure 29 is outlined.

pothesis. On the other hand, the fracturing may well have taken place later, during regional deformation, because weak fracturing also occurs in the contact zone between conglomerate and quartzite. In any case, some fracturing of the diabase probably took place at an early stage in connection with the synmagmatic spilitic alteration.

The primary textures of the sediments are well preserved. The strike is E-W, the dip is to the south and the stratigraphic top to the north. According to a palaeoenvironmental survey (Nikula 1988), the quartzite is a braided-river deposit of the distal part of an alluvial fan or an alluvial plain deposit, while the conglomerate is a debris flow deposit accumulated in the proximal part of an alluvial fan.

Albite diabase

The albite diabase is a subalkaline Fe tholeiite and its northern and middle parts were originally pyroxene cumulate (Figs. 27 and 28). The primary ophitic and cumulus textures are well preserved. Only near the contacts, in a 1-3 m wide zone, the texture is highly fractured and granoblastic. The mineral association of the least altered type (the dominant association of the diabase) is:

albite + tremolite-actinolite + epidote + magnetite + sphene.

Conglomerate and quartzite

The quartzite is blastoclastic, layered and cross-bedded. Quartz clasts dominate and albite clasts occur only near the diabase contact. The matrix is composed of sericite and quartz. This lack of albite except in the most altered zone is the most significant mineralogical dif-

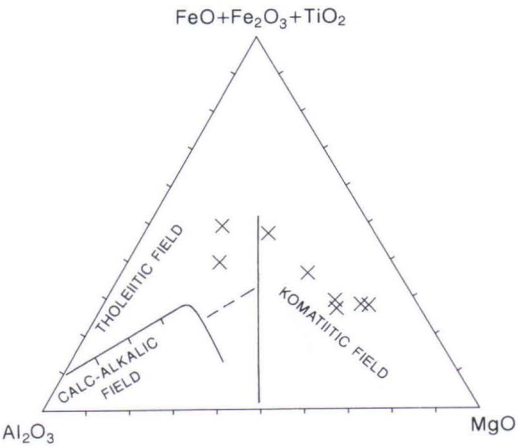

Fig. 27. Albite diabase from Isolaki on the Jensen cation plot diagram (Jensen 1976). Pyroxene cumulates are on the komatiitic side of the diagram.

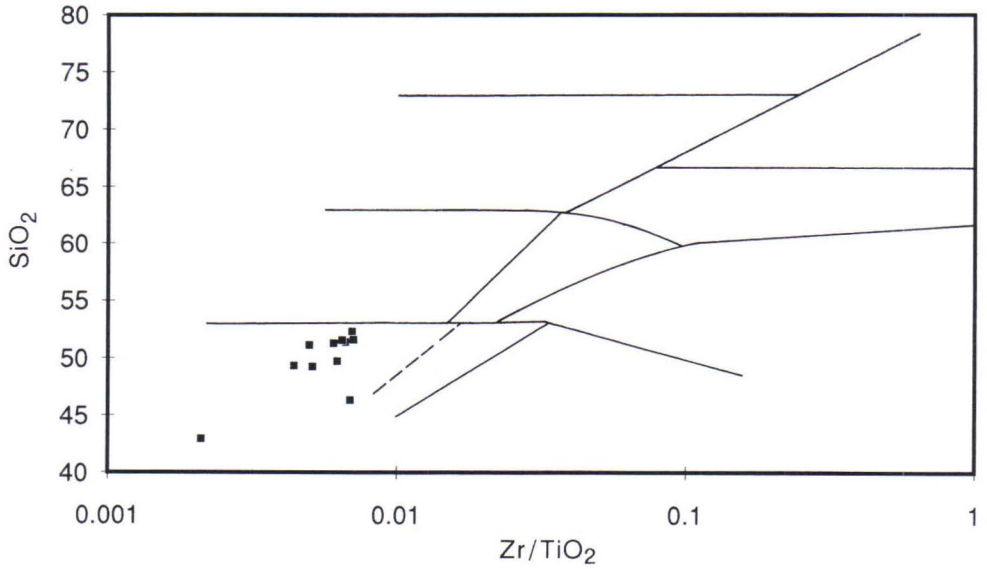

Fig. 28. SiO_2-Zr/TiO_2 diagram for albite diabase from Isolaki. Fields as in Figure 6, after Winchester and Floyd (1977). SiO_2 was recalculated on volatile-free basis.

ference between the quartzites of Isolaki (Kumpu quartzite) and the quartzites of the other sites (Lapponian quartzites). The conglomerate is blastoclastic, matrix-supported and massive or crudely bedded. It comprises clasts of quartz, phyllite, tuffite and albite diabase in a matrix of sericite-quartz-carbonate.

Alteration types

Six alteration types can be distinguished on the basis of the occurrence and replacement relationships of the secondary minerals (Fig. 29). The alteration in the albite diabase is characterized by amphibole, chlorite, biotite, carbonate and sericite (Tables 20 and 22, p. 90 and 91). In the quartzite and conglomerate, only albite-carbonate alteration was identified (Table 21, p. 91).

1. Most of the albite diabase is included in the **amphibole zone**, which is described above, in the general description of the diabase. The rock is moderately brecciated and the fractures are filled with tremolite-actinolite, epidote, albite and quartz.

2. The amphibole zone changes gradually into the **chlorite zone**. Chlorite replaces amphibole and epidote and the primary Mg-Fe silicates (olivine and pyroxene). Weak silicification is related to the chloritization. The most chloritized zones, where amphibole and epidote are totally replaced, are overlapped by biotitization. The mineral associations of the chloritized zones are:

albite + chlorite + tremolite-actinolite + epidote + magnetite + sphene + quartz and

albite + chlorite + biotite + magnetite + sphene + quartz.

The diabase is considerably more brecciated in the chloritized zones than in the amphibole zone and its texture is in places completely granoblastic. Fractures are filled with chlorite, quartz and biotite, in some places with pyrite and chalcopyrite, too.

3. The diabase margins are **biotitized**. Biotite has replaced chlorite at the southern margin and amphibole at the NW margin. The brecciation varies from weak (NW margin) to inten-

sive (S margin). The fractures are filled with biotite, quartz and pyrite. The diagnostic mineral association of the biotitized diabase is:

albite + biotite + quartz + magnetite.

4-6. Significant **carbonation** has taken place only in the contact zones diabase-sediment and quartzite-conglomerate and within 1-2 m wide zones in the diabase interior (Fig. 29). Carbonate has completely replaced epidote, chlorite and biotite and partially albite in the diabase. **Intensive albitization** is related only to the carbonation in quartzite and conglomerate. In addition, plagioclase is weakly **sericitized** at the diabase margins where the degree of carbonation is most intensive. The typical mineral composition of carbonated albite diabase is:

albite + carbonate + quartz + magnetite ± sericite.

The texture of intensively carbonated rocks is granoblastic. The rocks are brecciated and the fractures are filled with quartz, carbonate and pyrite.

Regional metamorphic recrystallization

No recrystallization related to regional metamorphism was found by investigation of thin sections from the Isolaki samples.

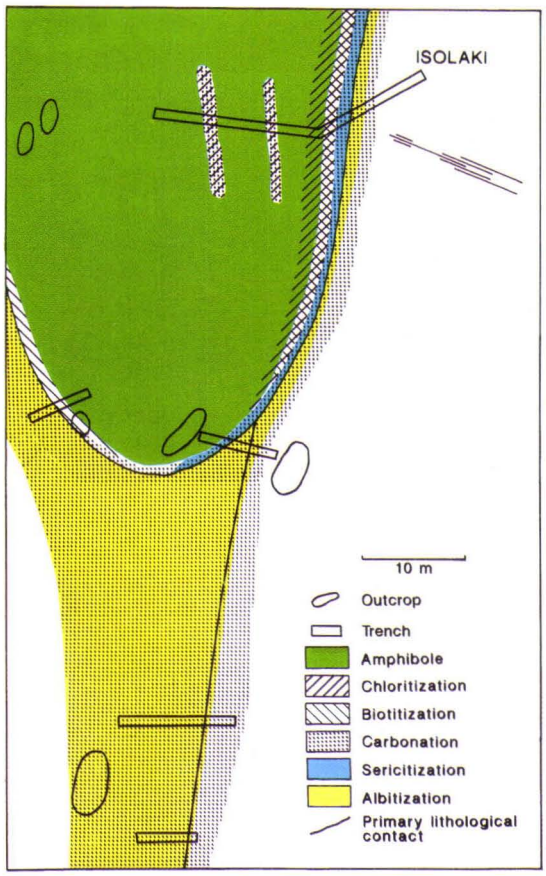

Fig. 29. Alteration types in the Isolaki area.

Palovaara

General structure

The bedrock (Fig. 30) is composed of two main units, Middle Lapponian sediments and Upper Lapponian mafic volcanic rocks and dykes, which are found chiefly above the sediments (Lehtonen and Rastas 1987, 1988). Some of the dykes, including all lamprophyres and a few albite diabases, are within the sediment pile, concordant with the sedimentary layers or cutting them at a low angle. In addition, there are Upper Lapponian ultramafic volcanic rocks interbedded with mafic lava units and dykes. The sediment pile consists mainly of phyllites, siltstones and quartzites, locally with thin beds of mafic and intermediate tuffite and ultramafic chrome-bearing marble.

The diabase dykes do not cut the lava units, and the chemical and petrographical data imply that they can be comagmatic and of the same age. The age relationship between albite diabase and lamprophyre is unclear; their mutual contacts are fractured and strongly altered. The lamprophyre dykes are, however, in a lower stratigraphic position than the bulk of the diabase dykes. The lamprophyre have thus prob-

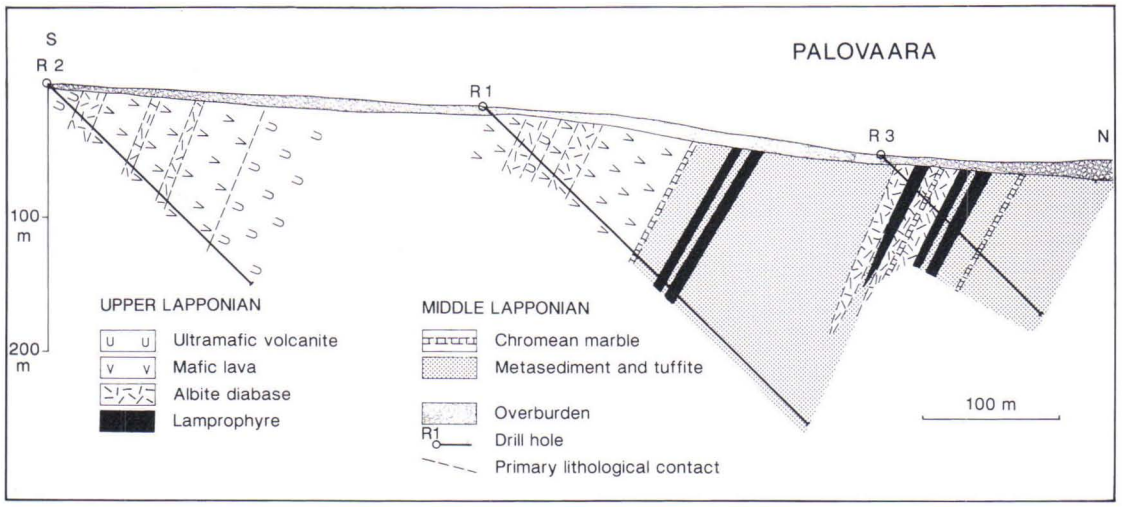

Fig. 30. Geology of the Palovaara site, chiefly based on diamond drillings. The drill log data have been integrated with the regional geological data from outcrops and exploration drilling (Lehtonen et al. 1984, 1985, Lehtonen and Rastas 1987, 1988). Also the drill hole numbers are shown.

ably intruded at an early phase of magmatism that was followed by the formation of albite diabase dykes. The strike of the bedding is E-W and the dip to the south. According to the sedimentary textures and the differentiation within the dykes, the stratigraphic top is to the south.

The deformation style is predominantly brittle, and all lithological units are variably fractured, both on a large and a small scale. The fracturing is most intensive in the most altered zones. The brittle deformation was followed by ductile deformation, during which layers containing sheet silicates were foliated.

Ultramafic volcanic rocks

The ultramafic volcanic rocks are basaltic komatiites (Fig. 31, Table 23, p. 94). It is difficult and in some cases impossible to distinguish between tuff and lava units, because the rocks are intensively altered. The most intensively altered ultramafic rock is chrome-bearing marble (Table 23), probably a tuffite. In addition, some of the massive ultramafic units may well be hypabyssal.

The texture of the least altered lava is massive, and locally it is possible to identify the original textures of olivine and pyroxene cumulates. In the pyroclastites, weakly altered types are not found; the least altered ones are lepidoblastic and banded, containing carbonate por-

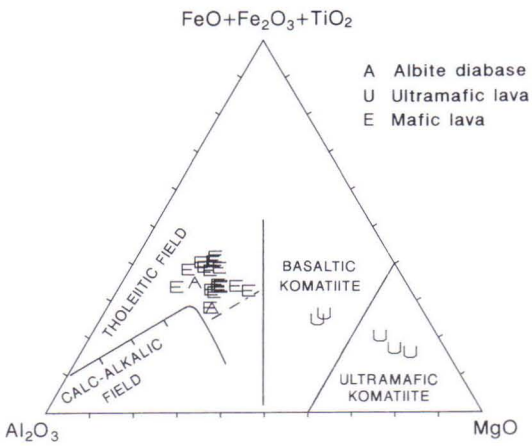

Fig. 31. Ultramafic and mafic lava and albite diabase from Palovaara on the Jensen cation plot diagram (Jensen 1976). The line separating basaltic and ultramafic komatiites is after Jensen and Pyke (1982).

phyroblasts. The mineral associations of the least altered ultramafics are:

Lava (more primitive type): talc + chlorite + serpentine + magnetite

Lava (less primitive type): tremolite-actinolite + biotite + chlorite + magnetite

Tuff: chlorite + talc + carbonate + magnetite ± quartz.

Mafic lava and albite diabase

Mafic lava and albite diabase comprise a homogeneous group both chemically (Table 24, p. 95) and mineralogically. They overlap both on the Jensen (1976) cation plot diagram (Fe tholeiite; Fig. 31) and on the SiO_2 vs. Zr/TiO_2 diagram (subalkaline; Fig. 32). The most significant difference between the diabase and the lava is textural: the lava units are fine-grained, locally porphyritic, spherulithic and amygdaloidal; the diabase units are coarser and do not contain phenocrysts or amygdales. Both are intergranular or subophitic. It is possible that some of the lithological units termed diabases are inner parts of thick lava beds, and that some smaller dykes have been termed lavas. The dominant mineral association of the least altered lava and diabase is:

albite + chlorite + magnetite.

Lamprophyre

The lamprophyre dykes at Palovaara are calc-alkalic, as shown by the Sc/Ta vs. Cr/V diagram (Fig. 9, p 27). The texture of the least altered types is biotite-phyric apatite-phyric and intergranular. The biotite phenocrysts (size 1-10 mm) are bent and broken. The groundmass consists of albite, biotite, chlorite and magnetite. In the most mafic types, the groundmass consists mainly of talc.

Tuffites and sediments

Sediments and tuffites compose most of the northern half of the area studied (Fig. 30). Intermediate and mafic tuffites occur as 0.1-2 m thick interlayers, forming about 10 vol. % of the sediment pile. The sediments and tuffites are in general intensively altered, and so chemical analyses were neccessary in order to distinguish between them. Only at the northern flank of the site is the degree of alteration so low that it is possible to identify the banded

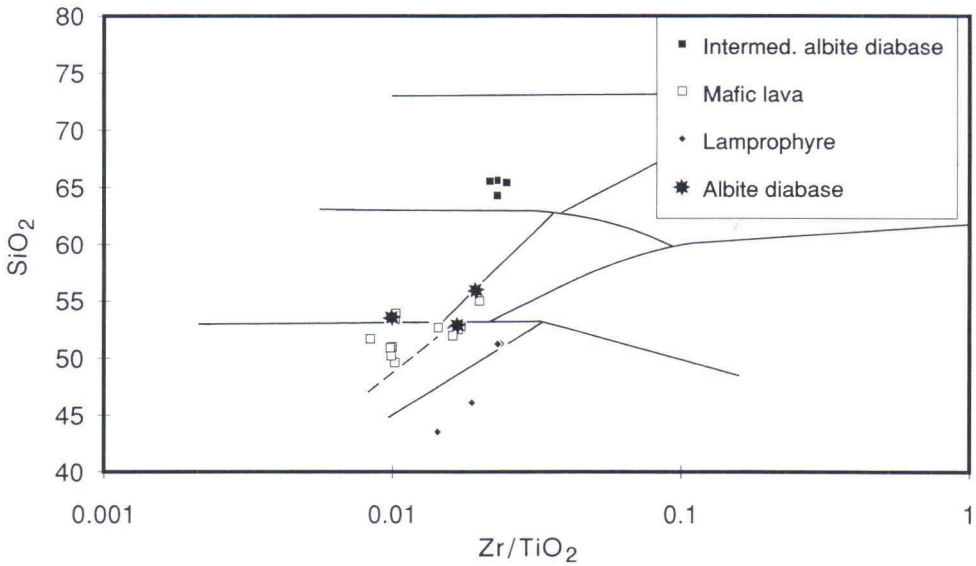

Fig. 32. SiO_2-Zr/TiO_2 diagram for mafic lava, albite diabase and lamprophyre from Palovaara. Fields as in Figure 6, after Winchester and Floyd (1977). SiO_2 was recalculated on volatile-free basis.

rocks as tuffites, conglomerates, quartzites, siltstones and phyllites by petrographical examination.

The texture of the least altered sediments is banded, weakly foliated, blastoclastic and granoblastic or lepidoblastic and the texture of the tuffites is banded and lepidoblastic-granoblastic. The dominating mineral associations are:

Quartzite, conglomerate: quartz + albite ± sericite

Siltstone: quartz + albite + biotite ± sericite

Tuffite: quartz + albite + chlorite ± biotite + magnetite.

Alteration types

Six alteration types can be distinguished on the basis of the occurrence and replacement relationships of the secondary minerals (Fig. 33). In the ultramafic volcanic rocks the alteration is characterized by amphibole, chlorite, biotite, carbonate and sericite; in the lamprophyre, albite diabase and mafic lava by chlorite, biotite, carbonate and sericite; and in the sediments and tuffites by albite, chlorite, carbonate and sericite. The alteration zones may follow the strike of the dykes as in Figure 33; it was not, however, possible to confirm this on the basis of the drilling profile, and there were no outcrops or excavated trenches at the site. The chemical composition of the lithological units in various alteration zones and combinations of zones at Palovaara is presented in Tables 23-26 (pp. 94-97).

1. The **albitized zones** here only consist of intensively albitized sediments. Thorough albitization was the first alteration stage in the sediments and it covered the sediment pile completely, since layers less altered than the albitized ones do not occur. All the sediments do not have a high albite content because the albite has partly decomposed during later alteration stages. The prevailing mineral association in the albitized zones is:

albite + quartz + rutile ± sericite.

The mineral assemblage of the albite zones includes 5% sericite, which is an early diagenetic mineral in these zones. Carbonate, formed at a later stage, is also present nearly everywhere. It is therefore probable that the occurrence of rutile is caused by weak carbonation of original Ti oxides and sphene, and not by albitization. The rocks are weakly brecciated and the fractures are filled with quartz and albite.

2. Only an ultramafic lava or a dyke at the

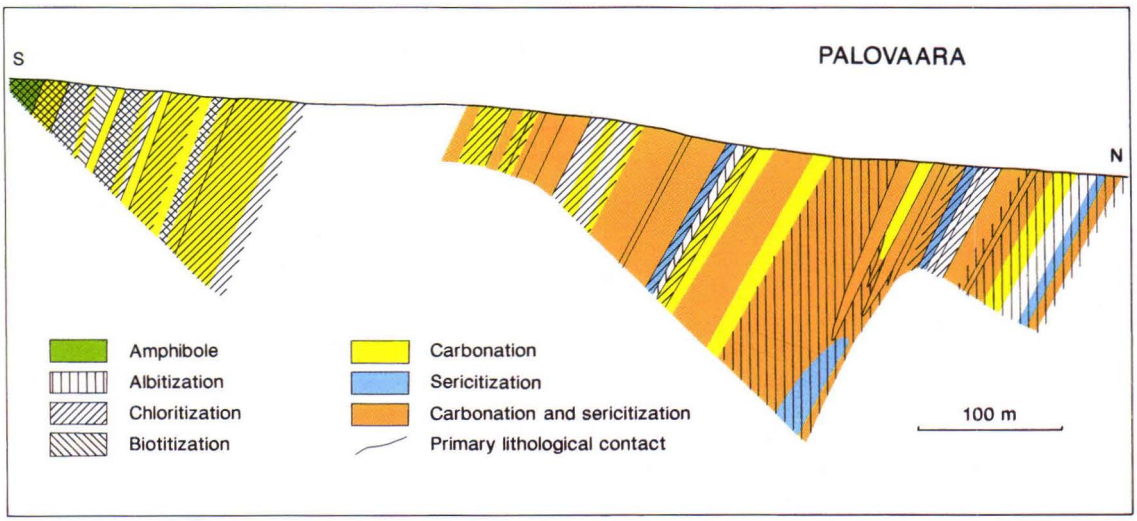

Fig. 33. Alteration types at Palovaara.

southern margin of the area studied is in the **amphibole zone**, which is overlapped by later chloritization and biotitization. Its dominating mineral association is:

tremolite-actinolite + biotite + chlorite + magnetite.

Tremolite-actinolite has completely replaced the primary Mg-Fe silicates (olivine and pyroxene) like in the amphibole zones of mafic rocks of the other sites. The primary texture is well preserved, only weakly brecciated. The fractures are filled with albite and tremolite-actinolite.

3. **Chloritized zones** include the majority of the least altered lava units, dykes and tuffites at Palovaara. Chlorite has replaced the amphibole, epidote and primary Fe-Mg silicates totally and the primary biotite of lamprophyre partially, and the rocks are weakly silicified. In places chlorite has also replaced albite. According to their mineral composition, the most chloritized lava and diabase units are hyalospilites. The ultramafic rocks were contemporaneously chloritized and steatitized. The dominating mineral associations of the chloritized zones are:

In albite diabase, mafic lava, tuffite: albite + chlorite + magnetite ± quartz

In ultramafic rock: talc + chlorite + magnetite

In lamprophyre: albite + biotite + chlorite + quartz + magnetite + apatite.

The chloritized rocks are thoroughly brecciated and the degree of brecciation varies from weak to very intensive, but it is generally possible to identify the primary magmatic textures. The fractures related to chloritization are filled with quartz, albite, chlorite, pyrite and chalcopyrite.

4. **Biotitization** has only taken place in the southern part of the area studied (Fig. 33) and in the lamprophyre. The secondary biotite has replaced only chlorite.

5. **Carbonation** covers the Palovaara site almost completely, but only zones wider than 5 m are shown in the alteration zone map (Fig. 33). Very weak carbonation can be observed throughout the area and in places 0.1-2 m wide, moderately carbonated zones occur. The weak carbonation has not changed the rocks significantly, only destroyed sphene and epidote.

In the moderately and intensively carbonated zones, the carbonates (chiefly Fe dolomite) replace all the other minerals except quartz, rutile and zircon. The primary textures can be identified in the weakly and moderately carbonated zones, but in intensively carbonated zones the texture is completely granoblastic and the primary features are difficult to identify. The degree of brecciation correlates positively with the degree of carbonation. The fractures are filled with carbonate, quartz, haematite and pyrite. The following mineral association was formed in all primary types of moderately and intensively carbonated rocks:

albite + carbonate + quartz + rutile ± sericite ± haematite.

6. Moderate and intensive **sericitization** (Fig. 3K) covers most of the middle and northern parts of the area studied, but overlaps the biotitization only in the lamprophyre. The sericitized zones regularly overlap the carbonated zones in the igneous rocks. The amount of carbonates is, however, very small in the intensively sericitized zones of the sediments. This low carbonate content most probably reflects the intensive sericitization and the strong decomposition of carbonates in these sediment units.

Potassium mica (currently muscovite) has replaced albite, biotite, chlorite and carbonates. In places, the degree of alteration was low and the pre-sericitization features are easily identified, but locally, especially in sediments and tuffites, the degree of alteration was very high. There, the carbonates and the albite were completely decomposed and in addition to sericitization, the rock underwent silicification and pyritization (Fig. 3K). Pyritization was an extremely irregular phenomenon and it has not been possible to find any pyritized zones extensive enough to be included in the map of alteration zones. The dominating mineral associa-

tions of the most strongly sericitized zones are:

In mafic lava and diabase: albite + sericite + carbonate + quartz + rutile

In sediments: sericite + quartz + rutile ± pyrite ± carbonate ± albite

In the igneous rocks, not even intensive sericitization destroyed the primary textures totally, although the rocks became partially granoblastic-lepidoblastic. On the other hand, the intensively sericitized sediments have totally lost their primary features, they are lepidoblastic and they have been foliated and folded during the regional ductile deformation. The brecciation is related to the sericitization and the breccia fractures are filled with sericite ± quartz and pyrite.

Regional metamorphic recrystallization

The lithological units of Palovaara were partially recrystallized during the regional metamorphism. The most significant processes were the recrystallization of sericite and the formation of schistosity in the sericitized sediments. In the ultramafics, nematoblastic tremolite-actinolite locally replaced biotite, chlorite, talc and carbonates, while lepidoblastic chlorite replaced talc and carbonates.

CHEMICAL CHANGES

Reactions

The chemical changes during the formation of secondary mineral associations are related to specific gas-fluid-mineral reactions (e.g., Giggenbach 1984). These reactions can be classified on the basis of various criteria, such as: hydration, carbonation, addition or loss of a particular anion or cation, change of pH or Eh, and breakdown or formation of a particular mineral or mineral assemblage. The last-mentioned criterion parallels the formation of the mineralogical zonation of an investigated site or deposit. Examples of various classifications are found in studies concerning ore deposits (Roberts and Reardon 1978, Kerrich 1983, Colvine et al. 1988, Pirajno 1992) and modern hydrothermal systems (Giggenbach 1981, Bird et al. 1984, Ragnarsdóttir et al. 1984).

One of the aims of the present study is to elucidate the conditions that prevailed during the formation of the typical alteration zones found in the areas studied. The chemical reactions are therefore classified according to their connections with this mineralogical zonation (Table 2, p. 52). Some of the reactions presented here can be connected with the formation of more than one alteration zone, especially if a reaction is considered to proceed in both directions: e.g., reaction [10] can be classified as belonging to either the chloritization or the biotitization category. The number of such cross connections would, however, be considerably greater if the classification were based on, e.g., hydration and anion and cation exchange. In that case reaction [1], e.g., could be classified as one of the following types: hydration, Na and S addition, or Mn, Mg and Ca loss.

Natural minerals are never pure end-member phases. Especially the sheet silicates are known to take significant amounts of trace elements in their lattices (Deer et al. 1962a). In addition, the exact compositions of the precursor minerals of completely altered rocks are not known. The exact stoichiometry of the reactions is therefore not shown in Table 2, but the minerals are symbolized by their names, so that their whole possible compositional range can be represented.

Table 2. Possible chemical reactions related to the formation of various alteration types. The connections between mineral reactions and depletion and enrichment of elements are also shown.

Amphibole zone formation:

[1] olivine + pyroxene + plagioclase + Ti magnetite + H_2O + Na^+ + SO_4^{2-} + H^+ <-> tremolite-actinolite + albite + epidote + sphene + magnetite + quartz + pyrite + Mn^{2+} + Mg^{2+} + Ca^{2+}

[2] clinopyroxene + primary biotite + plagioclase + K feldspar + Ti magnetite + H_2O + Na^+ + SO_4^{2-} + H^+ <-> tremolite-actinolite + albite + secondary biotite + epidote + sphene + magnetite + quartz + pyrite + Mn^{2+} + Mg^{2+} + Ca^{2+} + K^+

[3] plagioclase + Ca^{2+} + H_2O <-> epidote + albite + H^+

[4] olivine + $2H_2O$ + CO_2 <-> serpentine + $MgCO_3$

[5] serpentine + $3CO_2$ <-> talc + $3MgCO_3$ + $3H_2O$

Chloritization:

[6] olivine + pyroxene + plagioclase + Ti magnetite + H_2O + Mg^{2+} + SO_4^{2-} + H^+ <-> chlorite + sphene + haematite + quartz + pyrite + H_4SiO_4 + Ca^{2+} + Na^+ + K^+

[7] clinopyroxene + primary biotite + plagioclase + K feldspar + Ti magnetite + H_2O + Mg^{2+} + SO_4^{2-} + H^+ <-> secondary biotite + chlorite + sphene + haematite + quartz + pyrite + H_4SiO_4 + Ca^{2+} + Na^+ + K^+

[8] tremolite-actinolite + epidote + H_2O <-> chlorite + Ca^{2+} + Na^+ + K^+ + SiO_2

[9] albite + Fe^{2+} + Mg^{2+} + H_2O <-> chlorite + Na^+ + SiO_2 + H^+

[10] biotite + H^+ + H_2O <-> chlorite + Fe_3O_4 + K^+ + SiO_2

Biotitization:

[11] clinopyroxene, hornblende or actinolite + K^+ + H_2O <-> biotite + SiO_2 + magnetite + Ca^{2+}

[12] epidote + magnetite + quartz + K^+ + H_2O <-> biotite + Ca^{2+} + H^+

Albitization:

[13] anorthite + SiO_2(aq) + Na^+ <-> albite + epidote + H^+

[14] anorthite + H_4SiO_4 + Na^+ <-> albite + H_2O+ Ca^{2+}

[15] anorthite + SiO_2 + H_2O + H^+ + Na^+ <-> albite + sericite + Ca^{2+}

[16] K feldspar + Na+ <-> albite + K^+

[17] biotite + H^+ + Na^+ <-> albite + rutile + H_2O + Mg^{2+} + Fe^{2+} + Mn^{2+}

[18] sericite + SiO_2 + Na^+ <-> albite + K^+ + H^+

Carbonation (+ albitization or sericitization):

[19] actinolite + epidote + CO_2 + H_2O <-> chlorite + calcite + quartz

[20] Fe talc + Ca^{2+} + CO_3^{2-} + CO_2 <-> Fe dolomite + SiO_2 + H_2O

[21] sphene + CO_2 <-> calcite + rutile + SiO_2

[22] albite + $H(CO_3)^-$ + Ca^{2+} + K^+ <-> calcite + sericite + quartz + Na^+

[23] chlorite + SiO2 + epidote + CO_2 + Na^+ + Mn^{2+} <-> albite + Fe dolomite + H^+ + Fe^{2+} + Mg^{2+}

[24] chlorite + SiO2+ epidote + CO_2 + K^+ + Mn^{2+} <-> sericite + Fe dolomite + H^+ + Fe^{2+} + Mg^{2+}

[25] chlorite + Ca^{2+} + CO_2 + Mn^{2+} <-> Fe dolomite + SiO_2 + H_2O

[26] biotite + Ca^{2+} + Mn^+ + CO_2 + H^+ <-> Fe dolomite + sericite + quartz + rutile + Fe^{2+} + Mg^{2+} + K^+ + H_2O

Sericitization:

[27] chlorite + K^+ + H^+ <-> sericite + SiO_2 + Mg^{2+} + Fe^{2+} + H_2O

[28] biotite + OH^- <-> sericite + SiO_2 + Fe^{2+} + Mg^{2+} + K^+ + H_2O

[29] Fe dolomite + albite + K^+ + H^+ <-> sericite + SiO_2 + H_2O + Ca^{2+} + CO_2 + Na^+ + Mg^{2+} + Fe^{2+}

Talc formation:

[30] Mg^{2+} + SiO_2 + H_2O <-> talc + H^+

[31] albite + Fe^{2+} + Mg^{2+} + H_2O + O_2 <-> talc + Na^+ + H_4SiO_4 + $Al(OH)_4^-$

[32] chlorite + O_2 + H_4SiO_4 + Mg^{2+} + H_2S <-> talc + pyrite + H^+ + $Al(OH)_4^-$ + H_2O

Reactions related to sulphides:

[33] pyrite + H_2O <-> magnetite + H_2S + O_2

[34] Fe^{2+} + H_2S <-> pyrite + H^+

[35] chalcopyrite + SO_4^{2-} + H^+ <-> pyrite + Cu^+ + H_2O + S^{2-}

Table 2. Continued.

References to reactions. Chemical gains and losses when reactions proceed from left to right. Gains and losses are reverse when reactions proceed from right to left.

Reaction	Gains	Losses
[1] (Reed 1983, Hemley & Hunt 1992)	H_2O, Na, S	Mn, Mg, Ca, K, Cu, Co, Ni
[2] (modified after Reed 1983)	H_2O, Na, S	Mn, Mg, Ca, K, Cu, Co, Ni
[3] (Rosenbauer & Bischoff 1983)	H_2O, Ca	
[4] (Winkler 1979)	H_2O, CO_2	
[5] (Pirajno 1992)	CO_2	H_2O
[6] (Reed 1983)	H_2O, Mg, S	Si, Ca, Na, K, Ba, Cu, Co, Ni
[7] (modified after Reed 1983)	H_2O, Mg, S	Si, Ca, Na, K, Ba, Cu, Co, Ni
[8] (Colvine et al. 1988)	H_2O, Co, Ni	Mn, Ca, Na, K, Ba
[9] (Hemley & Hunt 1992)	H_2O, Fe, Mg	Na
[10] (Colvine et al. 1988)	H_2O	K, Rb, Cs
[11] (modified after Hemley & Hunt 1992)	H_2O, K	Ca, Ba
[12] (modified after Colvine et al. 1988)	H_2O, K, Cs, Rb, Ba	Ca
[13] (Janecky and Seyfried 1985)	Na, Si	
[14] (Morad et al. 1990)	Na, Si	Ca
[15] (Boles 1982)	H_2O, Na	Ca
[16] (Munhá et al. 1980)	Na	K, Rb, Cs, Ba
[17] (modified after Jasinski 1988)	Na	H_2O, Fe, Mn, Mg, K, Rb, Cs, Ba
[18] (Deer et al. 1962a, Jasinski 1988)	Na	Fe, K, Ba, Rb, Cs, Cr, V
[19] (Ames et al. 1991)	CO_2, H_2O	
[20] (Colvine et al. 1988)	CO_2, Ca	H_2O
[21] (Hunt & Kerrick 1977)	CO_2	U, Th and REE
[22] (modified after Jasinski 1988)	H_2O, Ca, K, Rb, Ba	Na
[23] (Kerrich 1983)	CO_2, Na, Mn	Fe, Mg, Ni, Co, Cu
[24] (Kerrich 1983)	CO_2, K, Mn	Fe, Mg, Co
[25] (Colvine et al. 1988)	CO_2, Mn, Ca	H_2O, Ni, Co
[26] (modified after Colvine et al. 1988)	CO_2, Mn, Ca	Fe, Mg, K, Rb, Cs, Ba, Br
[27] (Jasinski 1988)	K, Ba, Rb, Cs	H_2O, Fe, Mn, Mg
[28] (De Groot & Baker 1992)		H_2O, Fe, Mg, K
[29] (Reed & Spycher 1984, Kerrich 1983)	K, Ba, Rb, Cs	H_2O, CO_2, Fe, Mn, Mg, Ca, Na
[30] (Luce et al. 1985)	H_2O, Mg, (Fe)	
[31] (modified after Roberts & Reardon 1978)	H_2O, Fe, Mg	Si, Al, Na
[32] (Roberts & Reardon 1978)	Si, Mg, S	Al, Na
[33] (Colvine et al. 1988)	H_2O	S, Sb, As
[34] (Drummond & Ohmoto 1985)	Fe, S, As, Sb	
[35] (Reed 1983)	S	C

Mass balance calculations

The absolute abundances of major elements and trace elements of the lithological units suggest substantial variations in bulk chemical compositions in the areas studied. Simple inspection of tables of chemical analyses is not, however, satisfactory for the deduction of chemical changes. As Gresens (1967) and Costa et al. (1983) have pointed out, the assumption of constant volume without calculation of possible mass and volume changes in the mass balance studies may lead to highly erroneous results, except possibly in qualitative terms

such as for gross depletion or enrichment of highly mobile elements. The assumption of constant volume is typically based on the preservation of primary textures. For example Lesher et al. (1986) have, however, demonstrated that well-preserved primary textures are not inconsistent with a rock volume change of even ±70%.

The calculation of rock mass and volume changes and the application of these volume changes to the mass balance calculations follow the same procedure (Akella 1966, Gresens 1967, Grant 1986, Ames et al. 1991) as that one used in this study:

1. Samples from altered and unaltered zones are selected. In order to avoid erroneous results due to magmatic differentiation or sedimentary processes, the following criteria are applied: (1) the samples compared are from the same stratigraphic position, (2) they represent the same lithological unit and (3) they are from locations as close to each other as possible.

2. Elements that are usually treated as immobile (Winchester and Floyd 1977, Lesher et al. 1986, Ashley et al. 1988, MacLean 1990) are selected for observation. Their concentration ratios in unaltered rock (A) and altered rock (B) are compared.

3. If the concentration ratios within an element group are similar in A and B, but their absolute concentrations have changed, these elements have either been mobile to the same degree or the rock mass and volume has changed. When the elements used in this procedure are geochemically sufficiently different, the latter alternative becomes significantly more probable, because different elements are fixed to different minerals and therefore their mobility differs in the alteration processes. This is how the immobile elements are found. In the present study, Ti, Al and Zr were found immobile during all alteration stages and Ti (Zr in a few cases) was selected as the element on which to base the mass balance calculations.

4. The change in rock volume factor (= fv) is calculated by formula [1] using the rock densities of A and B and the concentrations of the most immobile element.

$$fv = g_A/g_B * X_A/X_B \qquad [1]$$

The relative changes in the concentrations of mobile elements are calculated by formula [2]:

$$Y_n = X_A/X_B * Y_B/Y_A \qquad [2]$$

Abbreviations in the formulae [1] and [2]:

g_A = density of rock A

g_B = density of rock B

X_A = concentration of "immobile" element X in rock A

X_B = concentration of "immobile" element X in rock B

Y_A = concentration of mobile element Y in rock A

Y_B = concentration of mobile element Y in rock B

Y_n = enrichment factor of element Y

5. The dimensionless enrichment factor Y_n indicates the relative gain or loss of the mobile element Y during the examined alteration process. For example, $Y_n = 1.5$ corresponds to a 50% increase compared with the original abundance of the element and $Y_n = 0.75$ correnponds to a 25% decrease. The enrichment/depletion relationships can be graphically illustrated on simple histograms where Y_n is on the Y axis and the elements on the X axis (e.g., Figs. 35 and 37, p. 60 and 66).

6. The enrichment factor perfectly shows the relative gains and losses, but because it is a relative factor, it easily exaggerates the importance of the changes in trace element concentrations and understates the main components. The absolute mass change in per cent units for element Y (= Y_d) is calculated by the formula [3], which gives the gains and losses directly in mass units, e.g., in grams per 100 grams of original rock.

$$Y_d = X_A/X_B * Y_B - Y_A \qquad [3]$$

The accuracy of the mass balance calculations depends on the analytical accuracy of concentrations and densities and on the pre-alteration equality of the samples compared. Thus, in the present study, gains and losses up to approx. 10% (Y_n = 0.9-1.1) for the major components (for silica up to 5%, Y_n = 0.95-1.05) and approx. 20% (Y_n = 0.8-1.2) for the trace elements are considered to be within the range of inaccuracy in the igneous rocks, whereas greater inaccuracy is possible in the sedimentary rocks chiefly because of their layered nature. The range of concentrations of trace elements is wide in various rock types and areas of the present study (cf., e.g., Tables 3 and 13, p. 57 and 76) and the concentration of an element may be over or below the analytical detection limit in different rocks. Only reliable analytical results were used in the calculations. Thus, the trace element sets in the enrichment/depletion figures are dissimilar. The calculations are normally based on comparisons between one of the altered samples and one of the least altered samples, but in some cases averages of similarly altered samples were compared with averages of the least altered samples.

In addition to the enrichment factor, formula [3] was applied for description of absolute mass changes in the present study. The analytical and sample inequality inaccuracies may cause errors in these calculations, too. The possible error effect increases as the absolute amount of element handled increases and its relative enrichment or depletion decreases, especially for SiO_2 or Al_2O_3, where the relative change is small. The method is reliable when the enrichment factor is small or large enough, i.e., <0.95 or >1.05 for SiO_2 and <0.9 or >1.1 for the other main components. Because the interpretation of this method may stress the significance of the main components and understate the relative changes in trace element concentrations, it was not applied to the latter ones. The mass balance calculations indicate that common chemical trends prevailed during the formations of similar alteration zones in the areas studied. The absolute mass changes were therefore calculated only once for each alteration type using the Eksymäselkä data as an example (Table 6, p. 61).

Because of the layering and the inhomogeneity of the sediments it can be difficult to find suitable sample pairs for the mass balance calculations. The mass balance calculation method may even give severely misleading results when applied to sedimentary rocks. Rather than the method of Gresens (1967), correlation diagrams of the type 'element vs. SiO_2/Al_2O_3' have proved to be suitable for the characterization of alterations in detrital sediments (Kalsbeek 1992). The use of this type of diagram is based on the following: (1) the SiO_2/Al_2O_3 of detrital sediments depends on the ratio of quartz/(feldspars + clay minerals) and is therefore closely correlated to the original grain size, because quartz is concentrated in the coarser fractions (Pettijohn et al. 1987, Taylor and McLennan 1985), (2) Al is normally immobile in alteration processes (Costa et al. 1983, Sturchio et al. 1986, Kerrich 1989), (3) the relative change (although not the absolute change) in Si concentrations of rocks is generally small compared with the mobilities of, e.g., alkaline and alkaline-earth elements (e.g., MacLean and Kranidiotis 1987, Elliot-Meadows and Appleyard 1991, Kalsbeek 1992), and (4) the assumption of small or insignificant rock mass and volume change during alteration. If, however, Si or Al was mobile, if there was a significant rock mass or volume change, or the sediment is not purely detrital but, e.g., actually a pyroclastite or a chemical precipitate, the diagrams of Si vs. SiO_2/Al_2O_3 and Al vs. SiO_2/Al_2O_3 most probably will show it as weak correlations and thus the further, possibly misleading use of the diagrams 'element vs. SiO_2/Al_2O_3' can be avoided.

Eksymäselkä

The least altered rocks

The chemical data of the least altered igneous rocks (Table 3) plotted on an alkali ratio diagram (Hughes 1973) indicate that most samples are not within the igneous field but in the spilite field (Fig. 34). This suggest that an early, thorough alkaline metasomatism affected lava and diabase. The feldspar of the least altered sediments and tuffites is albite, although K feldspar is also a typical mineral in quartzites and siltstones. Therefore, it is supposed that the least altered quartzite and tuffite (Table 4) were affected by albitization.

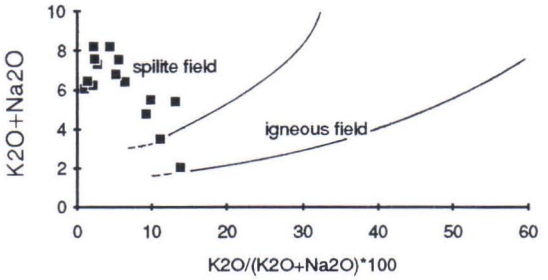

Fig. 34. The least altered igneous rocks at Eksymäselkä, plotted on the alkali ratio diagram of Hughes (1973).

Reaction [1] (Table 2) best describes the formation of the least altered zone, i.e. the amphibole zone in the mafic igneous rocks. The elements Si, Mn, Mg, Ca, Na, K, S, Cu, Ni and Co were mobile, the fluid was acid and weakly reducing, containing some CO_2 (indicated by the ultramafic rocks) and the rocks were moderately hydrated during the formation of the least altered zones.

The mass and volume changes and chemical mass balances related to the formation of the other alteration zones were calculated using formulae [1] and [2]. The analyses compared, their immobile element ratios and volume changes are presented in Table 5.

Chloritization and biotitization

The relative chemical changes connected with chloritization and biotitization of the Fe-Ti tholeiitic lava are presented in Figure 35A. It is highly probable that similar changes are related to chloritization and biotitization of the albite diabase, because its mineral and chemical compositions closely resemble the Fe-Ti tholeiites (cf. Figs. 5 and 6, p. 22 and 23, Table 3).

Within the accuracy of the analytical and mass balance calculation methods, the majority of the elements were immobile during chloritization and biotitization (Fig. 35A). The change in rock volume was approx. -10% (Table 5). The most significant relative chemical changes during chloritization were the losses of Si, Mn, Ca, Na, K, Sb, Ba, Br and Cu and the gains in S, Rb and Cr. The losses of Ca and Na and the gains in K, S, As, Rb and Ta (?) are related to biotitization.

The absolute gains and losses per 100 g of original rock based on formula [3] and immobility of Ti are presented in Table 6 (p. 61). The greatest absolute changes during chloritization were the losses of Si, Mg, Ca and Na and during biotitization the loss of Na and the gain in K. The losses of Al and Fe are not proven because the enrichment factors of Fe and Al are within the limits of the errors of the method.

The changes in the mineral association should explain the chemical changes. Reactions [6] and [9]-[11] (Table 2) in the igneous rocks and reactions [8] and [10] in the sediments and tuffites are related to the formation of the chlorite-biotite zones and associated with intensive hydration. Reactions [6], [10] and [35] imply that the hydrothermal fluid was acid and weakly reducing during chloritization and biotitization. In addition, its a_{K+} increased after chloritization, which made the biotite formation possible.

None of the chloritization reactions (Table 2) explains the enrichment of Rb (K is depleted) and the depletion of Sb, and none of the biotitization reactions the enrichment of As. Either

Table 3. Chemical composition of albite diabase and mafic lavas at Eksymäselkä. Major elements in wt. %, trace elements in ppm.

	Albite diabase														Fe-Ti tholeiite						Fe tholeiite	
	ultramafic cumulate		mafic albite diabase								intermediate type (albitite)				least altered (chloritized + biotitized)		carbonated		carbonated + sericitized		least altered (chloritized)	carbonated
	carbonated		least altered (chloritized)		chloritized + biotitized		carbonated		carbonated + sericitized		least altered (chloritized)		carbonated									
	avg	std	avg	std	avg	std	avg	std	avg	std	avg	std	avg	std	avg	std	avg	std	avg	std	avg	
SiO2	39.14	3.88	52.88	5.11	50.53	1.74	49.18	5.93	46.26	7.93	57.71	5.11	63.28	5.99	52.52	2.53	47.03	2.45	46.78	3.24	51.35	44.30
TiO2	0.52	0.17	2.29	0.64	2.37	0.28	2.07	0.54	1.85	0.14	1.88	0.47	1.33	0.56	2.37	0.31	1.74	0.54	2.62	0.22	1.50	1.39
Al2O3	4.23	1.10	13.30	1.88	13.53	0.82	12.94	1.61	11.04	2.20	14.01	0.90	14.07	1.21	14.66	1.50	13.59	1.85	13.17	1.70	14.50	12.70
Fe2O3t	12.58	0.94	16.77	3.97	19.31	1.96	8.22	4.19	10.12	3.87	13.95	4.54	1.91	0.59	15.17	1.27	15.49	0.87	7.38	1.74	14.87	12.18
MnO	0.17	0.08	0.11	0.12	0.11	0.04	0.15	0.03	0.29	0.13	0.04	0.02	0.07	0.03	0.10	0.04	0.17	0.05	0.23	0.04	0.09	0.18
MgO	28.47	1.61	4.31	1.47	4.24	0.70	4.44	2.55	4.63	1.05	2.91	1.17	1.95	1.08	4.50	0.73	5.94	0.81	4.60	0.92	7.34	6.86
CaO	2.46	1.72	3.89	3.89	3.51	1.30	7.28	1.39	9.36	3.13	1.74	1.05	4.25	1.76	3.90	2.34	4.94	1.09	9.21	1.84	3.72	6.85
Na2O	<0.01		5.32	2.05	4.46	1.16	6.14	1.49	3.19	0.89	7.05	0.62	7.80	0.64	4.99	0.77	4.24	0.55	2.82	2.04	3.03	4.17
K2O	<0.01		0.31	0.17	1.34	0.54	0.55	0.22	1.97	0.95	0.24	0.12	0.15	0.08	1.18	0.71	1.24	0.60	3.28	0.89	0.22	0.46
P2O5	0.05	0.01	0.20	0.03	0.17	0.04	0.17	0.09	0.15	0.04	0.24	0.08	0.34	0.16	0.26	0.04	0.17	0.08	0.29	0.06	0.14	0.11
sum	90.91	4.65	99.49	0.92	99.91	0.21	93.35	2.72	91.91	4.64	99.97	0.04	96.24	2.11	99.84	0.19	94.72	2.77	91.55	1.86	96.95	92.00
Br	<0.5		4.94	5.72	<2		0.76	0.48	<1		3.09	1.08	2.07	0.87	4.92	4.22	<2.2		5.56	4.15	0.75	0.76
S	400	287	270	324	2910	3019	4470	6631	4730	3935	1740	1720	290	799	290	253	190	132	920	1092	35	820
Sb	0.94	0.42	1.17	0.96	1.18	1.14	1.99	1.17	1.59	1.20	1.10	0.30	1.92	1.18	0.94	0.47	0.43	0.10	2.45	1.17	0.89	0.65
As	8.76	8.87	1.82	0.21	7.73	8.10	7.31	6.69	4.08	3.66	1.56	0.35	1.44	0.67	3.35	2.58	<1		4.86	4.58	2.06	2.86
W	<1		<1		<1		<1.3		<1		<1.3		<2		<0.8		<0.8		<0.8		<1	<1
Cs	<1		<1		<1		<1		<1		<1		<1.5		<1		<1		<0.5		<1	<1
Rb	9.8	3.8	14.2	10.5	45.2	22.6	20.4	7.9	32.7	15.2	17.3	7.9	23.9	12.8	32.2	19.9	33.2	14.6	58.3	12.4	10.9	11.2
Ba	49	16	<60		149	77	<80		267	207	<60		79	35	112	87	99	59	157	48	71	<50
Cu	10	10	50	49	<20		<20		<10		<10		<10		90	77	80	78	<30		60	420
Co	96	11	37	25	48	28	74	94	63	59	22	11	7.5	5.4	37	11	36	12	15	15	40	33
Ni	1150	194	50	26	<60		125	95	<50		<60		84	41	82	32	110	52	88	31	104	86
La	4.4	1.6	22.2	11.4	16.8	16.8	38.3	41.5	11.5	7.1	16.8	3.1	34.4	25.6	37.1	28.7	15.9	6.6	10.5	8.8	12.8	9.6
Sm	1.2	0.2	5.8	1.4	4.5	1.6	9.6	9.6	3.4	1.3	5.0	0.6	7.7	4.2	21.9	41.3	5.2	1.9	5.9	1.6	5.6	3.8
Sc	27	9	46	37	48.6	15.9	33	12	23	17	11	5	4.4	2.3	33	6	36	4	24	1	67	64
Ta	0.23	0.06	0.71	0.08	0.73	0.21	0.71	0.35	0.73	0.40	1.05	0.46	1.69	1.10	1.33	0.38	0.63	0.47	1.08	0.31	0.33	<0.5
V	120	32	400	155	480	77	310	138	390	38	240	94	100	64	330	65	300	21	380	42	310	270
Cr	6520	974	56	19	77	30	214	284	<60		<60		122	115	94	21	122	58	37	12	236	243
U	0.17	0.12	1.14	0.10	0.89	0.52	1.31	0.58	0.77	0.32	1.18	0.71	2.38	1.07	2.50	0.77	1.14	0.96	2.38	0.66	0.37	0.37
Th	0.69	0.12	3.48	1.86	2.48	3.29	3.51	2.96	5.12	5.17	10.15	7.45	14.52	8.62	3.84	1.02	2.08	1.34	2.76	0.84	1.30	1.15
Zr	50	17	170	34	130	29	160	29	140	40	260	74	350	191	220	37	160	64	220	51	120	100
n	3		4		14		5		3		6		9		8		3		5		2	1

Table 4. Chemical composition of sediments and pyroclastites at Eksymäselkä. Major elelments in wt. %, trace elemens in ppm.

	Quartzite		Siltstone					Intermediate tuffite							Mafic tuffite			
	albitized (chlor-biot -zone)		least altered (chlor-biot -zone)	intensively albitized + carbonated		carbonated + sericitized		least altered (chlor-biot -zone)	intensively albitized + weakly carb.		moderately carbonated	intensively albitized + carbonated		carbonated + sericitized	least altered (chlor-biot -zone)	carbonated	carbonated + sericitized	
	avg	std	avg	avg	std	avg	std	avg	avg	std	avg	avg	std	avg		avg	avg	std
SiO2	78.27	2.71	69.90	66.36	1.76	62.93	3.39	62.18	62.33	0.85	54.45	60.44	1.92	56.90	53.77	46.80	42.43	2.57
TiO2	0.16	0.04	0.39	0.45	0.07	0.50	0.16	0.45	0.63	0.05	0.53	0.50	0.10	0.49	0.65	0.51	0.60	0.22
Al2O3	11.80	1.95	15.21	14.01	0.52	14.59	1.87	13.01	15.94	0.45	13.98	14.59	1.09	13.45	17.64	13.41	11.59	1.21
Fe2O3t	1.31	0.34	3.09	1.43	0.38	4.52	2.07	8.63	6.53	0.20	7.72	2.61	1.48	7.04	10.75	8.79	6.69	1.52
MnO	0.03	0.00	0.07	0.05	0.02	0.08	0.03	0.03	0.05	0.01	0.06	0.08	0.03	0.07	0.02	0.09	0.20	0.03
MgO	0.77	0.25	1.41	1.93	0.19	3.08	1.23	7.75	1.80	0.57	7.64	2.77	0.90	7.15	9.54	9.07	7.20	1.56
CaO	1.07	0.51	1.75	3.60	0.32	2.84	1.41	0.47	2.52	0.79	3.12	4.22	0.78	2.81	0.28	6.93	8.94	3.50
Na2O	4.89	0.31	4.33	7.75	0.36	3.51	1.26	2.25	8.55	0.36	4.59	7.89	0.60	3.45	5.77	4.57	3.83	0.75
K2O	1.15	0.62	3.23	0.17	0.16	3.07	1.21	1.06	0.25	0.13	0.63	0.18	0.13	1.29	0.06	0.77	1.56	0.57
P2O5	0.07	0.02	0.11	0.10	0.06	0.10	0.02	0.10	0.11	0.07	0.10	0.20	0.13	0.09	0.13	0.12	0.11	0.05
sum	99.57	0.32	99.60	95.92	0.61	95.31	1.93	95.99	98.80	0.95	93.70	94.41	1.19	92.82	98.72	93.33	84.74	2.03
Br	<1		<1	1.79	0.47	0.82	0.41	0.67	0.75	0.36	<1	<1		<1	<1	<1	<1	
S	<30		70	50	46	40	20	40	30	16	70	50	30	<20	<30	45	100	89
Sb	0.67	0.05	0.80	1.33	0.59	1.20	0.53	1.13	0.81	0.19	0.81	1.35	0.43	1.20	1.10	0.64	1.22	0.28
As	1.18	0.42	1.49	1.26	0.70	1.17	0.77	1.20	1.25	0.32	0.70	1.82	0.89	1.79	1.54	1.50	1.73	1.04
W	0.76	0.08	2.83	7.29	5.54	<1		1.43	1.31	0.43	0.97	2.47	1.14	1.45	1.05	1.03	<1	
Cs	<1		<1	<2		<1		<1	<2		<1	<2		<1	<1	<1	<1	
Rb	19.3	12.7	64.1	30.8	3.9	49.8	29.0	39.2	23.1	10.3	28.7	28.0	11.6	66.8	<10	20.2	23.6	10.0
Ba	74	20	243	<90		175	97	61	<70		147	<90		196	<40	95	132	75
Cu	<10		<10	<10		<10		<10	<10		<10	<10		<10	<10	<10	<10	
Co	<3		2.8	<8		6.9	4.8	6.1	<5		9.1	6.8	1.9	6.2	23.3	15.6	13.1	14.7
Ni	<30		29	99	12	47	19	36	<70		66	90	39	<40	125	<50	42	13
La	9.8	7.2	26.3	8.3	3.9	25.2	12.9	27.0	3.8	0.6	155	22.1	14.6	27.8	62.2	36.8	25.0	11.1
Sm	1.5	0.6	4.9	2.4	0.4	4.3	1.5	4.1	1.9	0.3	8.0	4.5	2.0	3.4	7.9	5.2	4.9	1.3
Sc	3.2	1.0	7.8	4.3	1.1	13.3	3.0	11.5	19.6	11.6	18.3	9.4	6.4	16.9	10.4	14.7	28.2	23.9
Ta	0.22	0.02	0.60	0.59	0.07	0.81	0.26	0.64	0.74	0.11	0.86	<1		0.44	1.21	0.53	0.92	0.15
V	<20		60	60	10	80	17	90	90	43	90	50	11	70	110	100	90	52
Cr	34	4	96	106	47	111	23	114	194	19	158	125	21	114	157	103	106	79
U	0.60	0.11	1.87	0.88	0.44	1.87	0.69	1.64	0.64	0.31	1.62	0.82	0.58	1.77	3.06	2.80	1.53	0.62
Th	3.6	0.8	8.9	8.5	2.3	12.8	3.5	12.0	14.0	2.2	12.9	11.2	1.4	12.7	16.6	12.9	8.3	4.0
Zr	150	31	310	220	61	200	24	150	170	5	170	160	30	170	190	170	150	20
n	4		1	4		8		2	4		2	5		2	1	2	3	

Table 5. Eksymäselkä. Analyses compared in Figure 35, their densities, immobile element ratios and volume changes (= dV%). The samples of least altered rock are presented in italics. Abbreviations: ab = albitization, bt = biotitization, cb = carbonation, ch = chloritization, se = sericitization. Major elements in wt. % , trace elements in ppm.

alteration	chloritization ± biotitization			carbonation + albitization				sericitization						carbonation + sericitization			
rock	Fe-Ti tholeiite			albite diabase		siltstone		tuffite		siltstone		siltstone		Fe-Ti tholeiite			
sample	*127-1*	126-1	164-1	*42-29*	42-26	*44-10*	40-38	50-5	50-3	40-48	40-47	40-34	51-1	*164-1*	134-4	133-1	134-1
type		ch	ch+bt		cb		ab+cb	ab+cb	se	ab+cb	se	ab+cb	se			cb+se	
SiO2	*51.66*	52.77	51.33	*53.64*	55.59	*59.76*	62.99	39.70	48.96	61.15	63.57	63.07	62.01	*51.33*	48.95	44.56	48.32
TiO2	*2.25*	2.69	2.67	*2.14*	2.05	*0.60*	0.64	0.49	0.50	0.55	0.65	0.66	0.70	*2.67*	2.77	2.54	2.71
Al2O3	*12.97*	14.50	14.53	*15.64*	14.97	*14.51*	15.95	12.17	12.04	14.04	15.89	15.97	17.21	*14.53*	14.82	12.78	14.57
Fe2O3t	*13.97*	15.44	15.37	*16.67*	3.22	*9.91*	1.35	6.09	8.07	2.45	2.70	6.29	6.35	*15.37*	5.13	8.78	8.19
MnO	*0.17*	0.08	0.13	*0.02*	0.13	*0.04*	0.05	0.21	0.14	0.08	0.07	0.05	0.05	*0.13*	0.19	0.29	0.20
MgO	*4.47*	4.74	5.38	*3.49*	2.47	*7.35*	1.68	7.44	7.56	2.47	1.58	1.57	1.39	*5.38*	3.92	4.94	4.11
CaO	*8.14*	3.81	4.31	*0.43*	5.65	*0.76*	3.60	10.37	4.61	4.84	3.33	2.57	2.82	*4.31*	8.28	9.93	7.62
Na2O	*4.69*	4.94	4.04	*7.36*	8.34	*3.36*	8.91	4.31	1.66	7.59	7.23	8.92	8.14	*4.04*	3.90	3.37	5.26
K2O	*0.71*	0.54	1.70	*0.18*	0.06	*1.17*	0.07	1.66	3.30	0.30	1.16	0.19	0.99	*1.70*	3.27	2.80	2.08
P2O5	*0.24*	0.28	0.26	*0.26*	0.32	*0.13*	0.43	0.08	0.09	0.15	0.23	0.01	0.15	*0.26*	0.27	0.26	0.27
sum	*99.27*	99.79	99.72	*99.83*	92.80	*97.58*	95.66	82.52	86.93	93.61	96.40	99.30	99.81	*99.72*	91.50	90.25	93.33
Br	*5.94*	2.30	9.32	*2.13*	1.38	*<1*	<1	<1	<1	<1	<1	<1	<1	*9.32*	4.26	1.80	9.74
S	*80*	310	490	*1660*	2420	*70*	40	30	50	<20	30	<20	<20	*490*	90	2560	1520
Sb	*1.10*	0.67	1.44	*1.59*	2.12	*1.39*	1.71	1.52	1.51	1.10	1.43	0.75	1.24	*1.44*	3.67	1.03	1.40
As	*2.38*	3.41	7.09	*1.90*	1.23	*1.12*	1.81	0.73	1.90	1.77	1.71	0.86	1.14	*7.09*	1.83	12.6	5.54
W	*<1*	<1	<1	*<1*	<1	*1.42*	3.79	1.27	3.02	<2	<1.5	1.92	<1	*<1*	<1	<1	<1
Cs	*<1*	0.30	0.74	*<1*	<1	*<1*	<1	<1	<1	<1	<1	<1	<1	*<1*	<1	<1	<1
Rb	*8.5*	28.6	56.3	*<15*	<15	*23.8*	38.4	29.5	62.0	34.3	36.3	34.9	15.0	*56.3*	56.4	53.5	41.4
Ba	*84*	38	43	*<60*	<60	*79*	<100	66	149	<100	<100	<100	42	*43*	155	127	99
Cu	*90*	50	60	*<20*	<20	*<20*	<20	<20	<20	<20	<20	<20	<20	*60*	20	30	20
Co	*37*	42	57	*30*	20	*9.3*	8.2	6.8	5.1	7.2	7.3	<7	<3	*57*	3.4	38	22
Ni	*59*	66	85	*<60*	<60	*41*	<120	29	43	113	117	<120	<70	*85*	75	86	106
La	*22*	23.9	25.7	*20.7*	9.16	*24.2*	27.3	37.8	38.8	10.5	13.3	4.01	6.22	*25.7*	17	11.4	1.8
Sm	*6.4*	7.4	7.2	*5.5*	3.5	*3.9*	6.8	6.1	3.9	3.2	5.5	1.9	2.4	*7.2*	5.7	5.8	7.1
Sc	*32.2*	29.6	44.9	*13.3*	7.7	*12.9*	3.6	10.6	11.0	7.8	9.6	8.9	17.3	*44.9*	23.1	26.6	25.1
Ta	*1.16*	1.49	2.04	*1.02*	1.19	*0.59*	0.57	1.07	0.73	<1	<1	<1	0.88	*1.08*	1.04	0.93	0.97
V	*330*	300	410	*250*	110	*90*	60	60	80	40	30	30	130	*410*	380	410	420
Cr	*69*	113	81	*<60*	<60	*114*	<110	81	80	135	110	173	175	*81*	36	41	44
U	*2.30*	2.45	3.69	*1.14*	1.31	*2.25*	0.91	2.14	2.24	0.40	0.58	0.50	0.94	*2.04*	2.49	2.03	2.19
Th	*3.5*	4.1	3.7	*6.2*	4.7	*15.0*	12.4	12.8	13.5	11.7	12.9	11.4	14.6	*3.7*	2.5	2.3	2.6
Zr	*220*	230	200	*200*	200	*220*	200	170	180	180	210	170	160	*200*	210	200	210
Al/Ti	*5.76*	5.39	5.44	*7.31*	7.30	*24.1*	24.8	24.8	24.1	25.6	24.6	24.3	24.4	*5.44*	5.35	5.03	5.38
Al/Zr	*590*	630	727	*782*	749	*660*	798	716	669	780	757	939	1076	*727*	706	639	694
Ti/Zr	*102*	117	134	*107*	103	*27.3*	32.1	28.8	27.8	30.4	30.8	38.6	44.0	*134*	132	127	129
density (kg/m3)	*2846*	2797	2997	*2285*	2908	*2671*	2697	2846	2775	2661	2650	2681	2540	*2804*	2776	2806	2797
dV%		-12	-10		+33		-6		-4		-16		-12		-4	+6	-2
ref. to Fig. no.	35A			35B		35C		35D		35E		35E		35F			

these changes are related to a weak alteration that has not been identified, or the increase in Rb concentration is related to chlorite formation and the changes in Sb and As to pyrite formation.

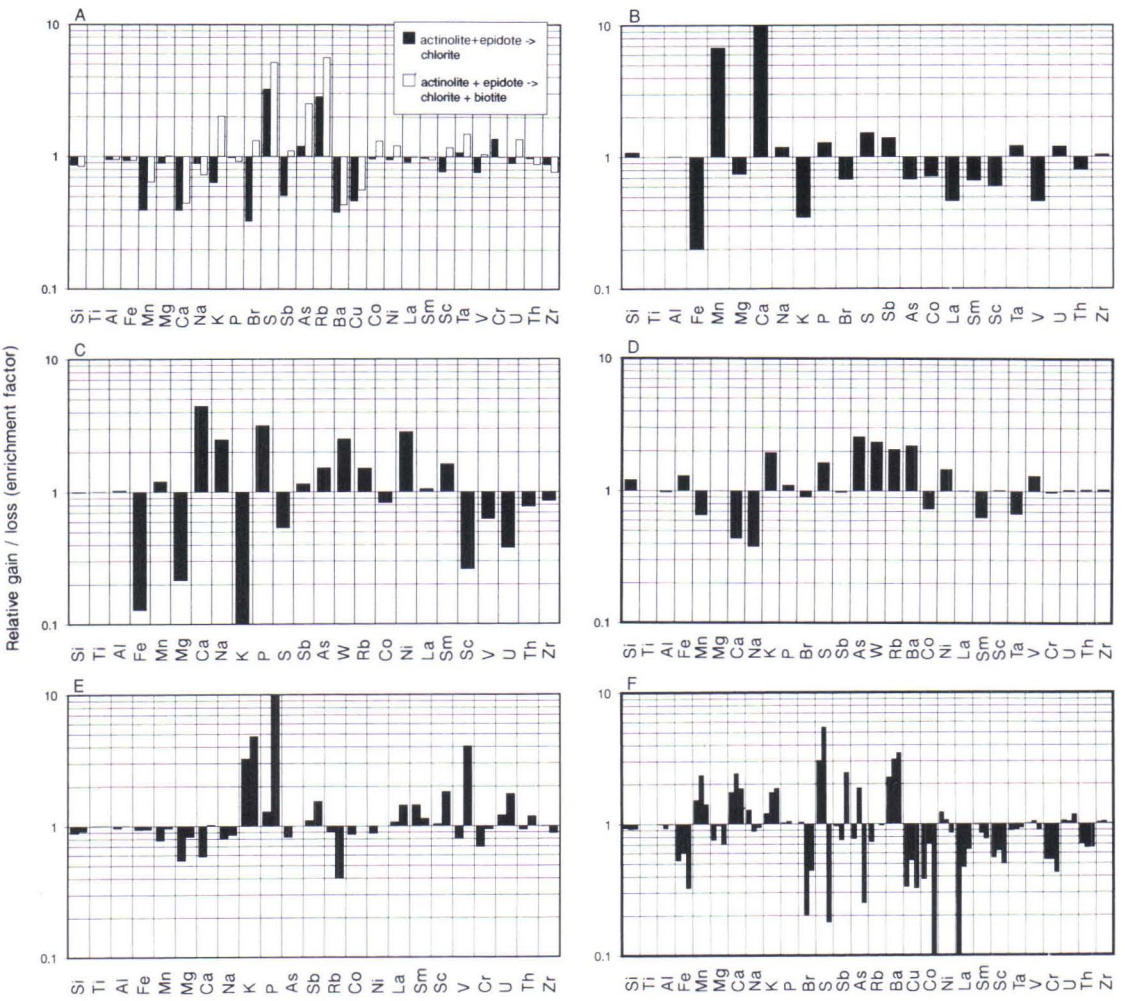

Fig. 35. Enrichment factors of the elements showing chemical gains and losses during the alterations at Eksymäselkä (y-axis). Only analytical results with small errors are used in the calculations, so that the element sets are different in the figures. The main components are presented in a typical order of analytical results. The general mobility of the trace elements decreases from left to right (Rose et al. 1979). The calculations are based on comparisons between one altered and one less altered sample unless otherwise idicated. Note the logarithmic scale of the y-axis. **A**: Chloritization and biotitization of Fe-Ti tholeiitic lava. Two altered samples are compared with the least altered type. **B**: Carbonation of albite diabase. **C**: Carbonation and intensive albitization of siltstone. **D**: Sericitization of carbonated intermediate tuffite. **E**: Sericitization of carbonated and intensively albitized siltstone. Two sericitized samples are separately compared with two carbonated and albitized samples. **F**: Carbonation and sericitization of the least altered Fe-Ti tholeiitic lava. Three altered samples are compared with the least altered type.

Carbonation and intensive albitization

The intensively albitized rocks are almost without exception carbonated. The calculated chemical changes (Figs. 35B., 35C, Table 6) and the correlation between the analytical data (Tables 3-5) indicate some common alteration trends, but also contrasts between rock types indicating the effect of the rock composition on the hydrothermal system.

The rock volume changes were approx. -5% - +30% (Table 5). The intensity of brecciation

Table 6. Absolute gains and losses of the main components in grams per 100 grams of original rock at Eksymäselkä calculated by formula [3] and immobile Ti. The figures in parentheses refer to enrichment factors within the limits of the errors of the method, i.e. the gain or loss shown is not reliable.

	Chloritization (Fe-Ti tholeiite)	Chloritization + biotitization (Fe-Ti tholeiite)	Carbonation (albite diabase)	Carbonation + intensive albitization (siltstone)	Sericitization (siltstone)	Carbonation + sericitization (Fe-Ti tholeiite)
SiO_2	-7.5	2-8.4	+4.4	(-0.86)	-7.3 ... (±0)	-4.4 ... -3.7
Al_2O_3	(-0.84)	(-0.73)	(±0)	(+0.41)	(-0.5 ... ±0)	(-1.1 ... -0.3)
Fe_2O_3t	(-1.1)	(-1.0)	-13.3	-8.6	(-0.4) ... +1.3	-10.4 ... -6.1
MnO	-0.10	-0.06	+0.12	+0.01	(-0.02) ... +0.02	+0.07 ... +0.2
MgO	-0.51	(+0.06)	-0.91	-5.8	-1.1 ... -0.3	-1.6 ... (-0.2)
CaO	-5.0	-4.5	+5.5	+2.6	-2.0 ... (±0)	+3.2 ... + 6.1
Na_2O	-0.56	-1.3	+1.4	+5.0	-1.7 ... -1.3	-0.5 ... +1.1
K_2O	-0.26	+0.72	-0.12	-1.1	+0.7 ... +1.1	+0.4 ... +1.5
P_2O_5	(-0.01)	(-0.02)	+0.07	+0.28	-0.2 ... +0.1	(±0)

and carbonation correlate positively with the increase in volume. Only a few elements were immobile (Figs. 35B and 35C). The chemical changes common to all rock types were the losses of Fe, Mg, K, Co, Sc, V and Th; the gains in Mn, Ca, Na and P; and the immobility of Ti, Al, Ta and Zr. Losses of Br, As, La and Sm and gains in Si, S and Sb also occurred in the igneous rocks and losses of S and U and gains in As, W, Rb, Ni, and Sm in the sediments and tuffites. The mobility of the REE is not supported by the normalized REE pattern of a moderately carbonated sample (Fig. 36), but Figures 35C and 35F imply that the REE may have been mobile when the alteration intensity was high, although the REE often are treated as immobile in alteration processes (Floyd and Winchester 1978, Sturchio et al. 1986, Michard 1989, Richards et al. 1991).

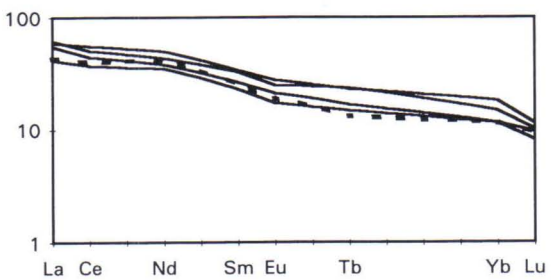

Fig. 36. Chondrite-normalized REE patterns of the intermediate type of the albite diabase. Solid lines: least altered types, dotted line: moderately carbonated type. Volume change during carbonation +30%. Normalizing values from Hickey and Frey (1982).

The largest absolute chemical changes (Table 6) in the igneous rocks were the losses of Fe and Mg and the gains in Si, Ca and Na, and in siltstone the losses of Fe, Mg and K and the gains in Ca and Na. The mobilities of Si (in silt) and Al (in silt and diabase) are questionable, because their enrichment factors are within the limit of error of the method.

The chemical changes can be combined with numerous mineral reactions, e.g., [17]-[26], which clearly show the importance of high f_{CO2} and a_{Na+}/a_{K+}, dehydration, and near neutral or alkaline pH during the alteration stage. Haematite and pyrite occur in places. This implies fluctuations in the f_{O2}, but since the haematite-bearing associations dominate, the conditions were chiefly oxidizing. Precipitation of pyrite (reaction [34]) in the fractures, which is in con-

cordance with pH increase, explains the gain of S, Sb and As. Apatite decomposition (because of decrease in pH caused by carbona-tion-related H^+ release to fluid) can explain the mobility of P, U, Th and REE (Deer et al. 1962b), but the decomposition of sphene [21] can also explain the mobility of U, Th and REE (Ribbe 1982, Pan et al. 1993).

Sericitization

A loss of rock volume seems to be related to sericitization, but if the sericitization and carbonation are treated as one alteration stage, the increase in rock volume was small (Table 5). This is supported by the alteration styles: the carbonation was related to intensive brecciation whereas the sericitization only to replacement.

The chemical changes calculated (Figs. 35D-35F, Table 6) and the comparison between the chemical compositions give distinct alteration trends for various alteration types (Tables 3-5). An uniform alteration trend observed in each lithological unit includes: gains in K and Ba, losses of Na and Co and immobility of Al, Ti and Zr. For most of the elements the alteration trends in different rock types differ from each other (cf. Figs. 35D-35F).

The calculation of the absolute chemical changes (Table 6) indicates the importance of the Si and Na depletion, the K enrichment and the connection between sericitization and carbonation. Mg and Ca depletions were locally significant in absolute numbers when sericite replaced carbonates.

The behaviour of most of the elements, like Fe, Mn, Mg, P, Sb, REE, Cr, Ni, U, S and V (cf. Figs. 35D and 35E, Table 6), seems complex in the sediments and tuffites. The reasons for this probably were the differences in the primary compositions and different pre-sericitization alterations. Most of the chemical changes can be combined with the carbonation reactions [21] and [24]-[26], with the sericitization reactions [18] and [27]-[29] and with the pyrite formation [34]. The Fe and V gains in sediments and tuffites (Figs. 35D and 35E, Table 6) are perhaps not related to alterations, but were caused by the primary differences between the magnetite contents of the specimens compared. The large Fe loss in the igneous rocks is related to carbonation, not sericitization (Table 6). The U, Th and REE mobilities are best explained by the decomposition of apatite and sphene.

The chemical connection between sericitization and carbonation is evident in the igneous rocks (Fig. 35F, Tables 2 and 6); carbonation of albite, chlorite, epidote and biotite may produce sericite (reactions [22], [24] and [26]). However, sericite evidently replaces carbonates in all lithological units (reaction [29]). This is explained by the Na^+ fixation to albite and H^+ release caused by albitization and carbonation (reactions [13], [17], [23]-[24]): the a_{Na+}/a_{K+} and pH of the fluid decreased, sericite precipitated and replaced carbonate. Thus, if sericitization took place at the same alteration stage as carbonation (and intensive albitization in sediments and tuffites), the deposition of carbonates and albite preceded the crystallization of sericite and composition of the fluid changed during the alteration stage.

Myllyvaara

The least altered rocks

The chemical compositions of the rocks in the alteration zones are presented in Tables 7-9. No unaltered rocks were found, which cannot be demonstrated by direct chemical methods, because common diagrams used to test the alterations of igneous rocks are not suitable for

Table 7. Myllyvaara. Chemical composition of lamprophyre dykes. Individual dykes are marked "LPFn", where "n" is an artifical number of a dyke. Major elements in wt. %, trace elements in ppm.

	Alkaline				Calc-alkaline									
	LPF 5			LPF 3	LPF17			LPF 7		LPF 14, LPF 18			LPF 16	LPF 9, LPF 10	
	least altered		intensively carbonated + sericitized	weakly carbonated	least altered		weakly carbonated	least altered		weakly carbonated		intensively albitized + carbonated	chloritized +albitized	weakly carbonated	intensively albitized + carbonated
	avg	std	avg		avg	std		avg	std	avg	std		avg		
SiO2	50.09	1.00	50.45	51.69	47.31	1.24	50.38	56.56	4.76	55.77	1.27	53.20	55.24	53.26	52.09
TiO2	3.24	0.06	2.41	3.99	2.72	0.47	2.27	1.12	0.37	1.99	0.07	1.72	1.40	1.03	1.07
Al2O3	11.05	0.40	11.15	13.02	13.35	0.75	15.37	15.85	2.13	12.12	0.71	15.90	15.88	9.27	12.88
Fe2O3t	13.53	0.80	4.79	5.99	16.95	1.98	8.68	6.61	3.07	5.78	2.74	1.44	11.96	9.48	1.96
MnO	0.03	0.02	0.10	0.04	0.04	0.01	0.05	0.03	0.01	0.03	0.01	0.06	0.05	0.04	0.04
MgO	8.09	0.66	6.55	5.32	9.55	1.47	7.19	3.82	2.59	6.52	1.16	3.42	3.95	11.48	6.73
CaO	3.61	0.68	7.13	7.53	2.67	0.65	4.25	3.74	2.18	5.93	1.52	6.23	2.66	4.32	6.63
Na2O	2.73	0.41	0.93	5.81	2.84	0.89	5.77	3.28	0.37	5.33	1.08	8.29	7.11	1.72	6.35
K2O	3.99	0.34	4.51	1.41	3.68	1.14	3.01	6.62	2.09	1.59	0.82	0.20	0.92	3.66	0.79
P2O5	2.52	0.07	1.59	2.75	0.54	0.09	0.57	0.58	0.28	1.04	0.05	0.89	0.65	1.38	0.59
sum	99.80	0.34	92.15	98.08	99.97	0.02	97.87	98.75	0.32	96.36	1.66	93.60	99.95	96.02	91.77
Br	<1		<1	<1	1.90	0.51	2.74	4.63	3.32	1.55	0.53	3.42	<1	<1	0.97
S	120	64	50	<10	150	282	<10	85	56	<10		<10	5	240	20
Sb	1.28	0.21	3.49	8.54	0.93	0.76	0.56	0.59	0.69	2.01	0.67	0.21	0.89	0.26	1.70
As	3.00	1.03	3.62	5.25	1.70	1.13	1.58	2.25	1.50	3.01	1.04	3.44	2.55	3.58	2.00
W	1.96	1.16	5.92	14.5	<1		0.67	<2		4.85	3.79	<1	0.64	<2	26.8
Cs	1.59	0.75	0.86	<1	2.44	1.02	2.01	<2		1.21	0.93	2.28	0.60	3.20	<1
Rb	162	39	137	49	113	39	97	122	28	55	38	144	16	156	29
Ba	4230	2196	2105	209	1985	439	1280	3860	1331	233	181	4490	196	1540	251
Cu	<10		<10	<10	<10		<10	<10		<10		<10	<10	<10	<10
Co	21.3	9.5	12.9	6.9	41.3	8.9	23.1	28.8	16.1	11.4	11.7	50.8	18.5	32.3	8.7
Ni	147	66	68	87	173	57	74	93	60	97	41	<40	120	341	84
La	176	55	184	166	38	3	42	99	75	132	21	44	26	51	76
Sm	18.9	6.0	20.2	23.7	5.6	0.3	6.1	10.9	7.6	13.3	1.3	6.4	4.8	12.0	10.0
Sc	37.1	4.4	39.5	44.2	48.7	6.3	35.5	33.9	13.7	25.6	2.6	58.7	24.0	22.0	23.1
Ta	9.90	6.65	16.3	12.9	0.80	0.11	1.10	4.58	7.42	1.17	0.12	<1	0.77	0.60	0.83
V	180	10	160	380	750	216	560	168	72	190	6	100	330	130	130
Cr	325	73	248	260	411	184	229	282	345	270	78	<40	117	583	381
U	6.35	3.02	7.55	9.21	3.07	0.81	4.19	4.21	1.85	4.43	0.39	2.99	3.27	4.36	2.56
Th	30.0	22.4	27.5	23.0	13.3	3.8	15.6	16.9	8.7	28.0	1.3	5.7	15.0	25.5	22.2
Zr	2200	192	1050	2690	330	38	430	390	120	830	58	360	260	340	290
n	4		2	1	4		1	4		3		1	2	1	1

Table 8. Chemical composition of sediments at Myllyvaara. Major elements in wt. %, trace elements in ppm.

	Quartzite		Siltstone											
			least altered (biotite ± sericite)		weakly albitized		weakly carbonated		intensively albitized + weakly carbonated		intensively albitized + intensively carbonated		intensively albitized + intensively carbonated + talc formation	
	avg	std	avg	std	avg	std	avg	std	avg	std	avg	std	avg	std
SiO2	79.50	4.39	62.46	3.62	65.03	2.44	66.12	2.41	67.18	0.90	46.96	10.13	51.26	4.87
TiO2	0.15	0.06	0.69	0.15	0.63	0.04	0.57	0.08	0.58	0.07	0.46	0.17	0.60	0.32
Al2O3	12.39	3.02	16.07	1.49	15.36	0.91	15.12	1.33	14.83	0.87	11.12	2.34	13.13	1.63
Fe2O3t	1.14	0.53	6.87	2.12	4.34	0.73	3.35	0.59	0.91	0.14	1.32	0.15	1.37	0.35
MnO	0.01	0.01	0.02	0.01	0.01	0.00	0.03	0.01	0.04	0.02	0.06	0.01	0.06	0.03
MgO	0.73	0.32	5.59	1.46	5.47	0.77	3.62	1.02	2.89	1.16	6.82	2.62	6.24	1.24
CaO	0.16	0.06	0.67	0.63	0.43	0.09	2.06	0.95	2.61	1.01	10.67	4.54	7.63	1.88
Na2O	2.86	2.17	1.91	1.28	5.62	0.70	1.26	1.16	7.94	0.38	5.94	1.29	7.02	0.88
K2O	2.75	1.57	4.95	1.57	2.33	0.41	4.90	1.12	0.17	0.10	0.20	0.11	0.12	0.02
P2O5	0.04	0.01	0.18	0.15	0.12	0.03	0.14	0.02	0.15	0.02	0.25	0.20	0.28	0.22
sum	99.83	0.09	99.56	0.55	99.46	0.58	96.52	1.56	97.39	0.98	83.86	5.83	87.77	2.57
Br	1.32	1.03	0.53	0.25	1.29	0.59	<1		1.88	0.86	1.41	0.53	1.60	0.83
S	<20		43	63	<20		28	26	<20		45	66	38	33
Sb	0.19	0.04	0.65	0.14	0.68	0.22	0.80	0.12	1.65	0.25	0.85	0.33	1.19	0.51
As	0.58	0.32	1.58	0.94	2.18	1.06	1.21	0.67	1.24	0.52	0.87	0.20	1.17	0.37
W	4.9	3.7	0.9	0.4	2.0	0.5	1.3	0.7	16.5	7.4	14.4	10.9	15.9	6.3
Cs	<1		1.25	0.52	<1		0.71	0.06	<1		<1		0.78	0.06
Rb	70	40	138	36	68	12	120	14	<10		<10		14	1
Ba	195	115	745	429	85	50	812	182	39	13	43	7	50	2
Cu	<10		<10		<10		<10		<10		<10		<10	
Co	2.8	1.0	11.6	3.1	9.3	2.1	7.4	1.5	3.1	1.4	3.0	1.1	5.0	1.4
Ni	<30		56	21	78	29	40	12	<40	13	<40		46	2
La	12.5	3.0	32.3	24.9	22.6	28.4	34.3	23.5	23.2	12.0	14.8	2.5	28.0	30.4
Sm	1.4	0.4	4.8	2.9	4.1	4.8	4.6	2.5	3.4	1.0	3.1	1.1	5.2	4.7
Sc	9.2	8.9	20.3	5.0	21.9	9.3	14.8	1.9	9.3	2.4	21.3	6.8	22.5	6.9
Ta	0.25	0.06	0.70	0.12	0.75	0.20	0.68	0.13	0.59	0.15	0.45	0.26	0.55	0.17
V	83	61	120	41	110	34	160	92	40	12	40	15	40	19
Cr	158	23	180	16	167	13	150	18	97	59	86	63	81	44
U	0.51	0.11	2.18	0.41	2.18	0.56	2.06	0.36	1.40	0.53	0.89	0.25	1.06	0.50
Th	3.15	0.78	14.1	2.0	13.8	2.5	12.6	3.0	12.2	2.3	7.51	2.73	7.97	0.85
Zr	148	53	190	95	220	27	170	94	200	6	120	54	170	67
n	4		8		5		5		3		5		4	

lamprophyres. The petrographical features in each lithological unit, however, imply several replacement reactions and chemical changes related to them. Some of reactions - [2] and [13] in lamprophyre dykes and [15] and [16] in sediments - have proceeded to the end, but some reactions (e.g., sericitization of biotite, [28]) have stopped before that. According to these reactions and the petrographical features, Fe, Mn, S, Cu, Ni, Co and the alkaline and alkaline-earth elements were mobile, the rocks were moderately hydrated, and the hydrothermal fluid was acid and weakly reducing.

CO_2 from the lamprophyre magma may also have been an altering agent during the formation of the least altered zones. According to Rock (1991), unaltered alkaline and calc-alkaline lamprophyres contain 2% CO_2 on an average. CO_2 is highly mobile and because there are no totally unaltered rock at Myllyvaara, it is difficult to estimate the primary CO_2 content of the lamprophyres. However, at least some lamprophyre units did not primarily contain any CO_2, because there are no carbonates in the

Table 9. Myllyvaara. Analyses compared in Figure 37, their densities, immobile element ratios and volume changes (= dV%). The samples of least altered rock are presented in italics. Abbreviations: ab = albitization, cb = carbonation, tc = talc formation. Intensity of alteration: w = weak, mod = moderate, int = intensive. Major elements in wt. %, trace elements in ppm. Number of samples calculated in each average is indicated in parentheses after the abbreviation "avg".

alteration	albitization + carbonation												talc formation	
rock	siltstone				lamprophyre								siltstone	
sample	*avg(8)*	avg(10)	avg(3)	avg(5)	*57-15*	57-16	*38-8*	36-11	*31-6*	36-11	*56-10*	37-4	avg(2)	57-8
type		w ab w cb	int ab w cb	int ab int cb		mod		mod		mod		int	int ab int cb	tc
SiO2	*62.46*	65.58	67.18	46.96	*55.67*	54.55	*50.76*	51.69	*50.40*	51.69	*50.72*	53.20	67.67	66.20
TiO2	*0.69*	0.60	0.58	0.46	*2.00*	1.92	*3.31*	3.99	*3.17*	3.99	*1.74*	1.72	0.56	0.63
Al2O3	*16.07*	15.24	14.83	11.12	*11.73*	11.69	*11.00*	13.02	*11.30*	13.02	*15.47*	15.90	14.34	15.83
Fe2O3	*6.87*	3.85	0.91	1.32	*8.65*	5.49	*14.16*	5.99	*14.07*	5.99	*11.67*	1.44	0.85	1.05
MnO	*0.02*	0.02	0.04	0.06	*0.03*	0.04	*0.02*	0.04	*0.02*	0.04	*0.02*	0.06	0.05	0.03
MgO	*5.59*	4.54	2.89	6.82	*7.82*	6.12	*7.48*	5.32	*7.64*	5.32	*4.96*	3.42	2.27	4.14
CaO	*0.67*	1.25	2.61	10.67	*4.27*	7.25	*3.16*	7.53	*3.32*	7.53	*3.47*	6.23	3.11	1.62
Na2O	*1.91*	3.44	7.94	5.94	*4.12*	5.69	*3.13*	5.81	*2.91*	5.81	*1.12*	8.29	7.75	8.34
K2O	*4.95*	3.62	0.17	0.20	*2.54*	1.03	*3.61*	1.41	*3.82*	1.41	*8.52*	0.20	0.17	0.16
P2O5	*0.18*	0.13	0.15	0.25	*1.08*	0.99	*2.47*	2.75	*2.45*	2.75	*0.90*	0.89	0.16	0.13
sum	*99.40*	98.26	97.32	83.80	*97.91*	94.77	*99.09*	97.55	*99.11*	97.55	*98.59*	91.35	96.91	98.13
Br	*0.53*	0.88	1.88	1.41	*1.11*	1.40	*<1*	<1	*<1*	<1	*4.75*	3.42	1.87	1.91
S	*43*	19	10	45	*0*	0	*50*	0	*130*	0	*940*	20	15	<10
Sb	*0.65*	0.74	1.65	0.85	*4.17*	2.16	*4.22*	5.25	*3.31*	5.25	*2.19*	3.44	1.07	1.56
As	*1.58*	1.69	1.24	0.87	*1.27*	2.18	*1.42*	8.54	*1.42*	8.54	*0.18*	0.21	1.78	1.39
W	*0.93*	1.65	16.5	14.4	*0.66*	5.86	*1.09*	14.5	*2.37*	14.5	*1.42*	0.82	17.9	11.1
Cs	*1.25*	<1	<1	<1	*<1*	<1	*2.31*	<1	*1.44*	<1	*2.74*	2.28	<1	<1
Rb	*138*	94	11	11	*100*	29	*177*	49	*186*	49	*205*	144	<20	<10
Ba	*745*	448	39	43	*440*	155	*5120*	160	*5010*	160	*8540*	4490	40	36
Cu	*<10*	<10	<10	<10	*<10*	<10	*<10*	<10	*<10*	<10	*<10*	<10	<10	<10
Co	*11.6*	8.3	3.1	3.0	*24.9*	4.9	*27.4*	6.9	*25.1*	6.9	*47.6*	50.8	3.2	3.1
Ni	*56*	59	35	38	*142*	88	*203*	170	*173*	170	*46*	37	<50	32
La	*32.3*	28.4	23.2	14.8	*127*	113	*207*	166	*217*	166	*34.9*	43.6	18.9	31.9
Sm	*4.8*	4.3	3.4	3.1	*13.1*	12.1	*22.6*	23.7	*22.5*	23.7	*6.0*	6.4	3.3	3.6
Sc	*20.3*	18.4	9.3	21.3	*28.2*	25.6	*38.1*	44.2	*39.9*	44.2	*44.1*	58.7	8.4	11.3
Ta	*0.70*	0.71	0.59	0.45	*1.16*	1.05	*11.4*	12.9	*15.9*	12.9	*0.72*	0.34	0.52	0.74
V	*116*	137	43	43	*190*	220	*180*	380	*190*	380	*320*	100	40	50
Cr	*180*	159	97	86	*350*	265	*253*	280	*287*	280	*56*	40	64	164
U	*2.18*	2.12	1.40	0.89	*4.63*	3.98	*7.46*	9.21	*4.29*	9.21	*3.34*	2.99	1.10	2.00
Th	*14.1*	13.2	12.2	7.5	*26.8*	27.8	*20.7*	23.0	*20.0*	23.0	*7.3*	5.7	11.2	14.3
Zr	*194*	195	203	120	*800*	800	*2330*	2690	*2260*	2690	*360*	360	200	210
Al/Ti	*23.4*	25.4	25.4	24.2	*5.87*	6.09	*3.33*	3.26	*3.56*	3.26	*8.91*	9.24	25.5	25.1
Ti/Zr	*35.4*	30.8	28.7	38.3	*25.0*	24.0	*14.2*	14.8	*14.0*	14.8	*48.2*	47.8	28.1	30.0
Al/Zr	*829*	782	730	926	*147*	146	*47.2*	48.4	*50.0*	48.4	*430*	442	717	754
density (kg/m3)	*2766*	2736	2618	2675	*2816*	2745	*2925*	2766	*2956*	2766	*2796*	2688	2612	2630
dV%		+16	+24	+54		+3		-8		-10		+4		-12
ref. to Fig.		37A	37B	37B		37C		37C		37C		37C		37D

least altered dykes. In addition, these dykes contain epidote and sphene that only are stable only when X_{CO2} is extremely low (Thompson 1971, Hunt and Kerrick 1977, Winkler 1979).

The volume changes and chemical mass balances related to the formation of more altered zones were calculated using formulae [1] and [2]. The compared analyses, their immobile

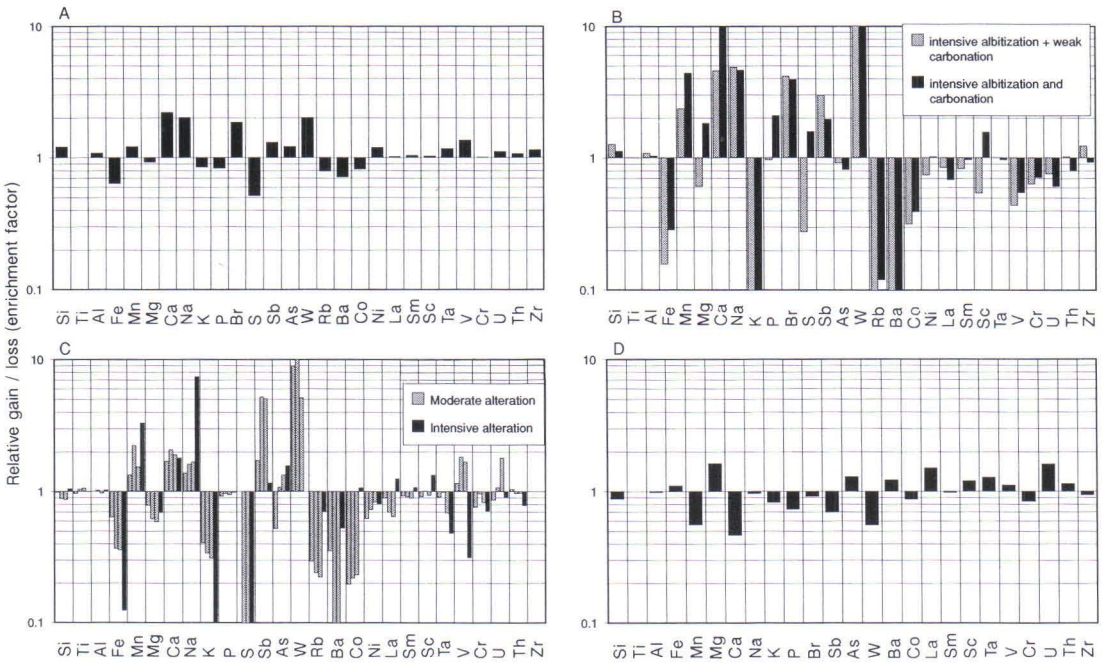

Fig. 37. Enrichment factors of the elements showing chemical gains and losses during the alterations at Myllyvaara (y-axis). Only analytical results with small errors are used in the calculations, so that the sets are different in the figures. The main components are presented in a typical order of analytical results. The general mobility of the trace elements decreases from left to right (Rose et al. 1979). The calculations are based on comparisons between average compositions, except in Figure C, where altered and least altered samples are compared one by one. Note the logarithmic scale of the y-axis. **A**: Weak albitization and carbonation of siltstone. **B**: Intensive albitization and weak carbonation (gray columns) and intensive albitization and intensive carbonation (black columns) of siltstone. **C**: Albitization and carbonation of lamprophyres. **D**: Talc formation of intensively albitized and moderately carbonated siltstone.

element ratios and volume changes are presented in Table 9.

Weak albitization and carbonation

The relative chemical changes related to weak albitization and carbonation of the siltstone are shown in Figure 37A, and the changes related to moderate albitization and carbonation of the lamprophyre in Figure 37C. The mass balance calculations indicate volume changes of -10% - +3% in the lamprophyre and approx. +15% in the siltstone (Table 9). This implies that, at this alteration stage, the brecciation was much more intensive in the siltstone than in the lamprophyre dykes.

Several elements were immobile or their mobility was minimal when the process of albitization and carbonation were weak or moderate. The alteration trends are nearly equal in the siltstone and in the lamprophyres: depletion of Fe, Mg, K, S, Rb, Ba and Co; enrichment of Si, Mn, Ca, Na, Br, Sb, W and V; and immobility of Ti, Al, Sc, Sm, Th and Zr. In addition, P, As, Ni, REE, Ta, Cr and U were mainly immobile during weak alteration, but became mobile with increasing alteration intensity. Reactions [16], [17], [21], [26] and [33] (Table 2) explain most of the chemical changes in the lamprophyres and reactions [16]-[18], [21] and [26] in the siltstone. Reactions indicate weakly acid, oxidizing conditions with high a_{Na+}/a_{K+} in the fluid. The acidity of the fluid probably lim-

ited the precipitation of carbonate. The changes in the concentrations of As, Sb and W remain unexplained; formation of scheelite is neccessary to explain the enrichment of W in the rocks.

Intensive albitization and carbonation

The chemical trends of weak alteration become more distinct with intensifying carbonation and albitization. The changes in rock volume are still dependent on the lithology: there is no remarkable change in the lamprophyres, but the volume increase in the siltstone is 20 - >50% (Table 9).

The chemical alteration trends in the siltstone were (Fig. 37B): depletion of Fe, K, Rb, Ba, Co, V, Cr and U and enrichment of Si, Mn, Ca, Na, Br, Sb and W. In the lamprophyres, the trends were (Fig. 37C): depletion of Si, Fe, Mg, K, S, Rb, Ba, Co, Ta and V and enrichment of Mn, Ca, Na, Sb, As and Sc. Thus, the trends of the main components and Sb, Rb, Ba, Co and V were equal in all lithological units regardless of the intensity of carbonation. The same reactions ([16]-[18], [21], [26] and [33]), equal f_{O2}, but increased f_{CO2}, a_{Na+}/a_{K+} and pH as in the weakly albitized and carbonated zones explain the chemical changes. The mobility of REE during the intensive carbonation is demonstrated by Figure 38: Eu and the HREE were enriched over the LREE in the carbonate-bearing fluids and in the extremely carbonated zones.

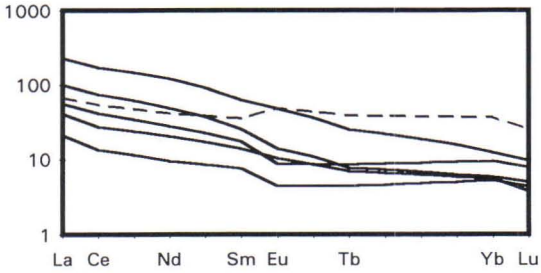

Fig. 38. Chondrite-normalized REE patterns of siltstone. Solid lines: weakly or moderately carbonated types (0.1-14% CO_2), dotted line: extremely carbonated type (34% CO_2). Volume change during extreme carbonation was 50%. Normalizing values from Hickey and Frey (1982).

Chloritization and talc formation

It was not possible to treat chloritization with mass balance calculations, because suitable sample pairs were not found. However, the mineral assemblages indicate that the chloritization reactions [9], [10], [19] and [27] took place. According to them, Fe, Mn, Mg, Ca, K, Rb, Ba Cu, Ni and Co were mobilized and the fluid was weakly acid, possibly CO_2-bearing, and its a_{Mg2+}/a_{K+} and a_{Mg2+}/a_{Na+} were high.

Talc formation only took place in the sediments. Rock volume was decreased (Table 9), thus replacement was the dominant alteration type and brecciation minimal. The chemical changes of the major components (Fig. 37D) well reflect the changes in mineral assemblages: talc mainly replaced dolomite [20] and filled fractures [30], but replaced albite [31] and chlorite [32] only in small amounts. The fluid was thus much like the chloritizing fluid, but its a_{Mg2+} was higher. Reactions that could explain the mobility of trace elements remain unclear. It is possible that the differences in the concentrations of trace elements between compared samples reflect the differences before talc formation.

Lehtovaara

The least altered rocks

The chemical data for the least altered albite diabase (amphibole zone type, Table 10, p. 68) lie inside the igneous field on an alkali ratio diagram (Fig. 39). This suggests that, in addi-

Table 10. Chemical composition of albite diabases and lamprophyres at Lehtovaara. Major elements in wt. %, trace elements in ppm.

	Albite diabase									lamprophyre	
	least altered (amphibole zone)		chloritized		biotitized		carbonated		sericitized + weakly carbonated	least altered (moderately carbonated)	intensively carbonated
	avg	std	avg	std	avg	std	avg	std			
SiO2	50.33	0.69	52.20	0.88	52.05	1.55	56.13	5.52	53.56	54.40	54.27
TiO2	0.80	0.04	0.81	0.05	0.86	0.07	0.66	0.07	0.89	1.80	1.79
Al2O3	12.41	0.22	14.79	0.50	14.06	0.99	12.12	1.02	14.40	14.52	15.11
Fe2O3t	15.72	0.89	15.86	0.99	17.09	2.23	4.34	0.61	19.55	4.73	1.66
MnO	0.16	0.03	0.09	0.01	0.04	0.01	0.09	0.03	0.07	0.04	0.05
MgO	6.21	0.27	5.77	0.91	5.24	0.73	3.54	1.08	2.45	4.35	2.51
CaO	10.40	0.75	6.62	2.02	3.53	1.40	7.36	2.43	2.40	4.84	6.20
Na2O	2.20	0.58	2.86	0.74	4.14	0.25	6.42	0.64	2.61	6.19	8.04
K2O	0.23	0.07	0.27	0.18	2.64	0.42	0.19	0.08	3.28	1.75	0.24
P2O5	0.06	0.00	0.06	0.01	0.07	0.01	0.05	0.01	0.08	1.27	1.27
sum	98.81	0.70	99.44	0.72	99.87	0.15	92.91	1.97	99.45	95.25	93.13
Br	0.36	0.10	0.77	0.57	<0.5		0.47	0.21	0.26	<0.5	<0.5
S	190	197	260	320	650	765	8180	4710	250	110	50
Sb	0.26	0.06	0.21	0.11	0.15	0.09	0.25	0.10	0.19	0.54	0.95
As	1.14	0.25	1.26	0.79	0.58	0.27	4.32	3.69	0.50	1.11	1.29
W	<1		0.85	0.33	1.41	0.59	17.0	14.1	<1	6.54	26
Cs	<0.7		<1		3.49	4.19	<1		0.70	0.62	<0.6
Rb	<10		<15		100	25	<15		10	60	<10
Ba	65	42	<50		154	113	35	11	441	491	<40
Cu	130	46	30	5	<10		50	32	<10	<10	<10
Co	49	4	48	6	54	34	116	64	24	23	<5
Ni	91	19	68	18	90	26	54	14	63	54	<40
La	1.2	0.5	1.3	0.5	3.5	1.7	7.1	4.7	2.7	138	162
Sm	1.2	0.1	1.1	0.3	1.6	0.5	1.4	0.3	1.2	14	16
Sc	50	4	42	8	35	6	25	28	35	23	10
Ta	<0.5		<0.5		<0.5		<0.5		0.12	1.36	1.66
V	380	12	350	50	380	43	90	58	400	200	150
Cr	158	19	47	19	57	35	<40		77	127	114
U	<0.2		<0.2		0.21	0.11	1.22	0.88	0.37	6.31	4.01
Th	<0.3		<0.3		0.33	0.09	0.52	0.25	0.19	17	20
Zr	50	5	50	11	50	5	50	6	60	490	480
n	7		5		4		3		1	1	1

tion to hydration, the alterations had a minor chemical effect on the least altered part of the diabase. The formation of the amphibole zones is fairly well characterized by reaction [1] (Table 2), according to which Mn, Mg, Ca, Na and S were mobile, but were not significantly enriched or depleted by the acid, weakly reducing fluid of the alteration type.

The least altered types of quartzite are the non-feldspathic and the K-feldspar-bearing ones, while layers in which albite has completely

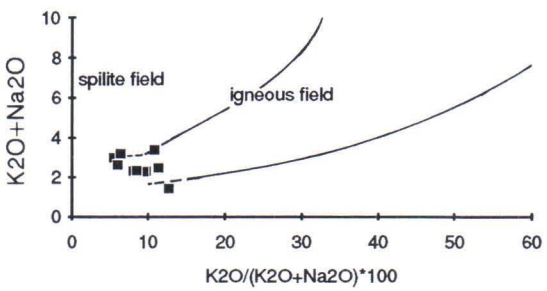

Fig. 39. The least altered albite diabase at Lehtovaara, plotted on the alkali ratio diagram of Hughes (1973).

Table 11. Chemical composition of quartzite at Lehtovaara.
Major elements in wt. %, trace elements in ppm.

	Quartzite									
	a non-feldspatic layer		K-feldspar partially albitized		feldspars totally albitized		feldspars and sericite albitized		albitized + carbonated	
	avg	std	avg	std	avg	std	avg	std	avg	std
SiO2	85.10	2.03	83.68	2.42	80.96	3.34	82.50	3.65	81.52	1.24
TiO2	0.10	0.01	0.11	0.04	0.19	0.09	0.17	0.09	0.15	0.03
Al2O3	8.13	1.10	9.20	1.46	10.72	1.84	9.75	1.21	10.04	0.55
Fe2O3t	1.94	0.51	1.46	0.27	1.99	0.82	0.81	0.17	1.44	0.35
MnO	0.01	0.01	0.01	0.00	0.01	0.01	0.02	0.01	0.01	0.00
MgO	1.23	0.67	0.28	0.10	0.78	0.54	0.33	0.40	0.88	0.34
CaO	0.15	0.20	0.09	0.05	0.13	0.15	0.56	0.79	0.58	0.18
Na2O	0.17	0.18	2.59	0.10	1.86	0.71	4.87	0.31	1.09	1.02
K2O	2.87	0.35	2.29	0.73	2.83	0.62	0.43	0.27	2.76	0.73
P2O5	0.01	0.00	0.01	0.01	0.01	0.01	0.02	0.00	0.02	0.03
sum	99.77	0.03	99.82	0.04	99.64	0.42	99.51	0.57	98.60	0.43
Br	0.38	0.21	1.83	1.53	0.59	0.43	1.63	2.09	0.23	0.06
S	<20		<20		<20		80	127	220	360
Sb	0.08	0.01	0.09	0.00	0.11	0.04	0.17	0.06	0.08	0.02
As	0.29	0.11	0.37	0.13	0.34	0.14	0.70	0.28	0.27	0.08
W	0.58	0.26	0.69	0.23	1.20	0.59	2.85	0.68	1.24	0.59
Cs	1.07	0.50	0.63	0.05	0.85	0.47	<0.5		0.64	0.19
Rb	76	11	59	25	74	17	14	8	71	18
Ba	133	70	364	94	380	162	66	39	440	245
Cu	<10		<10		<10		<10		<10	
Co	4.9	2.4	<3		5.0	4.1	4.9	2.0	4.0	1.7
Ni	<20		<30		<30		<30		<20	
La	12.5	7.7	8.8	7.1	11.0	4.7	15.4	0.5	11.4	6.4
Sm	1.5	0.7	1.2	0.7	1.4	0.5	1.8	0.4	1.2	0.5
Sc	2.6	0.3	2.9	1.1	4.7	1.7	3.5	2.1	3.5	0.3
Ta	0.21	0.08	0.32	0.04	<0.3		<0.3		0.29	0.09
V	30	10	20	15	50	19	50	46	40	12
Cr	25	2	29	9	39	17	48	28	37	7
U	0.36	0.07	0.52	0.12	0.55	0.18	1.06	0.98	0.43	0.08
Th	2.34	0.31	2.27	0.33	3.04	0.85	2.54	0.91	2.85	0.20
Zr	60	0	70	12	90	35	90	40	80	13
n	4		3		18		3		5	

replaced the other feldspars, i.e. zones of moderate albitization, cover wide areas. This is supported by the data of Table 11 and Figure 40 (p. 71). The sedimentary layers and albitized zones indicated in Figure 40 mostly overlap and are therefore presented as a single group in Figure 41 (pp. 72-73). The moderate albitization thus had no significant effect on the chemical composition of the quartzite except for the alkaline elements, and the chemical differences between the least altered types are mostly due to the primary differences between the sediment layers. Reactions [14] and [16] explain the albitization of the feldspars in the quartzites, implying a high a_{Na+}/a_{K+} in the fluid.

The volume changes and chemical mass balances related to the formation of the other diabase alteration zones were calculated using formulae [1] and [2]. The analyses compared, their immobile element ratios and volume changes are presented in Table 12.

Table 12. Lehtovaara. Analyses compared in Figure 42, their densities, immobile element ratios and volume change (= dV%). The samples of least altered rock are presented in italics. Major elements in wt. %, trace elements in ppm.

alteration	chloritization		biotitization		carbonation				carbonation + sericitization	
rock	albite diabase						lamprophyre		albite diabase	
sample	*39-2*	15-3	*52-4*	52-13	*39-2*	1042-1	*54-5*	54-4	*15-5*	55-2
SiO2	*50.87*	51.54	*51.02*	51.30	*50.87*	49.91	*54.40*	54.27	*51.08*	53.56
TiO2	*0.68*	0.74	*0.83*	0.87	*0.68*	0.64	*1.80*	1.79	*0.78*	0.89
Al2O3	*13.79*	14.70	*12.57*	13.44	*13.79*	13.12	*14.52*	15.11	*13.04*	14.40
Fe2O3t	*15.32*	16.62	*15.99*	17.42	*15.32*	4.76	*4.73*	1.66	*15.64*	19.55
MnO	*0.18*	0.08	*0.12*	0.04	*0.18*	0.12	*0.04*	0.05	*0.13*	0.07
MgO	*5.90*	6.23	*6.18*	6.22	*5.90*	4.78	*4.35*	2.51	*5.78*	2.45
CaO	*10.04*	6.42	*10.19*	2.98	*10.04*	10.06	*4.84*	6.20	*10.15*	2.40
Na2O	*2.43*	3.22	*2.06*	4.44	*2.43*	6.88	*6.19*	8.04	*2.34*	2.61
K2O	*0.16*	0.19	*0.22*	2.99	*0.16*	0.27	*1.75*	0.24	*0.13*	3.28
P2O5	*0.06*	0.06	*0.07*	0.07	*0.06*	0.06	*1.27*	1.27	*0.07*	0.08
Sum	*99.41*	99.79	*99.25*	99.77	*99.55*	90.61	*93.90*	91.13	*99.14*	99.29
Br	*0.54*	1.59	*<0.5*	<0.5	*0.54*	0.65	*<0.5*	<0.5	*0.36*	0.26
S	*270*	70	*520*	560	*270*	2750	*110*	50	*100*	250
Sb	*0.24*	0.24	*0.21*	0.07	*0.24*	0.34	*0.536*	0.951	*0.19*	0.19
As	*1.45*	1.14	*1.00*	0.37	*1.45*	2.14	*1.11*	1.29	*1.39*	0.50
W	*<1*	0.53	*<1*	<1	*0.73*	11.00	*6.54*	26.4	*0.30*	0.85
Cs	*<1*	<1	*0.50*	3.22	*<1*	<1	*0.62*	<1	*<1*	0.70
Rb	*<15*	<15	*7.3*	120	*<15*	13.8	*60.1*	9.2	*<15*	<15
Ba	*41*	<50	*41*	297	*41*	47	*491*	40	*45*	441
Cu	*160*	30	*140*	20	*160*	60	*<10*	<10	*110*	0
Co	*49*	44	*52*	38	*49*	48	*23.1*	3.05	*46*	24
Ni	*77*	67	*105*	86	*77*	45	*54.4*	36.7	*40*	63
La	*1.35*	<1	*1.07*	5.55	*1.35*	5.84	*138*	162	*1.91*	2.73
Sm	*1.05*	1.14	*1.35*	1.33	*1.05*	1.45	*13.8*	16.3	*1.35*	1.16
Sc	*48.4*	41.9	*46.6*	42.5	*48.4*	57.3	*22.8*	10.3	*47.7*	34.8
Ta	*<0.5*	<0.5	*<0.5*	<0.5	*0.24*	0.35	*1.36*	1.66	*0.26*	<0.5
V	*330*	330	*380*	390	*330*	160	*200*	150	*370*	400
Cr	*47*	36	*147*	91	*47*	35	*127*	114	*42*	77
U	*0.10*	0.20	*0.11*	0.36	*0.10*	0.57	*6.31*	4.01	*0.10*	0.37
Th	*<0.5*	<0.5	*0.21*	0.41	*<0.5*	<0.5	*17.2*	20.1	*<0.5*	<0.5
Zr	*50*	60	*50*	50	*50*	40	*490*	480	*50*	60
Al/Ti	*20.3*	19.9	*15.2*	15.5	*20.3*	20.4	*11.9*	11.4	*16.7*	16.1
Al/Zr	*2758*	2450	*2514*	2688	*2758*	3280	*296.3*	314.79	*2608*	2400
Ti/Zr	*136*	123	*165*	174	*136*	161	*36.8*	37.2	*157*	149
density (kg/m3)	*2972*	2893	*3059*	2924	*2972*	2449	*2580*	2561	*2973*	2837
dV%		-5		±0		+28		±0		-8
ref. to Fig.		42A		42B		42C		42D		42E

Intensive albitization of quartzite

The chemical changes that occurred during the intensive albitization of the quartzite are presented in Figure 41. On account of the primary compositional differences between the sediment layers, no sample pairs suitable for mass balance calculations was found. The

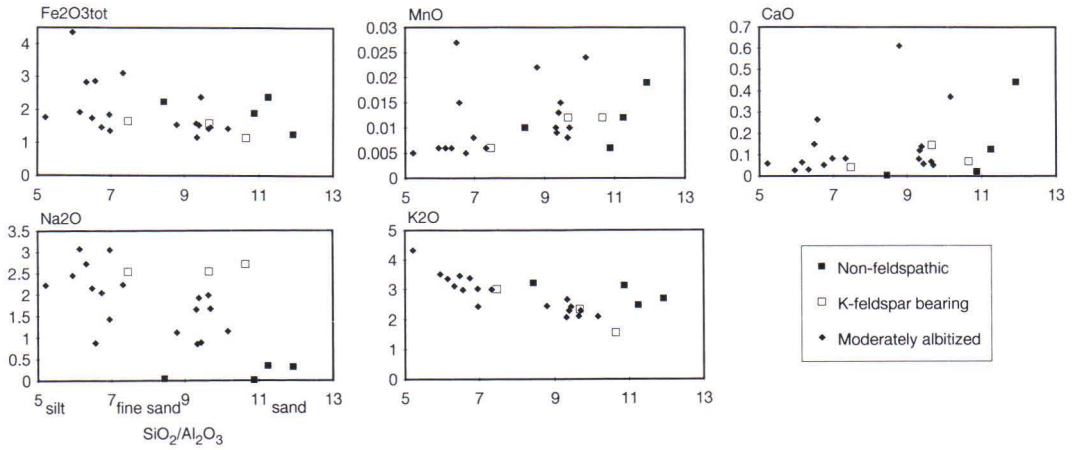

Fig. 40. Plots of the most mobile major elements vs. SiO_2/Al_2O_3 in the least altered types of quartzite at Lehtovaara. The ranges of SiO_2/Al_2O_3, a rough measure of the grain size of sediments (Taylor and McLennan 1985), for silt, fine sand and sand are indicated at the bottom of the figure.

grade of brecciation is extremely low and the Si vs. SiO_2/Al_2O_3 and Al vs. SiO_2/Al_2O_3 correlations are good, so that the volume change and Si and Al mobility connected with the alteration were probably low. Figure 41 gives only the alteration trends, which become more distinct if the change in concentration is large. Na, As, Sb and W enrichment and Fe, K, Ba and Rb depletion took place during the intensive albitization of the quartzites, whereas Si, Ti, Al, Co, Sc, Th, V and Zr were immobile. The mobility of the other elements is unclear, partly because of the overlapping weak carbonation and partly because of primary differences between the sediment layers. Reactions [14], [16] and [18] (Table 2) explain the mobility of the alkaline and alkaline-earth elements and imply a high a_{Na+}/a_{K+} and a_{Na+}/a_{Fe2+} fluid. The Fe loss can be explained by the albitization of sericite [18], as sericite can incorporate much more Fe than albite (Deer et al. 1962a, Smith and Brown 1988).

The enrichment of As and Sb is combined with weak sulphide formation, but the absolute amounts of As and Sb in the quartzite are low, and it is thus possible that the enrichment of these elements indicates a weak, reducing, but independent alteration stage postdating albitization and carbonation. This is also supported by the quartzite samples with the highest S concentrations, which are found in both the least altered and the intensively albitized and the carbonated zones (Fig. 41). This kind of alteration is related to late stage sericitization at Palovaara, but at Lehtovaara the latter is weakly developed and identifiable only in the albite diabase.

Chloritization

Several elements were immobile during chloritization of the albite diabase (Table 12 and Fig. 42A, p. 74). The rock volume loss was approx. 5% (Table 12). The most notable relative chemical changes were the losses of Si, Mn, Ca, S, As, Cu and Cr and the gains in Na, Br and U, most of which are explained by reactions [6], [8] and [9]. In addition, the depletion of S, As and Cu can be explained by sulphide decomposition (reactions [34] and [35]) and the enrichment of Br and U by their fixation in

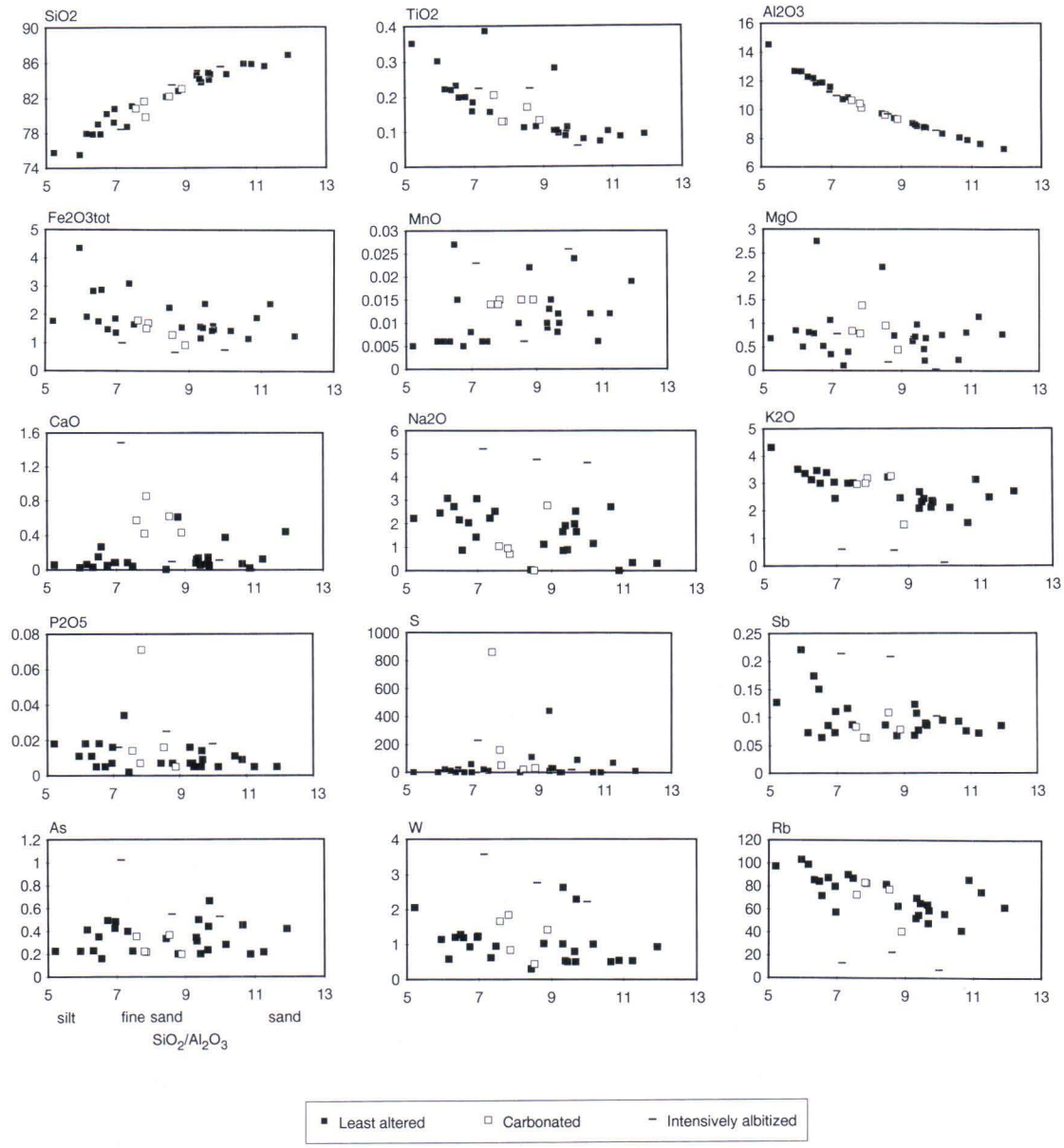

Fig. 41. Plots of major and trace elements vs. SiO_2/Al_2O_3 for the least altered, carbonated and intensively albitized types of quartzite at Lehtovaara. The ranges of SiO_2/Al_2O_3, a rough measure of the grain size of sediments (Taylor and McLennan 1985), for silt, fine sand and sand are indicated at the bottom of the figure.

the chlorite lattice, but the reason for the Cr depletion remains unclear. The reactions imply an acid, weakly reducing, intensively hydrating fluid.

Biotitization

Most elements were immobile during biotitization of the albite diabase and the volume

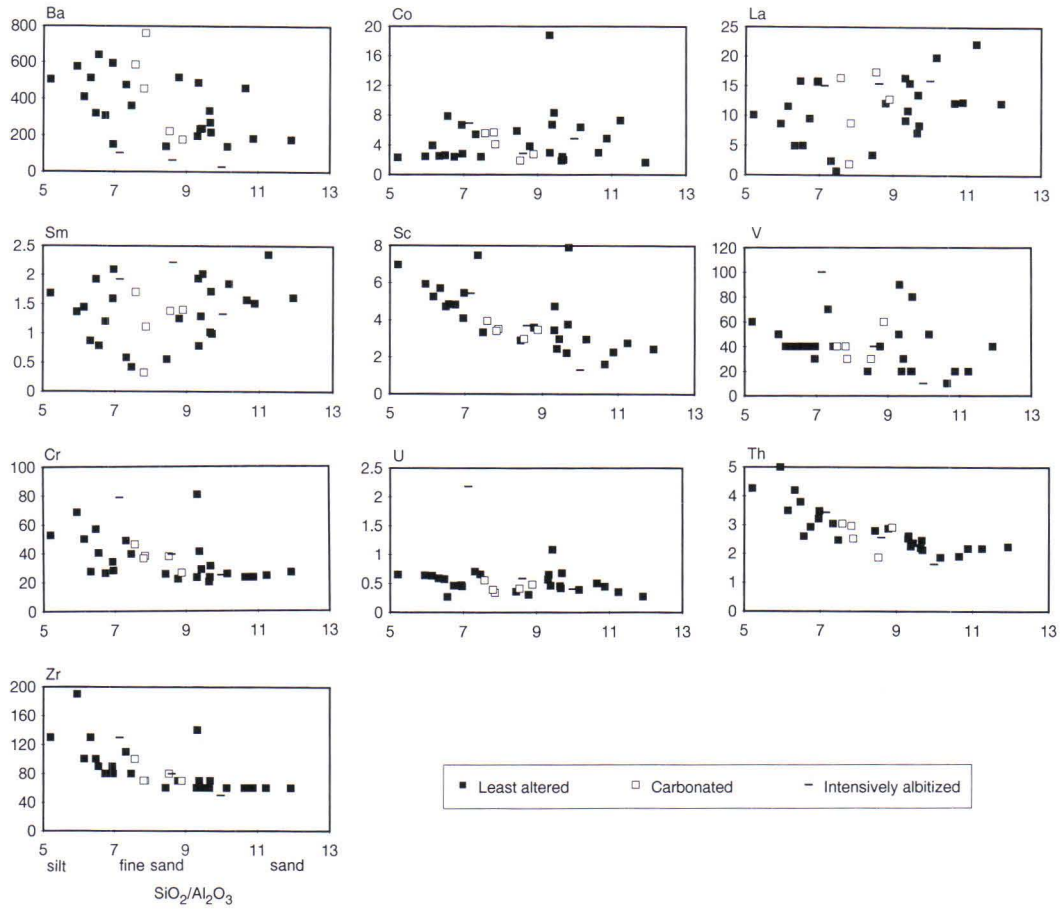

Fig. 41. Continued.

changes were negligible (Table 12 and Fig. 42B). Mn, Ca, Sb, As, Cu, Co and Cr were depleted and Na, K, Cs, Rb, Ba, La, U and Th enriched. The reactions [10] and [12] explain the mobility of Mn, alkaline and alkaline-earth elements, while the Sb, As, Cu, Co and Ni mobilities may be related to reactions [10] and [33]. The reactions imply a near-neutral or mildly acid, weakly reducing fluid with low a_{Ca2+}/a_{K+}. Only the reasons for La, Cr, U and Th mobility remain unclear, and it is possible that their mobility may be related to the later, weak carbonation, although the fluctuation in f_{O2} can also explain the mobility of U.

Carbonation

The chemical changes related to the carbonation of the quartzite were mostly insignificant (Fig. 41), and only Ca was indisputably mobile. The reason for the small obvious changes was the low intensity of carbonation.

The changes were far greater in the mafic rocks than in the quartzite. Iron, Mn, Mg, Cu, Ni, V and Cr concentrations decreased in the albite diabase (Fig. 42C) and Na, K, S, Sb, As, W, La, Sm, Sc and U increased, while in the lamprophyre (Fig. 42D) the Fe, Mg, K, S, Rb, Ba, Co, Ni, Sc, V and U concentrations de-

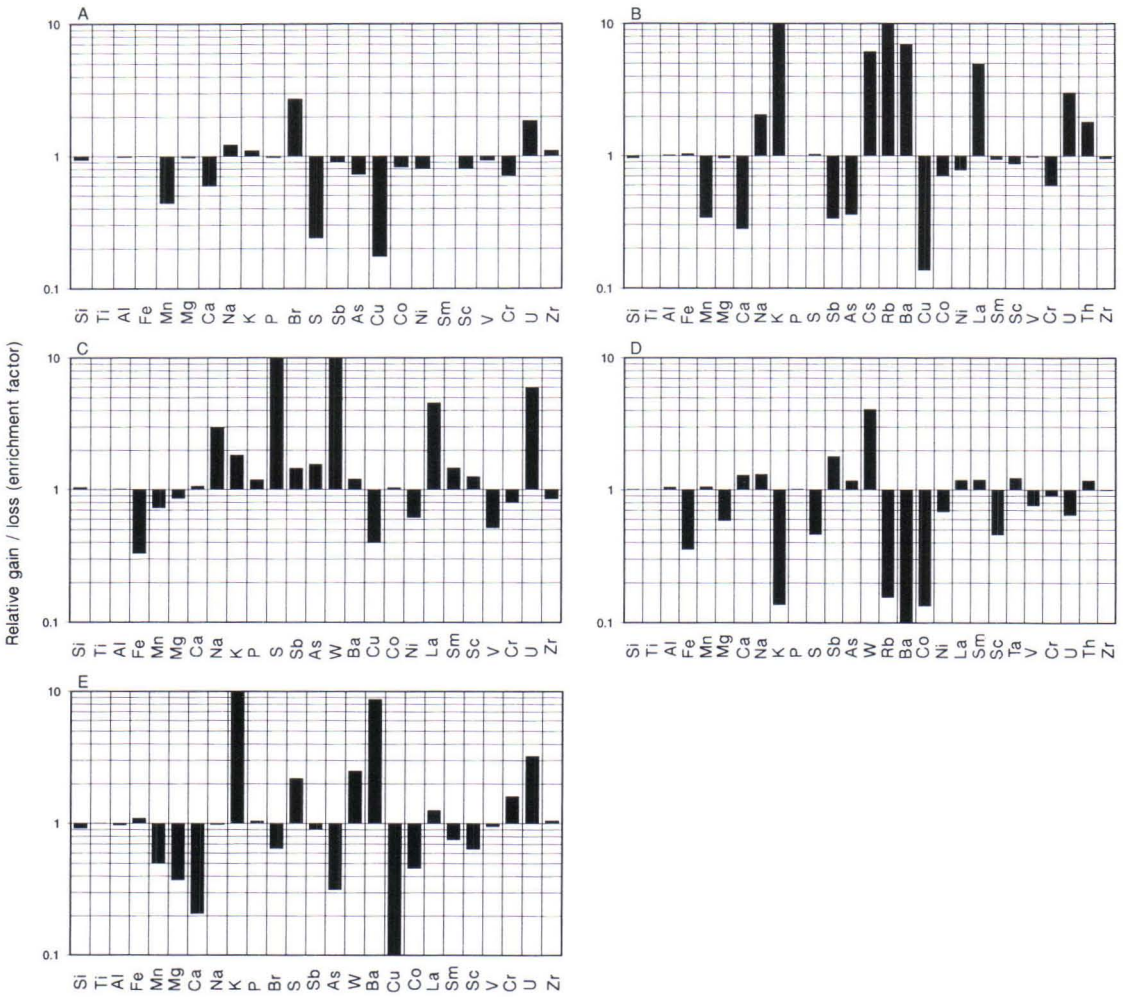

Fig. 42. Enrichment factors of the elements showing the chemical gains and losses during alterations in diabase and lamprophyre at Lehtovaara (y-axis). Only analytical results with small errors are used in the calculations, so that the element sets are different in the figures. The main components are presented in a typical order of analytical results. The general mobility of the trace elements decreases from left to right (Rose et al. 1979). The calculations are based on comparisons between one altered and one less altered sample. Note the logarithmic scale of the y-axis. **A**: Chloritization of albite diabase. **B**: Biotitization of albite diabase. **C**: Albitization and carbonation of albite diabase. **D**: Advanced albitization and carbonation of lamprophyre. **E**: Carbonation and sericitization of albite diabase.

creased and Ca, Na, Sb and W increased parallel with the progression of carbonation. The grade of brecciation is reflected in the rock volume changes, and only the albite diabase was brecciated intensively, giving a volume increase of nearly 30% in the highly carbonated zones (Table 12). The lamprophyre and quartzites did not brecciate and their volume did not change. The carbonation reactions [21], [23] and [26] explain most of the chemical changes in the albite diabase, [17] and [25] in the lamprophyre, and [29] in the quartzite. Reaction [33] or [34] will explain the mobility of S in each carbonated zone, and possibly that of Sb, As, Cu, Co and Ni. The reactions and the grade of the chemical changes imply to a dehydrating,

near-neutral, Na-rich fluid with fluctuating f_{O2} and f_{CO2}. Scheelite formation is required for thorough W enrichment.

The apparent increase in K concentration related to the carbonation of the albite diabase (Fig. 42C) is actually caused by the overlapping of the biotitized and carbonated zones in the carbonated sample used in the mass balance calculations. The grade of biotitization of this sample is so low, however (Table 12) that it most probably had no appreciable effect on the concentrations of the elements other than K.

Sericitization

The chemical changes demonstrated in Figure 42E and the comparison between the chemical compositions of the alteration types (Tables 10 and 12) indicate a distinct sericitization trend: losses of Si, Mn, Mg, Ca, Br, As, Cu, Co, Sm and Sc and gains in K, S, W, Ba, Cr and U. Most of the chemical changes can be combined with the carbonation and sericitization reactions [18], [21], [22], [24]-[26] and [28] (Table 2) and acid fluid with a low a_{Ca2+}/a_{K+} and a_{Na+}/a_{K+}. The reactions [33] and [34] explain the mobility of S, As, Cu and Co and scheelite formation the increase in W concentration. The acidity of the fluid may have been caused by H^+ release during carbonation, which implies that sericitization was a later phase of the carbonation stage. If this was the case, the small area covered by sericitization indicates that either the a_{K+} of the carbonating fluid or the H^+ release related to carbonation was high only in restricted areas at Lehtovaara.

Sivakkavaara

The least altered rocks

The chemical compositions of the rocks in the alteration zones are presented in Tables 13-16 (pp. 76-79). The chemical data for the least altered albite diabase and felsic dykes plotted on an alkali ratio diagram (Hughes 1973) indicate that most samples are inside the igneous field (Fig. 43). This suggests that, other than hydration, the alterations had only minor chemical effects on the inner part of the dykes. The occurrence of K feldspar and the low concentrations of hydrous minerals also indicate a very low grade of alteration in the interiors of the felsic dykes.

The formation of the least altered zones in the diabase dykes was characterized by a combination of reactions [1] and [8], but only by reaction [11] in the felsic dykes (Table 2). These reactions imply that Si, Mn, Mg, Ca, Na, S, Cu, Ni and Co were mobile in the diabase and Ca and K in the felsic dykes. The fluid was weakly acid and reducing in the diabase but may have been near neutral in the felsic dykes.

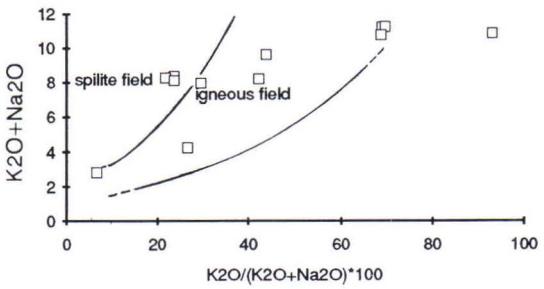

Fig. 43. The least altered igneous rocks at Sivakkavaara, plotted on the alkali ratio diagram of Hughes (1973).

The absolute element enrichments and depletions in the diabase and felsic dykes were weak however (Fig. 43), consisting only of modest gains and losses in the concentrations of the alkaline elements.

The mineral association of the least altered, inner part of the lamprophyre was probably formed by the decomposition of primary silicates and oxides by low pH, weakly reducing fluid (reaction [2]). Related to this reaction,

Table 13. Chemical compositions of albite diabases and lamprophyre at Sivakkavaara.
Major elements in wt. %, trace elements in ppm.

	Northern albite diabase			Southern albite diabase			lamprophyre			
	least altered (amhibole-biotite)		intensively carbonated + biotitized	least altered (amhibole-biotite)	intensively biotitized	carbonated + intensively biotitized	least altered (weakly carbonated)	carbonated		carbonated and sericitized
	avg	std						avg	std	
SiO2	50.96	1.08	46.37	50.60	48.81	51.25	48.50	46.17	0.57	46.50
TiO2	0.98	0.06	0.96	0.42	0.39	0.50	1.28	1.25	0.16	1.35
Al2O3	13.38	0.18	12.63	15.38	13.03	14.94	11.00	11.10	0.78	12.00
Fe2O3t	12.66	1.93	12.54	12.88	12.78	11.54	10.07	9.35	2.44	11.03
MnO	0.19	0.02	0.19	0.04	0.04	0.03	0.13	0.18	0.04	0.14
MgO	6.79	0.31	6.75	8.30	9.99	9.08	10.40	8.13	0.50	7.17
CaO	8.94	1.41	4.46	6.09	4.95	2.29	8.06	6.12	1.60	5.82
Na2O	2.12	0.52	3.51	3.11	2.27	3.42	2.16	2.78	0.63	2.79
K2O	1.81	0.88	3.97	2.70	5.81	4.26	2.74	3.54	0.80	3.61
P2O5	0.09	0.01	0.08	0.03	0.03	0.04	0.59	0.67	0.01	0.69
sum	98.92	1.10	91.77	99.17	98.35	97.69	95.60	91.87	1.88	93.70
Br	1.12	0.67	<1	<1	<1	<1	1.17	<1		<1
S	590	173	990	110	120	2610	140	1160	588	280
Sb	1.41	0.17	0.39	0.55	0.36	0.29	1.06	2.13	1.39	1.39
As	9.39	2.14	1.72	2.24	0.91	2.63	2.86	2.04	0.22	2.59
W	<1		2.26	<1	<1	<1	<1	18.2	15.7	11.6
Cs	1.05	0.38	3.98	1.43	4.29	4.29	3.55	3.21	2.14	4.00
Rb	54	25	156	74	191	192	99	103	76	156
Ba	629	300	1040	404	636	569	3490	2788	2525	2700
Cu	140	22	30	30	20	20	30	40	15	20
Co	42	4	25.8	26.4	25.4	79.7	43.2	17	12	58.2
Ni	80	26	65.8	106	139	146	116	105	53	79.4
La	5.61	0.91	16.7	3.49	51.5	17.0	52.7	80.4	22.1	65.1
Sm	2.36	0.36	4.31	1.17	5.70	<2	7.19	10.9	3.9	8.43
Sc	62	2	55.5	48.5	45	47.4	55.7	44	12	53.7
Ta	<0.2		0.16	<0.2	<0.2	<0.2	0.80	0.92	0.11	1.03
V	300	13	290	240	190	220	230	210	35	220
Cr	262	57	187	187	464	262	962	448	347	538
U	<0.3		0.86	<0.3	0.58	1.19	4.46	3.29	0.91	3.77
Th	0.56	0.20	0.60	<0.5	<0.5	0.60	25	23	5	26
Zr	90	9	70	30	30	40	380	390	65	400
n	6		1	1	1	1	1	3		1

Mn, S and the alkaline and alkaline-earth elements were mobile. More precise estimates are not possible, because unaltered lamprophyre does not exist and the common diagrams used to test alterations in igneous rocks are not suitable for lamprophyres.

The least altered type of quartzite is characterized by the albitization reactions [14], [16] and possibly [18], which all proceeded to the end. The fluid was near neutral and had high a_{Na+}/a_{K+}. The quartzite was depleted in K, Rb and Ca and enriched in Na, as supported by the average composition of the least altered quartzite (Table 15), the Na concentration in which is distinctly higher and Ca and K lower than in an average arkose quartzite as calculated by Pettijohn et al. (1987).

The volume changes and chemical mass balances related to the formation of the other alteration zones in the dykes were calculated

Table 14. Chemical compositions of felsic dykes at Sivakkavaara.
Major elements in wt. %, trace elements in ppm.

	Rhyolites		Quartz latites				Quartz trachyte	Trachytes		Lati-andesites
	least altered		least altered		carbonated + sericitized		least altered	least altered	carbonated	carbonated + sericitized
	avg	std	avg	std	avg	std	avg	avg		avg
SiO2	71.07	5.09	64.95	1.89	63.00	1.36	63.45	60.31	65.78	58.87
TiO2	0.25	0.05	0.61	0.28	0.72	0.01	0.64	0.82	0.73	0.92
Al2O3	14.69	2.55	15.96	1.08	15.47	0.25	15.80	14.19	15.79	12.69
Fe2O3t	2.79	1.26	4.25	1.62	3.04	0.81	6.58	8.31	4.30	7.26
MnO	0.10	0.09	0.08	0.05	0.11	0.03	0.09	0.07	0.10	0.16
MgO	0.98	0.44	1.65	0.61	1.49	0.11	0.47	1.78	0.97	2.46
CaO	1.35	0.84	2.62	0.67	4.67	0.28	1.08	2.35	2.31	7.24
Na2O	5.33	1.12	5.38	0.22	6.36	1.14	3.39	2.12	8.76	3.35
K2O	2.28	0.84	3.36	0.94	1.70	0.73	7.61	8.91	0.21	3.10
P2O5	0.11	0.04	0.16	0.01	0.13	0.00	0.12	0.42	0.14	0.71
sum	99.50	0.66	99.60	0.23	97.22	0.29	99.93	99.95	99.87	97.23
Br	1.02	0.49	0.80	0.08	<1		2.50	1.52	0.91	<1
S	1440	2131	620	531	2730	3208	350	340	1510	660
Sb	0.60	0.15	0.99	0.76	0.77	0.13	1.44	1.53	1.54	0.72
As	1.91	0.48	2.70	0.99	2.35	0.88	4.76	4.22	3.13	1.87
W	4.28	3.16	3.36	2.51	10.76	2.49	7.72	2.34	4.18	5.44
Cs	<0.5		0.72	0.32	<0.5		0.61	1.27	<0.5	<0.5
Rb	55	19	70	20	32	11	108	158	11	72
Ba	4728	2943	4477	1949	2527	837	6140	5665	6020	3495
Cu	<10		27	21	<20		<20	30	<20	<20
Co	6.0	7.5	4.9	5.4	12.8	13.3	3.8	11.3	2.9	7.8
Ni	<40		<40		<40		<40	<40	<40	<40
La	17.1	5.4	19.6	3.6	14.9	10.6	34.4	17.7	33.0	36.7
Sc	6.2	1.1	12.2	4.0	12.1	1.4	10.7	20.0	10.6	25.7
Ta	0.38	0.14	1.11	0.64	1.22	0.07	1.15	1.11	1.27	0.82
V	50	9	80	21	90	12	80	130	100	150
Cr	<40		<40		<40		<50	92	45.3	81.7
U	3.17	0.95	8.38	6.56	9.14	0.74	11.0	11.6	12.6	3.92
Th	10	2	45	40	28	9	33	30	33	15
Zr	180	23	320	110	340	32	370	320	390	240
n	8		3		3		2	2	1	2

using formulae [1] and [2]. The analyses compared, their immobile element ratios and volume changes are presented in Table 16.

Biotitization in albite diabases

Chemical changes related to the biotitization of albite diabase are difficult to present with accuracy, as no suitable pairs of samples were found for the mass balance calculations. The major component, S, Rb and Ba concentrations of the two most similar samples are compared in Figure 44A. Due to the primary differences between the samples (Table 16), the methodological error in this comparison is greater than in better established cases, so that enrichment factors between approx. 0.8 to 1.2 may be within the limits of the possible error. The most obvious chemical changes related to biotitization were the Mg, Ca and Na losses and K, S, Rb and Ba gains. The mineral assemblages indicate that reactions [10] and [12] were related to biotitization, as they explain fairly well the changes in the alkaline and alkaline-earth element concen-

Table 15. Chemical composition of quartzites, tuffs, tuffites and siliceous carbonate rocks at Sivakkavaara. Major elements in wt. %, trace elements in ppm.

	Average arkose (Pettijohn et al. 1987)	Quartzites					Tuffs		Tuffites	Siliceous carbonate rocks			
		least altered (albitized)		weakly carbonated + sericitized		moderately carbonated + sericitized	least altered (chlorite + biotite)	albitized + carbonated	chloritized + biotitized	tremolite-bearing		tremolite + phlogopite bearing	
		avg	std	avg	std				avg	avg	std	avg	std
SiO2	80.15	77.33	2.96	74.27	2.35	76.61	60.23	64.66	58.08	54.60	3.97	40.67	4.41
TiO2	0.31	0.20	0.05	0.21	0.04	0.20	0.57	0.51	0.55	0.23	0.01	0.27	0.06
Al2O3	9.04	13.03	1.73	14.01	1.70	11.70	13.98	12.90	13.48	4.97	0.88	6.43	1.34
Fe2O3t	2.39	1.09	0.25	1.45	0.38	1.95	7.25	4.61	9.33	3.25	0.27	6.34	4.08
MnO	0.21	0.04	0.01	0.04	0.01	0.05	0.05	0.09	0.04	0.09	0.02	0.08	0.02
MgO	0.52	0.38	0.18	0.87	0.40	1.28	10.57	4.61	10.02	15.42	0.44	16.07	1.14
CaO	2.81	0.31	0.16	1.00	0.46	1.85	0.17	2.73	0.01	15.03	3.88	17.35	6.53
Na2O	1.56	6.78	0.97	6.38	0.78	0.81	2.43	4.86	0.05	2.01	0.81	0.15	0.16
K2O	2.91	0.48	0.08	1.16	0.67	3.81	0.88	2.45	5.32	0.12	0.03	3.17	0.52
P2O5	0.10	0.09	0.02	0.08	0.01	0.08	0.05	0.03	0.01	0.44	0.04	0.44	0.16
sum	99.90	99.82	0.02	99.60	0.38	98.62	96.28	97.69	97.18	96.23	2.04	91.08	2.65
Br		7.24	0.39	5.33	1.45	2.09	0.86	0.91	0.52	18.9	24.5	<1	
S		20	39	50	60	50	30	330	<20	130	118	30	5
Sb		0.42	0.07	0.45	0.07	0.62	1.09	0.63	0.52	0.89	0.20	0.54	0.14
As		1.95	1.87	1.08	0.32	<0.5	1.06	1.86	0.47	5.17	0.20	4.42	1.68
W		<1		1.96	3.96	2.84	7.32	1.85	1.38	0.64	0.19	0.38	0.17
Cs		<1		<1		<1	<1	1.19	1.31	<1		2.87	1.25
Rb		14	5	28	17	83	20	90	137	8	0	122	39
Ba		218	50	551	285	1570	502	1440	2535	66	30	387	293
Cu		<10		<10		<10	<10	<10	<10	<10		<10	
Co		2.2	0.8	2.9	2.3	2.6	7.77	5.52	9.1	8.5	0.3	17.3	13.9
Ni		<40		<40		<40	<40	<40	<40	31	1	59	59
La		7.23	5.41	8.43	4.46	9.82	1.62	3.02	1.81	3.00	0.92	6.58	3.71
Sm		2.5	0.8	3.5	3.2	1.7	n.a.	n.a.	n.a.	n.a.		n.a.	
Sc		4.6	0.9	4.9	0.8	5.3	17.6	13.5	17.9	5.7	0.1	8.7	5.6
Ta		0.34	0.05	0.38	0.10	0.33	0.73	0.62	0.66	0.40	0.11	0.40	0.11
V		20	5	30	5	30	20	30	40	30	6	80	92
Cr		79	10	81	17	82	153	148	144	80	42	89	60
U		0.87	0.14	0.98	0.52	0.68	0.57	0.82	0.80	1.80	0.22	1.59	0.42
Th		4.67	0.63	4.38	0.51	5.43	4.01	2.73	2.33	4.62	1.25	5.38	1.81
Zr		170	50	180	32	190	190	280	200	140	10	140	27
n		6		9		1	1	1	2	3		4	

trations. The pyrite formation reaction [34] explains the increase in the S concentration. The reactions imply a reducing, near neutral or mildly acid, low a_{Ca2+}/a_{K+} and a_{Na+}/a_{K+} fluid.

Carbonation, albitization and sericitization

It is almost impossible to treat carbonation as a separate alteration stage at Sivakkavaara, because the sericitizated zones almost completely overlap with the carbonated zones (Fig. 21, p. 37). The chemical effect of sericitization was mostly small, however, as indicated by the minimal K gain or even K loss related to the formation of the albitized + carbonated + sericitized zones in several lithological units (Figs. 44D-44G). The alteration reactions indicate a high a_{Na+}/a_{K+} and f_{CO2}, near-neutral, H^+ releasing fluid, and the comprehensive loss of U implies oxidizing conditions. The H^+ release caused a substantial decrease in pH after carbonation

Table 16. Sivakkavaara. Analyses compared in Figure 44, their densities, immobile element ratios and volume changes (= dV%). The samples of least altered rock are presented in italics. Abbreviations: ab = albitization, bt = biotitization, cb = carbonation, se = sericitization. Major elements in wt. %, trace elements in ppm. Number of samples included in the average analysis is indicated in parentheses after the abbreviation "avg".

altera-tion	biotitization		biotitization + carbonation		albitization + carbonation + sericitization												
rock	diabase		diabase		trachyte		lamprophyre			quartz-latite		lati-andesite			rhyolite		
sample	*35-67*	35-2	*avg(5)*	35-17	*35-18*	35-21	*106-1*	100-2	100-1	*42-29*	42-31	*43-1*	42-62	42-63	*35-29*	35-32	*42-23*	42-24
SiO2	*48.95*	51.02	*51.36*	46.37	*62.31*	65.78	*48.50*	46.50	45.70	*63.99*	64.87	*62.43*	58.77	58.97	*70.76*	73.74	*67.80*	67.86
TiO2	*0.87*	0.97	*1.01*	0.96	*0.72*	0.73	*1.28*	1.35	1.36	*0.58*	0.63	*1.07*	0.92	0.92	*0.27*	0.27	*0.28*	0.28
Al2O3	*13.33*	13.71	*13.39*	12.63	*15.27*	15.79	*11.00*	12.00	12.00	*15.80*	16.78	*14.41*	12.74	12.64	*15.88*	14.79	*15.72*	15.53
Fe2O3t	*11.57*	14.82	*12.88*	12.54	*7.35*	4.30	*10.07*	11.03	10.58	*5.16*	2.46	*5.19*	8.52	5.99	*2.22*	1.92	*5.58*	2.37
MnO	*0.20*	0.20	*0.19*	0.19	*0.09*	0.10	*0.13*	0.14	0.14	*0.05*	0.07	*0.02*	0.16	0.17	*0.01*	0.07	*0.32*	0.09
MgO	*7.36*	6.72	*6.68*	6.75	*0.71*	0.97	*10.40*	7.17	7.86	*0.72*	0.57	*4.75*	2.45	2.46	*1.76*	0.53	*0.46*	0.45
CaO	*11.62*	7.53	*8.40*	4.46	*1.43*	2.31	*8.06*	5.82	5.36	*1.69*	5.10	*1.30*	6.47	8.00	*0.28*	0.51	*1.34*	4.64
Na2O	*2.59*	2.27	*2.03*	3.51	*3.48*	8.76	*2.16*	2.79	3.00	*3.42*	3.45	*5.46*	4.14	2.55	*6.35*	5.05	*6.44*	5.69
K2O	*0.19*	1.72	*2.13*	3.97	*7.73*	0.21	*2.74*	3.61	3.74	*7.82*	4.24	*2.86*	2.48	3.71	*1.97*	2.26	*1.79*	2.44
P2O5	*0.08*	0.08	*0.09*	0.08	*0.13*	0.14	*0.59*	0.69	0.66	*0.11*	0.11	*0.87*	0.72	0.70	*0.10*	0.09	*0.10*	0.10
sum	*96.75*	99.04	*98.15*	91.46	*99.22*	99.09	*94.94*	91.08	90.40	*99.34*	98.28	*98.37*	97.36	96.11	*99.60*	99.22	*99.83*	99.45
Br			*0.92*	<1	*1.94*	<1	*1.17*	0.25	1.33	*2.38*	0.86	*<1*	<1	<1	*1.22*	1.17	*0.90*	1.00
S	*260*	560	*658*	990	*340*	1510	*140*	280	1820	*400*	80	*4450*	510	810	*260*	1070	*1000*	280
Sb			*1.44*	0.39	*2.15*	1.54	*1.06*	1.39	3.68	*1.05*	0.62	*0.95*	0.82	0.63	*0.67*	0.79	*0.70*	0.53
As			*9.43*	1.72	*4.88*	3.13	*2.86*	2.59	2.19	*3.31*	1.43	*3.92*	1.76	1.98	*2.07*	1.92	*2.02*	1.3
W			*<1*	<1	*2.59*	4.18	*8.29*	11.6	36.1	*8.60*	13.8	*13.4*	6.87	4.00	*4.40*	9.48	*4.04*	6.17
Cs			*1.31*	3.98	*0.62*	0.35	*3.55*	4.00	0.92	*0.74*	0.55	*1.72*	0.58	0.60	*<0.5*	<0.5	*<0.5*	<0.5
Rb	*6.5*	48.8	*62.9*	156	*97.7*	10.7	*99.4*	156	15.7	*141*	69.1	*87.3*	56.3	86.9	*48.2*	50.3	*44.1*	51.4
Ba	*102*	572	*734*	1040	*6230*	6020	*3490*	2700	63	*4210*	6020	*2480*	3100	3890	*2190*	5220	*2100*	2230
Cu			*140*	30	*30*	<10	*<10*	<10	<10	*<10*	20	*6930*	10	20	*<10*	20	*<10*	20
Co			*42.7*	25.8	*2.37*	2.88	*43.2*	58.2	3.94	*5.16*	3.18	*9.17*	6.41	9.23	*2.77*	1.94	*11.0*	3.82
Ni			*79.4*	65.8	*27.0*	<40	*116*	79.4	43.8	*<40*	<40	*26.0*	36.0	35.3	*<40*	<40	*<40*	<40
La			*5.28*	16.7	*14.2*	33.0	*52.7*	65.1	103	*58.5*	11.0	*15.2*	46.8	26.6	*26.2*	22.9	*17.6*	10.6
Sm			*2.22*	4.31	*<10*	<10	*7.19*	8.43	15.3	*<10*	<10	*<10*	<10	<10	*<10*	<10	*<10*	<10
Sc			*62.0*	55.5	*13.9*	10.6	*55.7*	53.7	31.3	*9.26*	13.2	*23.9*	25.7	25.7	*7.12*	5.8	*6.44*	6.82
Ta			*<0.3*	<0.3	*1.10*	1.27	*0.80*	1.03	0.92	*0.95*	1.13	*1.36*	0.80	0.84	*0.64*	0.26	*0.52*	0.41
V			*304*	290	*90*	100	*230*	220	230	*70*	110	*150*	140	160	*40*	50	*50*	50
Cr			*257*	187	*<100*	45	*962*	538	89	*<40*	<40	*44*	74	89	*36*	<40	*<40*	<40
U			*0.36*	0.86	*14.0*	12.6	*4.46*	3.77	2.24	*13.3*	6.29	*14.9*	2.69	5.15	*2.96*	2.56	*4.54*	3.10
Th			*0.56*	0.60	*33.4*	32.8	*24.6*	25.7	17.5	*36.1*	34.2	*26.2*	15.7	14.5	*14.2*	12.4	*12.2*	11.9
Zr			*92*	70	*360*	390	*380*	400	390	*400*	380	*290*	240	240	*200*	200	*190*	200
Al/Ti	*15.3*	14.1	*13.3*	13.1	*21.1*	21.6	*8.6*	8.9	8.8	*27.1*	26.6	*13.5*	13.9	13.7	*59.5*	55.0	*55.9*	55.3
Al/Zr			*1456*	1804	*424*	405	*289*	300	308	*395*	442	*497*	531	527	*794*	740	*827.4*	777
Ti/Zr			*109*	137	*20.1*	18.7	*33.8*	33.7	34.9	*14.6*	16.6	*36.9*	38.3	38.4	*13.4*	13.5	*14.8*	14.1
density (kg/m3)	*2943*	2979	*2991*	2904	*2647*	2643	*2968*	2803	2740	*2645*	2647	*2547*	2658	2738	*2574*	2536	*2635*	2614
dV%		+13		+8		-1		+1	+2		-8		+11	+8		+1		+1
ref. to Fig.		44A		44B		44C			44D		44E		44F			44G		44G

and made sericite precipitation possible. The crystallization of chlorite instead of sericite indicates a higher a_{Mg2+}/a_{K+} and pH than during sericitization, but still acid conditions.

The effect of carbonation in the albite diabase becomes clearer when Figures 44B (biotitization + carbonation) and 44A (biotitization only) are compared. This suggests that the Sb,

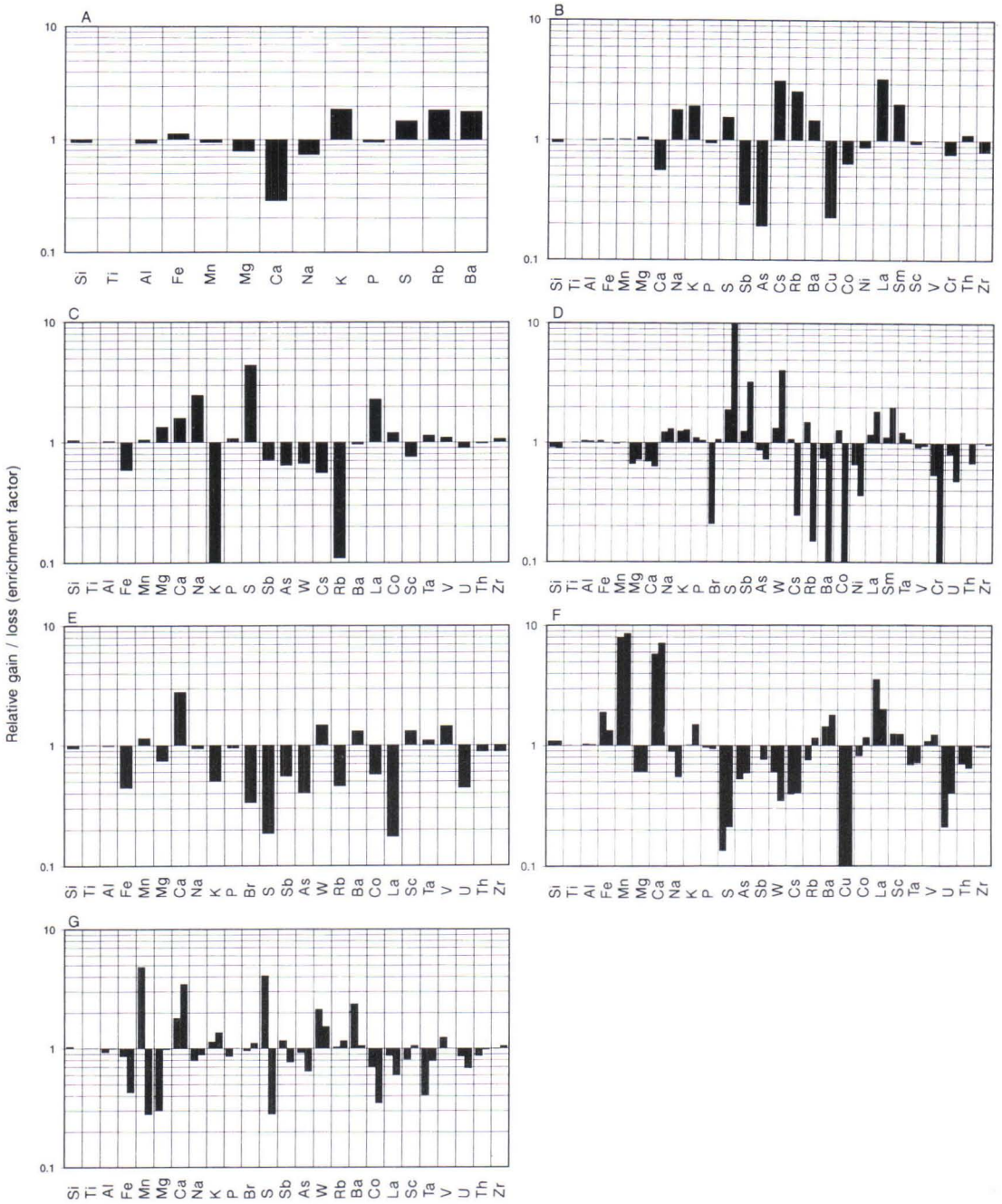

Fig. 44. Enrichment factors of the elements showing chemical gains and losses during the alterations in diabase and lamprophyre at Sivakkavaara (y-axis). The calculations are based on comparisons between one altered and one less altered sample, except in Figures D, F and G where two altered samples are compared with the least altered type. **A**: Biotitization of albite diabase. Since the samples do not have equal ratios of least mobile elements, the diagram gives only the trends in alteration. **B**: Biotitization and carbonation of albite diabase. **C**: Carbonation and albitization of trachytic dyke. **D**: Albitization, carbonation and sericitization of lamprophyre. **E**: Albitization, carbonation and sericitization of quartz-latitic dyke. **F**: Albitization, carbonation and sericitization of lati-andesitic dyke. **G**: Albitization, carbonation and sericitization of rhyolitic dyke.

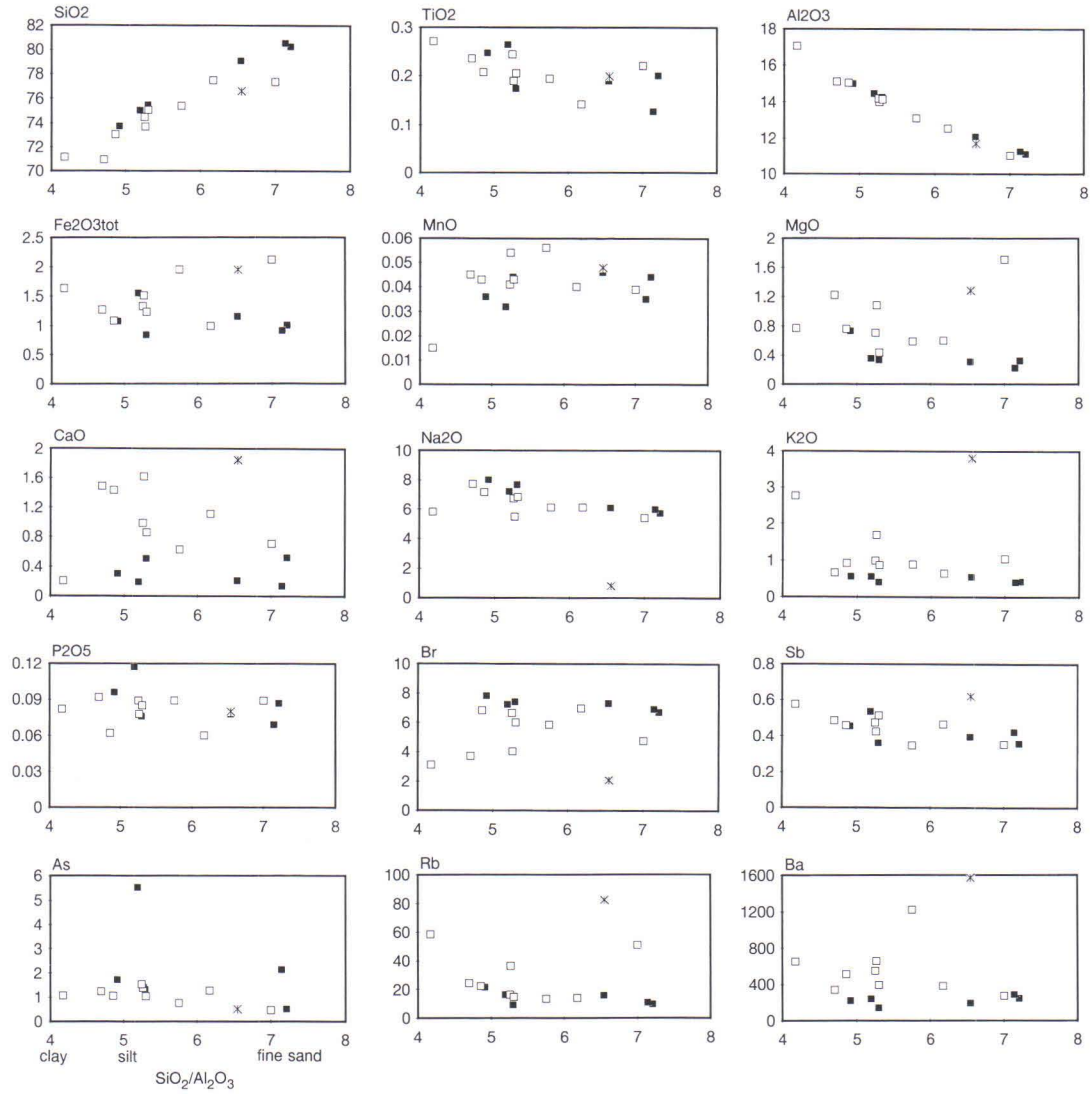

Fig. 45. Plots of major and trace elements vs. SiO_2/Al_2O_3 in the least altered, weakly carbonated and sericitized and moderately carbonated and sericitized types of quartzite at Sivakkavaara. The ranges of SiO_2/Al_2O_3, a rough measure of the grain size of sediments (Taylor and McLennan 1985), for clay, silt and fine sand are indicated at the bottom of the figure.

As, Cu and Co concentrations decreased, Mg, Ca, Na and REE increased and Ti, Fe, Mn, P and Th (and possibly also Si, Ni, Cr and Zr) were immobile. The albitization and carbonation reactions [17], [21], [23] and [26] explain most of the changes, but the increase in the REE concentrations does not fit with the decomposition of sphene (Pan et al. 1993), al-

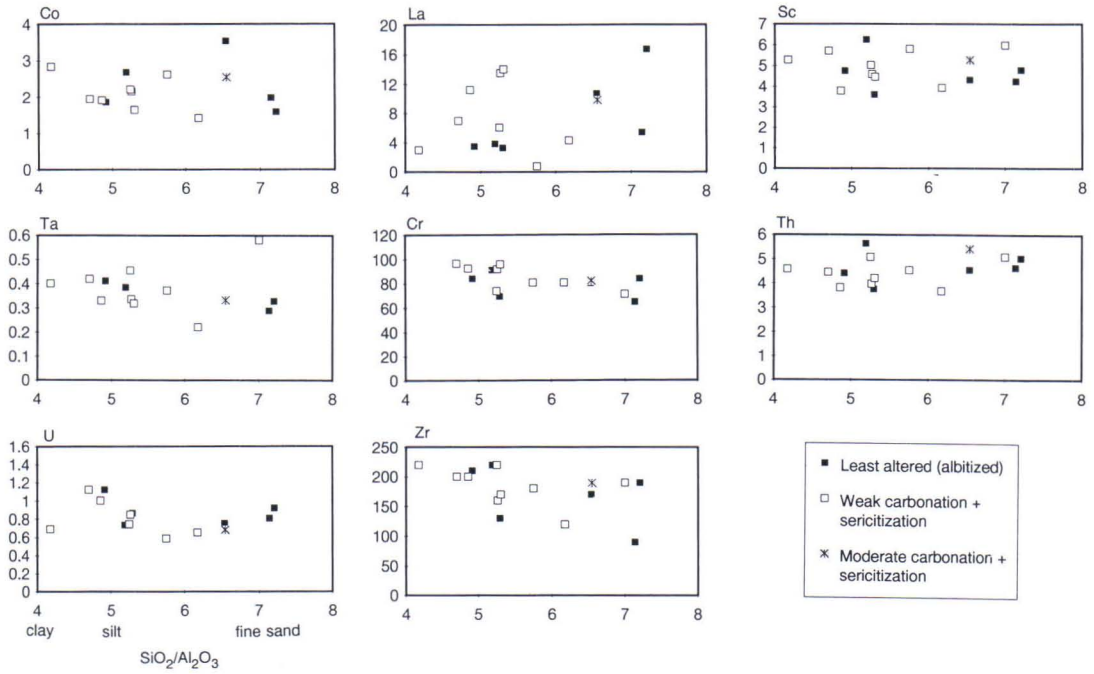

Fig. 45. Continued.

thought it fits well with intensive carbonation in general (Wood 1990a, 1990b). The produced decrease in the Sb and As concentrations imply sulphide decomposition (e.g., [34]), but because the S concentration did not decrease, it is possible that the sulphides only recrystallized and lost As and Sb.

Carbonation and albitization of a trachytic dyke is illustrated in Figure 44C. The chemical changes were losses of Fe, K, Sb, As, W, Cs, Rb and Sc and gains in Mg, Ca, Na, S and La. The albitization, carbonation and sericitization reactions [16], [21], [26] and [29] explain most of the changes.

Alteration in the lamprophyre reflects fairly "pure" carbonation (Fig. 44D), as the albitization and sericitization grades were low. The Si, Mg, Ca, As, Cs, Ba, Ni, Cr, U and Th concentrations decreased, Na, K, S, Sb and W increased and Ti, Al, Fe, Mn, P, Ta, V and Zr remained immobile. The changes are explained by reactions [17], [19], [21]-[23], [26] and [34] and by scheelite formation. The loss of Ca during carbonation is surprising, as the Ca silicates were obviously not replaced by an equivalent amount of Ca carbonate.

The changes related to the albitization, carbonation and sericitization of quartz-latitic, lati-andesitic and rhyolitic dykes are demonstrated in Figures 44E-44G. The chemical effects of albitization (reactions [14] and [16]) and sericitization (reactions [18], [22] and [27]-[29]) were minimal in these rocks because the alkali metal concentrations decreased or remained unchanged, which implies a low alkali metal concentration in the fluid. Carbonation (reactions [21], [25] and [26]) was more significant, as the Mn and Ca concentrations increased and Si, Fe, Na, La, U and Th were also mobile. In addition, the decreases in S, As and Sb concentrations imply the pyrite decomposition reaction [33]. Ti, Al and Zr were immobile

in each dyke, but P, V and Th were also immobile in most cases.

The rock volume change (Table 16) was approx. +10% in the diabase and the lati-andesitic dyke, which indicates a moderate grade of brecciation. The decrease of 8% in the volume of quartz-latite reflects the replacement nature of sericitization. In the other dykes the volume change was less than 2%, indicating a low brecciation grade.

Carbonation and sericitization alterations in quartzite differ from the corresponding ones in igneous rocks. Although no suitable pairs of samples were found for the mass balance calculations, the most notable chemical changes are clearly manifested by the element vs. SiO_2/Al_2O_3 diagrams (Fig. 45), in which the Mg, Ca, K, Rb and Ba concentrations increased and Na, Sb and Br decreased, implying low a_{Na+}/a_{Mg2+}, a_{Na+}/a_{Ca2+} and a_{Na+}/a_{K+} and a change in pH from near neutral (carbonation) to acid (sericitization). The changes are associated with the carbonation and sericitization reactions [22], [26], [28] and [29].

Honkavaara

The least altered rocks

The chemical data for the least altered albite diabase and mafic lava (Table 17, p.84) plotted on an alkali ratio diagram (Fig. 46) indicate that most samples are within the spilite field, implying an early alkaline metasomatic effect on the lava and diabase. The high Na and low K concentrations of the least altered types of felsic volcanic rock, quartzite and tuffite (Table 18) also imply alkaline metasomatism.

The formation of the least altered zones in the mafic lava and albite diabase is characterized by a combination of mineral reactions [1] and [8], those in the felsic volcanic rock by [1], those in the tuffite by [8] and [9] and those in the quartzite [14], [16] and [18] (Table 2). According to these reactions and in concordance with the chemical compositions (Tables 17 and 18), there were losses of the alkaline and alkaline-earth elements, with the exception of Na enrichment. The reactions also imply that the fluid had a high a_{Na+}/a_{K+} and was acid and weakly reducing.

The volume changes and chemical mass balances related to the formation of the other alteration zones were calculated using formulae [1] and [2]. The analyses compared, their immobile element ratios and volume changes are presented in Table 19.

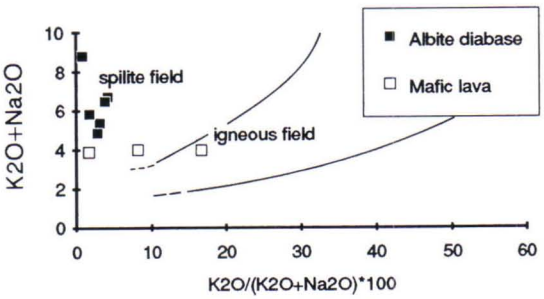

Fig. 46. The least altered igneous rocks at Honkavaara, plotted on the alkali ratio diagram of Hughes (1973).

Epidotization

The chemical changes that took place during epidotization of the albite diabase were not large (Fig. 47A) and if Si, Ti, Al, Sc, U and V were immobile, as seems to be realistic, there were no volume changes (Table 19) despite evident losses of Fe, Na and Br and gains in Mn, Ca, K, P, Ni and REE. A combination of reactions [1] and [3] will explain the chemical changes in the main components, implying an acid, reducing fluid with high a_{Ca} and low a_{Fe} and a_{Na}. Apatite formation explains the P and REE enrichments.

Table 17. Chemical compositions of mafic lavas and albite diabases at Honkavaara.
Major elements in wt. %, trace elements in ppm.

	Albite diabase											Mafic lava
	least altered (amhibole zone)		epidotized	chloritized + biotitized		carbonated		sericitized (intermed. types only)	dyke margin (biotitized + carbonated)		fragments in volc. breccia (carbonated)	amphibole zone + chloritized
	avg	std		avg	std	avg	std	avg	avg	std	avg	avg
SiO2	54.29	3.49	51.99	53.44	1.87	56.49	3.29	63.70	57.29	1.82	55.93	55.36
TiO2	1.78	0.19	1.63	1.68	0.28	2.05	0.28	2.63	0.58	0.06	1.69	1.39
Al2O3	14.14	0.55	14.03	14.48	0.70	15.35	1.20	20.63	14.75	0.37	14.42	12.68
Fe2O3t	12.70	4.10	7.71	14.50	2.34	2.85	3.07	1.62	7.15	3.18	10.06	14.59
MnO	0.05	0.01	0.06	0.06	0.02	0.10	0.02	0.03	0.04	0.02	0.10	0.09
MgO	4.53	0.86	5.25	5.14	0.77	3.30	0.67	0.63	7.12	2.38	5.56	8.17
CaO	5.41	2.12	11.75	3.53	1.97	6.16	1.10	0.45	3.20	2.89	3.32	1.94
Na2O	6.45	1.35	4.69	5.20	0.97	8.38	0.67	6.47	5.20	1.79	6.20	3.47
K2O	0.17	0.09	0.13	1.17	0.55	0.21	0.18	3.50	1.60	1.14	0.41	0.49
P2O5	0.18	0.04	0.17	0.19	0.03	0.26	0.14	0.18	0.27	0.02	0.21	0.18
sum	99.69	0.22	97.42	99.40	0.64	95.15	1.56	99.82	97.20	1.60	97.89	98.35
Br	4.09	1.55	2.89	1.42	0.90	1.78	1.03	1.48	<1		1.87	1.82
S	200	269	<20	1520	1759	1550	4728	30	1110	1272	470	760
Sb	0.36	0.11	0.34	0.74	0.36	1.10	0.21	2.04	0.45	0.14	0.72	0.13
As	1.65	0.64	2.32	2.02	3.40	0.91	0.67	0.96	1.00	0.86	0.57	0.37
W	<1		<1	<1		4.62	1.53	16.2	1.36	1.05	5.09	<1
Cs	<1		<1	<1		<1		<1	<1		<1	0.56
Rb	<15		<15	33.5	11.7	<10		63.8	45.0	35.2	<15	12.3
Ba	<50		<50	107	93.7	<50		230	356	413	41.1	<40
Cu	290	463	<20	460	779	1150	3397	40	150	300	510	530
Co	37.9	26.2	17.2	59.2	40.6	6.6	12.8	3.6	55.6	51.0	25.0	43.4
Ni	<50		56.3	77.2	20.9	<30		16.2	163	81.3	42.8	<40
La	23.6	8.0	26.9	45.0	41.0	46.8	54.8	17.9	47.7	24.1	14.5	16.1
Sm	5.92	1.19	5.67	7.94	4.61	10.6	9.47	<10	3.36	2.48	3.84	3.78
Sc	25.7	8.51	21.2	29.9	9.87	12.2	4.03	9.56	20.8	2.58	28.3	40.0
Ta	0.95	0.12	0.93	0.88	0.25	1.22	0.51	1.31	0.75	0.16	0.76	0.50
V	320	98	330	350	66	160	30	310	150	34	270	290
Cr	<40		<40	84	95	<40		28	318	57	47	48
U	1.96	0.90	2.67	1.93	0.63	3.00	0.96	2.66	5.65	1.33	1.21	0.45
Th	6.75	2.50	5.28	5.92	2.63	7.48	3.02	7.41	26.1	1.28	4.91	3.00
Zr	180	4	320	180	22	260	118	260	240	16	190	170
n	5		1	13		10		2	5		2	2

Chloritization

The chemical changes related to chloritization in the albite diabase are presented in Figure 47B. The chloritized sample used for the mass balance calculations (Table 19) also contained biotite, as the chloritized zones at Honkavaara are more or less biotitized everywhere. The effect of biotitization is partly avoided, however, by comparing Figures 47B and 47C, and bearing in mind that the difference in K_2O concentration between the samples used in diagram 47B is only 0.7 percentage units (Table 19).

The mass balance calculations indicate that the rock volume remained constant (Table 19). The most notable chemical changes, in addition to hydration, were losses of Ca, Na, Br and As and gains in Mg. The changes in Fe, K, P, S, Sb, As, Rb, Co, Ni, La, Sc and U concentrations remain unclear because of the overlapping biotitization, but were

Table 18. Chemical compositions of felsic volcanic rock, tuffite, quartzite and volcanic breccia at Honkavaara. Major elements in wt. %, trace elements in ppm.

	Quartzite	Tuffite						Felsic volcanic rock			Volcanic breccia	
	(albitized)	least altered (albitized)	chloritized + carbonated		carbonated		sericitized	least altered (amphibole)		carbonated	(lahar ?) carbonated	
	avg	avg	avg	std	avg	std		avg	std	avg	avg	std
SiO2	72.43	62.81	61.23	1.07	62.52	1.88	54.32	63.77	3.23	66.42	60.30	3.98
TiO2	0.42	0.67	0.67	0.04	0.63	0.02	0.77	0.52	0.08	0.50	0.61	0.16
Al2O3	14.22	16.28	15.28	0.45	14.89	0.35	19.11	14.75	0.57	13.50	15.18	2.48
Fe2O3t	1.97	7.19	6.59	2.16	5.10	1.79	7.19	7.78	1.59	5.06	3.64	1.55
MnO	0.06	0.05	0.06	0.03	0.07	0.02	0.07	0.03	0.01	0.04	0.07	0.03
MgO	0.93	1.25	3.20	1.06	2.60	0.63	3.25	1.38	0.91	1.76	3.20	1.95
CaO	1.55	2.07	3.72	2.31	4.48	1.04	4.55	2.73	1.23	3.04	4.99	2.79
Na2O	7.56	9.16	7.82	0.44	8.36	0.31	7.38	8.66	0.32	7.89	8.26	1.73
K2O	0.51	0.23	0.37	0.20	0.14	0.10	2.56	0.05	0.00	0.06	0.34	0.38
P2O5	0.14	0.15	0.11	0.06	0.16	0.05	0.16	0.13	0.02	0.12	0.18	0.08
sum	99.77	99.85	99.03	1.49	98.96	1.46	99.36	99.81	0.05	98.40	96.78	3.15
Br	2.43	1.07	1.18	0.08	1.66	0.65	<1	1.23	0.32	1.88	0.70	0.40
S	<10	<10	40	34	<10		30	<10		<10	<20	
Sb	0.65	1.05	0.60	0.33	0.73	0.22	0.96	0.15	0.04	0.47	0.64	0.24
As	0.70	0.78	<0.5		<0.5		0.76	0.88	0.08	0.68	0.70	0.41
W	3.80	2.10	1.94	0.88	4.19	1.33	3.24	<1		3.27	5.84	4.88
Cs	1.07	<1	<1		<1		<1	<1		<1	<1	
Rb	<15	<15	13.5	2.19	10.9	3.73	44.2	<15		<15	<15	
Ba	<50	<50	52.7	18.3	<50		164.0	<50		<50	48.0	30.3
Cu	<10	<10	80	85	<10		<10	<10		<10	<10	
Co	5.38	5.23	13.8	9.26	3.03	1.65	<10	6.05	3.19	1.62	2.82	1.68
Ni	63.9	<50	50.3	20.6	<50		<50	35.8	7.98	<50	37.9	24.8
La	2.83	44.3	15.0	7.06	10.0	2.88	69.1	15.6	6.01	15.3	16.6	20.6
Sm	0.78	6.28	2.47	0.90	1.55	0.38	7.67	3.22	0.98	3.71	3.12	2.30
Sc	13.2	18.3	24.5	8.94	21.8	7.85	44.8	13.4	2.49	8.49	13.9	6.60
Ta	0.60	0.82	1.05	0.45	0.88	0.19	1.21	0.57	0.31	0.72	0.81	0.26
V	50	100	80	22	70	6	150	110	28	220	90	32
Cr	97	159	202	44	199	64	218	122	27	99	151	63
U	0.83	1.70	2.25	1.70	1.20	0.43	1.40	1.47	0.47	0.95	1.89	1.58
Th	8.30	13.0	12.6	4.43	10.6	1.80	15.3	9.50	2.18	7.52	13.4	7.52
Zr	220	160	190	34	180	15	190	180	30	160	190	51
n	2	2	4		3		1	5		2	5	

probably small. Silicon, Ti, Al, Ta, V, Th and Zr were evidently immobile. The spilitization reaction [6] and the chloritization reactions [8] and [9] explain the changes sufficiently well, indicating an acid, weakly reducing fluid.

Biotitization

The rock volume remained constant during biotitization (Table 19). The chemical changes (Fig. 47C), when the preceding chloritization (Fig. 47B) is taken into account, were losses of Mg, Ca, Cs, La and U and the gains in Mn, K, S, Rb, Ba and Co. Most of these changes are related to the biotitization reactions [10] and [12], which indicate, that the fluid was reducing and near neutral or mildly acid, and to the pyritization reaction [34]. The La and U losses could have been caused by sphene decomposition and the P gain by apatite formation.

Table 19. Honkavaara. Analyses compared in Figures 47 and 48, their densities, immobile element ratios and volume changes (= dV%). The samples of least altered rock are presented in italics. Abbreviations: bt = biotitization, ch = chloritization, ep =epidotization. Major elements in wt. %, trace elements in ppm. The number of samples from which each average was calculated is indicated in parentheses after the abbreviation "avg".

altera-tion	epidotization, chloritization and biotitization				carbonation								sericitization			
rock	albite diabase								fels. volc. rock		tuffite		albite diabase		tuffite	
sample	*1044-1*	1044-3	40-11	40-2	*40-29*	36-2	*40-10*	39-3	*1044-18*	1044-23	*avg(2)*	avg(4)	*37-1*	40-6	*avg(2)*	avg(3)
type		ep	ch	bt												
SiO2	*53.73*	51.99	54.39	53.98	*51.87*	57.88	*52.48*	50.16	*66.82*	73.39	*62.81*	62.52	*53.09*	65.33	*62.81*	54.32
TiO2	*1.66*	1.63	1.62	1.65	*1.97*	2.36	*1.69*	1.79	*0.51*	0.46	*0.67*	0.63	*1.77*	2.57	*0.67*	0.77
Al2O3	*14.13*	14.03	14.25	14.16	*13.65*	16.84	*14.16*	13.89	*13.95*	12.63	*16.28*	14.89	*14.08*	19.63	*16.28*	19.11
Fe2O3	*9.94*	7.71	15.32	15.52	*15.93*	1.46	*15.59*	10.47	*8.14*	2.05	*7.19*	5.10	*14.41*	1.40	*7.19*	7.19
MnO	*0.06*	0.06	0.06	0.07	*0.05*	0.07	*0.08*	0.11	*0.04*	0.04	*0.05*	0.07	*0.04*	0.01	*0.05*	0.07
MgO	*4.92*	5.25	5.17	4.51	*5.15*	2.72	*5.01*	4.60	*0.43*	0.97	*1.25*	2.60	*4.66*	0.55	*1.25*	3.25
CaO	*8.95*	11.75	3.54	2.42	*5.57*	5.12	*4.11*	7.26	*1.44*	1.80	*2.07*	4.48	*4.94*	0.48	*2.07*	4.55
Na2O	*5.71*	4.69	4.50	5.41	*5.17*	9.14	*4.91*	7.56	*8.26*	7.30	*9.16*	8.36	*6.41*	6.60	*9.16*	7.38
K2O	*0.10*	0.13	0.78	1.91	*0.17*	0.16	*1.47*	0.38	*0.05*	0.07	*0.23*	0.14	*0.28*	3.02	*0.23*	2.56
P2O5	*0.13*	0.17	0.17	0.17	*0.15*	0.20	*0.17*	0.17	*0.13*	0.12	*0.15*	0.16	*0.19*	0.20	*0.15*	0.16
sum	*99.32*	97.42	99.80	99.80	*99.68*	95.94	*99.66*	96.38	*99.77*	98.82	*99.85*	98.96	*99.86*	99.79	*99.85*	99.36
Br	*3.74*	2.89	1.26	2.13	*2.79*	0.30	*1.53*	1.08	*1.41*	2.14			*2.58*	1.31		
S	*30*	<10	150	300	*210*	30	*1810*	860	*<20*	<20			*70*	60		
Sb	*0.35*	0.34	0.85	1.12	*0.42*	1.14	*0.91*	1.10	*0.20*	0.63			*0.45*	1.97		
As	*2.45*	2.32	0.30	1.41	*1.21*	1.52	*<1*	<1	*1.00*	0.83			*1.50*	0.30		
W	*<1*	<1	<1	<1	*1.23*	6.15	*0.70*	2.50	*1.00*	3.53			*0.70*	14.90		
Cs	*0.53*	<1	<1	0.34	*<1*	<1	*<1*	<1	*<1*	<1			*<1*	<1		
Rb	*<15*	<15	22.0	46.7	*<15*	<15	*42.8*	8.0	*<15*	<15			*8.8*	59.6		
Ba	*28.0*	30.0	<50	119	*<50*	<50	*<50*	43.0	*<50*	<50			*43.0*	173		
Cu	*<10*	<10	<10	<10	*1090*	10	*520*	1290	*<10*	<10			*30*	40		
Co	*17.8*	17.2	42.9	30.2	*49.1*	1.4	*45.3*	11.1	*3.06*	1.50			*31.3*	2.86		
Ni	*44.3*	56.3	62.9	87.7	*<50*	<50	*66.5*	69.0	*47.7*	23.0			*<50*	14.6		
La	*22.1*	26.9	12.5	12.4	*15.7*	135	*18.2*	14.4	*21.4*	13.8			*17.0*	24.1		
Sm	*4.76*	5.67	4.03	<10	*5.21*	15.7	*<10*	<10	*3.54*	3.56			*5.23*	<10		
Sc	*22.3*	21.2	26.8	22.7	*32.0*	20.9	*24.8*	22.3	*9.17*	5.37			*26.4*	7.82		
Ta	*0.86*	0.93	0.83	0.87	*0.88*	1.08	*0.76*	0.78	*0.86*	0.64			*0.88*	1.40		
V	*310*	330	330	310	*440*	160	*340*	390	*100*	130			*360*	250		
Cr	*<40*	<40	<40	<40	*<40*	<40	*<40*	42	*113*	80			*<40*	25		
U	*2.54*	2.67	1.31	2.02	*0.88*	3.79	*2.02*	2.08	*1.41*	1.07			*1.93*	2.42		
Th	*4.86*	5.28	4.99	5.16	*5.14*	7.76	*4.99*	5.73	*8.33*	4.94			*5.87*	6.38		
Zr	*170*	200	170	180	*180*	230	*170*	180	*160*	170			*180*	260		
Al/Ti	*8.53*	8.62	8.81	8.57	*6.93*	7.15	*8.39*	7.77	*27.19*	27.40			*7.95*	7.63		
Al/Zr	*831*	702	838	787	*758*	732	*833*	772	*872*	743			*782*	755		
Ti/Zr	*97*	81	95	92	*110*	102	*99*	99	*32*	27			*98*	99		
density (kg/m3)	*2832*	2920	2847	2835	*2911*	2612	*2820*	2823	*2629*	2639			*2915*	2664		
dV%		-1	+2	±0		-7		-3		+11				-25		
ref. to Fig.		47A	47B	47C		47D		47E		48A		48B		47F		48C

Carbonation

The chemical changes related to the carbonation of albite diabase are (Fig. 47D): losses of Si, Fe, Mg, Ca, K, Br, S, Cu, Co, Sc and V and

Table 19. Continued.

alteration	carbonation + sericitization					
rock	albite diabase					
sample	*40-43*	40-3	*40-29*	40-3	*40-48*	1044-38
SiO2	*52.35*	49.23	*51.87*	49.23	*59.07*	57.91
TiO2	*1.97*	2.29	*1.97*	2.29	*0.48*	0.55
Al2O3	*13.79*	16.68	*13.65*	16.68	*14.25*	15.48
Fe2O3	*16.29*	4.38	*15.93*	4.38	*5.46*	3.28
MnO	*0.04*	0.20	*0.05*	0.20	*0.06*	0.08
MgO	*4.89*	4.58	*5.15*	4.58	*4.81*	4.95
CaO	*3.83*	7.25	*5.57*	7.25	*6.55*	5.57
Na2O	*6.23*	4.54	*5.17*	4.54	*5.89*	7.70
K2O	*0.25*	3.27	*0.17*	3.27	*0.58*	0.96
P2O5	*0.17*	0.17	*0.15*	0.17	*0.23*	0.28
sum	*99.81*	92.58	*99.68*	92.58	*97.39*	96.75
Br	*6.17*	0.20	*2.79*	0.20	*2.58*	<1
S	*660*	50	*210*	50	*2550*	20
Sb	*0.42*	1.43	*0.42*	1.43	*0.28*	0.68
As	*2.17*	0.30	*1.21*	0.30	*1.59*	0.18
W	*1.40*	11.9	*1.23*	11.9	*1.40*	4.06
Cs	*<1*	<1	*<1*	<1	*<1*	<1
Rb	*15.0*	58.2	*14.0*	58.2	*15.0*	29.2
Ba	*75.0*	202	*66.0*	202	*68.0*	99.6
Cu	*280*	10	*1090*	10	*30*	10
Co	*77.7*	7.0	*49.1*	7.0	*79.7*	5.5
Ni	*<50*	33.2	*<50*	33.2	*110*	81.4
La	*29.1*	21.8	*15.7*	21.8	*73.9*	52.6
Sm	*7.40*	<10	*5.21*	<10	*<10*	7.10
Sc	*34.6*	25.8	*32.0*	25.8	*20.3*	17.6
Ta	*0.97*	1.01	*0.88*	1.01	*0.48*	1.07
V	*330*	340	*440*	340	*90*	120
Cr	*<50*	39	*<50*	39	*255*	260
U	*1.33*	2.20	*0.88*	2.20	*4.71*	4.64
Th	*6.89*	8.75	*5.14*	8.75	*25.4*	25.6
Zr	*180*	220	*180*	220	*210*	240
Al/Ti	*7.00*	7.29	*6.93*	7.29	*29.5*	28.4
Al/Zr	*766*	758	*758*	758	*679*	645
Ti/Zr	*110*	104	*110*	104	*23*	23
density (kg/m3)	*2873*	2511	*2911*	2511	*2831*	2603
dV%		-1		±0		-4
ref. to Fig.		47G		47G		47H

gains in Na, Sb, W, REE and U. The changes in the albite diabase fragment in volcanic breccia (Fig. 47E) are losses of Si, Al(?), Fe, Mg, K, Br, S, Rb, Co and La and the gains in Mn, Ca, Na, W and Cu. Thus the changes caused by carbonation in the dykes and volcanic breccia fragments are fairly uniform. The most significant difference is the behaviour of Ca, which is probably caused by higher pre-carbonation Ca depletion in the dykes and higher carbonation intensity in the volcanic breccia.

The losses of Fe, Co, Ni, La, Sc and Th and the gains in Si, Mg, Ca, K, Br, Sb, W and V are related to the carbonation of felsic volcanic rock (Fig. 48A). The absolute K_2O gain is in fact negligible, only 0.02 percentage units. The carbonation trend of the main components in the tuffite (Fig. 48B) is Mn, Mg and Ca gain and Fe and K loss. Carbonation in felsic volcanic rock and tuffite closely resembles carbonation in the albite diabase dykes and the fragments of volcanic breccia, the main difference being Mg, which is depleted in the diabase and enriched in the more felsic rocks. This contrast is most probably caused by the pre-carbonation differences in composition, in that the mafic rocks had 3-5 fold higher Mg concentrations than the felsic volcanic rock and tuffite (cf. Tables 17 and 18). The intensity of brecciation was greater in the felsic volcanic rock than in the albite diabase, as indicated by the volume changes of +10% in the felsic volcanic rock and -7 - +3% in the albite diabase (Table 19).

Reactions [21]-[23], [25], [26] and [33] explain most of the chemical changes in the albite diabase and [25], [26] and [33] in the felsic volcanic rock and tuffite. Reaction [23], which consists of albitization in addition to carbonation, explains the Na gain in the albite diabase. Scheelite formation is the probable explanation for the comprehensive W enrichment of the carbonated zones. The alteration reactions indicate a near-neutral, H^+-releasing fluid with fluctuating f_{O2}, pyrite and magnetite being stable in the fractures and magnetite and haematite in the wall rock.

Sericitization

The greatest relative and absolute chemical

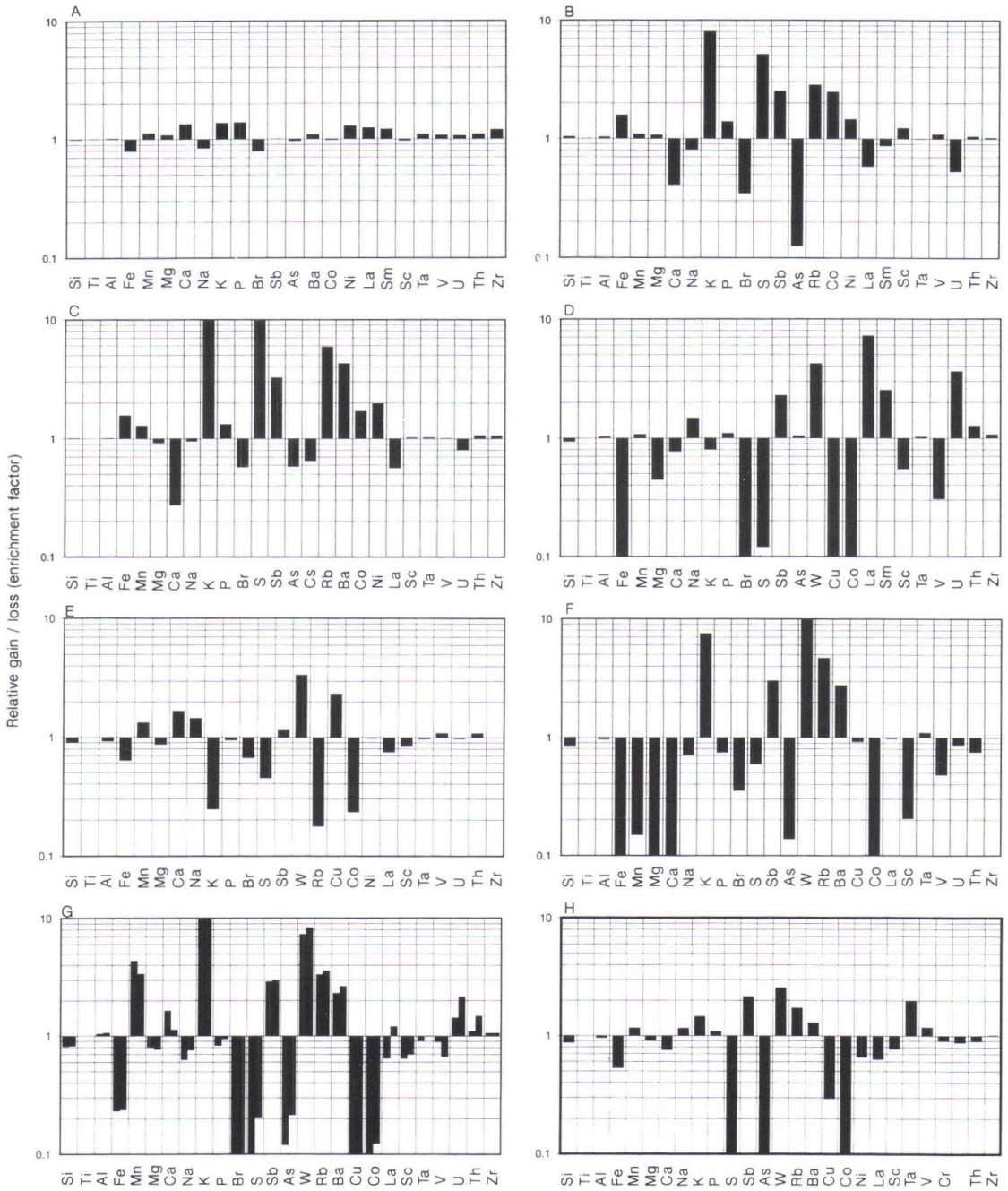

Fig. 47. Enrichment factors of the elements showing the chemical gains and losses during alterations in albite diabase at Honkavaara (y-axis). The calculations are based on comparisons between one altered and one less altered sample unless otherwise indicated. Note the logarithmic scale of the y-axis. **A**: Epidotization of albite diabase. **B**: Chloritization and weak biotitization of albite diabase. **C**: Intensive biotitization of albite diabase (= no chlorite left). **D**: Carbonation of albite diabase. **E**: Carbonation of the albite diabase fragment in volcanic breccia. **F**: Sericitization of albite diabase. **G**: Carbonation and sericitization of albite diabase. Two altered samples are compared with the least altered type. **H**: Carbonation and sericitization of the albite diabase dyke margin fragment in volcanic breccia.

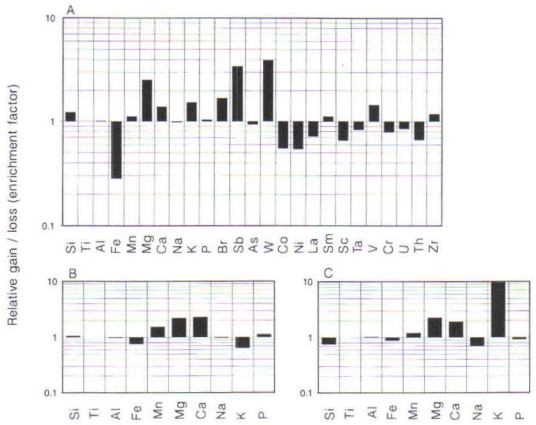

Fig. 48. Enrichment factors of the elements showing the chemical gains and losses during alterations in felsic volcanic rock and tuffite at Honkavaara (y-axis). The main components are presented in a typical order of analytical results. The general mobility of the trace elements decreases from left to right (Rose et al. 1979). The calculations are based on comparisons between one altered and one less altered sample. Since the samples in Figures B and C do not have equal ratios of the least mobile elements, the diagrams give only the trends in alteration. **A**: Carbonation of felsic volcanic rock. **B**: Carbonation of tuffite. **C**: Sericitization of tuffite.

and volume changes at Honkavaara (-25%, Table 19) are related to the sericitization of the albite diabase (Fig. 47F): Si, Fe, Mn, Mg, Ca, Na, P, Br, S, As, Co, Sc, V and U losses and K, Sb, W, Rb, and Ba gains. Since carbonation preceded sericitization, the apparent Fe, Br, Co, Sc and V losses and W gain are actually related to carbonation. The rest of the changes are combined with the sericitization reactions [18] and [27]-[29], which also indicate dehydration and CO_2 loss. The late replacements of carbonates by chlorite [25] and talc [20] were weak and cannot be identified in the chemical compositions. The fluid during sericitization was acid possibly as a result of H^+ release in carbonation and had low $a_{alkaline\text{-}earth}/a_{K+}$ and a_{Na+}/a_{K+} caused by alkaline-earth and Na precipitation during carbonation and albitization. The talc and chlorite were precipitated by a slightly less acid fluid with high a_{Mg2+}.

The alteration trend in the tuffite (Fig. 48C) is different from that in the albite diabase. It is highly probable that the Mn, Mg and Ca gains were inherited from the preceding carbonation, because there was no formation of talc or chlorite related to sericitization in the tuffite.

Finally, because of their wide occurrence and close connection, a combination of carbonation and sericitization in the albite diabase is presented in Figures 47G and 47H. Again a similarity in alteration styles between the diabase dykes and the diabase fragments in the volcanic breccia is indicated. This does not mean, however, that carbonation and sericitization took place before the formation of the volcanic breccia, as the breccia matrix is also carbonated and sericitized.

Isolaki

The least altered rocks

The chemical compositions of the least altered albite diabase (Table 20, p. 90) plotted on an alkali ratio diagram (Hughes 1973) indicate that some of the samples lie inside the igneous field but some are enriched in potassium (Fig. 49). This suggests that, apart from hydration, the alterations had a minimal chemical effect on part of the amphibole zone of the albite diabase while another part was affected by K

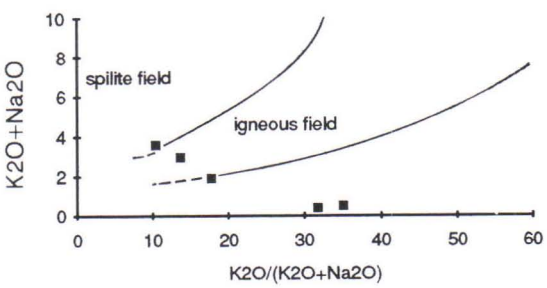

Fig. 49. The least altered albite diabase samples at Isolaki, plotted on the alkali ratio diagram of Hughes (1973).

Table 20. Chemical compositions of albite diabase at Isolaki.
Major elements in wt. %, trace elements in ppm.

	Albite diabase					
	least altered (amphibole)		biotitized	biotitized + carbonated	carbonated + sericitized	fragment in conglomerate (carbonated + sericitized)
	avg	std	avg	avg		
SiO2	49.65	2.06	45.87	48.19	43.98	38.36
TiO2	1.34	0.66	2.79	0.85	1.75	0.64
Al2O3	5.80	2.03	12.73	4.63	12.43	2.99
Fe2O3t	16.28	4.64	21.81	11.02	11.20	8.14
MnO	0.17	0.04	0.14	0.33	0.20	0.29
MgO	12.66	3.20	5.28	13.77	4.72	8.82
CaO	10.48	2.82	5.12	13.13	8.70	16.70
Na2O	1.57	1.32	5.07	0.76	4.60	0.02
K2O	0.28	0.13	0.63	1.16	1.66	1.23
P2O5	0.05	0.01	0.07	0.04	0.09	0.04
sum	98.27	1.38	99.50	93.87	89.33	77.21
Br	0.90	0.23	0.90	0.63	1.18	<0.5
S	170	139	1260	550	140	40
Sb	1.88	0.30	2.19	1.39	2.08	1.37
As	8.99	2.57	17.35	7.98	6.59	1.54
W	<2		<2	<2	<2	<2
Cs	<1		<1	1.67	<1	<1
Rb	11.3	1.99	18.3	41.0	34.4	28.3
Ba	80.7	43.4	108	65.7	472	237
Cu	<20		1280	<20	<20	<10
Co	62.4	6.03	79.1	54.3	11.4	8.25
Ni	230	66.6	110	243	82.3	94.8
La	6.07	2.78	7.16	8.45	15.5	3.28
Sm	<5	<5	<5	<5	<5	<5
Sc	62.7	11.7	29.7	55.0	24.5	41.1
Ta	0.24	0.05	0.53	<0.3	<0.3	0.15
V	340	193	770	210	520	160
Cr	484	415	<50	602	<50	652
U	7.14	9.49	4.56	4.56	2.99	1.37
Th	1.55	1.24	1.26	0.62	<0.5	<0.5
Zr	90	47	90	50	90	40
n	5		2	2	1	1

metasomatism. Petrographic investigations indicate that the K enrichment was combined with weak biotitization, thus the K-enriched samples in Figure 49 do not actually represent the least altered diabase but a weakly biotitized diabase. The formation of the least altered zone in the albite diabase is characterized by reaction [1] (Table 2), which implies hydration by an acid, weakly reducing fluid and mobility of the alkaline and alkaline-earth elements.

The chemical composition of the least altered quartzite (Table 21) closely resembles an average, non-feldspathic sericite quartzite, and since there are no petrographic indications of secondary sericitization, it is treated as unaltered rock. The chemical and mineralogical composition of the conglomerate varies, and there are abundant signs of carbonation. On the

Table 21. Chemical compositions of quartzite and conglomerate at Isolaki. Major elements in wt. %, trace elements in ppm.

	Quartzite			Conglomerate
	unaltered		carbonated + albitized	
	avg	std		avg
SiO2	89.31	1.14	68.86	60.50
TiO2	0.16	0.03	0.50	0.92
Al2O3	6.03	0.65	12.99	12.46
Fe2O3t	1.50	0.20	1.63	3.28
MnO	0.02	0.01	0.07	0.14
MgO	0.25	0.05	1.71	2.87
CaO	0.09	0.03	3.88	6.26
Na2O	0.01	0.02	6.99	5.05
K2O	2.15	0.24	0.18	1.37
P2O5	0.05	0.04	0.15	0.16
sum	99.57	0.04	96.96	93.00
Br	0.85	0.27	<0.5	1.14
S	50	8	60	50
Sb	0.78	0.12	1.57	2.54
As	1.97	0.32	2.28	2.87
W	<1		<2	<2
Cs	<0.5		<0.5	0.67
Rb	47.3	6.53	14.2	33.7
Ba	426	84.8	56.0	167
Cu	<10		<10	<10
Co	3.66	1.01	5.51	5.95
Ni	<40		<40	45.3
La	20.3	5.39	23.6	25.5
Sm	<5	<5	<5	<5
Sc	4.72	0.62	6.16	8.57
Ta	0.20	0.04	0.42	0.65
V	20	5	40	90
Cr	41.0	7.18	<50	<50
U	3.87	1.03	5.20	2.59
Th	4.96	1.21	6.69	5.81
Zr	140	28	140	180
n	4		1	2

other hand, carbonates are typical primary components of a conglomerate matrix. Thus, it is almost impossible to confirm that the conglomerate was carbonated by secondary processes or remained totally unaltered.

The volume changes and chemical mass balances related to the formation of the more altered diabase types were calculated using formulae [1] and [2]. The analyses compared, their immobile element ratios and volume changes are presented in Table 22.

Table 22. Isolaki. Analyses compared in Figure 50, their densities, immobile element ratios and volume changes (= dV%). The samples of least altered rock are presented in italics. Major elements in wt. %, trace elements in ppm.

alteration	biotitization + carbonation		carbonation + sericitization	
rock	albite diabase			
sample	*030-7*	034-3	*030-2*	031-3
SiO2	*50.97*	47.77	*49.70*	38.36
TiO2	*1.14*	0.71	*0.90*	0.64
Al2O3	*5.76*	3.56	*4.06*	2.99
Fe2O3	*13.31*	10.31	*13.06*	8.14
MnO	*0.18*	0.14	*0.19*	0.29
MgO	*13.17*	14.65	*14.80*	8.82
CaO	*11.05*	13.60	*13.54*	16.70
Na2O	*1.56*	0.09	*0.31*	0.02
K2O	*0.34*	1.75	*0.17*	1.23
P2O5	*0.05*	0.04	*0.05*	0.04
sum	*97.53*	92.62	*96.77*	77.21
Br	*<1*	<1	*0.70*	0.40
S	*70*	750	*150*	40
Sb	*1.67*	1.46	*1.94*	1.37
As	*6.34*	8.24	*10.2*	1.54
W	*<2*	<2	*<2*	<2
Cs	*0.92*	2.52	*<1*	<1
Rb	*12.0*	70.0	*9.77*	28.3
Ba	*<70*	69.9	*60.0*	237
Cu	*20*	<10	*50*	0
Co	*52.6*	53.7	*63.8*	8.25
Ni	*213*	281	*292*	94.8
La	*10.8*	8.01	*5.97*	3.28
Sm	*<5*	<5	*<5*	<5
Sc	*72.1*	49.0	*77.2*	41.1
Ta	*<0.3*	<0.3	*0.25*	0.15
V	*280*	180	*210*	160
Cr	*329*	662	*937*	652
U	*5.30*	1.32	*23.7*	1.37
Th	*1.18*	0.88	*0.98*	<1
Zr	*80*	50	*60*	40
Al/Ti	*5.06*	5.05	*4.53*	4.67
Al/Zr	*720*	712	*677*	748
Ti/Zr	*142*	141	*150*	160
density (kg/m3)	*2886*	2949	*3137*	2862
dV%		+58		+54
ref. to Fig.		50A		50B

Chloritization, biotitization, carbonation and sericitization

On account of the overlapping alterations and the parallelism between the alteration zones and the zones formed by magmatic differentiation, the variations in the chemical compositions presented in Table 20 are a combination of differentiation and secondary alterations, and only two suitable pairs of samples were found for the mass balance calculations (Table 22). As a consequence of the nature of the alteration style in these pairs, none of the alteration types can be treated separately.

The petrographical investigations imply that reaction [6] caused the formation of chloritized zones, that the diabase was hydrated and that Si, Mg, Ca, Na, K, S, Ba, Cu, Co, and Ni were mobilized by a acid, reducing fluid.

Most elements in the albite diabase were enriched by a combination of biotitization + carbonation (Fig. 50A), while only Na and U were depleted and Ti, Al, La(?), Sc, V, Th(?) and Zr were immobile. The volume change was large, +58% (Table 22). The biotitization reactions [10] and [12], carbonation reactions [19], [21], [23] and [26] and pyrite formation reaction [34] explain the Mn, Ca, K and trace element gains. Quartz precipitation in the fractures explains the Si enrichment. The formation of carbonate with higher Fe and Mg concentrations than the silicates it replaced may be the reason for the Fe and Mg enrichment.

A diabase fragment in the conglomerate is highly carbonated and moderately sericitized. The chemical changes within this fragment (Fig. 50B) were losses of Fe, Mg, Na, S, As, Cu, Co, Ni, REE and U and gains in Si (?), Mn, Ca, K, Rb and Ba. Th volume change was +54% (Table 22). Reactions [18], [21]-[26], [28] and [33] are possible explanations for the alterations. The carbonation-related and biotitization-related mineral associations in both the dyke and the diabase fragment in the conglomerate imply a near-neutral or mildly alkaline, oxidizing fluid with high f_{CO2} and low a_{Na+}/a_{K+}.

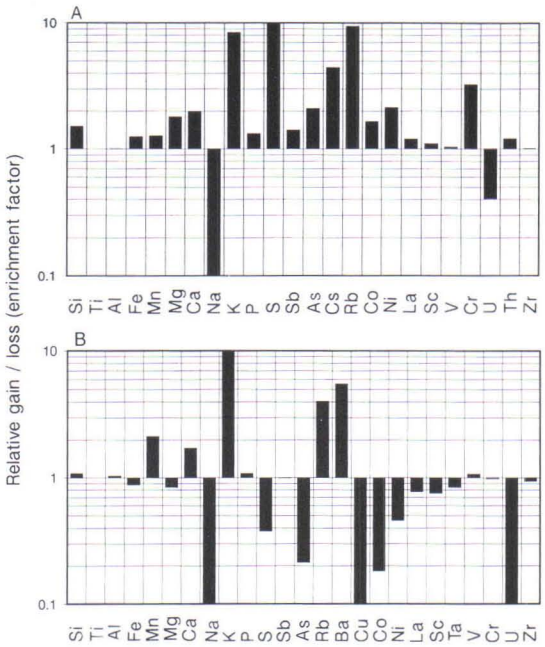

Fig. 50. Enrichment factors of the elements showing the chemical gains and losses during alterations in the albite diabase at Isolaki (y-axis). Only analytical results with small errors are used in the calculations, so that the element sets are different figures. The main components are presented in typical order of analytical results. The general mobility of the trace elements decreases from left to right (Rose et al. 1979). The calculations are based on comparisons between one altered and one less altered sample. Note the logarithmic scale of the y-axis. **A**: Biotitization and carbonation of albite diabase. **B**: Carbonation and sericitization of the albite diabase fragment in conglomerate.

The only alteration in the quartzite is carbonation + albitization in the diabase contact zone. The trend in alteration, according to the correlation between unaltered and altered quartzite compositions (Table 21), consist of losses of Si and K and gains in Ti, Al, Mn, Mg, Ca and Na, if the rock volume was conserved, but if Al was immobile, the rock volume will have decreased by about 50% and the related chemical changes will have been Si, Fe and K losses and Ti, Mn, Mg, Ca and Na gains. Some of the apparent changes may actually have beeen caused by the primary differences between altered and unaltered types, as the difference in Ti concentrations, for example, is easi-

ly explained by a sediment layer with higher detrital Ti mineral content in the altered type. The albitization reactions [17] and [18] explain the Fe, Na and K mobility and dolomite formation the Mn, Mg and Ca enrichments. The fluid was similar to the carbonating fluid that affected the diabase, except that its a_{Na+}/a_{K+} was much higher.

Palovaara

The least altered rocks

The least altered rocks in the area are the ultramafic rocks of the amphibole and chlorite-serpentine-talc zones (Table 23, p. 94), chloritized lamprophyre, mafic lava and albite diabase (Table 24, p. 95), albitized + weakly carbonated quartzite and siltstone and chloritized + albitized tuffite (Table 25, p. 96). The chemical data for the least altered igneous rocks plotted on an alkali ratio diagram (Fig. 51) indicate that the mafic rocks lie distinctly within the spilite field and those ultramafic rocks which have enough K and Na for the purposes of the diagram lie in a zone where the igneous field gives way to the spilite field. This suggests a Na-metasomatic effect on the ultramafic and mafic lava and diabase. The high Na concentration in the least altered sediments and tuffites (Table 25) suggests an altered nature for these as well.

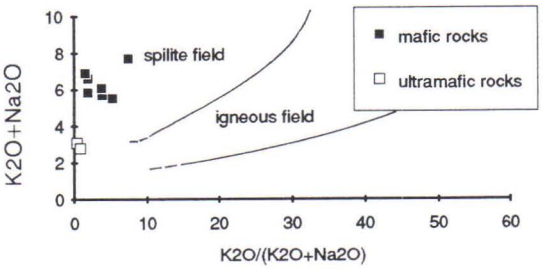

Fig. 51. The least altered igneous rocks at Palovaara, plotted on the alkali ratio diagram of Hughes (1973).

The formation of the chloritized zones in the mafic lava and albite diabase is characterized by a combination of reactions [6] and [8] (Table 2), that in the ultramafic rock by [1] and [8] in the amphibole zone and [4], [5] and [32] in the chlorite-serpentine-talc zone, and by [2], [8] and [10] in the lamprophyre. These reactions and the chemical compositions (Tables 23 and 24) imply that significant hydration, gains in S and Na and losses of Cu, Co, Ni and the alkaline and alkaline-earth elements except for Mg and Na were related to the formation of the alteration zone. The fluid was a reducing one, contained some CO_2 (as indicated by the ultramafic rocks) and its a_{Na+}/a_{K+} was high. The fluid in the mafic rocks was acid, but that in ultramafic rock was near-neutral, because carbonates were precipitated.

The least altered zones of quartzite and siltstone are characterized by the albitization reactions [14], [16] and [18] (K, Rb and Ca loss; Na gain), the carbonation of albite [22] (Ca and Mg gain) and the decomposition of sphene [21], which imply a near neutral fluid with high a_{Na+}/a_{K+} and moderate f_{CO2}. The comparison between the Palovaara quartzite (Table 25) and an average arkose quartzite (Table 15, p. 78) supports the assumed changes, as the Mg and Na concentrations at Palovaara are higher than those in the average arkose quartzite of Pettijohn et al. (1987), K lower and Ca roughly equal.

The least altered type of tuffite is rare, and only one chemical analysis is available (Table 25), so that little can be said about the alterations that formed it, but the chloritization and albitization reactions [8], [10] and [14] were probably the most important. This is supported by the high Mg and Na and low Ca and K concentrations in the rock.

The volume changes and chemical mass bal-

Table 23. Chemical compositions of ultramafic volcanic rocks and chrome-bearing marbles at Palovaara. Major elements in wt. %, trace elements in ppm.

	Ultramafic lava (more primitive)				Ultramafic lava (less primitive)			Ultramafic tuff			Chrome-bearing marble	
	least altered (serpentine + chlorite + talc)		carbonated		least altered (amphibole + chlorite + biotite)	carbonated	carbonated + sericitized	chloritized + carbonated		carbonated + sericitized	intensively carbonated + sericitized	
	avg	std	avg	std	avg			avg	std		avg	std
SiO2	44.95	1.65	42.22	0.91	47.69	39.15	37.27	37.52	1.43	39.36	38.47	2.10
TiO2	0.40	0.05	0.37	0.01	0.63	0.60	0.67	0.63	0.33	0.67	0.41	0.11
Al2O3	6.23	1.11	5.14	0.32	8.90	8.03	9.04	6.25	2.08	6.77	6.51	1.90
Fe2O3t	14.86	1.49	10.06	3.74	13.91	19.36	12.98	15.71	4.96	13.87	9.69	3.83
MnO	0.07	0.02	0.12	0.05	0.18	0.21	0.25	0.19	0.07	0.28	0.37	0.18
MgO	30.56	2.91	29.66	0.52	14.25	13.11	8.39	18.56	6.16	10.80	11.80	3.04
CaO	2.03	1.87	6.12	1.90	7.45	3.72	7.53	5.21	2.44	4.70	8.83	5.30
Na2O	<0.01		<0.01		1.34	<0.01	<0.01	<0.01		<0.01	<0.01	
K2O	0.01	0.00	<0.01		1.57	0.01	3.36	0.07	0.06	2.65	2.53	0.68
P2O5	0.04	0.00	0.03	0.00	0.08	0.04	0.04	0.06	0.05	0.06	0.04	0.02
sum	99.13	0.31	93.72	3.42	95.99	84.24	79.52	84.21	3.80	79.16	78.66	1.81
Br	<1		<1		<1	<1	<1	<1		<1	<1	
S	660	208	150	44	910	30	900	320	156	380	1340	1369
Sb	2.07	1.17	0.66	0.32	1.72	0.45	1.04	0.63	0.14	0.61	0.75	0.41
As	46.5	26.2	1.62	1.56	6.29	0.87	4.87	0.91	0.15	2.09	2.63	2.20
W	<2		<2		<2	<2	<2	<2		<2	<2	
Cs	<1		<1		<1	<1	0.95	<1		0.36	<1	
Rb	<10		<10		42.1	<10	126	<10		56.8	55.8	5.83
Cu	<20		<20		<20	<20	<20	<20		<20	<20	
Ba	<60		<60		<60	<60	240	<60		74	148	26
Co	105	21.2	71.7	9.67	70.9	60.8	58.3	42.1	12.2	16.4	24.7	12.4
Ni	1427	155	1623	110	268	662	341	912	433	409	375	233
La	0.36	0.14	0.74	0.41	10.5	1.07	5.19	4.55	3.84	3.88	3.96	3.65
Sm	0.46	0.19	0.72	0.41	2.88	1.30	2.94	1.69	0.89	1.91	<5	
Sc	29.5	2.9	28.8	0.8	45.0	37.2	68.2	28.6	4.6	23.9	33.4	16.5
Ta	<0.3		<0.3		0.19	<0.3	<0.3	0.20	0.07	0.13	0.10	0.03
V	180	40	140	0	240	230	250	190	64	240	190	70
Cr	3530	427	3947	47.3	1490	1140	1600	2117	671	1410	2177	265
U	<0.3		<0.3		0.58	<0.3	0.44	0.30	0.19	0.43	0.69	0.34
Th	<0.5		<0.5		1.70	<0.5	<0.5	<0.5		0.56	0.25	0.07
Zr	30	0	30	6	90	40	50	60	32	60	40	6
n	3		3		2	1	1	3		1	3	

ances related to the formation of the more altered zones were calculated using formulae [1] and [2]. The analyses compared, their immobile element ratios and volume changes are presented in Table 26.

Biotitization

The chemical changes related to biotitization in the mafic lava and albite diabase (Fig. 52A) are losses of Si, Na and Sb and the gains in Mn, Mg, K, S, Cs, Rb, Cu, Co, Ni and Cr. Most of these changes are associated with the biotitization reactions [10] and [12], the pyritization reaction [34] and a reducing, near-neutral, low a_{Na+}/a_{K+} fluid which released H^+. The Na loss is related to the replacement of albite by biotite. The chemical changes caused by the biotitiza-

Table 24. Chemical compositions of mafic lavas, albite diabases and lamprophyres at Palovaara.
Major elements in weight per cent, trace elements in ppm.

	Mafic lava and albite diabase								Lamprophyres, each analyse represent separate dyke			
	least altered (chloritized)		chloritized + biotitized		chloritized + carbonated		carbonated + sericitized		chloritized	chloritized + carbonated	carbonated	carbonated + sericitized
	avg	std	avg	std	avg	std	avg	std				
SiO2	52.09	2.43	51.25	1.64	50.72	2.35	46.42	3.82	51.20	45.45	43.56	44.90
TiO2	1.94	0.53	1.38	0.61	1.74	0.78	1.90	0.63	0.90	0.67	0.53	0.51
Al2O3	14.89	0.93	14.31	0.60	14.59	0.69	13.69	1.28	17.80	11.05	6.20	7.46
Fe2O3t	16.81	2.65	17.12	1.25	12.69	4.90	10.96	4.29	12.03	9.45	11.90	10.70
MnO	0.05	0.01	0.06	0.01	0.10	0.04	0.18	0.07	0.04	0.14	0.12	0.13
MgO	4.24	1.00	5.94	1.05	4.45	0.97	4.11	0.60	5.05	8.70	24.23	20.60
CaO	2.29	0.55	2.07	0.83	4.25	1.53	5.88	2.72	2.86	6.93	5.27	6.41
Na2O	6.08	0.71	4.30	0.97	6.11	1.31	4.86	1.23	6.84	3.25	0.00	0.11
K2O	0.23	0.16	2.32	1.30	0.48	0.41	2.08	0.64	2.07	2.23	2.14	3.26
P2O5	0.24	0.06	0.19	0.07	0.22	0.09	0.23	0.07	0.61	0.86	0.52	0.60
sum	98.85	0.38	98.93	0.70	95.35	2.15	90.30	4.18	99.39	88.72	94.46	94.68
Br	<1		<1		<1		<1		2.48	1.69	<1	<1
S	1030	522	990	635	1280	1110	1240	768	7310	2040	80	140
Sb	0.94	0.22	0.52	0.15	0.70	0.41	1.19	0.50	0.41	0.56	0.83	0.28
As	3.14	1.41	4.33	3.03	4.75	2.30	3.14	2.40	4.15	4.36	8.44	3.14
W	<2		<2		<2		<2		<2	<2	<2	<2
Cs	<1		1.68	0.73	<1		<1		1.40	2.58	2.54	3.41
Rb	9.67	3.09	76.4	40.7	15.7	13.3	51.4	25.3	53.4	79.5	73.0	86.7
Ba	40.9	8.46	91.1	42.9	48.6	21.1	102	35.3	320	2270	883	1750
Cu	110	128	60	63	60	77	<20		<20	<20	<20	<20
Ni	58.4	20.5	54.9	30.9	52.4	20.6	50.3	18.5	91.4	83.6	908	727
Co	37.6	9.78	48.1	12.4	43.6	23.4	33.1	18.5	47.4	30.5	75.2	68.8
La	18.9	4.86	22.4	5.9	17.5	9.0	25.6	24.4	297	125	87.5	124
Sm	5.41	1.08	5.82	2.03	6.32	1.11	6.20	0.99	42.6	17.7	12.3	<20
Sc	28.8	5.01	37.1	2.52	28.9	7.45	27.0	6.01	17.6	36.8	34.3	30.4
Ta	0.83	0.34	0.82	0.44	0.75	0.31	0.87	0.24	0.57	1.02	0.99	0.61
V	360	51	310	49	340	86	350	85	170	150	130	120
Cr	67.9	33.9	155	116	86.6	53.7	67.3	42.7	<60	349	1430	1260
U	1.10	0.20	1.00	0.11	1.20	0.29	1.37	0.29	9.66	4.73	2.68	5.06
Th	3.13	0.43	3.30	0.43	3.05	0.84	2.83	0.56	29.0	24.2	12.9	21.9
Zr	200	23	190	29	190	32	190	18	210	160	100	130
n	7		11		13		18		1	1	1	1

tion in the lamprophyre dykes were different because of the different pre-biotitization compositions (Table 24), the relative K gain in particular having presumably been smaller. The lack of biotitization-related brecciation is supported by the roughly constant rock volume (Table 26).

Carbonation

The chemical changes related to the carbonation of the igneous rocks at Palovaara are presented in Figures 52B-52D. Carbonation was characterized by losses of Si, Mg, K, S, As, Sb and Co and the gains in Mn, Ca and REE in the ultramafic units, losses of Sb and Cr and gains in Mn, Ca, Na, K, S, Cu, and Co in the mafic lava and diabase and losses of Fe, Na, K, P, As, Cs, Rb and La and the gains in Si, Mn, Ca, Ta, Cr and U in the lamprophyre dykes. The common features are Mn and Ca gains and the immobility of Ti, Al, Sc(?), V, Th and Zr. The

Table 25. Chemical composition of tuffite and sediments at Palovaara
Major elements in wt. %, trace elements in ppm.

	Quartzite		Siltstone						Tuffite		
	albitized + carbonated		albitized + carbonated		carbonated + sericitized		carbonated + sericitized + intensively pyritized		albitized + chloritized	carbonated + sericitized + pyritized	
	avg	std	avg	std	avg	std	avg	std		avg	std
SiO2	71.02	4.04	59.15	6.31	51.85	20.84	45.51	9.63	56.40	49.27	2.85
TiO2	0.24	0.11	0.48	0.03	0.50	0.30	0.87	0.14	0.53	1.10	0.17
Al2O3	13.22	1.25	14.12	1.59	12.44	7.42	14.44	4.01	15.50	12.43	1.26
Fe2O3t	2.07	0.45	4.59	3.20	6.41	2.83	6.47	1.08	13.11	8.66	3.28
MnO	0.08	0.03	0.09	0.05	0.23	0.25	0.18	0.10	0.04	0.28	0.08
MgO	1.89	0.70	3.71	1.51	4.53	4.23	4.93	2.24	8.20	5.09	0.76
CaO	3.14	1.42	4.33	3.69	7.65	10.15	8.93	5.28	0.84	5.68	3.29
Na2O	5.40	1.74	6.54	1.64	0.09	0.11	0.07	0.06	4.80	0.05	0.10
K2O	1.54	1.32	0.51	0.30	4.84	2.98	4.73	1.14	0.37	4.43	0.56
P2O5	0.10	0.03	0.13	0.02	0.13	0.07	0.22	0.30	0.07	0.08	0.01
sum	98.70	1.57	93.66	3.43	88.66	15.07	86.35	7.25	99.87	87.06	2.65
Br	1.43	0.63	0.74	0.35	<1		<1		<1	<1	
S	60	39	70	35	560	377	23400	23132	80	4530	3331
Sb	0.46	0.33	1.03	0.21	0.74	0.67	0.82	0.49	0.237	0.82	0.42
As	<0.6		<0.6		0.81	0.58	98.4	69.9	1.04	26.9	19.7
W	2.97	2.22	9.67	10.4	<2		<2		<2	2.64	1.75
Cs	<1		<1		<1		<1		<1	<1	
Rb	37.9	36.2	14.1	6.36	153	118	95.5	31.4	<10	96.3	21.9
Ba	179	153	37.5	10.6	416	510	372	243	54.2	287	151
Cu	<10		<10		<10		140	139	20	80	87
Co	2.73	0.56	5.27	4.34	11.6	7.60	194	111	40.7	64.0	68.7
Ni	25.6	11.1	52.8	41.8	49.1	4.26	132	22.9	46.9	105	27.8
La	9.19	5.75	17.8	14.5	29.8	22.6	55.6	68.9	12.6	7.65	2.69
Sm	2.86	0.56	<10		6.97	1.33	11.6	10.8	<10	2.57	0.39
Sc	5.34	2.36	9.15	3.62	12.7	5.34	37.8	13.7	48.1	46.5	4.16
Ta	0.32	0.16	0.71	0.14	0.61	0.39	0.38	0.26	0.232	0.36	0.14
V	50	29	60	20	100	53	240	80	240	260	21
Cr	73.4	26.7	117	52.0	122	50.3	180	52.2	356	195	41.9
U	0.98	0.32	1.31	0.73	1.99	1.10	2.88	2.26	1.08	1.07	0.55
Th	4.53	3.26	10.7	7.1	7.76	5.59	7.70	9.05	2.29	0.91	0.62
Zr	150	61	220	37	140	92	110	51	80	100	34
n	9		6		4		3		1	7	

differences in relative changes are caused the nature of the pre-carbonated rock types. Thus, since the lamprophyre dykes had high LIL element concentrations and the ultramafic rocks high sulphide concentrations, the lamprophyre dykes were apt to lose LILE and the ultramafic rocks to lose S, As, Sb and Co.

The mass balance calculations show that the effect of brecciation on the rock volume (Table 26) was negligible in the ultramafic rock (volume change -5%), small in the albite diabase and mafic lava (volume change +5%), and moderate in the lamprophyre (volume change +15%).

REE mobility is depicted in Figure 53, which indicates a weak LREE gain and HREE loss during carbonation of a mafic lava, with a high Eu loss, but contrasts with Figure 52C. The REE were obviously leached in one place and deposited in an other during carbonation, and dissolved REE were deposited where the car-

Table 26. Palovaara. Analyses compared in Figure 52, their densities, immobile element ratios and volume changes (= dV%). The samples of least altered rock are presented in italics. Abbreviations: cb = carbonation, se =sericitization. Major elements in wt. %, trace elements in ppm. The number of samples from which each average was calculated is indicated in parentheses after the abbreviation "avg".

alteration	biotitization		carbonation						carbonation + sericitization						sericitization	
rock	mafic lava		ultramafic lava		mafic lava		lamprophyre		mafic lava and albite diabase						ultramafic tuff	
sample	*1-19,1*	2-157,0	*2-202,3*	2-181,5	*1-19,1*	1-23,7	*1-182,7*	3-34,3	*avg(2)*	1-107,6	*2-109,7*	2-119,3	*1-114,6*	1-38,5	avg(3)	1-55,9
type															cb	cb+se
SiO2	*52.92*	49.83	*45.17*	42.96	*52.92*	50.52	*42.40*	41.60	*53.14*	50.37	*54.86*	49.81	*47.48*	38.06	37.52	39.36
TiO2	*2.31*	2.32	*0.34*	0.36	*2.31*	2.24	*0.90*	0.79	*1.78*	1.59	*0.92*	1.01	*2.57*	2.34	0.63	0.67
Al2O3	*14.32*	14.27	*5.01*	5.38	*14.32*	13.95	*11.10*	9.35	*16.02*	14.54	*15.23*	16.78	*14.01*	13.21	6.25	6.77
Fe2O3	*18.06*	19.59	*13.79*	13.80	*18.06*	17.69	*14.26*	11.20	*15.17*	12.30	*13.07*	5.06	*20.31*	7.58	15.71	13.87
MnO	*0.03*	0.05	*0.05*	0.06	*0.03*	0.07	*0.04*	0.13	*0.05*	0.12	*0.05*	0.13	*0.07*	0.23	0.19	0.28
MgO	*3.82*	4.88	*33.45*	30.26	*3.82*	3.60	*17.33*	14.70	*3.64*	3.27	*5.91*	3.22	*4.78*	4.47	18.56	10.80
CaO	*1.66*	1.57	*0.94*	4.24	*1.66*	3.66	*3.43*	7.98	*1.93*	4.36	*2.31*	6.82	*3.13*	10.97	5.21	4.70
Na2O	*5.72*	4.52	*<0.01*	<0.01	*5.72*	6.28	*0.56*	0.01	*6.78*	5.87	*5.44*	6.45	*5.83*	4.72	0.01	0.01
K2O	*0.11*	2.01	*0.01*	0.00	*0.11*	0.14	*5.05*	3.06	*0.34*	1.33	*0.22*	2.36	*0.23*	2.07	0.07	2.65
P2O5	*0.30*	0.29	*0.03*	0.03	*0.30*	0.29	*2.38*	0.64	*0.21*	0.20	*0.13*	0.12	*0.30*	0.22	0.06	0.06
sum	*99.25*	99.34	*98.78*	97.08	*99.25*	98.43	*97.45*	89.46	*99.05*	93.95	*98.13*	91.76	*98.70*	83.86	84.22	79.17
Br	*<1*	<1	*<1*	<1	*<1*	<1	*<1*	<1	*<1*	<1	*<1*	<1	*<1*	<1	<1	<1
S	*500*	660	*780*	200	*500*	640	*250*	190	*1065*	1170	*1660*	3360	*1320*	2030	323	380
Sb	*1.10*	0.53	*3.42*	1.03	*1.10*	0.65	*0.47*	0.44	*0.72*	0.61	*0.71*	0.95	*1.11*	0.99	0.63	0.61
As	*2.83*	2.97	*75.0*	3.42	*2.83*	2.48	*27.1*	0.53	*3.24*	2.25	*2.57*	7.79	*3.08*	3.28	0.91	2.09
W	*<2*	<2	*<2*	<2	*<2*	<2	*<2*	<2	*<2*	<2	*<2*	<2	*<2*	<2	<2	<2
Cs	*0.63*	2.22	*<1*	<1	*0.63*	<1	*5.54*	2.93	*<1*	<1	*<1*	<1	*<1*	<1	<1	0.36
Rb	*8.50*	86.9	*<10*	<10	*8.50*	<10	*148*	86.4	*11.1*	30.4	*6.00*	33.3	*11.6*	38.1	8.50	56.8
Ba	*33.6*	<80	*<60*	<60	*33.6*	<60	*3090*	2290	*48.2*	82.0	*35.0*	136	*39.0*	97.6	44.0	74.0
Cu	*40*	100	*<20*	<20	*40*	110	*<20*	<20	*<20*	<20	*<20*	<20	*<20*	<20	<20	<20
Co	*40.0*	54.9	*83.7*	68.6	*40.0*	51.6	*52.2*	57.4	*27.3*	26.8	*53.1*	82.4	*32.9*	53.8	42.1	16.4
Ni	*81.2*	107	*1600*	1560	*81.2*	80.4	*428*	463	*45.0*	47.2	*70.2*	43.3	*33.0*	46.7	912	409
La	*26.6*	29.0	*0.27*	1.11	*26.6*	20.8	*177*	77.7	*14.4*	12.1	*23.1*	36.9	*15.6*	2.93	4.55	3.88
Sm	*7.36*	8.34	*0.64*	1.19	*7.36*	6.30	*<20*	<20	*<5*	<5	*<5*	<5	*<5*	<5	1.69	1.91
Sc	*29.0*	35.4	*26.2*	29.7	*29.0*	27.9	*39.6*	28.2	*30.5*	33.0	*35.9*	24.6	*29.4*	22.4	28.6	23.9
Ta	*1.26*	1.43	*<0.3*	<0.3	*1.26*	1.08	*0.47*	0.72	*0.45*	0.54	*0.59*	0.62	*0.94*	0.91	0.20	0.13
V	*360*	390	*130*	140	*360*	340	*180*	170	*365*	380	*260*	290	*430*	470	187	240
Cr	*68.7*	93.7	*3980*	3930	*68.7*	35.0	*456*	671	*53.0*	32.0	*135*	148	*32.0*	52.7	2117	1410
U	*1.05*	1.09	*<0.3*	<0.3	*1.05*	0.93	*3.71*	4.47	*1.26*	1.67	*0.96*	1.47	*0.91*	1.56	0.30	0.43
Th	*3.59*	3.64	*<0.5*	<0.5	*3.59*	3.22	*23.8*	20.0	*3.08*	2.81	*3.41*	4.24	*2.37*	2.09	<0.5	0.56
Zr	*230*	230	*30*	30	*230*	220	*130*	120	*180*	170	*180*	190	*180*	170	63	60
Al/Ti	*6.21*	6.15	*14.9*	15.1	*6.21*	6.23	*12.3*	11.8	*9.00*	9.16	*16.6*	16.5	*5.45*	5.65	9.86	10.1
Al/Zr	*623*	620	*1670*	1793	*623*	634	*854*	779	*890*	855	*846*	883	*778*	777	987	1128
Ti/Zr	*100*	101	*112*	119	*100*	102	*69.4*	65.8	*98.8*	93.4	*51.1*	53.4	*143*	138	100	112
density (kg/m3)	*2900*	2925	*2969*	2939	*2900*	2847	*2840*	2820	*2833*	2797	*2858*	2784	*2979*	2859	2910	2934
dV%		-2		-5		+5		+15		+14		-7		+15		-6
ref. to Fig.		52A		52B		52C		52D		52E		52E		52E		52F

bonation intensity was greatest (e.g., in the ultramafic rock, Fig. 52B).

The carbonation reactions [5], [20] and [25] and the pyrite decomposition reaction [33] explain most of the chemical changes in the ultramafic rocks. Carbonation also explains the Si

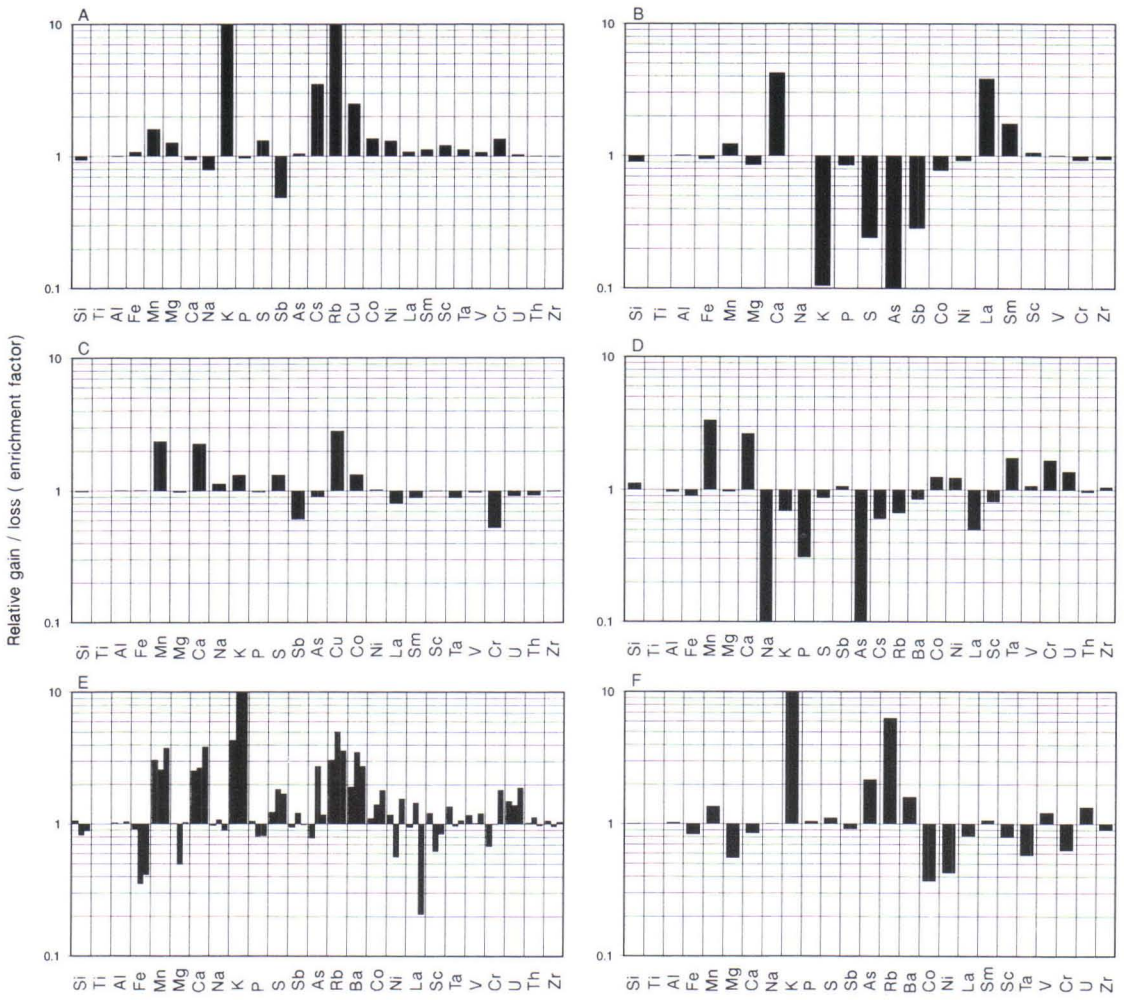

Fig. 52. Enrichment factors of the elements showing chemical gains and losses during the alterations at Palovaara (y-axis). Only analytical results with small errors are used in the calculations, so that the element sets are different figures. Main components are presented in a typical order of analytical results. The general mobility of the trace elements decreases from left to right (Rose et al. 1979). The calculations are based on comparisons between one altered and one less altered sample, except in Figure E. Note the logarithmic scale of the y-axis. **A**: Biotitization of mafic lava and albite diabase. **B**: Carbonation of ultramafic lava. **C**: Carbonation of mafic lava and albite diabase. **D**: Carbonation of lamprophyre. **E**: Carbonation and sericitization of mafic lava and albite diabase. Three altered samples are compared with the least altered type. **F**: Sericitization of carbonated ultramafic tuffite.

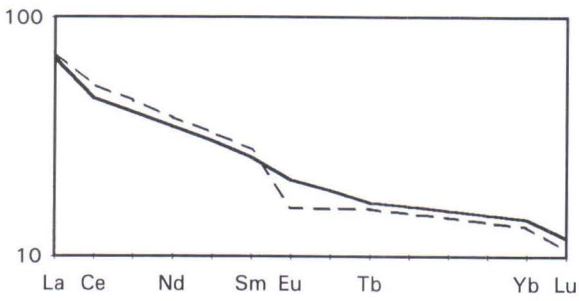

Fig. 53. Chondrite-normalized REE patterns for a mafic lava. Solid line: chloritized and biotitized type, dotted line: carbonated type. The mass balance calculations suggest no significant volume change. Normalizing values from Hickey and Frey (1982).

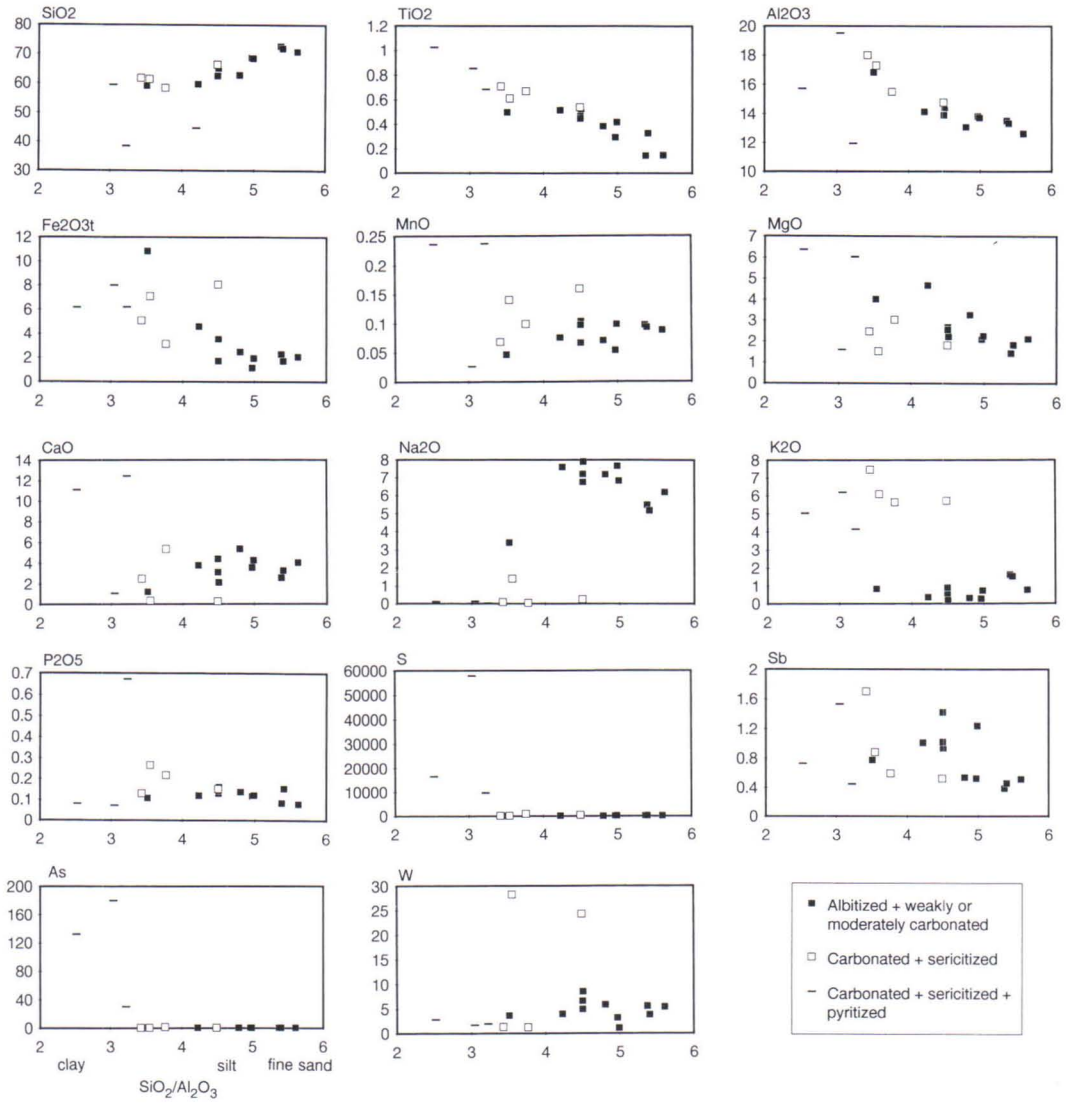

Fig. 54. Plots of major and trace elements vs. SiO_2/Al_2O_3 in the weakly carbonated (+ albitized), carbonated + sericitized, and carbonated + sericitized + intensively pyritized types of sediment at Palovaara. The ranges of SiO_2/Al_2O_3, a rough measure of the grain size of sediments (Taylor and McLennan 1985), for clay, silt and fine sand are indicated at the bottom of the figure.

loss, provided that silica from talc and chlorite decomposition (reactions [20] and [25], respectively) did not precipitate but was dissolved in the fluid. The reactions that explain the chemical changes in the albite diabase, mafic lava and lamprophyre are [21], [22], [25] and [26]. Additionally, chalcopyrite precipitation explains the S and Cu gains in the mafic lava and albite diabase, and apatite decomposition the P loss in the lamprophyre.

Sericitization and pyritization

Sericitization is common in mafic lava and

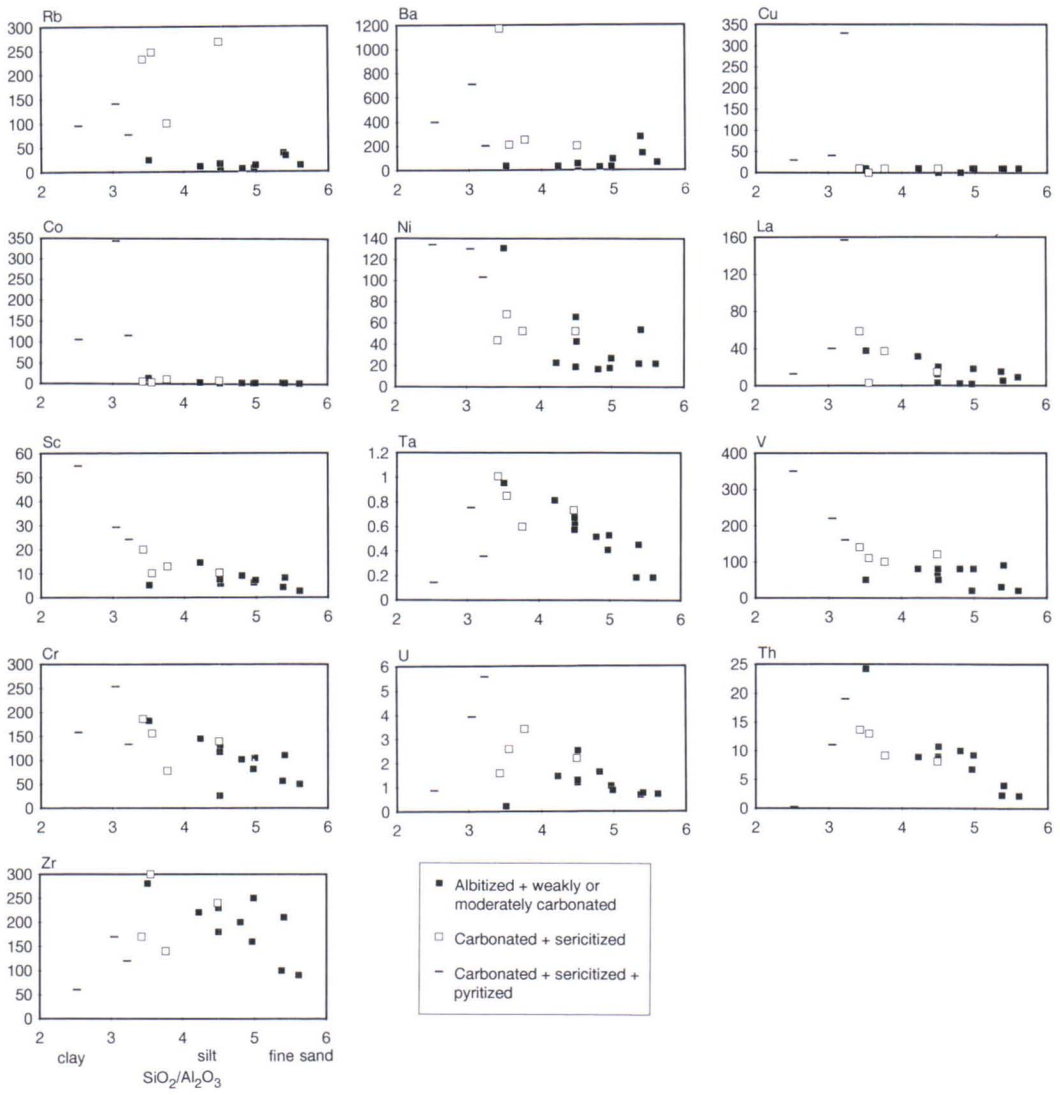

Fig. 54. Continued.

albite diabase, but because it overlaps with carbonation, the chemical changes related to the sericitized zones are actually a combination of carbonation and sericitization (Fig. 52E): loss of Fe and gains in Mn, Ca, K, S, Rb, Ba and U, and in some cases also losses of Si, Mg, P, Ni, La, Sc and Cr and/or gains in As, Co, Ni, La, Ta and Cr. These chemical changes can be explained by a combination of the carbonation and sericitization reactions [18]-[29], pyrite formation [34] and apatite decomposition. The reason for the U gain may have been a change in f_{O2} conditions (from oxidizing to reducing).

The problem of overlapping carbonation exists in the ultramafic rocks, too. A carbonated sample of ultramafic tuff is compared with a

carbonated and sericitized one in Figure 52F, the maximum error in the mass balance calculations arising from the layered nature of the tuff is assumed to be at least ±10% for the main components and ±40% for the trace elements. The most obvious chemical changes are losses of Fe, Mg, Ca, Co, Ni and Ta and the gains in Mn, K, As, Rb and Ba. The changes in Mg and Mn concentrations are probably caused by carbonation (cf. Figs. 52B and 52F). Other changes are combined with the sericitization of chlorite and of talc. The alterations in the igneous rocks suggest that the H^+ released by carbonation caused a substantial pH decrease, and that sericite crystallization followed soon after carbonation.

The sericitization of sediments and tuffites differs from that of igneous rocks. Although no suitable pairs of samples were found for the mass balance calculations, Figure 54 demonstrates the most obvious compositional changes, which were loss of Na and gains in Mn, K, Rb and Ba related to sericitization, and losses of Al(?), Na and Ta and gains in Mn, K, S, As, Rb, Ba, Cu and Co related to sericitization and intensive pyritization. On account of the primary differences between the samples compared, overlapping carbonation and possible volume changes, the alteration trend for most of the elements is unclear. The apparent Al depletion implies that a significant volume increase was related to the formation of pyrite ± quartz-filled fractures in the most markedly pyritized zones. The compositional changes are associated with the sericitization reactions [18], [22] and [28] and the pyritization reactions [33] and [34]. An additional sericitization reaction that occurred in the tuffites was [27]. These reactions imply distinctly acid, weakly reducing (?) fluid with a significant a_{S2-} and a very low a_{Na+}/a_{K+}.

GEOTHERMOMETRY AND GEOBAROMETRY

The mineral parageneses, both hydrothermal and metamorphic, at each study site - like the association of the amphibole zones actinolite + albite + epidote + quartz + sphene + magnetite - represent greenschist facies conditions. This gives a rough estimate of approx. 220-450°C for the alteration and metamorphic temperatures (Laird 1980, Moody et al. 1983, Schiffman and Fridleifsson 1991, Shau and Peacor 1992).

Potentially suitable minerals for geothermometry at the sites are chlorite and the calcite-dolomite and muscovite-paragonite pairs, while the tremolite-actinolite is useful for geobarometry. In practice, it was not possible to use the muscovite-paragonite pair, because the Na_2O content of the white mica was found to be 0.5% in every sample analysed. This very low paragonite content makes the error too large for geothermometry applications (Chatterjee 1972, Baltatzis and Wood 1977).

Ca-amphibole geobarometry

Ca-amphibole geobarometry is based on equilibrium in the reaction [36] (Brown 1977, Clark et al. 1989):

[36] crossite + epidote + water <->
Ca amphibole + albite + chlorite + Fe oxide

The exact stoichiometry of the reaction depends on compositional variations in the minerals, especially Fe^{2+}/Mg^{2+} and Fe^{3+}/Al^{3+}. Ca amphibole will have fixed Na content at its M_4 site at given temperature and pressure when it coexists with albite, chlorite and iron oxide. Geobarometry only works when f_{O2} is buffered by iron oxide, so that the most reliable pressure estimates are obtained when Ca amphibole is in contact with iron oxide. The Fe^{2+}/Mg^{2+} and Fe^{3+}/Al^{3+} of amphibole have a minimal effect on the amount of Na of the M_4 site, but when the pressure is >2 kb, the NaM_4 content correlates inversely with Al in tetrahedral coordination (Al^{IV}). The mineral assemblage amphibole + albite + chlorite + Fe oxide also roughly buffers Al^{IV} with respect to temperature. Thus, at constant pressure, the Al^{IV} content of Ca amphibole increases and NaM_4 decreases as the temperature rises. (Brown 1977, Clark et al. 1989)

After the mineral formula has been calculated for a total cation charge of 46, pressure is estimated using a NaM_4 vs. Al^{IV} diagram. Amphiboles which have formed in hydrothermal systems at very low pressures, lie in an area of this diagram where NaM_4 is ≤ 0.05 and Al^{IV} ≤ 1while the regional metamorphic amphiboles are in areas of higher NaM_4 and Al^{IV} (Brown 1977, Bird et al. 1984, Trzcienski et al. 1984, Sveinbjörnsdóttir 1992).

Amphibole geobarometry results

Two types of amphibole can be recognized at each site (Figs. 3A and 3J, p.18 and 20): (1) an early hydrothermal type which has replaced the primary Fe-Mg silicates (olivine and pyroxene), and (2) a late metamorphic type which has replaced the early amphibole, chlorite and biotite. The calculated formulae for these are presented in Appendix 1. The early type at each site and the late type at Myllyvaara and Isolaki consist of tremolite-actinolite, whereas at the other sites the late type is actinolitic hornblende.

The distribution of amphiboles into two groups in the NaM_4 vs. Al^{IV} diagram (Fig. 55) indicates that regional metamorphism had no effect on the composition of the early, hydrothermal amphibole. Both Brown (1977) and Trzcienski et al. (1984) describe similar situations with amphiboles formed at several pressures in one sample.

The NaM_4 vs. Al^{IV} diagrams show that the early amphiboles were formed at very low pressures (<0.5 kb) and that nearly all of the early amphibole analyses are in the hydrothermal region. The occurrence of early amphibole completely covers the amphibole zones at the sites, indicating that pressure during the formation of these zones was near hydrothermal conditions for the Earth's surface. Only at Myllyvaara did two analyses come close to the 2 kb isobar. These samples, which contain more NaM_4 than the rest of the early amphiboles, are not known for certain to be in equilibrium with Fe oxide, however, and the geobarometry is not reliable in this case.

Most of the late amphibole was formed at pressures of 2-3 kb (Fig. 55). This supports the results of the petrographic investigations, i.e. that the late amphibole which replaced the hydrothermal minerals was formed during regional metamorphism and that the hydrothermal alteration was not related to the regional metamorphism.

The compositions of the late amphibole at Myllyvaara, Isolaki and Palovaara are not as simple to interpret as those at the other sites. At Myllyvaara, the mineral association that includes the late amphibole does not contain Fe oxide, representing a kind of regional metamorphic amphibole that tends, according to Brown (1977), to be located in a lower pressure region of the NaM_4 vs. Al^{IV} diagram than it should. At Isolaki, no indication of regional metamorphic recrystallization was found and the late amphibole indicates very low pressure. This implies that the later, fracture filling amphibole was most probably formed during hydrothermal alteration. At Palovaara, amphibole only occurs in an ultramafic rock, where the mineral association is amphibole + chlo-

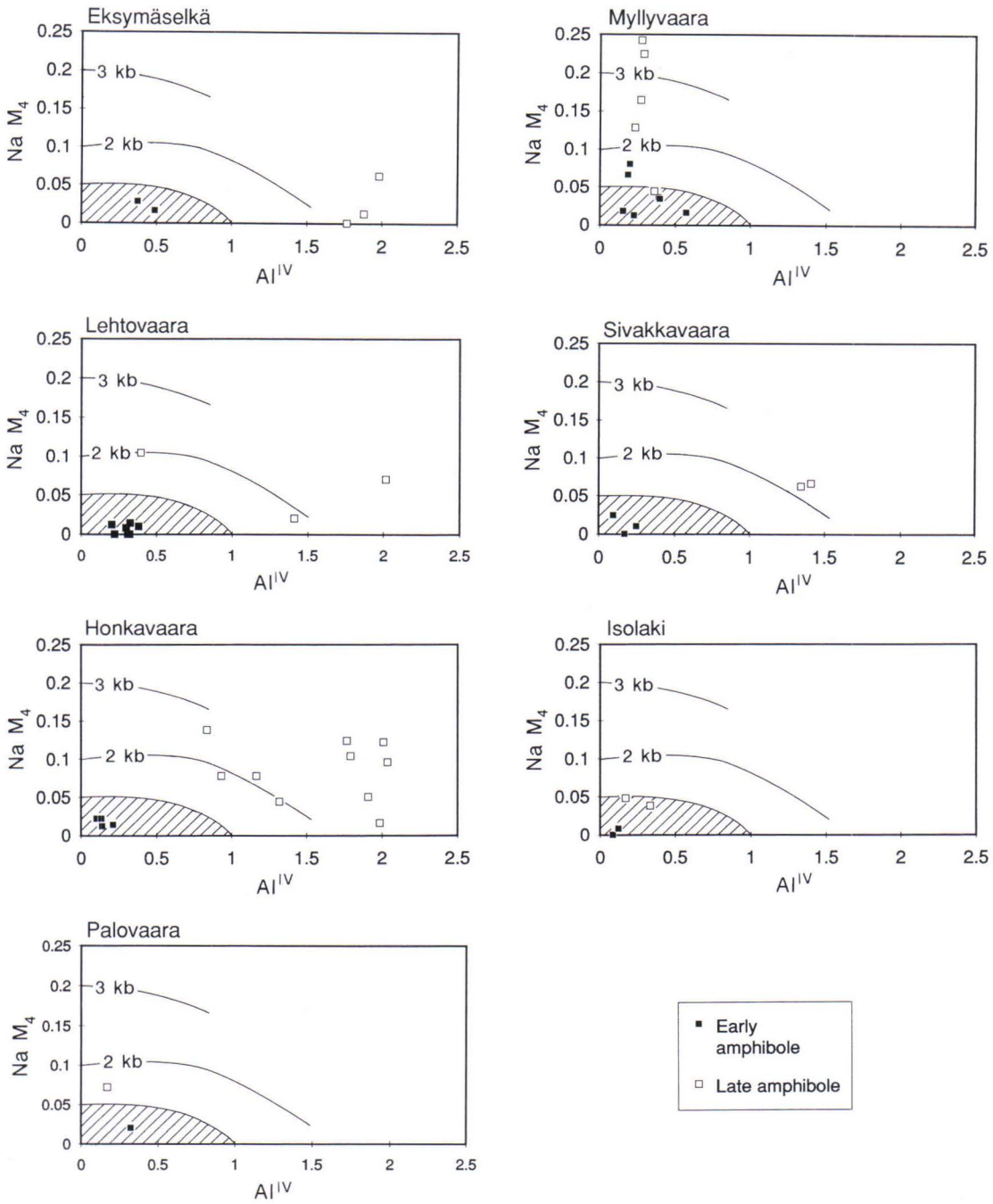

Fig. 55. NaM_4 vs. Al^{IV} plot for the amphiboles. The isobars are from Brown (1977). The area of hydrothermal amphiboles formed near earth surface conditions is hatched (Brown 1977, Bird et al. 1984, Sveinbjörnsdóttir 1992). The formulae for the amphiboles were calculated based on a total cation charge of 46 using the RECALC program of Powell and Holland (1988).

rite + biotite + albite + magnetite. The albite content of the rock is very low, and thus, the pressure estimate obtained from the NaM_4 vs. Al^{IV} diagram is not as valid as is an estimate for amphibole in a mafic rock. The trend is nevertheless the same as at the other sites, in that the pressure was very low during hydrothermal alteration and higher during regional metamorphism.

Chlorite geothermometry

Chlorite geothermometry has been developed chiefly for studying ore deposits and recently active geothermal systems (Cathelineau and Nieva, 1985, Kranidiotis and MacLean 1987, Cathelineau 1988), and has been successfully applied to ore deposits and fossil hydrothermal systems (Bettison and Schiffman 1988, MacLean and Hoy 1991, Offler and Whitford 1992, Pankka 1992) and to regional metamorphic conditions (e.g., Bevins et al. 1991). It is based on the positive correlation between temperature and Al^{IV} content, which has proved to be good (R = 0.97) in some modern geothermal areas where the variation in other thermodynamic variables is not temperature-dependent (Cathelineau and Nieva 1985, Cathelineau 1988). Based on this relationship, Cathelineau (1988) gives formula [4], where the Al^{IV} of chlorite is the only variable. Bevins et al. (1991) show that this formula works well with some low grade regional metamorphic rocks.

$$T/°C = -61.92 + 321.98Al^{IV} \quad [4]$$

Kranidiotis and MacLean (1987) show in their critique that the Fe/(Fe + Mg) of chlorite should also be taken in account, because the Al^{IV} of chlorite increases in parallel with the Fe content at constant temperature. They demonstrate that the corrected formula [5] works well in the case of the Phelps Dodge mineralization and its wall rocks (Kranidiotis and MacLean 1987).

$$T/°C = 106Al^{IV} + 0.7Fe/(Fe + Mg) \quad [5]$$

Chlorite must be in equilibrium with an Al-rich phase (e.g., epidote, albite, sericite) and quartz, i.e., the system has to be Al and SiO_2-saturated before formula [5] can be used. In Al-undersaturated systems, formula [5] gives approx. 50° lower temperatures than it should, but the correlation between the real and calculated temperatures is still roughly linear and good (Kranidiotis and MacLean 1987). If this is recognized, chlorite in ultramafic rocks and chlorite-talc and chlorite-carbonate veins can also be used for geothermometry.

The effect of pressure on the shape or position of the chlorite solid solution field is poorly understood. The chlorites used for geothermometry calibration are formed at pressures of 0.1-0.7 kb (Cathelineau and Nieva 1985) and geothermometry has been shown to be workable at pressures up to 2-3 kb (Bevins et al. 1991). Since a higher pressure may have a significant effect on Al^{IV}/Si substitution (Kranidiotis and MacLean 1987), geothermometry should be limited to chlorites that were obviously formed in low-pressure environments and not recrystallized or formed at pressures higher than 2-3 kb. On the other hand, it has been shown by Kranidiotis and MacLean (1987), Bevins et al. (1991) and Offler and Whitford (1992) that the composition of early, hydrothermal chlorite does not change during later, low grade regional metamorphism.

Calculation method

Amphibole geobarometry indicates that pressure of the regional metamorphism at the

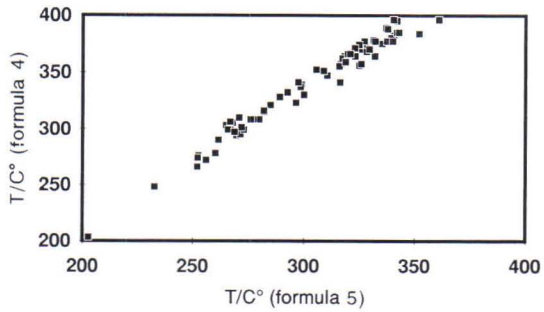

Fig. 56. Chlorite geothermometry correlations. Chlorite temperatures on the y-axis are calculated after Cathelineau (1988) and those on the x-axis after Kranidiotis and MacLean (1987). No addition of 50° was made to the temperatures of the Al-undersaturated ultramafic rocks.

present sites was 2-3 kb (Fig. 55). The chlorite is locally recrystallized, but it is still possible to find large amounts of hydrothermal, non-recrystallized chlorite at each site, which warrants the use of chlorite geothermometry. The chlorite compositions and formation temperatures calculated from formulae [4] and [5] are presented in Figure 56, Table 27 (p.106) and Appendix 2.

Formula [4] always gives higher temperatures for the present chlorites than formula [5], except in the case of the most ultramafic rocks (Fig. 56 and App. 2) or if the temperatures of ultramafic rocks are corrected by 50°. According to Sveinbjörnsdóttir (1992), formula [4] gives systematically high temperatures, although there was an evident positive correlation between actual temperature and Al^{IV} content in Icelandic chlorites. This suggests that temperatures calculated from formula [5] may be considered more realistic for the chlorites examined here than those given by formula [4].

Chlorite geothermometry results

Chloritization temperatures varied both between and within the areas (Table 27). The lowest temperatures prevailed in a tuffite at Sivakkavaara (272°C), a moderately brecciated zone of an albite diabase dyke at Honkavaara (278°C) and lamprophyre dykes and sediments at Myllyvaara (265-287°C). A low temperature (270°C) was also found at Eksymäselkä, but it applies to an ultramafic cumulate of albite diabase, which is Al-undersaturated, and thus the accuracy of the temperature calculation is poor. The highest chloritization temperatures apply to the interiors of large albite diabase dykes at Eksymäselkä and Lehtovaara (360°C and 346°C, respectively). This supports the theory that the dykes formed the heat source for the hydrothermal system. The temperatures of the late chloritization stage (chlorite replacing carbonate) were roughly the same as those that prevailed during formation of the chlorite zones.

Carbonate geothermometry

The Mg content of calcite and the partition of $FeCO_3$ between calcite and dolomite are temperature-dependent when calcite and dolomite are in equilibrium, and the effect of pressure on this equilibrium is small (Bickle and Powell 1977). Anovitz and Essene (1987) present calculation formulae based on this equilibrium and calibrated over the temperature range 250-700°C (Anovitz and Essene 1987, formula 23, p. 407 and formula 31, p. 409). These formulae enable the temperatures at which the mineral pairs calcite-ankerite and calcite-Fe-dolomite were formed to be calculated. This greatly increases the applicability of the method in the hydrothermally altered areas of the CLGB, where ankerite is common and dolomite is normally Fe-rich.

Table 27. Chlorite geothermometry at the sites. Temperatures are calculated from formula [5], with 50° added to those for Al-underaturated ultramafic rocks. The relationship between the Fe/(Fe + Mg) of chlorite and the whole rock (Fig. 57, p. 110) is also indicated. The rocks are non-brecciated unless otherwise shown. Only late stage chlorite occurs at Myllyvaara.

Site	Lithological unit	T_{avg}/°C	Fe/(Fe+Mg) equilibrium with whole rock
Eksymäselkä	Ultramafic cumulate of albite diabase, Al-undersaturated	270	yes
	Ultramafic cumulate of albite diabase, Al-undersaturated	320	yes
	Albite diabase, 4 m from dyke margin, intensively brecciated	340	yes
	Albite diabase, 100 m from dyke margin	360	yes
	Fe-tholeiitic lava	323	yes
Myllyvaara	Lamprophyre dyke interior, thorough chloritization	279	no
	Highly brecciated siltstone, chlorite replacing albite	265	no whole rock analysis
	Highly brecciated quartzite, chlorite filled fractures	287	no whole rock analysis
	Highly brecciated siltstone, chlorite replacing carbonate	270	no whole rock analysis
	Highly brecciated siltstone, chlorite replacing carbonate	267	yes
Lehtovaara	Albite diabase, 40 m from dyke margin	346	yes
	Albite diabase, 20 m from dyke margin	331	no
	Albite diabase, late chlorite replacing carbonate	342	no
Sivakkavaara	Albite diabase, 6 m from dyke margin	325	near equilibrium
	Tuffite, 10 m from diabase contact	272	yes
	Interior of lamprophyre dyke 10 m wide	301	yes
	Lamprophyre, late chlorite replacing carbonate	321	near equilibrium
Honkavaara	Albite diabase, 10 m from dyke margin, intensively brecciated	328	near equilibrium
	Albite diabase, 25 m from dyke margin, slightly brecciated	278	no
	Felsic volcanic rock, late chlorite replacing carbonate	295	no
Isolaki	Ultramafic cumulate of albite diabase, Al-undersaturated, slightly brecciated	309	yes
	Albite diabase, 3 m from dyke margin, intensively brecciated	329	no
Palovaara	Ultramafic lava or dyke interior, Al-saturated (no Al-correction)	301	yes
	Albite diabase, 2 m from dyke margin, intensively brecciated	332	yes
	Tuffite layer 3 m thick between lamprophyre dykes 5 m wide, moderately brecciated	331	yes

Carbonate geothermometry results

It was difficult to find calcite-dolomite or calcite-ankerite pairs at the sites that were in equilibrium, the major problem being the scarcity of calcite, as Fe-dolomite is the dominant carbonate at every site and in most of the lithological units. A number of carbonate pairs suitable for geothermometry were found only at Lehtovaara, while none was found at Myllyvaara, Isolaki and Palovaara and only 2 or 3 pairs at Eksymäselkä, Sivakkavaara and Hon-

Table 28. Carbonate geothermometry at the sites. The temperatures are calculated after Anovitz and Essene (1987). The geothermometry ranges of the early stage chlorites are also shown.

Site	Lithological unit	Carbonate type	T_{carb}/°C	T_{chlo}/°C
Eksymäselkä	Ultramafic cumulate of albite diabase	fracture fill, porphyroblast	371-384	318-357
	Albite diabase	fracture fill	314	
Lehtovaara	Albite diabase	fracture fill	450-463	326-343
	Albite diabase	porphyroblast	457-501	
	Albite diabase	fracture fill	470-488	
	Albite diabase	fracture fill	342-455	
Sivakkavaara	Albite diabase	fracture fill	425	270-298
	Trachyte dyke	fracture fill	389-406	
Honkavaara	Albite diabase	porphyroblast	306	276-326

kavaara. The carbonate analyses and the calculated temperatures are presented in Appendix 3. The relationships between carbonate geothermometry, lithological units and chloritization temperatures are presented in Table 28. Carbonate geothermometry was applied to the Myllyvaara rocks and was presented in preliminary publications arising from the present research (Eilu 1992, 1993), but upon revision, the calcite-dolomite mineral pairs proved not to be in equilibrium.

The chlorite and carbonate geothermometry results partially overlap at Eksymäselkä, Lehtovaara and Honkavaara, i.e., carbonation evidently took place at the same temperatures as chloritization. This points to one, common hydrothermal system and a relatively short time span for carbonation and chloritization. The rest of the carbonation temperatures are higher than the chloritization temperatures and could indicate either a resetting during the regional metamorphism or increasing temperature in the hydrothermal system.

If the main heat source for the hydrothermal system was the albite diabase dykes, no temperature increase would have been possible after chloritization and before regional metamorphism, as the dykes were already cooling during chloritization and no other potential heat source can be found for the period between the dyke intrusions and the metamorphism. The carbonate temperature range of 380-500°C also points to resetting during the regional metamorphism, as it fits well with the regional metamorphic mineral associations at the sites, where the index mineral is actinolitic hornblende. The carbonation temperatures of 450-500°C, at Lehtovaara in particular fit significantly better with a regional metamorphic system than with a near-surface hydrothermal system, in which the highest temperatures are normally approx. 400-430°C (e.g., Seewald and Seyfried 1990). In addition, if carbonates reset more easily than silicates during thermal events (Mottl and Holland 1978, Offler and Whitford 1992), it is probable that the present carbonates would have been less liable to retain their hydrothermal compositions than the chlorites.

ALTERATION CONDITIONS

Hydrothermal solutions are activated at various stages in the geodynamic evolution of rifted basins. Hydrothermal or diagenetic fluids begin to form during diagenetic processes with the movement of pore water during early compaction of the sedimentary pile (Boles 1982, Aagaard et al. 1990, Pirajno 1992). The intrusion of mafic magma into sediments results in fracturing and heating of the pore fluid, and soon afterwards the temperature in the dyke-sediment contact may rise to a maximum of approx. 400°C (Pirajno 1992). The heated fluid would then be set into convective motion in a hydrothermal system, facilitated by the high permeability of the sediments.

The temperature range of igneous-sedimentary hydrothermal systems can be wide. Elders at al. (1992) describe the Salton Sea hydrothermal system, which contains three main temperature zones: a chlorite-calcite zone at 180-320°C, a biotite zone at 320-345°C and an actinolite-clinopyroxene zone at >345°C. Albite and quartz are stable in each zone. According to Magenheim and Gieskes (1992), the temperature in the Guaymas Basin (Gulf of California) dyke-sediment hydrothermal system is >300°C in the deep-seated part, where a greenschist mineral assemblage is forming, and 20-200°C in the shallow part, where hydrothermal fluids emanate onto the sea floor. The zones of elevated temperatures and hydrothermal mineral assemblages can be several hundred metres or even a kilometre thick, and reach several kilometres laterally (Bird and Norton 1981, Elders et al. 1992). A combination of a few wide mineral assemblage zones (hundreds of metres - kilometres) and several narrower ones (metres - tens of metres) is more typical of fossil hydrothermal systems, corresponding to large-scale temperature zoning and small-scale chemical zoning of the system (Fyon and Crocket 1982, Hayba et al. 1985, Henley and Hedenquist 1986, Kishida and Kerrich 1987, Elliot-Meadows and Appleyard 1991).

The lithological associations in the CLGB indicate volcanic-sedimentary evolution with substantial hypabyssal magmatism in a rift zone (Räsänen et al. 1989, Ward et al. 1989, Lehtonen et al. 1992). Alteration processes are obviously related to specific stages of the geological evolution of the CLGB. The sediments were being altered for the first time during their diagenesis, before the tholeiitic and lamprophyre magmatisms. Most of the alteration is clearly synmagmatic and related to the widespread diabase magmatism, although alteration conditions varied, alteration took place in several stages and weak alterations related to lamprophyre dykes and felsic dykes cannot be ruled out. Regional metamorphism and deformation followed and partially overprinted the alterations, but did not notably destroy the textures and chemical compositions formed during the alteration stages in the areas of the central part of the CLGB studied here.

Each alteration type is described in the following and the formation conditions are discussed with reference to modern hydrothermal systems, related experimental research and analogous areas with fossil hydrothermal systems. Although each alteration type is discussed separately, it is evident that they have clear mutual relationships and most of the alteration zones were formed simultaneously under different conditions.

Amphibole zones

A mineral assemblage of the least altered, mafic and intermediate igneous rocks at the sites, actinolite + albite + epidote + sphene + magnetite ± quartz ± chlorite ± pyrite, and a

low grade of brecciation with epidote, actinolite and albite-filled fractures are characteristic of the mafic rocks in the amphibole zones at each site. These rocks are orthospilites (Cann 1969).

The chemical and physical conditions related to the formation of the orthospilite assemblage can only be considered indirectly, because the sites lack any chemically unaltered rocks. Mineral assemblages and fracture fills similar to the amphibole zones are currently being formed in the basaltic and andesitic reservoir rocks of the Icelandic high-temperature (>250°C) geothermal systems (Tómasson and Kristmansdóttir 1972, Kristmansdóttir 1983, Sveinbjörnsdóttir 1992) and in submarine hydrothermal systems (Humpris and Thompson 1978a, 1978b, Alt et al. 1986, Alt 1992, Edmond 1992). Experimental evidence and theoretical models suggest that the mineral assemblages form by interaction between mafic volcanic rocks and sea water at temperatures of 300-430°C, pressures of 0.2-1 kb and relatively low water-rock ratios (w/r) (w/r = 1-5, if T = 300-350°C and p = 0.4-0.6 kb) (Seyfried and Bischoff 1977, Bischoff and Seyfried 1978, Hajash and Chandler 1981, Reed 1983, Thompson 1983, Bowers and Taylor 1987, Seewald and Seyfried 1990, Delaney et al. 1992). In the synmagmatic hydrothermal system, sea water penetrates through dykes and lava flows while they are still hot, resulting in convective systems which involve fluid flow along discrete cracks (Lister 1983).

Reaction [1] (Table 2), based on the above-mentioned experiments best describes the formation of the amphibole zone in basaltic rocks and related chemical changes. In rocks containing primary biotite, e.g. lamprophyres, reaction [2] applies. The fluid present during the alteration must be reducing and low pH, as the result rocks become enriched in Na, S and H_2O and depleted in Fe, Mn, Mg, Ca, K, Ba, Rb, Cu, Ni and Co. The existence of pillow lava at Eksymäselkä site and at several sites in an analogous stratigraphic position in the CLGB supports the submarine nature of the synmagmatic hydrothermal system.

Compared with recent, unaltered tholeiitic lavas (MORB and continental types; Hughes 1973, De la Roche et al. 1980, Meyer et al. 1985, Wilkinson 1986), the tholeiites of the amphibole zones have lower Mn and Ca and higher Na and volatile concentrations. The amphibole zone data plotted on Hughes (1973) alkali ratio diagrams (Figs. 34, 39, 43, 46, 49 and 51) demonstrate that most of the rocks are depleted in K, probably together with Ba, Rb and Cs. The mineral assemblages indicate that the f_{CO2} of the system was very low (epidote and sphene stable), and amphibole geobarometry unambiguously points to formation under near-surface conditions (Fig. 55, p. 103). Thus the amphibole zones were formed at temperatures of 300-430°C, pressures of <0.5 kb and relatively low rock-fluid ratios, in the manner of a replacement process supported by a low brecciation grade. The fluid leached Mn, Mg, Ca, K, Ba, Rb and Cs, precipitated Na and hydrated the rocks. It is probable that mobile transition metals such as Zn, Ag, Cu, Ni and Co were leached from the rocks (Thompson 1983, Janecky and Seyfried 1987, Seewald and Seyfried 1990), although it cannot be proved from the present data.

The chlorite geothermometer data (Table 27, p. 106) confirm the above-mentioned temperature range, since the chloritization most probably took place in the higher w/r areas of the same hydrothermal systems. Especially when there is both chlorite and actinolite in the equilibrium mineral assemblage and the chlorite and whole rock are in chemical equilibrium (Fig. 57), the chlorite geothermometry most probably also indicates the temperature of actinolite formation (Table 27). Examples of such assemblages exist in the albite diabase dykes at Eksymäselkä, Lehtovaara and Sivakkavaara and the ultramafic lava at Palovaara, which give temperatures of 360°C, 340°C, 320°C, and 300°C, respectively. If no chlorite occurs in the amphibole zone, chlorite geothermometry will give a

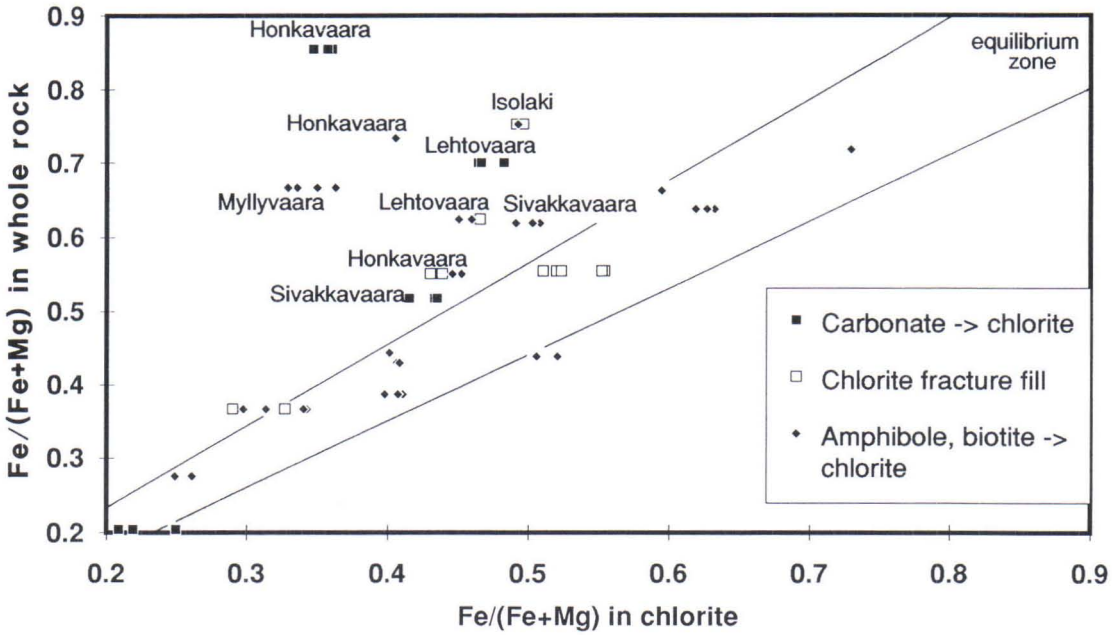

Fig. 57. Fe/(Fe + Mg) in whole rock and chlorite. Non-equilibrium cases are indexed by the name of the site. The area in which the whole rock and chlorite are in Fe/(Fe + Mg)-equilibrium within the limits of analytical accuracy is outlined and forms a diagonal zone. The carbonate->chlorite alteration and all of the Myllyvaara cases represent late stage chloritization.

minimum temperature for the amphibole alteration, because chlorite-bearing assemblages without amphibole are formed at lower or equal temperatures in hydrothermal systems relative to amphibole-bearing assemblages, but never higher temperatures (Bird and Norton 1981, Mottl 1983b, Sveinbjörnsdóttir 1992).

Epidotization

At Honkavaara, where intensive epidotization has taken place, the mineral association gradually changes from amphibole alteration to epidotization and seems to be in equilibrium. The mass balance calculations indicate Fe, Na and Br loss and Mn, Ca, K, P, Ni and REE gain, which are explained by a combination of reactions [1] and [3] (Table 2) and apatite formation. According to experimental evidence (Reed 1983), epidotization takes place in submarine hydrothermal systems with a higher w/r value than in the case of orthospilite formation described above (w/r approx. 10, if T = 300-350°C and p = 0.4-0.6 kb), but Ca enrichment is necessary for intensive epidotization. In addition, a very low f_{CO_2} is essential for epidote stability (Winkler 1979).

Chloritization

The Fe/(Fe + Mg) relationship between whole rock and chlorite (Table 27, p.106, Fig. 57) indicates that an equilibrium between the rock and fluid was widely attained during chloritization at Eksymäselkä, Sivakkavaara and Palovaara, was attained in some places at Myllyvaara, Lehtovaara and Isolaki and was almost attained at Honkavaara. Most of the cases of greatest deviation from Fe/(Fe + Mg) equilibrium represent post-carbonation conditions, when sericitization and talc formation took place in addition to the late-stage chloritization.

At those sites where the whole rock/chlorite equilibrium conditions are indicated by the Fe/(Fe + Mg) relationship (Fig. 57), the temperature ranges shown by the chlorite geothermometry (Table 27) were most probably attained completely in the chloritizing zones, and the chlorite composition parallels the composition of the surrounding rock. This is supported by descriptions of currently active hydrothermal systems (Mottl 1983b, Bird et al. 1984, Reed and Spycher 1984, Henley and Hedenquist 1986, Hemley and Hunt 1992). On the other hand, in the case of a non-equilibrium Fe/(Fe + Mg) relationship the temperature given by the chlorite is only the temperature of the fluid and the immediately adjacent wall rock in the fractures (Giggenbach 1981, Henley et al. 1984, Sveinbjörnsdóttir 1992, Lonker et al. 1993).

In the Fe/(Fe + Mg) non-equilibrium cases the chlorite composition primarily depends on the composition of the hydrothermal fluid (Bischoff and Seyfried 1978, Reed and Spycher 1985), and in all these instances the Mg content is higher in the chlorite than in the surrounding rock (Fig. 57). This suggests a Mg-rich hydrothermal fluid, which would be sea water in modern hydrothermal systems (Seyfried and Bischoff 1981, Mottl 1983a, Ragnarsdóttir et al. 1984, Shau and Peacor 1992, Lonker et al. 1993). Since non-equilibrium chloritization (apart from cases of carbonate replacement) is petrographically similar to equilibrium chloritization, it is highly probable that both the equilibrium and non-equilibrium cases were caused by the same kind of hydrothermal system with sea water as the deriving fluid. Also, the total range of the chlorite geothermometry results (265-360°C, Table 27) fits well with the chloritization conditions of modern submarine hydrothermal systems (Spiess et al. 1980, Stakes and O'Neill 1982, Rosenbauer and Bischoff 1983, Mottl 1983b, Bowers and Taylor 1987, Alt 1992).

The hypothesis of a sea water origin for the hydrothermal fluid fits well with the general characteristics of the amphibole and chlorite zones. Chlorite-bearing mineral assemblages are frequently formed in modern submarine synmagmatic hydrothermal systems (Humphris and Thompson 1978a, Mottl 1983b, Reed 1983, Shau and Peacor 1992). The temperature of the chlorite-forming sea water-derived fluid is >230°C, and it is reducing and of low pH. The gradual change from an amphibole-dominated mineral association to a chlorite-dominated one - i.e., from orthospilite to hyalospilite (Cann 1969) - depends on the w/r, as demonstrated in Table 29.

Experimental results suggest that direct chloritization of magmatic mineral assemblages (reaction [6], Table 2) and indirect chloritization via the chloritization of actinolite, albite and epidote (reactions [8] and [9]) best describe the formation of the chloritized zones in mafic

Table 29. Relationship between w/r and silicate mineral assemblage in basaltic rocks altered in a submarine hydrothermal system (when T = 300-350°C, p = 0.4-0.6 kb) (Mottl 1983b).

w/r	mineral assemblage
<5	actinolite + albite + epidote + quartz
5-35	chlorite + actinolite + albite + epidote + quartz
35-50	chlorite + albite + quartz
>50	chlorite + quartz

and intermediate rocks and related chemical changes. The chloritization reactions in rocks containing primary biotite, e.g. lamprophyres, are [7]-[10], and those in ultramafic rocks are a combination of reactions [4]-[6]. These replacements are also recognizable in the chlorite zones at the present sites. During chloritization under high w/r conditions (w/r >35 in Table 29) the rocks become enriched in Mg, Mn, S and H_2O and depleted in Si, Ca, Na, K, Ba, Rb, Cs, Cu and Zn, while under moderate w/r conditions, when both actinolite and chlorite are stable, the chemical changes lie between those related to the formation of the non-chloritic mineral associations of amphibole zones and that of intensively chloritized zones. (Mottl 1983b, Reed 1983, Colvine et al. 1988, Hemley and Hunt 1992)

All three chlorite-bearing mineral associations described in Table 29 occur at the present sites. The dominant association at Lehtovaara and Honkavaara is chlorite + actinolite + albite + epidote ± quartz and that at the other sites chlorite + albite + quartz, which represent moderate and high w/r, respectively. The occurrence of a very high w/r association, chlorite + quartz, is restricted to extremely fractured zones 1 mm - 50 cm wide.

The mass balance calculations for chloritization (Figs. 35A, 42A and 47B) indicate that Mn, Ca, Na, K, Br, As, Ba and Cu were usually leached from the rocks into the fluid and that the rocks were only enriched in H_2O. Iron, S, Sb, Rb, Ni, Co and U were also mobile in some cases. The changes in main component and H_2O concentrations formed the dominant part of the absolute mass changes. Most of these chemical changes are in good accordance with those observed in modern submarine hydrothermal systems and with the results of the experiments on chloritization under conditions of moderate and high w/r (Humphris and Thompson 1978a, Mottl 1983a, Reed 1983, Rosenbauer and Bischoff 1983). Evident Mg enrichment is indicated at Honkavaara, but the apparent Mg mobility was negligible at the other sites. The lack of Mg enrichment scale large enough to be indicated by the mass balance calculations is in accordance with the restricted occurrence of the mineral association chlorite + quartz (Table 29). This is also explained by the cases of Fe/(Fe + Mg) non-equilibrium between chlorite and whole rock (Fig. 57), for extremely high w/r prevailed in such narrow zones that it is seen only as Mg enrichment in chlorite compositions but not in whole rock samples.

Biotitization

Biotite has predominantly replaced the other mafic silicates, by what the mass balance calculations and petrography indicate to have been essentially an equal volume replacement process. The alteration was peaceful with respect to deformations, and no fracturing took place. Biotite-filled fractures are abundant, but these had already formed at the chloritization stage and biotite merely replaced the chlorite fracture fill material.

The most important chemical changes related to biotitization were Ca and Na leaching into the fluid and K, Cs, Rb, Ba and S precipitation from the fluid. Some transition metals such as Fe, Mn, Cu, Co and Ni were also mobile locally. The chemical changes are best described by the biotitization reactions [10]-[12] and [17] and the sulphide formation reactions [33]-[35] (Table 2) and by a weakly reducing, near neutral or mildly acid fluid with low a_{Na+}/a_{K+} and a_{Ca2+}/a_{K+}. No carbonates were precipitated with the biotite. This implies either a low f_{CO2} or the prevention of simultaneous carbonate precipitation by the release of H^+ in the biotitization reactions.

It was not possible to evaluate the tempera-

ture of the biotitization stage directly, but the carbonate geothermometry also gives temperatures for biotitization when this was part of the main hydrothermal stage, as suggested by the contrast between the chemical changes involved in biotitization and carbonation + albitization, and when the carbonates did not re-equilibrate during regional metamorphism. This is probable at Eksymäselkä (314-384°C), Honkavaara (306°C) and locally at Lehtovaara (342°C), while the rest of the carbonate temperatures (Table 28, p. 107) most probably reflect regional metamorphic conditions.

Potassium metasomatism is not possible at the above-mentioned temperatures in a submarine hydrothermal system of subalkaline rocks as the rocks begin to lose K when the temperature rises above 150°C and the total K loss occurs at temperatures above 300°C whatever the w/r may be (Mottl 1983b). Ba, B, Li and Rb behave like K (Munha et al. 1980, Mottl 1983a and 1983b). Thus, if biotitization at the present sites was related to a submarine hydrothermal system, a K source must be found. Sediments surrounding the igneous rocks could be such a source, as there are extensive sediment piles at each site which originally had K_2O concentrations of 2-5 wt-% and which were depleted in K during the alterations (cf., Tables 8 and 11 and Figs. 37B and 41). A sedimentary source of K is also supported by the position of the biotitized zones near dyke-sediment contacts.

Rubidium and barium could also have a sedimentary source, because they behave geochemically like K. The biotitizing fluid also contained S, Fe, Mn, Cu, Co and Ni locally, which were probably derived from the formation of the amphibole and chlorite zones of the mafic igneous rocks. The origin of K and other LIL elements may also lie to some extent in altered lamprophyres, which had high LILE concentrations primarily. This portion in the total LILE of the hydrothermal fluids was small, however, because of the low total mass of the lamprophyre dykes relative to that of the altered sediments. The lack of K-enrichment haloes around the lamprophyre dykes also supports the negligible importance of lamprophyre-derived LILE in the alteration processes. Granitization or granite-derived fluids can similarly cause significant LILE enrichment (Eugster and Wilson 1985, Colvine et al. 1988), but this is improbable at the present sites because no signs of granitic influence, e.g., pegmatites, were found.

Albitization and carbonation

Diagenetic albitization

Albitization of feldspars commonly takes place during the diagenesis of sediments (Boles 1982, Ko and Hesse 1987, Milliken 1988 and 1992, Aagaard et al. 1990, Morad et al. 1990). In modern sediment basins, plagioclase begins to albitize rapidly when the temperature in the sediment pile exceeds 75-100°C, and it is totally albitized at temperatures above 100-130°C. Potassium feldspar albitizes slowly in the temperature range 60-150°C, and quartz is not replaced by albite in diagenesis. Complete albitization of feldspars in sandstones is achieved 1-5 Ma after deposition at the above-mentioned temperatures, whereupon the provenance information contained in the feldspars of the sediments is completely lost. Behr et al. (1983), Morad (1986), and Ko and Hesse (1987) have shown that similar diagenetic albitization also took place during Proterozoic and Palaeozoic times.

Albitization proceeds by a dissolution-precipitation mechanism rather than by solid-state diffusion (Aagaard et al. 1990), and albite does not replace the original feldspar grain by grain

everywhere, but aggregates of small albite crystals may replace the original plagioclase or K-feldspar grains, the clastic forms of which will thus be destroyed. Those albite aggregates form at temperatures of 60-90°C, when the precipitation velocity of albite is less than the dissolution velocity of the original feldspar (Milliken 1988, Saigal et al. 1988). At temperatures above 90-100°C, when the precipitation velocity of albite reaches the dissolution velocity of the original feldspar, perfect albite pseudomorphs may form after the original feldspar clasts.

Albitization of a sedimentary layer is related to the addition of Na, which presumably originates from evaporites. There are indeed in many cases of intrastratal evaporites (e.g. in the North Sea and Mexican Gulf Coast basins) in which the clastic sediments have albitized (Land and Milliken 1981, Saigal et al. 1988). The diagenetic albitization of feldspars does not necessarily require a pore fluid of high salinity and/or high a_{Na+}, however, and the proximity of evaporites is not essential. According to Morad et al. (1990), an external Na source is not necessary either, if there are interbedded shales in which sheet silicates alternate in diagenesis. The chloritization of smectite and kaolinization of detrital Na-bearing micas can liberate enough Na for albite formation.

Chloritization of smectite and illitization of smectite, kaolinite and dickite in the sediment pile are especially important processes for the albitization of K feldspar, which, unlike anorthite, is stable in the P-T conditions during diagenesis. Therefore, in addition to the availability of Na^+ ions, a contemporaneous K-precipitating process is a prerequisite for the albitization of K feldspar, i.e. the a_{Na+}/a_{K+} of the fluid must remain high. The illitization of clay minerals, which takes place in the same temperature range as the albitization of feldspars (beginning at 60°C), is an effective K-fixing process, as the clay minerals donate Na to the fluid at the same time (Milliken 1988, Aagaard et al. 1990, Saigal et al. 1990). Ion exchange between the sheet silicate-rich and feldspar-rich sedimentary layers causes the former to become enriched in K and the latter in Na. Overpressurization of the sediment layers caused by tectonic effects or impermeable cap rock accelerates albitization, because the alteration of clay minerals is accelerated (Ko and Hesse 1992) and Na^+ ions are already abundantly available at 60°C. On the other hand, if illite formation is insufficient, the albitization of K feldspar will remain partial despite the total albitization of plagioclase and the good availability of Na.

Some albitization reactions that can take place under diagenetic conditions are presented in Table 30.The reactions suggest that the albitizing fluid is weakly acid and calcite, clay minerals and K mica form as by-products when feldspars are albitized. In addition to silt and clay horizons, the by-products precipitate in the pores of the albitizing sediment, and calcite in particular may totally fill the pore space, thus stopping the flow of fluid and interrupting albitization (Aagaard et al. 1990, Morad et al. 1990).

Least altered sediments

The average chemical compositions of the least altered sediments at the sites studied indicate albitization. The Na concentrations of the feldspar-bearing quartzites are higher than those for an average arkose quartzite presented by Pettijohn et al. (1987), for example, and the

Table 30. Some common albitization reactions that can take place under diagenetic conditions.

[37] 2Quartz + $0.5H_2O$ + Anorthite + Na^+ + H^+ -> Albite + 0.5Kaolinite + Ca^{2+}	(Boles 1982)
[38] Anorthite + HCO_3^- + H^+ + H_2O -> Kaolinite + Calcite	(Morad et al. 1990)
[39] 2K feldspar + $9H_2O$ + $2H^+$ + $2Na^+$ -> 2Albite + Kaolinite + $2K^+$ + $4H_4SiO_4$	(Land and Milliken 1981)
[40] 2K feldspar + 2.5Kaolinite + Na^+ -> Albite + 2Illite + 2Quartz + $2.5H_2O$ + H^+	(Morad et al. 1990)

Ca and K concentrations generally significantly lower (cf. Tables 15, 18 and 25, p. 78, 85, 96). In cases where the Ca concentration of an albitized quartzite equals that of an average arkose, the petrography of the rock displays an above-average carbonate content but no Ca-bearing feldspar.

Albite is the only feldspar in the sediments at all the sites except Lehtovaara. Potassium feldspar exists at Lehtovaara in addition to albite, but only in a small part of the area. The albite content of the least altered sediments regularly varies according to the layering and does not depend on brecciation or the distance from dykes or lava units, which most probably played an essential role in the formation of the other alteration types and zones. The originally feldspar-rich layers (arkosites, silts) now contain more albite than the originally feldspar-poor layers (orthoquartzites, sericite quartzites). An albite pseudomorph or an aggregate of small albite crystals may exist at the site of an original feldspar clast. The K-feldspar-bearing quartzite of Lehtovaara is partially albitized, small albite crystals replacing the K-feldspar clasts. Carbonate porphyroblasts occur regularly in the least altered, albitized sediments, but the carbonate content is low, <0.1-1 vol.-%. All these features and the unfractured texture of the rocks imply complete or almost complete diagenetic albitization of the sediments. This also means that the possible provenance information contained in the feldspars of the Lapponian sediments at these sites has been completely lost.

If albitization took place under normal diagenetic conditions, the alteration temperature must have been 60-150°C. The sediments of the Central Lapland greenstone belt (CLGB) are Palaeoproterozoic in age, apparently deposited in a continental rift (Ward et al. 1989, Lehtonen et al. in prep.), and the geothermal gradient of the CLGB basins was very probably steeper than in the modern sedimentary basins in which diagenetic albitization has been described. Therefore, the albitization may have taken place at significantly shallower depths and lower pressures than in the modern sedimentary basins, where the albitization depth is 2.5-4 km and the pressure 0.4-0.7 kb.

The origin of the Na needed for diagenetic albitization remains unresolved, but a combination of the following sources would seem most probable:

(1) Evaporites. There are no Na-bearing evaporites in the CLGB today, but there may well have been once, as there are still Ca-Mg carbonate rocks in its sedimentary associations (Lehtonen et al. 1984 and 1985). The abundance of scapolite throughout the greenstone belt (e.g., Mikkola 1941, Tuisku 1985) similarly points to evaporite deposits as a regional phenomenon (Vanko and Bishop 1982, Sleep 1983, Kalsbeek 1992), although scapolite is not an abundant mineral at the present sites. The scapolite-bearing carbonate rocks of Sivakkavaara could be altered evaporites, but there are no signs of evaporite layers at the other sites.

(2) Clay minerals. Since only the feldspars are albitized in the least altered types of sediment, an evaporite-based pore fluid of high salinity and a_{Na+} is not necessary and Na release from clay minerals becomes a reasonable possibility. K-mica-bearing, fine-grained layers which may originally have contained Na-bearing clay minerals are found at the sites, and are especially common at Eksymäselkä, Myllyvaara and Palovaara, where the diagenetic alteration of clay minerals may have been the most important Na source. Where this process dominated, the coarse-grained sediments were enriched in Na and depleted in K, Rb and Ba while reverse changes took place in the fine-grained sediments. This process would explain the relatively high K concentration of some of the least altered fine-grained sediments and the early sericitization of the least altered silt horizons at Myllyvaara.

(3) Sea water. The tidal deposition environment of the Lapponian clastic sediments (Nikula 1988) suggests that the original pore fluids of the sediments were derived from sea water.

Hence at least some of the Na needed for the diagenetic albitization of feldspars may have originated from sea water.

Hydrothermal albitization and related carbonation

Several albitized zones whose formation cannot be explained by diagenetic albitization or the albitization of plagioclase related to the formation of amphibole and chlorite zones exist at the sites. Their brecciation grade is frequently high and the calculated rock volume and total mass change is from ±0% to over +50%, but most typically +10 - +25%. These zones are also without exception carbonated. The intensities of albitization and especially carbonation vary considerably between and within the zones. Albitization and carbonation were roughly contemporaneous processes, although carbonates have replaced albite in some cases and carbonate-filled fractures cross-cut albite crystals.

Two types of albitized and carbonated zones have been encountered: (1) zones 1-200 m wide at diabase dyke-country rock contacts, and (2) breccia zones 0.5-20 m wide away from the contacts but commonly parallel to them. The two zone types are identical in their mineralogy and texture.

The best examples of the contact-type alteration are a zone about 200 m wide to the east of the Eksymäselkä albite diabase intrusion (Fig. 7, p. 24), the carbonated zones 10-20 m wide at Lehtovaara (Fig. 15, p. 32) and zones 20-70 m wide bordering the albite diabase in the northern part of the Honkavaara area (Fig. 25, p. 42). The weakly albitized and carbonated zones at Myllyvaara (Fig. 11, p. 29) represent the non-contact alteration type. In places, especially at Palovaara (Fig. 33, p. 49), several albitized and carbonated zones are fused together to form one extensive zone.

Alteration related to albitization and carbonation was in many cases so intensive that all mineralogical traces of the earlier alterations were lost. Also, the greatest chemical changes related to any alteration type at the sites took place during albitization and carbonation. Typical changes were losses in Fe, Mg, K, Cs, Rb, Ba, Cu, Co, Ni, V, Cr, U, Th and H_2O and gains in Mn, Ca, Na, Sb, W and CO_2. In addition, Si, Br, S and As were consistently mobile and P, REE, Sc and Ta mobile in some cases, but their mobility trends were not constant. If absolute mass changes are considered, the Fe, Mg, K and H_2O losses and Ca, Na and CO_2 gains may be said to have been the most significant. Ti, Al, Zr were immobile, as also were Si, P, REE, Sc, Ta, V, Cr, U and Th in cases where alteration was less intensive.

The decomposition of amphibole, chlorite, talc, biotite and magnetite will explain the depletion of Si, Fe, Mg, Cu, Co and Ni (reactions [17], [19], [20] and [23]-[26]; Table 2), and correspondingly the decomposition of K feldspar, biotite and sericite ([16], [17], [26] and [29]) will explain the K, Cs, Rb, Ba and Br depletion, whereas the decomposition of sphene, magnetite and apatite (e.g., [21]) is responsible for the depletion of P, REE, Sc, Ta, V, Cr, U and Th. The Mn, Ca, REE and scarce Mg enrichments are related to carbonation ([19] and [23]-[26]) and the Na enrichment to albitization ([16]-[18], [23] and [29]). The S, Sb and As depletions and enrichments are explained by pyrite decomposition and formation ([33]-[35]).

Problems were encountered with the calcite-dolomite geothermometry, as described in the chapter on carbonate geothermometry, as suitable mineral pairs were only found at a few sites. Thus all geothermometry results do not correlate with the other indications of alteration conditions, although they correspond quite well to the regional metamorphic conditions. The carbonate temperatures at Eksymäselkä, Lehtovaara, Sivakkavaara and Honkavaara, 306-425°C, match with the hydrothermal conditions of the amphibole alteration and chloritization, but the temperature range of 389-425°C for the Sivakkavaara carbonates devi-

ates from the temperature of the late chlorite (321°C), although it fits well with the occurrence of regional metamorphic amphibole (actinolitic hornblende). Thus the hydrothermal temperatures during the formation of the albitized and carbonated zones were probably from 270°C to 380°C.

All of the above-mentioned features together indicate that the alteration was caused by a synmagmatic hydrothermal system during cooling of the dykes and lava flows, and contemporaneously with amphibole alteration and chloritization, i.e. spilitization, or soon after. In particular, the location of most of the alteration zones at the contacts of the dykes and the parallelism of the rest of them with the dyke contacts are features that clearly indicate that the dykes, which largely intruded into the sediment piles, were the main heat source for the hydrothermal system. No chemical difference was found between the carbonation + albitization that occurred around the lamprophyre dykes and that around the albite diabase dykes (cf. Figs. 35 and 37, p. 60 and 66), which implies albite diabase-related alterations in and near the lamprophyre dykes. The genetic relationship and overlapping temperature ranges of spilitization and biotitization in mafic rocks and carbonation + albitization in the diabase contact zones and sedimentary wall rocks is analogous to the zonation of modern and fossil submarine dyke-sediment hydrothermal systems, involving one wide temperature zone and a few chemically different zones (Fyon and Crocket 1982, Edmond 1992, Elders et al. 1992, Stakes 1992, Magenheim and Gieskes 1992).

The alteration patterns at Sivakkavaara form an exception to the above spilitization relationship. If the spilitization reactions ([2] or [7]) had affected the felsic dykes there would not be any K feldspar left, but as it is, the felsic dykes only are albitized, carbonated and sericitized in their contact zones and, contrary to the diabase and lamprophyre, are not spilitized. Thus, the post-spilitization alterations are related to the intrusion of the felsic dykes, which formed the heat source during the alteration stage. This alteration pattern indicates that the hydrothermal system related to the albite diabase dykes of Sivakkavaara was no longer active during the intrusion of the felsic dykes.

It has been proposed that pervasive albite-carbonate alteration would also have been possible after regional metamorphism and deformation in the CLGB (Härkönen and Keinänen 1989, Ward et al. 1989, Korkiakoski 1992), but no signs of any post-metamorphic alteration stage were found in the albitized and carbonated zones at the present sites. Contemporaneity of the alteration processes is also supported by the opposite Ca, Na, K, Cs, Rb and Ba trends in albitization and carbonation vs. biotitization, the opposite Mn, Mg, Ca and Na trends in albitization and carbonation vs. spilitization and the overlap of the chlorite and carbonate temperatures. Because sea water-derived fluid is considered essential for spilitization (Mottl 1983b, Reed 1983, Janecky and Seyfried 1987), contemporaneity of albitization + carbonation and spilitization would imply a sea water source for most of the Na needed for albitization.

The concentration of CO_2 in the hydrothermal fluid must have been significant, because carbonation-sensitive minerals such as epidote and sphene are lacking in the alteration zones. The f_{CO2} of the fluid nevertheless fluctuated during the formation of the zones, as is demonstrated by the variable carbonate content, the variable amounts of less CO_2-sensitive minerals such as chlorite, and the alternating REE mobility (cf. Figs. 36, 38 and 53, p. 61, 67 and 98), as REE are predominantly mobile in the form of carbonate complexes under neutral and weakly alkaline hydrothermal conditions at temperatures up to a few hundred degrees (Humphris 1984, Brookins 1990, Wood 1990a and 1990b, Lottermoser 1992). Intensive albitization and a large K loss imply a high a_{Na+}/a_{K+} in the fluid, and low stability of the micas and carbonate deposition point to near-neutral or

mildly alkaline conditions (Stakes and O'Neill 1982, Henley and Brown 1985, Reed and Spycher 1985). The f_{O2} probably varied, as pyrite, magnetite and haematite was deposited with the carbonates, but the widespread magnetite decomposition, stability of haematite and rutile, scarcity of sulphides and U depletion indicate predominantly oxidizing conditions (Large 1977, Nesbitt and Kelly 1980, Henley and Brown 1985). The composition of the fluid in the intensively altered zones was uniform, with high f_{CO2}, a_{Na+}/a_{K+} and fluid-rock ratio, as indicated by the tendency to form the mineral assemblage Fe-dolomite + albite + quartz + rutile regardless of the nature of the original rock, i.e. the system was fluid-dominated and the fluid was in equilibrium with this mineral assemblage.

There are several possible CO_2 sources, and it is highly probable that there were no single source at any of the sites. The most intensive carbonation took place in the igneous rocks and their immediate vicinity. This may locally indicate a magmatic source for CO_2, as is also supported by the presence of lamprophyre dykes (Rock 1987, 1991). On the other hand, there are extensive areas of carbonate rocks and signs of evaporites in the CLGB (Lehtonen et al. 1984, Tuisku 1985). Since the magmas at the present sites usually intruded into sediments, it is probable that the CO_2 of the sediments, from both fluid and solid phases, was mobilized and took part in the hydrothermal carbonation. Without isotope investigations it is not possible, however, to prove the sedimentary origin of the CO_2. Palovaara, where carbonation was most intensive, is indeed situated near known sedimentary carbonate rocks, but the rocks at Sivakkavaara are not highly carbonated, although the dykes and carbonate rocks are in contact.

Albitization and carbonation at Isolaki

The conditions under which the carbonation and albitization of albite diabase took place at Isolaki could be explained in the same manner as the formation of similar zones at the other sites, but it would have been impossible for the quartzite to be carbonated and albitized in a synmagmatic hydrothermal system because the radiometric age determinations (Lehtonen 1987) show the quartzite to be more than 200 Ma younger than the diabase.

The diabase-sediment and quartzite-conglomerate contact zones are fractured, and would thus have formed a permanent flow path for fluids, i.e. upflowing magmatic or deep metamorphic fluids, downward or upward flowing meteoric or sea water or a combination of these with a_{Na+}/a_{K+} high, f_{CO2} moderate or high, and pH near neutral. The temperature of a fracture zone-related hydrothermal system can be relatively low and its influence on the rocks slow, but because its duration can be some orders of magnitude longer than that of a synvolcanic hydrothermal system (Mottl 1983b, Craw et al. 1989, Lalou et al. 1990, Criss et al. 1991, Minissale 1991), this extremely slow process can also alter the rocks considerably. As a consequence of the age of sedimentation, that of carbonation and albitization must be 1.9 Ga or less, which indicates that alteration probably took place during the Svecokarelian orogeny, which lasted from approx. 2.0 to 1.8 Ga (Lehtonen et al. 1992), and that the synorogenic silicic plutonism formed the heat source for the hydrothermal system.

It is possible that the sericite quartzite near the fracture zone was partly zeolitized at first and that the zeolites were subsequently altered to albite and carbonate by a CO_2 influx or by a pH change in the hydrothermal system. Zeolitization takes place at a low temperature (generally <250°C; Kristmansdóttir 1975, Bird et al. 1984) if f_{CO2} is low (Thompson 1971, Winkler 1979) or the pH high (Lambert et al. 1988). If the CO_2 of the fluid came from the carbonate-bearing matrix of the conglomerate, however, no zeolitization would have been possible, as the f_{CO2} was most probably high from the onset of the hydrothermal system.

A fracture zone-related hydrothermal system can also deposit chlorite, biotite, carbonate and albite in the albite diabase. If the diabase was not affected by a submarine hydrothermal system, the weakly altered amphibole zone (Fig. 29) could not have been formed before the regional metamorphism. This is not likely, however, because the amphibole geobarometry and the petrography of the diabase do not suggest any notable recrystallization during regional metamorphism but point to a very low pressure which was close to the hydrothermal conditions prevailing near the Earth's surface.

Sericitization

Sericitized zones occur in the same manner as carbonated and albitized zones, either in the dyke-wall rock contact zones or apparently independently but parallel to the dykes (see Figs. 7 and 21, p. 24 and 37). The sericitized zones vary in width from 30 cm to 100 m. The sericite frequently fills narrow fractures, but calculations show that the brecciation related to sericitization was negligible as far as the rock mass balance was concerned and that sericitization was essentially a replacement process with a decrease in rock volume.

Since the sericite replaced carbonates, sericitization must have taken place after carbonation (Fig. 3D). The carbonated and sericitized zones overlap, however, so that the alteration processes must be related to each other. Some mineral reactions ([22], [24] and [26]; Table 2) also require roughly simultaneous carbonate and sericite formation.

Typical chemical changes related to sericitization were losses of Si, Fe, Mn, Mg, Ca, Na, P, Br, Cu, Co, Ni and CO_2 and gains in K, Cs, Rb, Ba, S, Sb, W and H_2O. Titanium, Al and Zr were immobile everywhere and Si, P, REE, Sc, Ta, V, Cr, U and Th locally. The main changes in absolute mass were in the main components and volatiles.

The following relationships between element mobilities and mineral reactions are relevant to sericitization. The decomposition of chlorite and biotite (reactions [24] and [26]-[28]; Table 2) explains the depletions in Fe, Mg, Mn, Cu, Co, Ni and possibly Br; epidote decomposition ([24]) some of the depletions in Fe, Ca and Mn; carbonate decomposition ([29]) most of the Ca and Mn depletions and part of the Mg and Fe depletions; and albite decomposition ([18], [22] and [29]) the Na depletions. Each of the above-mentioned reactions except [26] will explain the enrichment of K, Cs, Rb and Ba. A Si loss into the fluid instead of the SiO_2 precipitation presupposed in the reaction formulae ([18], [22], [24] and [26]-[29]) will explain the general Si depletion. The P depletion is related to apatite decomposition and the S and Sb enrichments to pyrite formation ([33] and [34]).

Sericitization requires an acid fluid (commonly pH <5.5) with low a_{Na+}/a_{K+} and a_{Na+}/a_{H+} and moderate a_{K+}/a_{H+} (Montoya and Hemley 1975, Giggenbach 1984, Henley and Brown 1985, Reed and Spycher 1985, Saunders and Tuach 1991) as shown in Figure 58, and possibly very high w/r (>50-100; Lesher et al. 1986, MacLean and Hoy 1991). In addition, the Mg and Ca depletions imply low a_{Mg2+}/a_{K+} and a_{Ca2+}/a_{K+} and the Si depletion silica undersaturation in the fluid. f_{O2} was moderate with respect to the possible pH scale, and certainly not very high, because no haematite was formed, nor very low, because no pyrrhotite was formed (Fig. 59).

The sericitization temperature varied between the sites, but the temperature estimates remain fairly crude as muscovite-paragonite geothermometry could not be used. Sericitiza-

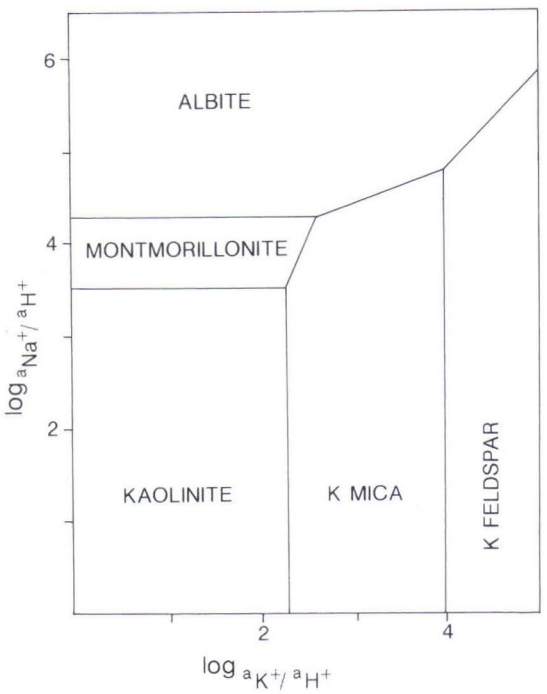

Fig. 58. Activity diagram for the ideal system K_2O-Na_2O-Al_2O_3-SiO_2-H_2O at 250°C with quartz present (Henley and Brown 1985).

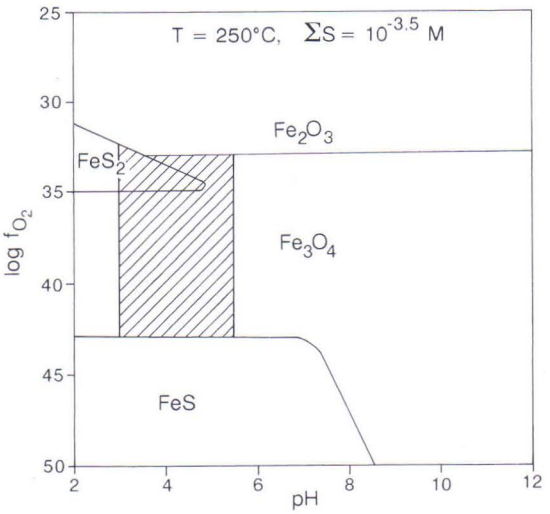

Fig. 59. Stability fields of Fe-O-S minerals in a f_{O_2}-pH space at 250°C for low values of total dissolved sulphur (S = $10^{-3.5}$M) (Large 1977). The possible f_{O_2}-pH region during sericitization at the sites is hatched.

tion can take place in hydrothermal systems of low pressure and in the temperature range <150-350°C (Bird et al. 1984, Lesher et al. 1986, Robinson and Merchant 1989, Ames et al. 1991, MacLean and Hoy 1991, Cooke 1992). These carbonate geothermometry results referring to the carbonation conditions fit with the upper part of the sericitization temperature range. Carbonate geothermometry may thus give the sericitization temperature in those rocks in which sericitization and carbonation overlap: 314°C at Eksymäselkä, 342°C at Lehtovaara, and 306°C at Honkavaara (Table 28). Late chloritization is related to sericitization at some sites, and the geothermometry of the late-stage chlorite also provides sericitization temperatures (Table 27): 342°C at Lehtovaara, 321°C at Sivakkavaara and 295°C at Honkavaara.

The change from albitization and carbonation to sericitization requires a decrease in pH and/or temperature, as both favour sericite deposition and a pH decrease also favours carbonate and albite decomposition (Giggenbach 1984, Henley and Hedenquist 1986, Saunders and Tuach 1991). Some carbonation and albitization reactions which took place at the sites ([17], [23] and [24]) released H^+, causing a significant pH decrease in the fluid. This change in pH was probably the reason for the sericite precipitation and the replacement of the carbonates. A close relationship between carbonation and sericitization also is supported by the negligible difference between the carbonation and late chloritization temperatures at Honkavaara (11°) and Lehtovaara (0°).

Sericitization and pyritization at Palovaara

Sericitization at Palovaara was more intensive and had strikingly more sulphidation related to it, chiefly pyritization, than at the other sites. The major chemical differences between the sericitized zones in Palovaara and those at the other sites are the higher S, As, Cu and Co concentrations and greater grade of enrichment of these elements in the sediments and tuffites of Palovaara. Also the brecciation related to sericitization was more intensive, and the rock volume increase was probably significant in the sediments and tuffites.

The intensive sulphidation indicates that the sulphur content of the hydrothermal fluid was higher than at the other sites and the high sericitization intensity implies a lower pH. The fluid carried Fe, Cu and Co in particular, most probably in bisulphide and chloride complexes (Large 1977, Drummond and Ohmoto 1985, Reed and Spycher 1985). The f_{O2} of the fluid may have been within the range of sericitization at the other sites because pyrite becomes stable instead of magnetite when the total sulphur content of the fluid is high, pH low and f_{O2} steady (Large 1977, Nesbitt and Kelly 1980, Henley and Brown 1985, Huston and Large 1989). The sericitization temperatures at Palovaara remain unknown, because the calcite-dolomite, muscovite-paragonite and chlorite geothermometries cannot be employed.

The sediments and tuffites at Palovaara contain a few totally sericitized zones in which the mineral association is sericite + quartz ± rutile. These zones are brecciated, with their fractures filled with pyrite ± quartz. This extremely intensively altered assemblage implies a boiling zone in the hydrothermal system (Giggenbach 1981, Drummond and Ohmoto 1985, Reed and Spycher 1985). When a hydrothermal, sulphide-bearing, silica-rich fluid boils, a CO_2 ± HCl-bearing gaseous phase separates out, the temperature of the residual fluid decreases and its pH suddenly increases, whereupon the fluid becomes oversaturated, the bisulphide and chloride complexes are decomposed and sulphides and silica are precipitated (Tómasson and Kristmansdóttir 1972, Henley et al. 1984, Reed and Spycher 1985, Spycher and Reed 1989). As and Sb may be precipitated with sulphides (Spycher and Reed 1989). A large proportion of the sulphides at Palovaara occur as fracture fill material, as is typical of precipitation from a boiling fluid (Reed and Spycher 1985, Merchant 1986). The gaseous phase that separates out during boiling is low in pH and may leach the surrounding rocks effectively, leaving only a Si-Al-rich residue with an assemblage of silica + clay minerals or silica + sericite (Giggenbach 1981 and 1984, Kerrich 1983, Drummond and Ohmoto 1985, Reed and Spycher 1985, Steinthorsson et al. 1987). During regional metamorphism, the residue recrystallizes to a quartz-muscovite schist, a rock similar to the most markedly sericitized sediments and tuffites at Palovaara.

Intensive sericitization is generally found to be more typical of subaerial than subaqueous hydrothermal systems and the occurrence of a boiling zone is commonly considered an indication of subaerial alteration conditions (Giggenbach 1984, Merchant 1986, Christenson 1989, Robinson and Merchant 1989), although Kerrich (1983) and Hall (1992) demonstrate that highly aluminous rocks with argillic alteration are formed as a product of submarine near-seafloor hydrothermal leaching in the presence of an acid vapour phase with CO_2 that has evolved from the boiling of a CO_2-rich hydrothermal fluid. Dill et al. (1992) show that sericitization has taken place in modern submarine hydrothermal systems. Thus, the boiling zones at Palovaara do not inevitably mean that the system was subaerial.

Late chloritization and talc formation

Late chloritization is characteristic of the Eksymäselkä, Myllyvaara, Sivakkavaara and Honkavaara sites, and late talc formation of Myllyvaara and Honkavaara. The alteration is contemporaneous with sericitization, because the late chlorite and talc have the same mode of occurrence as sericite and are apparently in equilibrium with it.

The chlorite geothermometry (Table 28) suggests that the alteration temperature of the late chloritization and talc formation was relatively high, from 265°C (Myllyvaara) to 342°C (Lehtovaara). Thus, the alteration took place at only slightly lower temperatures than the spilitic chloritization and carbonation (cf. Tables 27 and 28, pp. 106-107), the pH of the fluid being lower than during carbonation (Fig. 60) but slightly higher than during sericitization (Giggenbach 1984). The f_{O2} of the system remains unclear except at Myllyvaara, where the conditions were moderately oxidizing, as magnetite and rutile are obviously in equilibrium with the late chlorite.

Talc formation, low Fe/(Fe + Mg) in chlorite and the decomposition of carbonate indicate that the Mg concentration and the a_{Mg2+}/a_{Fe2+} and a_{Mg2+}/a_{Ca2+} were high in the fluid. The contemporaneity of sericitization, chloritization and talc formation suggests that chlorite or talc was precipitated when the a_{Mg2+}/a_{Na+} and a_{Mg+}/a_{K+} ratios were high enough for them but too high for micas (Giggenbach 1984), while talc was precipitated instead of chlorite when the a_{Mg2+} was highest, the pH was slightly higher (Fig. 60) and/or the activity of Al was low (Large 1977, Roberts and Reardon 1978, Bird et al. 1984, Luce et al. 1985).

The Fe/(Fe + Mg) relationships (Fig. 57, p. 110) indicate that the greatest deviations from the chlorite-whole rock equilibrium in the hydrothermal system existed during late chloritization. As was shown in the discussion of early chloritization, this non-equilibrium suggests a Mg-rich hydrothermal fluid comparable to sea water in modern hydrothermal systems. The geothermometry of the late stage chlorites (265-342°C, Table 27) also fits with the chloritization conditions of modern submarine hydrothermal systems (Stakes and O'Neill 1982, Mottl 1983b, Alt 1992). An equilibrium was found between late stage chlorite and whole rock at Myllyvaara (Table 27), representing conditions that prevailed in highly brecciated siltstone, where the w/r was so high that a Mg enrichment was possible throughout.

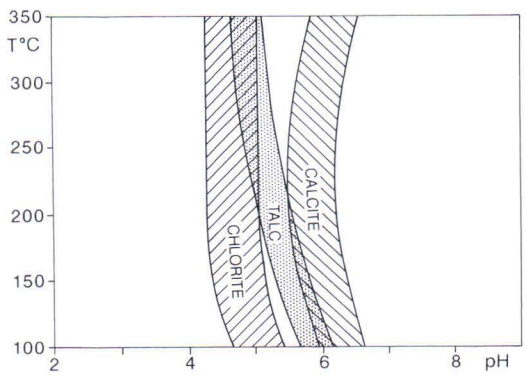

Fig. 60. Relative stabilities of ideal composition Mg chlorite, talc and calcite in relation to pH and temperature (Large 1977).

The formation of talc in areas with no primary Mg-rich rocks (Myllyvaara and Honkavaara) also supports the assumption of a submarine hydrothermal system, as talc is a common product of modern submarine hydrothermal alteration capable of being produced by mixing of a Mg-poor and silica-rich hydrothermal fluid with unmodified, Mg-bearing sea water (Spiess et al. 1980, Stakes and O'Neil 1982, O'Neil and Stakes 1983, Alt et al. 1986, Shau and Peacor 1992). The mixing can take place on the sea floor or in highly brecciated zones of the upflow channels of a submarine hydrothermal system (Costa et al. 1980, Lonsdale et al. 1980, Costa et al. 1983, Aggarwal and Nesbitt 1984).

Indeed, talc was formed in the most brecciated zones at Myllyvaara, which may thus have been upflow zones in which the two fluids were mixed.

A Mg gain from sedimentary pore fluids is not totally ruled out in talc formation, however (Lonsdale et al. 1980), and talc formation in previously Mg-poor areas is therefore not sufficient evidence for assuming submarine conditions, although it fits well with the other evidence for a submarine system and a sea water origin for the hydrothermal fluids.

Alteration styles and conditions

The alteration styles and conditions, with related mineral associations and chemical changes, are summarized separately for each site in Tables 31-37 (pp. 124-130).

SUMMARY AND CONCLUSIONS

A NW-SE striking rift zone was formed in an Archaean continent at the present site of the CLGB in Palaeoproterozoic times (Räsänen et al. 1989, Ward et al. 1989, Lehtonen et al. 1992), and the Middle Lapponian sediments were deposited in this rift in shallow marine and fluviatile environments (Nikula 1988) and were soon albitized under diagenetic conditions.

Upper Lapponian igneous activity in the central part of the CLGB probably began with small-volume lamprophyric magmatism and was followed by a voluminous tholeiitic phase approx. 2.2 Ga ago. Small-scale hydrothermal systems may have been active in combination with the lamprophyre dykes, and large-scale hydrothermal activity causing comprehensive, widespread alterations was generated by the tholeiitic magmatism. The main heat sources were the dykes and sills, and the fluids were predominantly derived from sea water. The temperature zonation was weakly developed in the system, as most of the alterations took place in same temperature range, but the chemical zonation was more complex (Tables 31-37). The igneous rocks were spilitized, and their wall rocks were simultaneously albitized and carbonated. Biotitization took place between the spilitizing and carbonating zones, in the margins and breccia zones of the igneous bodies. During the evolution of the hydrothermal system, the carbonating zones expanded and also covered the most markedly brecciated zones of the igneous rocks and the marginal zones. Sericitization soon followed and overprinted carbonation, as the composition of the hydrothermal fluid changed.

Two smaller-scale alteration stages followed those related to the tholeiitic intrusions: (1) felsic magmatism, manifested by several dykes at the Sivakkavaara site, generating small-scale carbonating, albitizing and sericitizing hydrothermal systems locally after the cessation of the diabase-related hydrothermal systems; (2) fracture zone-related carbonation and albitization taking place locally in the CLGB during the Svecokarelian orogeny, as displayed in the sediments of the Isolaki site.

The alteration stages related to the geological evolution of the central part of the CLGB is described more precisely below.

Table 31. Alteration conditions at Eksymäselkä, in chronological order from left to right.

Alteration type	Diagenetic albitization (Chl-Bt zone in sediments)	Amphibole (diabase and lava)	Chlorite-biotite (diabase, lava and tuffite)	Albite - carbonate	Sericite - chlorite
Mineral association	Qz+Ab+Ser+Mgt ± Hm, Crb, Bt	Act+Ep+Ab+Chl+ Mgt+Ilm/Sp	Chl+Ab+Mgt ± Qz, Ilm, Bt	Ab+Crb+Qz+Rt ± Ser, Mgt, Hm	Ser ± Chl
Alteration style	thorough	thorough	thorough or selective	thorough or selective	selective
Brecciation grade	nil	weak	weak - intensive	weak - intensive	weak
Fracture fill	-	Ep, Ab	Chl, Qz, Bt, Ab, (Py, Cp)	Crb, Ab, Qz, (Py, Cp)	Ser
Gains	feldspar-rich: Na ? mica-rich: K, Cs, Rb, Ba ?	Na, H_2O	CHL: Mg, S, Rb, Cr, H_2O BT: K, S, As, Rb, Ta, H_2O	Mn, Ca, Na, S, Sb, As, CO_2	K, (Cs, Rb, Ba)
Losses	feldspar-rich: K, Cs, Rb, Ba ? mica-rich: Na ?	Fe, Mn, Mg, Ca, K, Cs, Rb, Ba, Cu, Ni, Co	CHL: Si, Mn, Ca, Na, K, Br, Sb, Ba, Cu	Fe, Mg, K, Rb, Ba, Ni, Co, Sc, V, Th, H_2O	Si, Mn, Ca, Na, Co, CO_2
Volume change	±0% ?	?	-10%	-10 - >+30%	-15 - -5%
T	60-150°C ?	≥340-360°C	(270-) 320-360°C	314-384°C ?	≤314°C ?
p	low	<0.5 kb	<0.5 kb	low	low
f_{O2}	?	reducing	reducing	predominantly high	?
f_{CO2}	low	very low	very low	moderate - high	low
pH	weakly acid	acid	acid	near neutral	distinctly acid
Fluid	sediment pore fluid ± sea water ± evaporite-derived fluid	evolved sea water	evolved sea water ± sediment-derived K-rich fluid ?	evolved sea water + magmatic and/or sediment-derived CO_2	evolved sea water ± fresh sea water ?

Abbreviations: CHL = chloritization, BT = biotitization. Ab = albite, Act = actinolite, Bt = biotite, Chl = chlorite, Cp = chalcopyrite, Crb = carbonate, Ep = epidot
Hm = haematite, Ilm = ilmenite, Mgt = magnetite, Qz = quartz, Py = pyrite, Rt = rutile, Ser = sericite, Sp = sphene.

Table 32. Alteration conditions at Myllyvaara, in chronological order from left to right.

Alteration type	Diagenetic albitization (= Bt-Ser zones in sediments)	Amphibole - biotite (lamprophyre)	Albite - carbonate	Chlorite - Talc
Mineral association	Qz+Ab+Bt+Ser+Mgt ± Hm, Crb	Bt+Act+Ab+Mgt+Sp ± Kfs, Ep	Ab+Dol+Qz+Rt ± Hm	Chl+Ab+Qz+Rt ± Mgt, Dol Tc+Ab+Dol+Qz+Rt
Alteration style	thorough	thorough	weak: selective intensive: thorough	thorough (CHL) or selective (CHL, TC)
Brecciation grade	very weak	weak	moderate - intensive	weak - intensive
Fracture fill	Qz, Ser	Qz, Ser, Bt	Qz, Ab, Dol, Hm	Chl±Qz, Tc
Gains	feldspar-rich: Na ? mica-rich: K, Cs, Rb, Ba ?	Na, H_2O ?	Mn, Ca, Na, Br, Sb, W, CO_2	Mg, H_2O
Losses	feldspar-rich: K, Cs, Rb, Ba ? mica-rich: Na ?	Fe, Mn, Mg, Ca, K, Ba, Cu, Ni, Co, CO_2 ?	Fe, Mg, K, S, Rb, Ba, Co, Ni, V, Cr, Th, H_2O	Si, Mn, Ca, K, CO_2
Volume change	±0% ?	?	-10 - > +50%	TC: -10%, CHL: ?
T	60-150°C ?	≥300°C ?	≥265°C ?	265-287°C
p	low	<0.5 kb ?	<0.5 kb ?	low
f_{O2}	?	reducing	high	moderate
f_{CO2}	low	?	moderate - high	low
pH	weakly acid	acid	weakly acid -> near neutral	weakly acid
Fluid	sediment pore fluid ± sea water ± evaporite-derived fluid	evolved sea water	evolved sea water ± magmatic and/or sediment-derived CO_2-fluid	evolved hydrothermal fluid + fresh sea water ?

Abbreviations: CHL = chloritization, TC = talc formation. Ab = albite, Act = actinolite, Bt = biotite, Chl = chlorite, Dol = dolomite, Ep = epidote, Hm = haematite, Ilm = ilmenite, Kfs = K-feldspar, Mgt = magnetite, Qz = quartz, Rt = rutile, Ser = sericite, Sp = sphene, Tc = talc.

Table 33. Alteration conditions at Lehtovaara, in chronological order from left to right.

Alteration type	Diagenetic albitization (quartzite)	Amphibole (diabase)	Chlorite (diabase)	Biotite (diabase)	Albite - carbonate	Sericite (- chlorite)
Mineral association	Qz+Ab+Mgt ± Ser, Crb, Bt	Act+Ep+Ab+ Mgt ± Sp, Ilm	Chl+Ab+Mgt+ Qz ± Ep, Sp	Bt+Ab+Qz+Mgt ± Chl, Ep	Ab+Crb+Qz+Rt ± Bt, Mgt, Hm	Ab+Ser(Chl)+Crb+ Qz+Rt
Alteration style	thorough	thorough	thorough	selective	thorough or selective	thorough
Brecciation grade	nil	very weak	weak - intensive	moderate - intensive	moderate - intensive	nil
Fracture fill	-	Ep, Qz	Chl, Qz, Py	Bt, Qz, Mgt	Crb, Bt, Qz, Py	-
Gains	Na ?	H_2O	Na, Br, U, H_2O	Na, K, Cs, Rb, Ba, La, U, Th, H_2O	Ca, Na, Sb, As, W, CO_2, (La, Sm, S)	DB: K, S, W, Ba, Cr, U QTZ: As, Sb ?
Losses	K, Cs, Rb, Ba ?	?	Mn, Ca, S, As, Cu, Cr	Mn, Ca, Sb, As, Cu, Co, Cr	Fe, Mn, Mg, K, Rb, Ba, Cu, Co, Ni, V, H_2O	Si, Mn, Mg, Ca, Br, As, Cu, Co, Sm, Sc, CO_2
Volume change	±0% ?	?	-5%	±0%	±0 - +28%	-8%
T	60-150°C ?	≥345°C	330-345°C	ca. 340°C ?	ca. 340°C ?	ca. 340°C
p	low	<0.5 kb	<0.5 kb	low	low	low
f_{O2}	?	reducing	reducing	reducing	moderate - high	moderate ?
f_{CO2}	low	very low	very low	low	low - high	high
pH	weakly acid	acid	acid	acid - near neutral	near neutral	weakly acid
Fluid	sediment pore fluid ± sea water ± evaporite-derived fluid	evolved sea water	evolved sea water	evolved sea water + sediment-derived K-rich fluid ?	evolved sea water + magmatic and/or sediment-derived CO_2	evolved hydrothermal fluid ± sea water ?

Abbreviations: DB = albite diabase, QTZ = quartzite. Ab = albite, Act = actinolite, Bt = biotite, Chl = chlorite, Crb = carbonate, Ep = epidote, Hm = haematite, Ilm = ilmenite, Mgt = magnetite, Qz = quartz, Py = pyrite, Rt = rutile, Ser = sericite, Sp = sphene.

Table 34. Alteration conditions at Sivakkavaara, in chronological order from left to right.

Alteration type	Diagenetic albitization (quartzite)	Amphibole - chlorite (diabase)	K feldspar (felsic dykes)	Biotite (diabase)	Carbonate - albite	Sericite - chlorite
Mineral association	Qz+Ab+Mgt ± Ser, Rt, Bt	DB: Act+Ep+Ab+Chl+Mgt LP: Act+Ep+Bt+Ab+Mgt+Sp	Kfs+Pl+Qz+ Mgt ± Bt, Ep, Sp	Bt+Ab+Qz+Mgt	Ab+Crb+Qz+Rt ± Mgt, Bt, Ser, Py	Ser ± Chl
Alteration style	thorough	thorough	thorough	thorough or selective	thorough or selective	selective
Brecciation grade	nil	weak	nil	nil	weak - intensive	weak
Fracture fill	-	Ep, Ab, Chl, Qz	-	-	Crb, Qz, Bt	Ser
Gains	Na ?	H_2O, (Na ?)	(K, H_2O ?)	K, S, Rb, Ba, H_2O	Mn, Ca, Na, W, La, CO_2, (S, Sb, Sm)	SER: K, Rb, Ba CHL: Mg, H_2O
Losses	K, Cs, Rb, Ba ?	(CO_2, K, Cs, Rb, Ba ?)	(Ca ?)	Mg, Ca, Na	Fe, Mg, K, As, Cs, Co, U, (Rb, Ba, Cu, Ni, Th)	CO_2 (Na, Mg, As ?)
Volume change	±0% ?	?	?	? (CHL+BT: +13%)	-8 - +10%	?
T	60-150°C ?	DB: ≥325°C, LP: ≥300°C	?	300-320°C?	ca. 300 - 320°C ?	ca. 320°C
p	low	<0.5 kb	?	low	low	low
f_{O2}	?	reducing	?	reducing	predominantly oxidizing	?
f_{CO2}	low	very low	very low	very low	moderate - high	low
pH	weakly acid	acid	near neutral ?	near neutral - mildly acid	near neutral	acid
Fluid	sediment pore fluid ± sea water ± evaporite-derived fluid	evolved sea water	?	evolved sea water + sediment-derived K ?	evolved sea water + magmatic and/or sediment-derived CO_2	evolved hydrothermal fluid ± fresh sea water ?

Abbreviations: DB = albite diabase, LP = lamprophyre. BT = biotitization, CHL = chloritization, SER = sericitization. Ab = albite, Act = actinolite, Bt = biotite, Chl = chlorite, Cp = chalcopyrite, Crb = carbonate, Ep = epidote, Hm = haematite, Ilm = ilmenite, Mgt = magnetite, Pl = plagioclase, Qz = quartz, Py = pyrite, Rt = rutile, Ser = sericite, Sp = sphene.

Table 35. Alteration conditions at Honkavaara, in chronological order from left to right.

Alteration type	Diagenetic albitization (sediments)	Amphibole (diabase, volcanic rocks)	Epidote (diabase)	Chlorite	Biotite	Carbonate - albite	Sericite - chlorite - talc
Mineral association	Qz+Ab+Rt ± Hm	Act+Ep+Ab+Mgt ± Chl, Sp, Bt	Ep+Act+Sp ± Ab, Mgt, Ap	Chl+Bt+Ab+Mgt +Sp ± Qz, Ep, Rt	Bt+Chl+Ab+Mgt ± Qz, Act, Rt	Ab+Crb+Qz+Rt ± Ser, Hm	Ser/Chl/Tc+ Ab+Qz+Mgt
Alteration style	thorough	thorough	highly localized	selective	selective	thorough or selective	selective
Brecciation grade	nil	weak	weak	weak - intensive	nil	weak - intensive	weak - moderate
Fracture fill	-	Act, Ep, Ab, Qz	Ep, Ap	Chl, Py, Cp	-	Crb, Qz	Ser, Chl, Tc
Gains	feldspar-rich: Na ? mica-rich: K, Cs, Rb, Ba ?	Na, H_2O	Mn, Ca, K, P, Ni, REE	Mg, H_2O	Fe, Mn, K, P, S, Sb, Rb, Ba, Co, Ni	Mn, Ca, Na, Sb, W, U, CO_2, (REE)	SER: K, Sb, Rb, Ba CHL, TC: Mg, H_2O
Losses	feldspar-rich: K, Cs, Rb, Ba ? mica-rich: Na ?	Mg, Ca, K, Cs, Rb, Ba	Fe, Na, Br	Ca, Na, Br, As	Ca, Cs, La, U	Fe, Mg, K, Br, S, Cu, Co, H_2O, (Si, Sc)	Si, Mn, Mg, Ca, Na, P, S, As, U, CO_2
Volume change	±0% ?	?	±0%	±0%	±0%	-7 - ±0%	-25 - ±0%
T	60-150°C ?	>330°C	≥330°C	270-325°C	ca. 306°C ?	306°C	295°C
p	low	<0.5 kb	<0.5 kb	<0.5 kb	low	low	low
f_{O2}	moderate ?	reducing	reducing	reducing	reducing	dominantly high	moderate ?
f_{CO2}	low	very low	very low	very low	low	moderate - high	low
pH	weakly acid	acid	acid	acid	near neutral - mildly acid	near neutral	distinctly acid
Fluid	sediment pore fluid ± sea water ± evaporite-derived fluid	evolved sea water	evolved sea water	evolved sea water	evolved sea water + sediment-derived K-rich fluid ?	evolved sea water + magmatic and/or sediment-derived CO_2	evolved hydrothermal fluid ± fresh sea water ?

Abbreviations: CHL = chloritization, SER = sericitization, TC = talc formation. Ab = albite, Act = actinolite, Ap = apatite, Bt = biotite, Chl = chlorite, Cp = chalcopyrite, Crb = carbonate, Ep = epidote, Hm = haematite, Mgt = magnetite, Qz = quartz, Py = pyrite, Rt = rutile, Ser = sericite, Sp = sphene, Tc = talc.

Table 36. Alteration conditions at Isolaki, in chronological order from left to right.

Alteration type	Amphibole (diabase)	Chlorite (diabase)	Biotite (diabase)	Carbonate - albite - sericite
Mineral association	Act+Ep+Ab+Mgt+Sp	Chl+Ab+Mgt+Sp+Qz ± Act, Bt	Bt+Ab+Qz+Mgt	Ab+Crb+Qz+Mgt ± Ser, Rt, Hm
Alteration style	thorough	selective	thorough or selective	thorough or selective
Brecciation grade	moderate	moderate - intensive	moderate - intensive	weak - intensive
Fracture fill	Act, Ep, Ab, Qz	Chl, Qz, Bt, Py, Cp	Bt, Qz, Py	Crb, Qz, Py
Gains	(Na, H_2O ?)	H_2O, (Mg, S ?)	Fe, K, S, Cs, Rb, Ba, H_2O ?	DB: Mn, Ca, K, Cr, CO_2 QZT: Mn, Mg, Ca, Na, CO_2, Ti (?)
Losses	(K, Cs, Rb, Ba ?)	Ca, Na, K, Cs, Rb, Ba, Cu ?	Ca, Na ?	DB: Na, U, H_2O QZT: Si, Fe, K ?
Volume change	±0% ?	?	?	>+50%
T	>310°C	310-330°C	?	very low ?
p	<0.5 kb	<0.5 kb	low	low ?
f_{O2}	reducing	reducing	?	fluctuating: moderate - high
f_{CO2}	very low	very low	low	moderate - high
pH	acid	acid	near neutral - mildly acid	near neutral - mildly alkaline
Fluid	evolved sea water	evolved sea water	evolved sea water + sediment-derived K-rich fluid ?	deep magmatic, metamorphic and/or sedimentary, containing CO_2 ± K

Abbreviations: DB: albite diabase, QZT: quartzite. Ab = albite, Act = actinolite, Bt = biotite, Chl = chlorite, Cp = chalcopyrite, Crb = carbonate, Ep = epidote, Hm = haematite, Mgt = magnetite, Qz = quartz, Py = pyrite, Rt = rutile, Ser = sericite, Sp = sphene.

Table 37. Alteration conditions at Palovaara, in chronological order from left to right.

Alteration type	Diagenetic albitization (sediments)	Amphibole (ultramafic rocks)	Chlorite - talc	Biotite	Carbonate - albite	Sericite - pyrite
Mineral association	Qz+Ab+Rt ± Ser	Act+Chl+ Bt+Ab+Mgt ± Ab	UM: Tc+Chl+Mgt ± Srp MA: Chl+Ab+Mgt+Qz LP: Bt+Chl+Ab+Qz+Mgt	Bt+Chl+Ab+Qz +Mgt	Ab+Crb+Qz+Rt ± Ser, Hm	Ser+Qz+Rt ± Py, Ab, Crb
Alteration style	thorough	thorough	thorough	selective	thorough or selective	thorough or selective
Brecciation grade	very weak	weak	weak - intensive	nil	moderate - intensive	moderate - intensive
Fracture fill	Qz, Ab	Act, Ab	Qz, Ab, Chl, Py, Cp	-	Crb, Qz, Hm, Py	Ser, Py, Qz, Cp
Gains	feldspar-rich: Na ? mica-rich: K, Cs, Rb, Ba ?	Na, H_2O	Mg, Na, S, H_2O	Mn, Mg, K, S, Cs, Rb, Cu, H_2O	Mn, Ca, Na, CO_2 (S, Cu)	Mn, K, S, As, Rb, Ba, Co, U, H_2O
Losses	feldspar-rich: Na ? mica-rich: K, Cs, Rb, Ba ?	Mg, Ca, K ?	Fe, Ca, K, Cs, Rb, Ba ?	Na, Sb, (Si ?)	Fe, Mg, K, As, Cs, Rb, Ba, Cu, Co, Ni, H_2O	Na, CO_2, (Fe, Mg, Ni, La, Sc ?)
Volume change	±0% ?	?	?	±0%	-5 - +15%	-10 - +20% ?
T	60-150°C ?	≥300°C	300-330°C	?	?	?
p	low	<0.5 kb ?	<0.5 kb ?	low	low	low
f_{O2}	?	reducing	reducing	reducing	predominantly high	reducing
f_{CO2}	low	low	low	low	moderate - high	low (- moderate)
pH	weakly acid	acid	weakly acid ?	near neutral - mildly acid	near neutral	distinctly acid
Fluid	sediment pore fluid ± sea water ± evaporite derived- fluid	evolved sea water	evolved sea water	evolved sea water + sediment-derived K-rich fluid ?	evolved sea water + magmatic and/or sediment-derived CO_2	evolved hydrothermal fluid ?

Abbreviations: LP = lamprophyre, MA = albite diabase, mafic lava and tuffite, UM = ultramafic rock. Ab = albite, Act = actinolite, Bt = biotite, Chl = chlorite, Cp = chalcopyrite, Crb = carbonate, Hm = haematite, Mgt = magnetite, Qz = quartz, Py = pyrite, Rt = rutile, Ser = sericite, Sp = sphene, Srp = serpentine, Tc = talc.

Diagenesis

Most of the Middle Lapponian clastic sediments, even in the upper parts of the sediment pile, were thoroughly albitized during the diagenesis - before the Upper Lapponian magmatism - in the high heat flow regime that prevailed in the rift. Pore fluid of sea water and evaporite origin was an essential source of sodium, and the fine-grained, clayey beds bound the liberated potassium while donating additional Na for the albite (Fig. 61). The alteration temperature was 60-150°C, pressure <0.5 kb, f_{CO2} low and the fluid weakly acid, very much like the situation in modern diagenetic albitizing systems (Boles 1982, Ko and Hesse 1987, Milliken 1988 and 1990, Aagaard et al. 1990). Any provenance information originally contained in the feldspars of the Lapponian sediments was completely lost upon diagenetic albitization at the sites.

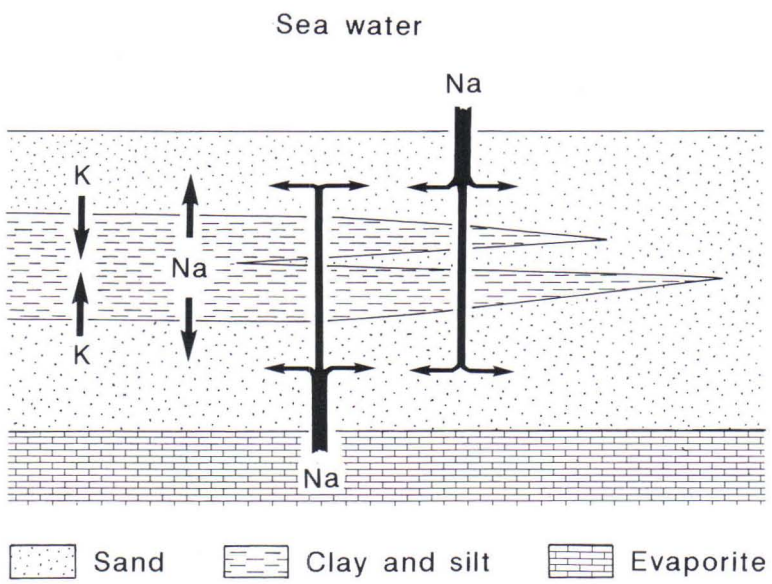

Fig. 61. Simplified model for diagenetic albitization of the Middle Lapponian sediment pile in the CLGB.

Lamprophyre magmatism

It is probable that the Upper Lapponian magmatic activity in the CLGB rift zone may have started with alkaline magmatism, as manifested by the presence of several lamprophyre dykes. In the absence of any radiometric date or contact relationships, even the relative age of the lamprophyre dykes remains open to discussion. In any case, the Middle Lapponian sediments were already consolidated when the lamprophyre magma intruded into them.

It remains unresolved here whether there was any alteration related to the lamprophyre magmatism. Small hydrothermal systems could have been connected with the lamprophyre dykes, using the lamprophyres as their heat source. This is indicated by the bleached haloes

around some of the lamprophyre dykes (Figs. 11 and 21, p. 29 and 37). These alterations could also be related to the tholeiitic magmatism, however, implying that the fractured lamprophyre dykes and their wall rocks merely formed good flow paths for fluids and were thus sensitive to alteration. The latter interpretation is supported by the lack of any petrographical or chemical difference in carbonation + albitization between the areas around the lamprophyre and albite diabase dykes.

Tholeiitic magmatism

Continued rifting ca. 2.2 Ga ago caused deep fractures in the crust, and substantial hypabyssal tholeiitic magmatism occurred in the central part of the CLGB (Kallio 1980, Tyrväinen 1983, Ward et al. 1989, Lehtonen et al. 1992). Great masses of magma solidified as dykes and sills in the sediment piles. The upper Lapponian tholeiitic and komatiitic volcanic rocks were extruded under submarine conditions, covering the rift sediments and dykes. The chemical and petrographical similarity and contact relationships between the volcanic rocks and dykes imply their contemporaneity and comagmatism, though no reliable radiometric age determinations exist for the volcanic rocks.

Magma intrusions caused additional brecciation and fracturing in the consolidated sediments, and the pore fluids of the country rocks, sea water and magmatic fluids were easily able to flow along these fracture zones. The hot, slowly cooling diabase and lava masses heated their wall rocks and the fluids, so that fractures were formed in the dykes and lava flows during cooling, bringing the fluids into direct interaction with the igneous bodies along these fractures. Penetration of the fluids into the still hot rocks further increased the brecciation grade, and the extensive hydrothermal systems demonstrated in Figure 62 were formed in the greenstone belt.

A sea water-dominated hydrothermal fluid of low pH and Eh and having a very low f_{CO2} and high a_{Na+}/a_{K+} predominated in the lava and dyke units, and locally in the pyroclastites. Because of the mafic composition of the rocks, spilitic alteration assemblages were formed (Fig. 62) with a zonation chiefly depending on the w/r of the system: yielding amphibole-dominated (low w/r) and chlorite-dominated (high w/r) zones (Seyfried and Bischoff 1981, Mottl 1983a, Reed 1983, Lonker 1993). The Fe/(Fe + Mg) relationships between chlorite and whole rock indicate an equilibrium between the fluid and rock during chloritization. Intensive epidotization took place locally at Honkavaara in a low w/r but high Ca enrichment regime. The temperature of the hydrothermal system was 270°C, probably 300-430°C in connection with amphibole alteration and epidotization, and 270-360°C in connection with chloritization. The prevailing pressure was ≤0.5 kb.

An exchange of elements between igneous and sedimentary rocks took place in the hydrothermal system (Fig. 62), as indicated by the biotitization of the igneous rocks, chiefly near their contacts with sediments. Biotitization followed the spilitization of these zones, but took place before carbonation + albitization. Its greatest chemical effect was the K-metasomatism of the tholeiites, as their K content increased ten-fold in several zones. The most probable origin for the K is the K-rich, fine-grained sediments intruded by the dykes, as it is improbable that the originally K-poor tholeiites could have been able to supply enough K to the hydrothermal system. The conditions during biotitization were roughly the same as during spilitization, except that the a_{Na+}/a_{K+} was lower and pH higher in the fluid.

The main effect of the synmagmatic hydro-

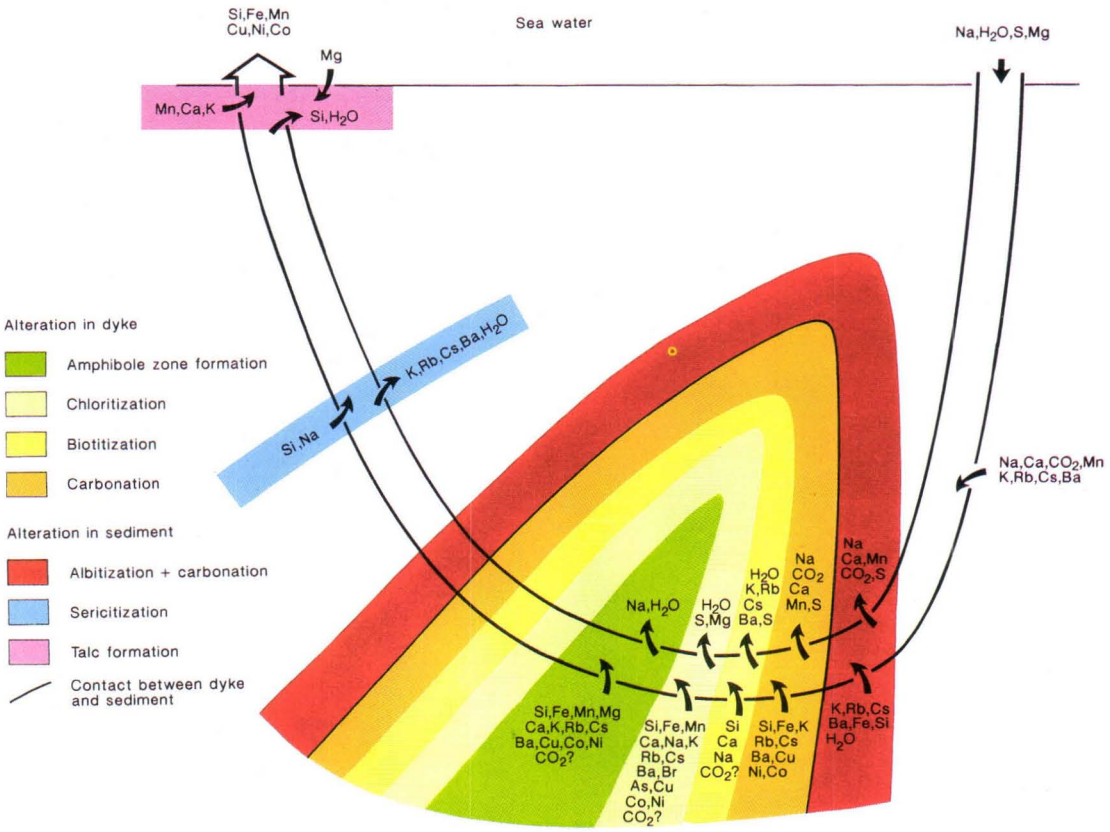

Fig. 62. Simplified model for a dyke-related hydrothermal system in a steady state. Analogous element exchange to the shown to the right of the amphibole zone also takes place in the alteration zones above and to the left of it. Sericitization is only shown at some distance from the dyke, but will also have taken place at a later stage in some parts of the carbonated zones, possibly with chloritization or talc formation.

thermal system on the country rocks of the lavas and dykes was carbonation and intensive albitization. The reason for the high intensity of carbonation was most probably the high pH and the good availability of CO_2 in the sediments. Smaller amounts of CO_2 may have come from the magmatic fluids. A high a_{Na+}/a_{K+} was required for albitization and most of the additional Na needed came from the sea water which flowed into the hydrothermal system, but some may have come from the biotitizing zones and from the pore fluid of the sediments (Fig. 62).

The pH of the carbonating and albitizing system was near neutral or mildly alkaline, and its f_{CO2} was high. f_{O2} varied significantly, but it was mainly at a high level. The chemical changes related to the carbonation and intensive albitization of the sediments and tuffites were large, and most elements were mobilized, even the REE. A number of components had the opposite trends during carbonation and albitization from those that occurred in biotitization (Ca, Na, K, Cs, Rb and Ba) or spilitization (Mg, Fe and Ca and volatiles). This supports the hypothesis that the spilitization and biotitization of the igneous rocks and the carbonation and albitization of the wall rocks took place in

one hydrothermal system and were contemporaneous.

Carbonation and albitization took place in the igneous rocks after spilitic alterations and biotitization. During the evolution of the dyke-heated hydrothermal system, the zones of higher pH expanded and covered the most markedly brecciated zones and the marginal zones of the igneous rocks, thus making carbonate precipitation possible. Carbonate geothermometry (306-384°C) suggests that the temperature in the hydrothermal system was not significantly lower than during the spilitic chloritization of the igneous rocks.

A substantial H^+ release and lowering of a_{Na+}/a_{K+} was related to carbonation and albitization, so that a lowering of the pH and sericitization of the carbonates soon followed. Sericitization also indicates a low f_{CO2}, a_{Mg2+}/a_{K+}, a_{Ca2+}/a_{K+}, and a_{Na+}/a_{H+} and a moderate a_{K+}/a_{H+} in the fluid. f_{O2} and f_{S2} fluctuations are indicated by the formation of magnetite or pyrite. f_{S2} was relatively high only at Palovaara, where significant pyritization was associated with the sericitization. Boiling may have been related to the most intensive sericitization and pyritization in Palovaara, causing a lower pH than at the other sites.

pH was a little higher locally and the activity of Mg^{2+} significantly higher, as Mg-chlorite or talc was precipitated instead of sericite. The Fe/(Fe + Mg) relationships between the chlorite and whole rock indicate that disequilibrium between the fluid and rock prevailed during the alteration stage. The equilibrium was only attained in the most markedly brecciated siltstone at Myllyvaara. The local Mg enrichments (Mg chlorite and talc) require a Mg-rich fluid, suggesting that the hydrothermal fluid that evolved was mixed with fresh sea water in places in the upflow zones of the hydrothermal system. The related chlorites were formed at temperatures of approx. 270-340°C, a range which fits well with spilitization and also supports the close association of sericitization with the synmagmatic hydrothermal system.

Felsic dykes

Felsic dykes were intruded at the Sivakkavaara site after the cooling and cessation of the albite diabase-related hydrothermal system. Small-scale albitization, carbonation and sericitization took place at dyke-wall rock contacts and in other fractured zones, but the interiors of the dykes remained virtually unaltered. The alterations indicate similar P-T and chemical conditions to those related to carbonation and sericitization combined with the diabase-related hydrothermal systems.

Alteration related to fracture zones

The texture and petrography of the carbonated and albitized fracture zones of Isolaki closely resemble the corresponding zones at the other sites, except that the sediments are not albitized at all outside the fracture zone and the alteration zone is connected with both diabase-sediment and conglomerate-quartzite contacts. In addition, carbonation and albitization of the sediments was not possible within the synmagmatic hydrothermal system which spilitized the albite diabase, but took place later, because the sediments are at least 200 Ma younger than the

diabase.

The alteration in the sediments most probably took place in a long-lived hydrothermal system related to the fracture zones. The origin of the carbonating and albitizing fluid remains unresolved, as roughly all fluid sources and their combinations are possible. In any case, the a_{Na+}/a_{K+} of the fluid was high, a_{Ca2+} and f_{CO2} moderate or high, and its pH alkaline or near neutral. The alteration probably took place during the Svecokarelian orogeny 1.9-1.8 Ga ago, and the synorogenic plutonism formed the heat source for the hydrothermal system.

Effects of regional metamorphism

Regional metamorphism with ductile deformation took place after the hydrothermal alterations at each site except Isolaki. Although it caused partial recrystallization of the sheet silicates in places, a good foliation was rarely formed. In addition, partial recrystallization took place in the diabases, lavas and sediments. The most common products being actinolitic hornblende to replace tremolite-actinolite and biotite, and metamorphic biotite to replace chlorite, magmatic biotite and hydrothermal biotite. The recrystallizations did not significantly destroy the textures, mineral associations, chemical gradients and zonations caused by the hydrothermal alterations, however.

Adinoles of the Central Lapland greenstone belt

As mentioned in the introduction, the use of the term *adinole* has been popular in research concerning the greenstone belts of northern Finland. In the central parts of the CLGB, rocks that can be called adinoles *sensu stricto* (Rosenbusch 1923) evidently exist at several sites, but do necessarily not cover particularly wide areas. Only the intensively albitized ± carbonated sediments in direct contact with the albite diabase dykes are undoubtedly true adinoles, and most of the other altered rock types are not. The bleached diabases are by definition not adinoles, though they were formed in the same hydrothermal systems which formed the true adinoles, neither are most of the pale Middle Lapponian sediments adinoles, because they were only albitized during diagenesis, nor can the rocks which were altered in fracture zone-related processes, such as the albitized and carbonated sediments of Isolaki, be considered adinoles.

ACKNOWLEDGEMENTS

I am grateful to many people who have contributed to the production of this work. The research would not have been possible without the work carried out in Lapland by my colleagues at the Geological Survey of Finland. Discussions with Matti I. Lehtonen, who started the Adinole Research Project and was principally responsibilty for it in its early stages,

were important for the progress of the work, and further discussions with Eero Hanski, Hannu Idman, Esko Kontas, Esko Korkiakoski, Tuomo Manninen, Pekka Pihlaja, Jorma Räsänen, Kalevi Rasilainen, Jyri Rastas, Pentti Rastas and Ahti Silvennoinen were neccessary to gain an understanding of the geological evolution and structure of Central Lapland. Matti Pajunen gave significant advice on the mineral formulae calculations.

Continuous support and encouragment was received from Professor Heikki Papunen and Dr Hannu Huhma, who were the supervisors of the work and also critically reviewed the manuscript. I must also thank Professor Papunen for directing me to research into hydrothermal systems, a topic which has proved to be especially interesting and absorbing. Professor Jyrki Lehtovaara and Dr Pekka Nurmi, the official referees of the manuscript, did sterling work and are acknowledged with gratitude.

Special thanks are due to Jukka Välimaa, who participated in the fieldwork, and Jukka Alakunnas, Hannu Kairakari and Vesa Perttunen who assisted with the computing. Fruitful discussions were held with Tapio Glumoff and Seppo Roos in the early stages of the work. Pentti Kouri provided the XRD analyses in cases of difficult mineral indentification, and Lassi Pakkanen and Bo Johansson performed the microprobe analyses for the geothermometry and geobarometry. Soili Ahava, Viena Arvola and Ritva Kotiranta drew the figures, Reijo Lampela assisted in the photographical work and Sini Autio assisted in the editing. Ritva Ääri and Tuula Wan are thanked for their assistance in administrative questions - formal and informal - at the University of Turku. Carola Eklundh and Malcolm Hicks revised the language of the manuscript and made a number of useful corrections.

Finally, and most important, I thank my wife Tarja for her patience and impatience which she expressed in just the right proportions during the preparation of this work.

REFERENCES

Aagaard, P., Egeberg, P.K., Saigal, G.C., Morad, S. & Björlykke, K., 1990. Diagenetic albitization of detrital K-feldspars in Jurassic, lower Cretaceous, and Triassic clastic reservoir rocks from offshore Norway, II. Formation water chemistry and kinetic considerations. J. Sediment. Petrol. 60, 575-581.

Aggarwal, P.K. & Nesbitt, B.E., 1984. Geology and geochemistry of the Chu Chua massive sulfide deposit, British Columbia. Econ. Geol. 79, 815-825.

Agrell, S.O., 1939. The adinoles of Dinas Head, Cornwall. Miner. Mag. 25, 305-337.

Akella, J., 1966. Calculation of material transport in some metasomatic processes. Neues Jahrb. Miner. Abh. 104, 316-329.

Alt, J.A., 1992. Hydrothermal alteration of a 2 km "reference section" of upper ocean crust, DSDP/ODP hole 504B. In: Schiffman, P., Day, H.W. and Beiersdorfer, R.E. (conv.) The transition from basalt to metabasalt: environments, processes, and petrogenesis. Abstracts and program. A meeting on 8-16 September, 1992, by the IGCP 294: Very low grade metamorphism. (no page numbers)

Alt, J.A., Honnorez, J., Laverne, C. & Emmermann, R., 1986. Hydrothermal alteration of a 1 km section through the upper oceanic crust, Deep Sea Drilling Project Hole 504B: mineralogy, chemistry, and evolution of seawater-basalt interactions. J. Geophys. Res. 91, 10309-10335.

Ames, D.E., Franklin, J.M. & Froese, E., 1991. Zonation of hydrothermal alteration at the San Antonio gold mine, Bisset, Manitoba, Canada. Econ. Geol. 86, 600-619.

Amstutz, G.C. (ed.), 1974. Spilites and spilitic rocks. IUGS, Ser. A, 4. 482 p.

Anovitz, L.M. & Essene, E.J., 1986. Phase equilibria in the system $CaCO_3$-$MgCO_3$-$FeCO_3$. J. Petrol. 28, 389-414.

Ashley, P.M., Dudley, R.J., Lesh, R.H., Marr, J.M. & Ryall, A.W., 1988. The Scuddles Cu-Zn prospect, an Archean volcanogenic massive sulphide

deposit, Golden Gove District, western Australia. Econ. Geol. 83, 918-951.

Baltatzis, E. & Wood, B.J., 1977. The occurrence of paragonite in chloritoid schists from Stonehaven, Scotland. Mineral. Mag. 41, 211-216.

Bates, R.L. & Jackson, J.A., 1987. Glossary of geology. 3rd edition. Alexandria: American Geological Institute. 788 p.

Behr, H.-J., Ahrendt, H., Martin, H., Porada, H., Röhrs, L. & Weber, K., 1983. Sedimentology and mineralogy of Upper Proterozoic playa-lake deposits in the Damara Orogen. Pp. 577-610 in: Martin, H. and Eder, F.W. (eds.) Intracontinental fold belts. Berlin: Springer-Verlag. 945 p.

Bettison, L.A. & Schiffman, P., 1988. Compositional and structural variations of phyllosilicates from the Point Sal ophiolite, California. Am. Miner. 73, 62-76.

Bevins, R.E., Robinson, D. & Rowbotham, G., 1991. Compositional variations in mafic phyllosilicates from regional low-grade metabasites and application of the chlorite geothermometer. J. Metamorph. Geol. 9, 711-721.

Bickle, M.J. & Powell, R., 1977. Calcite-dolomite geothermometry for iron-bearing carbonates. Contr. Miner. Petrol. 59, 281-292.

Bird, D.K. & Norton, D.L., 1981. Theoretical prediction of phase relations among aqueous solutions and minerals: Salton Sea geothermal system. Geochim. Cosmochim. Acta 45, 1479-1493.

Bird, D.K., Schiffman, P., Elders, W.A., Williams, A.E. & McDowell, S.D., 1984. Calc-silicate mineralization in active geothermal systems. Econ. Geol. 79, 671-695.

Bischoff, J.L. & Seyfried, W.E., 1978. Hydrothermal chemistry of seawater from 25° to 350°C. Am. J. Sci. 278, 838-860.

Björlykke, A., Nilsen, K.S. & Ekberg, M., 1991. Geology of the Bidjovagge gold-copper deposit, northern Norway. Pp. 489-491 in: E.A. Ladeira (ed.) Brazil Gold '91. Rotterdam: Balkema. 823 p.

Boles, J.R., 1982. Active albitization of plagioclase, Gulf Coast Tertiary. Am. J. Sci. 282, 165-180.

Bowers, T.S. & Taylor, H.P., Jr., 1987. Some calculations pertaining to an integrated chemical and stable-isotope model of the origin of mid-ocean ridge hydrothermal systems. Pp. 633-655 in: Helgeson, H. (ed.) Chemical transport in metasomatic processes. Dordrecht: D.Reidel Publishing Co. 782 p.

Brookins, D.G., 1990. Aqueous geochemistry of rare earth elements. Pp. 201-226 in: Lipin, B.R. and McKay, G.A. (eds.) Geochemistry and mineralogy of rare earth elements. Reviews in Mineralogy 21. Miner. Soc. Am. 348 p.

Brown, E.H., 1977. The crossite content of Ca-amphibole as a guide to pressure of metamorphism. J. Petrol. 18, 53-72.

Browne, P.R.L., 1978. Hydrothermal alteration in active geothermal fields. Ann. Rev. Earth Planet Sci. 6, 229-250.

Cann, J.R., 1969. Spilites from the Carlsberg Ridge, Indian Ocean. J. Petrol. 10, 1-19.

Cathelineau, M., 1988 Cation site occupancy chlorites and illites as a function of temperature. Clay Minerals 23, 471-485.

Cathelineau, M. & Nieva, D., 1985. A chlorite solid solution geothermometer: Los Azufres (Mexico) geothermal system. Contr. Mineral. Petrol. 91, 57-76.

Chatterjee, N.D., 1972. Upper stability limit of the assemblage paragonite + quartz and its natural occurrences. Contr. Mineral. Petrol. 34, 288-303.

Christenson, B.W., 1989. Fluid inclusion and stable isotope studies in the Kawerau hydrothermal system, New Zealand: Evidence for past magma-fluid interaction in the active system. Pp. 155-158 in: Miles D.L. (ed.) Water-rock interaction WRI-6. Proceedings of the 6th International Symposium. Rotterdam: Balkema. 819 p.

Clark, M.E., Carmichael, D.M., Hodgson, C.J. & Fu, M., 1989. Wall-rock alteration, Victory gold mine, Kambalda, western Australia. Processes and P-T-X_{CO2} conditions of metasomatism. Econ. Geol. Monograph 6, 445-459.

Cole, J.W., 1986. Volcanism in the Taupo Volcanic Zone. Pp. 23-35 in: Henley, R.W., Hedenquist, J.W. and Roberts, P.J. (eds.) Guide to the active epithermal (geothermal) systems and precious metal deposits of New Zealand. Monogr. Ser. Mineral Depos. 26, 211 p.

Colvine, A.C., Fyon, J.A., Heather, K.B., Marmont, S., Smith, P.M. & Troop, D.G., 1988. Archean lode gold deposits in Ontario, Canada. Ontario Geol. Surv. Misc. Paper 139. 136 p.

Coombs, D.S., 1974. On the mineral facies of spilitic rocks and their genesis. Pp. 373-385 in: Amstutz, G.C. (ed.) Spilites and spilitic rocks. IUGS, Ser. A, 4. 482 p.

Cooke, D.R., 1992. Numerical models of mineral deposition for the Acupan vein system, Philippines. Pp. 1579-1582 in: Kharaka, Y.K. and Maest, A.S. (eds.) Water-Rock Interaction. Proceedings of the 7th International Symposium on Water-Rock Interaction-WRI-7, Park City, Utah, USA, 13-18 July 1992. Rotterdam: A.A. Balkema. 1686 p.

Costa, U.R., Barnett, R.L. & Kerrich, R., 1983. The Mattagami Lake mine Archean Zn-Cu sulfide deposit, Quebec: Hydrothermal coprecipitation of talc and sulfides in a sea-floor brine pool-evidence from geochemistry, $^{18}O/^{16}O$, and mineral chemistry. Econ. Geol. 78, 1144-1203.

Costa, U.R., Fyfe, W.S., Kerrich, R. & Nesbitt, H.W., 1980. Archean hydrothermal talc evidence for high ocean temperatures. Chem. Geol. 30, 341-349.

Craw, D., Johnstone, R.D. & Rattenbury, M.S., 1989. Tectonic-hydrothermal Au-Cu mineralization in a metamorphic-meteoric fluid mixing zone, Westland, New Zealand. Pp. 167-169 in: Miles D.L. (ed.) Water-rock interaction WRI-6. Proceedings of the 6th International Symposium. Rotterdam: Balkema. 819 p.

Criss, R.E., Fleck, R.J. & Taylor, H.P.Jr., 1991. Tertiary meteoric hydrothermal systems and their relation to ore deposition, northwestern United States and southern British Columbia. J. Geophys. Res. 96, 13335-13356.

Deer, W.A., Howie, R.A. & Zussmann, J., 1962a. Rock forming minerals 3. Sheet silicates. London: Longman. 270 p.

Deer, W.A., Howie, R.A. & Zussmann, J., 1962b. Rock forming minerals 5. Non-silicates. London: Longman. 371 p.

De Groot, P.A. & Baker, J.H., 1992. High element mobility in 1.9-1.86 Ga hydrothermal alteration zones, Bergslagen, central Sweden: relationships with exhalative Fe-ore mineralizations. Precambrian Res. 54, 109-130.

Delaney, J.R., Robigou, V., McDuff, R.E. & Tivey, M.K., 1992. Geology of vigorous hydrothermal system on the Endreavour Segment, Juan de Fuca Ridge. J. Geophys. Res. 97, 19663-19682.

De la Roche, H., Leterrier, J., Granclaude, P. & Marchal, M., 1980. A classification of volcanic and plutonic rocks using R_1R_2-diagram and major-element analyses - its relationships with current nomenclature. Chem. Geol. 29, 183-210.

Dill, H.G., Gauert, C., Holler, G. & Marchig, V., 1992. Hydrothermal alteration and mineralization of basalts from the spreading zone of the East Pacific Rise (7°S-23°S). Geol. Rundsch. 81, 717-728.

Drummond, S.E. & Ohmoto, H., 1985. Chemical evolution and mineral deposition in boiling hydrothermal systems. Econ. Geol. 80, 126-147.

Edmond, J.M., 1992. Results of water rock interactions in mid-ocean ridges. Pp. 885-889 in: Kharaka, Y.K. and Maest, A.S. (eds.) Water-Rock Interaction. Proceedings of the 7th International Symposium on Water-Rock Interaction-WRI-7, Park City, Utah, USA, 13-18 July 1992. Rotterdam: A.A. Balkema. 1686 p.

Eilu, P., 1990. Hydroterminen muuttuminen Kittilän Eksymäselässä ja Myllyvaarassa. Unpubl. Phil. Lic. Thesis. Univ. Turku. 84 p. (in Finnish)

Eilu, P., 1992. Hydrothermal alteration in two Palaeoproterozoic volcanic associations in northern Finland. Pp. 1491-1494 in: Kharaka, Y.K. and Maest, A.S. (eds.) Water-Rock Interaction. Proceedings of the 7th International Symposium on Water-Rock Interaction-WRI-7, Park City, Utah, USA, 13-18 July 1992. Rotterdam: Balkema. 1686 p.

Eilu, P., 1993. Hydrothermal alteration in some volcano-sedimentary associations in Central Finnish Lapland. Geological Survey of Finland Current Research 1991-1992. Geol. Surv. Finland, Spec. Paper 18, 5-13.

Eilu, P. & Idman, H., 1988. Hydrothermal alteration in the lower part of an Early Proterozoic greenstone complex at Palovaara, Enontekiö, northwestern Finland. Bull. Geol. Soc. Finland. 60, Part 2, 115-127.

Elders, W.A., McKibben, M.A. & Williams, A.E., 1992. The Salton Sea hydrothermal system, California, USA: A review. Pp. 1283-1288 in: Kharaka, Y.K. and Maest, A.S. (eds.) Water-Rock Interaction. Proceedings of the 7th International Symposium on Water-Rock Interaction-WRI-7, Park City, Utah, USA, 13-18 July 1992. Rotterdam: A.A. Balkema. 1686 p.

Elliot-Meadows, S.R. & Appleyard, E.C., 1991. The alteration geochemistry and petrology of the Lar Cu-Zn deposit, Lynn Lake Area, Manitoba, Canada. Econ. Geol. 86, 486-505.

Elo, S., Lanne, E., Ruotoistenmäki, T. & Sindre, A., 1989. Interpretation of gravity anomalies along the Polar Profile in the northern Baltic Shield. Tectonophysics 162, 135-150.

Eriksson, B. & Hallgren, U., 1975. Beskrivning till berggrundskartbladen Vittangi NV, NO, SV, SO. Sveriges Geol. Unders., Ser. Af 13-16. 203 p.

Eskola, P., 1925. On the petrology of eastern Fennoscandia I. The mineral development of basic rocks in the Karelian formations. Fennia 45 (19), 1-93.

Eugster, H.P. & Wilson, G.A., 1985. Transport and deposition of ore-forming elements in hydrothermal systems associated with granites. Pp. 87-98 in: Papers presented in High heat production (HHP) granites, hydrothermal circulation and ore genesis Conference, St. Austell, Cornwall, England, 22-25 September, 1985. Inst. Min. Met. London. 591 p.

Fiala, E., 1974. Some notes on the problem of spilites. Pp. 9-22 in: Amstutz, G.C. (ed.) Spilites and spilitic rocks. IUGS, Ser. A, 4. 482 p.

Floyd, P.A. & Winchester, J.A., 1978. Identification and discrimination of altered and metamorphosed volcanic rocks using immobile elements. Chem. Geol. 21, 291-306.

Fournier, R.O., 1989. Geochemistry and dynamics of the Yellowstone National Park hydrothermal system. Ann. Rev. Earth Planet. Sci. 17, 13-53.

Frietsch, R., 1966. Berggrund och malmer: Svappa-

vaara-fältet, Norra Sverige. Sveriges Geol. Unders. Ser. C 604. 282 p. (in Swedish)

Fyon, J.A. & Crocket, J.H., 1982. Gold exploration in the Timmins district using field and lithological characteristics of carbonate alteration zones. In: Hodder, R.W. and Pertuk, W. (eds.) Proceedings of the CIM Gold Symposium, September 1980. Can. Inst. Min. Metall. Spec. vol. 24, 113-129.

Gaál, G., 1990. Tectonic styles of early Proterozoic ore deposition in the Fennoscandian Shield. Precambrian Res. 46, 83-114.

Giggenbach, W.F., 1981. Geothermal mineral equilibria. Geochim. Cosmochim. Acta 45, 393-410.

Giggenbach, W.F., 1984. Mass transfer in hydrothermal alteration systems - A conceptual approach. Geochim. Cosmochim. Acta 48, 2693-2711.

Gjelsvik, T., 1958. Albittrike bergarter i den karelske fjellkjede på Finnmarksvidda, Nord-Norge. Norges Geol. Unders., Bull. 203, 60-72. (in Norwegian)

Grant, J. A., 1986. The isocon diagram - a simple solution to Gresens' equation for metasomatic alteration. Econ. Geol. 81, 1976-1982.

Gresens, R.L., 1967. Composition-volume relationships of metasomatism. Chem. Geol. 2, 47-65.

Hackman, V., 1925. Porkosen-Pahtavaaran rautamalmikentän geologiasta. Geol. Surv. Finland, Geotekn. julk. 39. 41 p. (in Finnish)

Hackman, V., 1927. Studien über den Gesteinsaufbau der Kittilä-Lappmark. Bull. Comm. Geol. Finlande 79. 105 p. (in German)

Hajash, A. & Chandler, G.W., 1981. An experimental investigation of high-temperature interactions between seawater and rhyolite, andesite, basalt and peridotite. Contr. Miner. Petrol. 78, 240-254.

Hall, J.M., 1992. Interaction of submarine volcanic and high-temperature hydrothermal activity proposed for the formation of the Agrokipia, volcanic massive sulfide deposits of Cyprus. Can. J. Earth Sci. 29, 1928-1936.

Härkönen, I. & Keinänen, V., 1989. Exploration of structurally controlled gold deposits in the Central Lapland greenstone belt. In: Autio, S. (ed.) Geological Survey of Finland, Current Research 1988. Geol. Surv. Finland, Spec. Paper 10, 79-82.

Hayba, D.O., Bethke, P.M., Heald, P. & Foley, N.K., 1985. Geologic, mineralogic, and geochemical characteristics of volcanic-hosted epithermal precious-metal deposits. Pp. 129-167 in: B.R. Berger and P.M. Bethke (eds.) Geology and geochemistry of epithermal systems. Rev. Econ. Geol. 2. 298 p.

Hemley, J.J. & Hunt, J.P., 1992. Hydrothermal ore-forming processes in the light of studies in rock-buffered systems: II. Some general geologic applications. Econ. Geol. 87, 23-43.

Henley, R.W. & Brown, K.L., 1985. A practical guide to the thermodynamics of geothermal fluids and hydrothermal ore deposits. Pp. 25-44 in: Berger, B.R. and Bethke, P.M. (eds.) Geology and geochemistry of epithermal systems. Rev. Econ. Geol. 2. 298 p.

Henley, R.W. & Hedenquist, J.W., 1986. Introduction to the geochemistry of fossil and active geothermal systems. Pp. 1-22 in: Henley, R.W., Hedenquist, J.W. and Roberts, P.J. (eds.) Guide to the active epithermal (geothermal) systems and precious metal deposits of New Zealand. Monogr. Ser. Miner. Depos. 26, 211 p.

Henley, R.W., Truesdell, A.H. & Barton, P.B. Jr., 1984. Fluid-mineral equilibria in hydrothermal systems. Rev. Econ. Geol. 1. 267 p.

Hickey, R.L. & Frey, F.A., 1982. Geochemical characteristics of boninite series volcanics: implications for their source. Geochim. Cosmochim. Acta 46, 2099-2115.

Holmsen, P., Padget, P. & Pehkonen, E., 1957. The Precambrian geology of Vest-Finnmark, northern Norway. Norges Geol. Unders., Bull. 201. 107 p.

Hughes, C.J., 1973. Spilites, keratophyres and the igneous spectrum. Geol. Mag. 109, 513-527.

Huhma, H. & Meriläinen, K., 1991. Provenance of paragneisses from the Lapland granulite belt. Abstract. In: Tuisku, P. and Laajoki, K. (eds.) Metamorphism, deformation and structures of crust. Res. Terrae, Ser. A 5, p. 26.

Humphris, S.E., 1984. The mobility of the rare earth elements in the crust. Pp. 317-342 in: Henderson, P. (ed.) Rare earth element geochemistry. Amsterdam: Elsevier. 510 p.

Humphris, S.E. & Thompson, G., 1978a. Hydrothermal alteration of oceanic basalts by seawater. Geochim. Cosmochim. Acta 42, 107-125.

Humphris, S.E. & Thompson, G., 1978b. Trace element mobility during hydrothermal alteration of oceanic basalts. Geochim. Cosmochim. Acta 42, 127-136.

Hunt, J.A. & Kerrick, D.M., 1977. The stability of sphene: experimental redetermination and geologic implications. Geochim. Cosmochim. Acta 41, 279-288.

Huston, D.L. & Large, R.R., 1989. A chemical model for the concentration of gold in volcanogenic massive sulfide deposits. Ore Geol. Rev. 4, 171-200.

Inkinen, O., 1979. Copper, zinc, and uranium occurrences at Pahtavuoma in the Kittilä greenstone complex, northern Finland. Econ. Geol. 74, 1153-1165.

Irvine, T.N. & Baragar, W.R.A., 1971. A guide to chemical classification of common volcanic rocks.

Can. J. Earth Sci. 8, 523-548.

Janecky, D.R. & Seyfried, W.E., Jr, 1985. The solubility of magnesium-hydroxide-sulfate-hydrate in seawater at elevated temperatures and pressures. Am. J. Sci. 283, 831-860.

Janecky, D.R. & Seyfried, W.E., Jr, 1987. Transition metal mobility in oceanic ridge crest hydrothermal systems at 350 °C-425 °C. Pp. 657-668 in: Helgeson, H. (ed.) Chemical transport in metasomatic processes. Dordrecht: D.Reidel Publishing Co. 782 p.

Jasinski, A.W., 1988. Activity diagrams for the MgO-Na_2O-K_2O-SiO_2-Al_2O_3-H_2O-HCl system in the temperature range 298 to 623 K and 1 bar pressure: application to the 1900 Ma phlogopite-Mg-chlorite-sericite schists of W. Bergslagen, Sweden. Geol. Mijnbouw 67, 379-395.

Jensen, L.S., 1976. A new cation plot for classifying subalkalic volcanic rocks. Ontario Div. Mines, Misc. Pap. 66. 22 p.

Jensen, L.S. & Pyke, D.R., 1982. Komatiites in the Ontario portion of the Abitibi belt. Pp. 147-157 in: Arndt, N.T. and Nisbet, E.G. (eds.) Komatiites. Mainz: Max-Planck Institute of Chemistry. 526 p.

Kallio, M., 1980. Keski-Lapin liuskealue Itä-Kittilän ja Länsi-Sodankylän osalta. Osa II: Rakenne ja stratigrafia. Kuhmon ja Kittilän malmiprojekti, Raportti 29, Oulun yliopisto. 67 p. (in Finnish)

Kallio, M., Kärkkäinen, N. & Sarapää, O., 1980. Keski-Lapin liuskealue Itä-Kittilän ja Länsi-Sodankylän osalta. Osa I: Petrografinen kuvaus ja kallioperäkartta. Kuhmon ja Kittilän malmiprojekti, Raportti 28, Oulun yliopisto. 88 p. (in Finnish)

Kalsbeek, F., 1992. Large scale albitization on Qeqertakavsak island, northeast Disko Bugt, West Greenland. Chem. Geol. 95, 213-233.

Kärkkäinen, N., 1980. Keski-Lapin liuskealue Itä-Kittilän ja Länsi-Sodankylän osalta. Osa IV: Metamorfoosi. Kuhmon ja Kittilän malmiprojekti, Raportti 31, Oulun yliopisto. 88 p. (in Finnish)

Kerrich, R., 1983. Geochemistry of gold deposits in the Abitibi greenstone belt. Can. Inst. Mining Metall. Spec. vol. 27, 74 p.

Kerrich, R., 1989. Lithophile element systematics of gold vein deposits in Archean greenstone belts: implications for source processes. Econ. Geol. Monograph 6, 508-519.

Kishida A. & Kerrich R., 1987. Hydrothermal alteration zoning and gold concentration at the Kerr-Addison Archean lode gold deposit, Kirkland Lake, Ontario. Econ. Geol. 82, 649-690.

Ko, J. & Hesse, R., 1987. Provenance, albitization and carbonate cementation of Middle Ordovician greywackes, Cloridorme formation, Gaspe Peninsula, Quebec. Geol. Assoc. Canada, Miner. Assoc. Canada, May 25-27, 1987. University of Saskatchewan. Joint Annual Meeting. Program and abstracts. 111 p.

Ko, J. & Hesse, R., 1992. Illite/smectite diagenesis in overpressurized and normally pressurized environments, Beaufort-Mackenzie Basin, Arctic Canada. Pp. 1173-1176 in: Kharaka, Y.K. and Maest, A.S. (eds.) Water-Rock Interaction. Proceedings of the 7th International Symposium on Water-Rock Interaction-WRI-7, Park City, Utah, USA, 13-18 July 1992. Rotterdam: A.A. Balkema. 1686 p.

Korja, A., Korja, T., Luosto, U. & Heikkinen, P., 1993. Seismic and geoelectric evidence for collisional and extensional events in the Fennoscandian Shield - implications for Precambrian crustal evolution. Tectonophysics 219, 129-152.

Korkiakoski, E., 1992. Geology and geochemistry of the metakomatiite-hosted Pahtavaara gold deposit in Sodankylä, northern Finland, with emphasis on hydrothermal alteration. Geol. Surv. Finland, Bull. 360. 96 p.

Kortelainen, V., 1986. Levitunturin ja sen lähiympäristön klastisten kivien sedimentologia Kittilässä, Pohjois-Suomessa. Pp. 29-30 in: Laajoki, K., Paakkola, J. and Gehör, S. (eds.) Suomen kallioperän sedimentologia. Res Terrae, Ser. B, 9. 30 p. (in Finnish)

Korvuo, E., 1991. The Saattopora mine. Pp. 33-37 in: Tuisku, P. and Laajoki, K. (eds.) Excursion guide to Lapland, 21-24 August. Metamorphism, deformation and structure of the crust. Res Terrae Ser. A, 6. 75 p.

Kranidiotis, P. & MacLean, W.H., 1987. Systematics of chlorite alteration at the Phelps Dodge massive sulfide deposit, Mattagami, Quebec. Econ. Geol. 82, 1898-1911.

Kristmannsdóttir, H., 1975. Hydrothermal alteration of basaltic rocks in Icelandic geothermal areas. Second UN Symposium on development and utilization of geothermal resources. San Francisco, California. May 20-29, 1975. 441-445.

Kristmannsdóttir, H., 1983. Chemical evidence from Icelandic geothermal systems as compared to submarine geothermal systems. Pp. 291-320 in: Rona, P.A., Boström, K., Laubier, L. and Smith, K.L., Jr (eds.) Hydrothermal processes at seafloor spreading centers. New York: Plenum Press. 796 p.

Laird, J., 1980. Phase equilibria in mafic schist from Vermont. J. Petrol. 21, 1-37.

Lalou, C., Thompson, G., Arnold, M., Brichet, E., Druffel, E. & Rona, P.A., 1990. Geochronology of TAG and Snakepit hydrothermal fields, Mid-Atlantic Ridge: witness to a long and complex hydrothermal history. Earth Planet. Sci. Lett. 97, 113-128.

Lambert, D.D., Malek, D.J. & Dahl, D.A., 1988.

Rb-Sr and oxygen isotopic study of alkalic rocks from the Trans-Pecos magmatic province, Texas: Implications for the petrogenesis and hydrothermal alteration of continental alkalic rocks. Geochim. Cosmochim. Acta 52, 2357-2367.

Land, L.S. & Milliken, K.L., 1981. Feldspar diagenesis in the Frio Formation, Brazoria county, Texas Gulf Coast. Geology 9, 314-318.

Lång, K., Gaál., G. & Starostin, V., 1984. Structural and petrographical features, some Precambrian stratabound base metal deposits of Finland (Outokumpu, Vihanti, Riikonkoski). 27th Internat. Geol. Congr. Moskva, 4-14 Avgusta. Tesizy = Abstracts. Abstract section 12, 186-187.

Lanne, E., 1979. Vuotoksen ja Kittilän alueiden geofysikaalisten tietojen tulkinnasta. Summary: On the interpretation of geophysical data from the Vuotos and Kittilä areas, northern Finland. Geol. tutk.l. Tutk.rap. - Geol. Surv. Finland, Rep. Invest. 25. 38 p.

Large, R.R., 1977. Chemical evolution and zonation of sulfide deposits in volcanic terrains. Econ. Geol. 77, 549-572.

Le Bas, M.J., Le Maitre, R.W., Streckeisen, A. & Zanettin, B., 1986. A chemical classification of volcanic rocks based on the total alkali-silica diagram. J. Petrol. 27, 745-750.

Lehmann, E., 1974. Spilitic magma. Characteristics and mode of formation. Pp. 23-58 in: Amstutz, G.C. (ed.) Spilites and spilitic rocks. IUGS, Ser. A, 4. 482 p.

Lehtonen, M. & Rastas, P., 1987. Aluetutkimukset, Keski-Lappi. Pp. 4-18 in: Manninen, T., Hanski, E. ja Kesola, R. (eds.) Lapin vulkaniittiprojekti, vuosikertomus 1986. Geologian tutkimuskeskuksen arkisto, raportti K/1987/1. 47 p. (in Finnish)

Lehtonen, M. & Rastas, P., 1988. Aluetutkimukset, Keski-Lappi. Pp. 4-15 in: Manninen, T., Hanski, E. ja Kesola, R. (eds.) Lapin vulkaniittiprojekti, vuosikertomus 1987. Geologian tutkimuskeskuksen arkisto, raportti K/1988/1. 47 p. (in Finnish)

Lehtonen, M., Rastas, P., & Räsänen, J., 1989. Keski-Lapin vulkaniittitutkimukset. Pp. 9-39 in: Manninen, T. (ed.) Tulivuorenkivet Kolarista Kuusamoon. Lapin vulkaniittiprojektin ekskursio ja esitelmäseminaari 5.-10.6.1989. Geol. tutk.k. Opas - Geol. Surv. Finland, Guide 23. 78 p. (in Finnish)

Lehtonen, M.I., 1987. Adinolikivet. Pp. 32-36 in: Manninen, T., Hanski, E. and Kesola, R. (eds.) Lapin vulkaniittiprojekti, vuosikertomus 1986. Geologian tutkimuskeskuksen arkisto, raportti K/1987/1. 47 p. (in Finnish)

Lehtonen, M.I., 1988. Adinolikivet. Pp. 35-38 in: Manninen, T., Hanski, E. and Kesola, R. (eds.) Lapin vulkaniittiprojekti, vuosikertomus 1987. Geologian tutkimuskeskuksen arkisto, raportti K/1988/1. 46 p. (in Finnish)

Lehtonen, M.I., 1989a. Adinolikivet. Pp. 34-35 in: Manninen, T. and Kesola, R. (eds.) Lapin vulkaniittiprojekti, vuosikertomus 1988. Geologian tutkimuskeskuksen arkisto, raportti K/20.3/1989/1. 44 p. (in Finnish)

Lehtonen, M.I., 1989b. The Lapland Volcanite Project. In: S. Autio (ed.) Geological Survey of Finland, Current Research 1988. Geol. Surv. Finland, Spec. Paper 10, 19-21.

Lehtonen, M.I. & Manninen, T., 1986. Adinolikivet. Pp. 25-28 in: Lehtonen, M., Manninen, T., and Rastas, P. (eds.) Lapin vulkaniittiprojekti, vuosikertomus 1985. Geologian tutkimuskeskuksen arkisto, raportti K/1986/1. 33 p. (in Finnish)

Lehtonen, M.I., Manninen, T., Rastas, P., Väänänen, J., Roos, S.I. & Pelkonen, R., 1984. Geological map of Central Lapland, northern Finland 1 : 250 000. Geol. Surv. Finland. Helsinki.

Lehtonen, M.I., Manninen, T., Rastas, P., Väänänen, J., Roos, S.I. & Pelkonen, R., 1985. Keski-Lapin geologisen kartan selitys. English summary and discussion: Explanation to the geological map of Central Lapland. Geol. tutk.k. tutk.rap. Geol. Surv. Finland. Rep. Invest. 71. Helsinki. 55 p.

Lehtonen, M.I., Manninen, T., Rastas, P. & Räsänen, J., 1992. On the early Proterozoic metavolcanic rocks in Finnish Central Lapland. Pp. 65-85 in: Balagansky, V.V. (ed.) Correlation of Lower Precambrian Formations of the Karelian-Kola Region, Russia and Finland. The Russian Academy of Science, Kola Science Centre, Geological Institute: Apatity. 86 p.

Lehtonen, M.I., Eilu, P., Kortelainen, V., Lanne, E., Manninen, T., Rastas, P., Räsänen, J., & Virransalo, P. (in prep.) Keski-Lapin vulkaniitit. Lapin vulkaniittiprojektin raportti. Summary: Volcanic rocks in the Central Lapland area, northern Finland. A report of the Lapland Volcanite Project. Geol. tutk.k. tutk.rap. - Geol. Surv. Finland, Rep. Invest.

Lesher, C.M., Gibson, H.L. & Campbell, I.H., 1986. Composition-volume changes during alteration of andesite at Buttercup Hill, Noranda District, Quebec. Geochim. Cosmochim. Acta 50, 2693-2705.

Lister, C.R.B., 1983. The basic physics of water penetration into hot rock. Pp. 140-168 in: Rona, P.A., Boström, K., Laubier, L. and Smith, K.L., Jr (eds.: Hydrothermal processes at seafloor spreading centers. New York: Plenum Press. 796 p.

Lonker, S.W., Franzon, H. & Kristmansdóttir, H., 1993. Mineral-fluid interactions in the Reykjanes and Svartsengi geothermal systems, Iceland. Am. J. Sci. 293, 605-670.

Lonsdale, P.F., Bischoff, J.L., Burns, V.M., Kast-

ner, M. & Sweeney, R.E., 1980. A high-temperature hydrothermal deposit on the seabed at a Gulf of California spreading center. Earth Planet. Sci. Lett. 49, 8-20.

Lottermoser, B.G., 1992. Rare earth elements and hydrothermal ore formation processes. Ore Geol. Rev. 7, 25-41.

Luce, R.W., Cygan, G.L., Hemley, J.J. & D'Angelo, W.M., 1985. Some mineral stability relations in the system CaO-MgO-SiO_2-H_2O-HCl. Geochim. Cosmochim. Acta 49, 525-538.

MacKenzie, W.S., Donaldson, C.H. & Guildford, C., 1982. Atlas of igneous rocks and their textures. London: Longman. 148 p.

MacLean, W.H., 1990. Mass change calculations in altered rock series. Mineral. Depos. 25, 44-49.

MacLean, W.H. & Hoy, L.D., 1991. Geochemistry of hydrothermally altered rocks at the Horne mine, Noranda, Quebec. Econ. Geol. 86, 506-528.

MacLean, W.H. & Kranidiotis, P., 1987. Immobile elements as monitors of mass transfer in hydrothermal alteration: Phelps Dodge massive sulphide deposit, Mattagami, Quebec. Econ. Geol. 82, 951-962.

Magenheim, A.J. & Gieskes, J.M., 1992. Hydrothermal discharge and alteration in near-surface sediments from the Guaymas Basin, Gulf of California. Geochim. Cosmochim. Acta 56, 2329-2338.

Manninen, T., 1991. Sallan alueen vulkaniitit. Lapin vulkaniittiprojektin raportti. English summary: Volcanic rocks in the Salla Area, northeastern Finland. A report of the Lapland Volcanite Project. Geol. tutk.k. Tutk.rap. - Geol. Surv. Finland, Rep. Invest. 104. 97 p.

Merchant, L.J., 1986. Mineralization in the Thames District-Coromandel. Pp. 147-164 in: Henley, R.W. Hedenquist, J.W. and Roberts, P.J. (eds.) Guide to the active epithermal (geothermal) systems and precious metal deposits of New Zealand. Monogr. Ser. Mineral Depos. No. 26, 211 p.

Meriläinen, K., 1961. Albite diabases and albitites in Enontekiö and Kittilä, Finland. Bull. Comm. Geol. Finlande 195. 75 p.

Metamorphic, Structural and Isotopic Age Map, Northern Fennoscandia, 1988. 1:1 mill. Helsinki: Geological Surveys of Finland, Norway and Sweden.

Meyer P.S., Sigurdsson, H. & Sigvaldason, G.,E., 1985. Petrological and geochemical variations along Iceland's Neovolcanic Zone. J. Geophys. Res. 90, 10043-10072.

Michard, A., 1989. Rare earth element systematics in hydrothermal fluids. Geochim. Cosmochim. Acta 53, 745-750.

Mikkola, E., 1937. Suomen geologinen yleiskartta. Kivilajikartta. Sodankylä (lehti C7). The General Geological Map of Finland. Pre-quaternary rocks. Sheet C7, Sodankylä. Helsinki: Suomen geologinen toimikunta.

Mikkola, E., 1941. Suomen geologinen yleiskartta. Lehdet B7-C7-D7, Muonio, Sodankylä ja Tuntsajoki. Kivilajikartan selitys. English summary: The general geological map of Finland. Sheets B7-C7-D7, Muonio, Sodankylä and Tuntsajoki. Explanation to the map of rocks. 286 p.

Milliken, K.L., 1988. Loss of provenance information through subsurface diagenesis in Plio-Pleistocene sandstones, northern Gulf of Mexico. J. Sediment. Petrol. 58, 992-1002.

Milliken, K.L., 1992. Chemical behavior of detrital feldspars in mudrocks versus sandstones, Frio Formation (Oligocene), South Texas. J. Sediment. Petrol. 62, 790-801.

Minissale, A., 1991. The Lardello geothermal field: a review. Earth Sci. Rev. 31, 133-151.

Montoya, J.W. & Hemley, J.J., 1975. Activity relations and stabilities in alkali feldspar and mica alteration reactions. Econ. Geol. 70, 577-583.

Moody, J.B., Meyer, D. & Jenkins J.E., 1983. Experimental characterization of the greenschist/amphibolite boundary in mafic systems. Am. J. Sci. 283, 48-92.

Morad, S., 1986. Albitization of K-feldspar grain in Proterozoic arkoses and greywackes from southern Sweden. N. Jb. Miner. Mh. 10, 145-156.

Morad, S., Bergan, M., Knarud, R. & Nystuen, J.P., 1990. Albitization of detrital plagioclase in Triassic reservoir sandstones from the Snorre Field, Norwegian North Sea. J. Sediment. Petrol. 60, 411-425.

Mottl, M.J., 1983a. Hydrothermal processes at seafloor spreading centers: application of seawater-basalt experiments. Pp. 199-224 in: Rona, P.A., Boström, K., Laubier, L. and Smith, K.L., Jr (eds.) Hydrothermal processes at seafloor spreading centers. New York: Plenum Press. 796 p.

Mottl, M.J., 1983b. Metabasalts, axial hot springs, and the structure of hydrothermal systems at mid-ocean ridges. Geol. Soc. Am. Bull. 94, 161-180.

Mottl, M.J. & Holland H.D., 1978. Chemical exchange during hydrothermal alteration of basalt by seawater - I. Experimental results for major and minor components of seawater. Geochim. Cosmochim. Acta 42, 1103-1115.

Munhá, J., Fyfe, W.S. & Kerrich, R., 1980. Adularia, the characteristic mineral of felsic spilites. Contr. Mineral. Petrol. 75, 15-19.

Nesbitt, B.E. & Kelly, W.C., 1980. Metamorphic zonation of sulfides, oxides and graphite in and around the orebodies at Ducktown, Tennessee. Econ. Geol. 75, 1010-1021.

Nikula, R., 1988. Paleosedimentology of Precambrian tidal Virttiövaara and fluvial Värttiövaara quartzite formations in Sodankylä, northern Finland. In: Laajoki, K. and Paakkola, J. (eds.) Sedimentology of the Precambrian formations in eastern and northern Finland. Geol. Surv. Finland, Spec. Paper 5, 177-188.

Nurmi, P., Lestinen, P. & Niskavaara, H., 1991. Geochemical characteristics of mesothermal gold deposits in the Fennoscandian Shield, and a comparison with selected Canadian and Australian deposits. Geol. Surv. Finland, Bull. 351. 101 p.

Ödman, O.H., 1939. Urbergsgeologiska undersökningar inom Norrbottens län. Sveriges Geol. Unders. Ser. C, 426. 100 p. (in Swedish)

Offler, R. & Whitford, D.J., 1992. Wall-rock alteration and metamorphism of a volcanic-hosted massive sulfide deposit at Que River, Tasmania: petrology and mineralogy. Econ. Geol. 87, 686-705.

O'Neil, J.R. & Stakes, D.S., 1983. Mineralogy and stable isotope geochemistry of hydrothermally altered rocks from the East Pacific Rise and the Mid-Atlantic Ridge. U.S. Geol. Surv. Prof. Pap. p. 149.

Paakkola, J., 1971. The volcanic complex and associated manganiferous iron formations of the Porkonen-Pahtavaara Area in Finnish Lapland. Bull. Comm. Geol. Finland 247. 83 p.

Padget, P., 1959. Leucodiabase and associated rocks in the Karelidic zone of Fennoscandia. Geol. Fören.Stockholm Förh. 81, 316-332.

Pan, Y., Fleet, M.E. & MacRae, N.D., 1993. Late alteration in titanite ($CaTiSiO_5$). Redistribution and remobilization of rare earth elements and implications for U/Pb and Th/Pb geochronology and nuclear waste disposal. Geochim. Cosmochim. Acta 57, 355-367.

Pankka, H., 1992. Geology and mineralogy of Au-Co-U deposits in the Proterozoic Kuusamo volcanosedimentary belt, northeastern Finland. A dissertation. Michigan Technological University, Geology. 233 p.

Pankka, H.S. & Vanhanen, E.J., 1992. Early Proterozoic Au-Co-U mineralization in the Kuusamo district, northeastern Finland. Precambrian Res. 58, 387-400.

Pettijohn, F.J. Potter, P.E. & Siever, R., 1987. Sand and sandstone. 2nd ed. New York: Springer-Verlag. 553 p.

Pihlaja, P. & Manninen, T., 1993. Pre-Quaternary rocks, Sheet 3723 Peurasuvanto, Geological Map of Finland, 1 : 100 000. Espoo: Geological Survey of Finland.

Piirainen, T. & Rouhunkoski, P., 1974. General features of the spilitic rocks in Finland. Pp. 191-205 in: Amstutz, G.C. (ed.) Spilites and spilitic rocks. IUGS, Ser. A, 4. 482 p.

Piispanen, R., 1972. On the spilitic rocks of the Karelidic belt in western Kuusamo, northeastern Finland. Acta Univ. Oul., Ser. A, 4, Geol. 2. 73 p.

Pirajno, F., 1992. Hydrothermal mineral deposits. Berlin: Springer-Verlag. 709 p.

Powell, R. & Holland, T.J.B., 1988. An internally consistent dataset with uncertainties and correlations: 3. Applications to geobarometry, worked examples and a computer program. J. Metamorph. Geol. 6, 173-204.

Ragnarsdóttir, K.V., Walther, J.W. & Arnórsson, S., 1984. Description and interpretation of the composition of fluid and alteration mineralogy in the geothermal system, at Svartsengi, Iceland. Geochim. Cosmochim. Acta 48, 1535-1553.

Räsänen, J., Hanski, E. & Lehtonen, M.I., 1989. Komatiites, low-Ti basalts and andesites in the Möykkelmä area, Central Finnish Lapland. A report of the Lapland Volcanite Project. Geol. tutk.k. Tutk.rap. - Geol. Surv. Finland, Rep. Invest. 88. Espoo. 41 p.

Rastas, P., 1984. Pre-Quaternary rocks, Sheet 2732 Kittilä, Geological Map of Finland, 1:100 000. Espoo: Geologicl Survey of Finland.

Reed, M.H., 1983. Seawater-basalt reaction and the origin of greenstones and related ore deposits. Econ. Geol. 78, 466-485.

Reed, M.H. & Spycher, N.F., 1984. Calculation of pH and mineral equilibria in hydrothermal waters with application to geothermometry and studies of boiling and dilution. Geochim. Cosmochim. Acta 48, 1479-1492.

Reed, M.H. & Spycher, N.F., 1985. Boiling, cooling and oxidation in epithermal systems: a numerical modelling approach. Pp. 249-272 in: B.R. Berger and P.M. Bethke (eds.) Geology and geochemistry of epithermal systems. Rev. Econ. Geol. 2. 298 p.

Reino, J., 1973. Pohjois-Suomessa esiintyvien albitiittien petrografiasta ja geokemiasta. Unpubl. M.Sc. Thesis, Univ. Oulu. 75 p. (in Finnish)

Ribbe, P.H., 1982. Titanite. Pp. 137-154 in: Ribbe, P.H. (ed.) Orthosilicates. Mineralogical Society of America: Reviews in mineralogy, 5. 450 p.

Richards, J.P., McCulloch, M.T., Chappell, B.W. & Kerrich, R., 1991. Sources of metals in the Porgera gold deposit, Papua New Guinea: Evidence from alteration, isotope, and noble metal geochemistry. Geochim. Cosmochim. Acta 55. 565-580.

Roberts, R.G. & Reardon, E.J., 1978. Alteration and ore-forming processes at Mattagami Lake Mine, Quebec. Can. J. Earth Sci. 15, 1-21.

Robinson, B.W. & Merchant, R.J., 1989. Mineralization, fluid inclusion and sulphur isotope studies of the Thames-Tapu area, Hauraki goldfield, New Zealand. Pp. 589-592 in: Miles, D.L. (ed.) Water-

rock interaction WRI-6. Proceedings of the 6th International Symposium. Rotterdam: Balkema. 819 p.

Rock, N.M.S., 1987. The nature and origin of lamprophyres: an overview. Pp. 191-226 in: Fitton, J.G. & Upton, B.G.J. (eds.) Alkaline igneous rocks. Geol. Soc. Spec. Publ. 30. 568 p.

Rock, N.M.S., 1991. Lamprophyres. London: Blackie and Son Ltd,. 285 p.

Rose, A.W., Hawkes, H.E. & Webb, J.S., 1979. Geochemistry in mineral exploration. 2nd edition. London: Academic Press. 657 p.

Rosenbauer, R.J. & Bischoff, J.L., 1983. Uptake and transport of heavy metals by heated seawater: a summary of the experimental results. Pp. 177-197 in: Rona, P.A., Boström, K., Laubier, L. and Smith, K.L., Jr (eds.): Hydrothermal processes at seafloor spreading centers. New York: Plenum Press. 796 p.

Rosenbusch, H., 1923. Elemente der Gesteinlehre. 4. neubearb. Stuttgart: Aufl. von A. Osnann. (in German)

Saigal, G.C., Morad, S., Björlykke, K., Egeberg, P.K. & Aagaard, P., 1988. Diagenetic albitization of detrital K-feldspar in Jurassic, lower Cretaceous, and Tertiary clastic reservoir rocks from offshore Norway, I. Textures and origin. J. Sediment. Petrol. 58, 1003-1013.

Sarapää, O., 1980. Keski-Lapin liuskealue Itä-Kittilän ja Länsi-Sodankylän osalta. Osa III: Vulkaniittien geokemia. Kuhmon ja Kittilän malmiprojekti, Raportti 30, Oulun yliopisto. 56 p. (in Finnish)

Saunders, C.M. & Tuach, J., 1991. Potassic and sodic alteration accompanying gold mineralization in the Rattling Brook deposit, western White Bay, Newfoundland Appalachians. Econ. Geol. 86, 555-569.

Saverikko, M., 1988. The Oraniemi arkose-slate-quartzite association: an Archaean aulacogen fill in northern Finland. In: Laajoki, K. and Paakkola, J. (eds.) Sedimentology of the Precambrian formations in eastern and northern Finland. Geol. Surv. Finland Spec. Paper 5, 189-212.

Schiffman, P. and Fridleifsson, G.O., 1991. The smectite-chlorite transition in drillhole NJ-15, Nesjavellir geothermal field, Iceland: XRD, BSE and electron microprobe investigations. J. Metamorph. Geol. 9, 679-696.

Seewald, J.S. & Seyfried, W.E., Jr., 1990. The effect of temperature on metal mobility in subseafloor hydrothermal systems: constrains from basalt alteration experiments. Earth Planet. Sci. Lett. 101, 388-403.

Seyfried, W.E., Jr & Bischoff, J.L., 1977. Hydrothermal transport of heavy metals by seawater: the role of seawater/basalt ratio. Earth Planet. Sci. Lett. 34, 71-77.

Seyfried, W.E., Jr & Bischoff, J.L., 1981. Experimental seawater-basalt interaction at 300°C, 500 bars, chemical exchange, secondary mineral formation and implications for the transport of heavy metals. Geochim. Cosmochim. Acta 45, 135-147.

Shau, Y-H. & Peacor, D.R., 1992. Phyllosilicates in hydrothermally altered basalts from DSDP Hole 504B, Leg 83 - a TEM and AEM study. Contr. Mineral. Petrol. 112, 119-133.

Silvennoinen, A., 1985. On the Proterozoic stratigraphy of northern Finland. In: Laajoki, K. and Paakkola, J. (eds.) Proterozoic exogenic processes and related metallogeny. Geol. Surv. Finland, Bull. 331, 107-116.

Skiöld, T., 1987. Aspects of the Proterozoic geochronology of northern Sweden. Precambrian Res. 35, 161-167.

Sleep, N.H., 1983. Hydrothermal convection at ridge axes. Pp. 71-82 in: Rona, P.A., Boström, K., Laubier, L. and Smith, K.L.,Jr (eds.): Hydrothermal processes at seafloor spreading centers. New York: Plenum Press. 796 p.

Smith, J.V. & Brown, W.L., 1988. Feldspar minerals. 1. Crystal textures, physical, chemical, and microtextural properties. 2nd edition. Berlin: Springer-Verlag. 828 p.

Spiess, F.N., Macdonald, K.C., Atwater, T., Ballard, L., Carranza, A., Cordoba, D., Cox, C., Diaz Garcia, V.M., Franceteau, J., Guerrero, J., Hawkins, J., Haymon, R., Hessler, R., Juteau, T., Kastner, M., Larson, L., Luyenduk,B., Macdougall, J.D., Miller, S., Normark, W., Orcutt, J. & Rangin, C., 1980. East Pacific Rise: hot springs and geophysical experiments. Science 207, 1421-1433.

Spycher, N.F. & Reed, M.H., 1989. Evolution of Broadlands-type epithermal ore fluid along alternative p-T paths: Implications for the transport and deposition of base, precious, and volatile metals. Econ. Geol. 84, 328-359.

Stakes, D.S., 1992. Hydrothermal alteration of mafic sills and basement in Middle Valley, a sediment segment of the Juan de Fuca Ridge. In: Schiffman, P., Day, H.W. and Beiersdorfer, R.E. (conv.) The transition from basalt to metabasalt: environments, processes, and petrogenesis. Abstracts and program. A meeting on 8-16 September, 1992, by the IGCP 294: Very low grade metamorphism. (no page numbers)

Stakes, D.S. & O'Neill, J.R., 1982. Mineralogy and stable isotope geochemistry of hydrothermally altered oceanic rocks. Earth Planet. Sci. Lett. 57, 285-304.

Steinthórsson, S., Oskarsson, N., Arnórsson, S. &

Gunnlaugsson, E., 1987. Metasomatism in Iceland: Hydrothermal alteration and remelting of oceanic crust. Pp. 355-387 in: Helgeson H. (ed.) Chemical transport in metasomatic processes. Dordrecht: D.Reidel Publishing Co. 782 p.

Sturchio, N.C., Muelenbachs, K. & Seitz, M.G., 1986. Element redistribution during hydrothermal alteration of rhyolite in an active geothermal system: Yellowstone drill cores Y-7 and Y-8. Geochim. Cosmochim. Acta 50, 1619 -1631.

Sveinbjörnsdóttir, A.E., 1992. Composition of geothermal minerals from saline and dilute fluids - Krafla and Reykjanes, Iceland. Lithos, 27, 301-315.

Taylor, R.S. & McLennan, S.M., 1985. The continental crust: its composition and evolution. An examination of the geochemical record preserved in sedimentary rocks. Oxford: Blackwell Scientific Publications. 312 p.

Thompson, A.B., 1971. P CO_2 in low-grade metamorphism: zeolite, carbonate, clay mineral, prehnite relations in the system $CaO-Al_2O_3-SiO_2-CO_2-H_2O$. Contr. Mineral. Petrol. 33, 145-161.

Thompson, G., 1983. Basalt-seawater interaction. Pp. 225-278 in: Rona, P.A., Boström, K., Laubier, L. and Smith, K.L., Jr (eds.): Hydrothermal processes at seafloor spreading centers. New York: Plenum Press. 796 p.

Tómasson, J. & Kristmansdóttir, H., 1972. High temperature alteration minerals and thermal brines, Reykjanes, Iceland. Contr. Mineral. Petrol. 36, 123-134.

Trzcienski, W.E. Jr., Carmichael, D.M. & Helmstaedt, H., 1984. Zoned sodic amphibole: indicator of changing pressure and temperature during tectonism in the Bathurst area, New Brunswick, Canada. Contr. Miner. Petrol. 85, 311-320.

Tuisku, P., 1985. The origin of scapolite in the Central Lapland schist area, Northern Finland; preliminary results. In: Laajoki, K. and Paakkola, J. (eds.) Proterozoic exogenic processes and related metallogeny. Geol. Surv. Finland, Bull. 331, 159-173.

Tyrväinen, A., 1983. Pre-Quaternary rocks of the Sodankylä and Sattanen map-sheet areas, sheets 3713 and 3714. Explanation to the maps of Pre-Quaternary rocks. Geological Map of Finland, 1: 100 000. 59 p.

Vallance, T.G., 1974. Spilite degradation of a tholeiitic basalt. J. Petrol. 15, 79-96.

Vanko, D.A. & Bishop, F.C., 1982. Occurrence and origin of marialitic scapolite in the Humboldt lopolith, N.W. Nevada. Contr. Mineral. Petrol. 81, 277-289.

Ward, P., Härkönen, I. & Pankka, H.S., 1989. Structural studies in the Lapland greenstone belt, northern Finland and their application to gold mineralization. In: S. Autio (ed.) Geological Survey of Finland, Current Research 1988. Geol. Surv. Finland, Spec. Paper 10, 71-78.

Wilkinson, J.F.G., 1986. Classification and average chemical compositions of common basalts and andesites. J. Petrol. 27, 31-62.

Winchester, J.A. & Floyd, P.A., 1977. Geochemical discrimination of different magma series and their differentiation products using immobile elements. Chem. Geol. 20, 325-343.

Winkler, H.G., 1979. Petrogenesis of metamorphic rocks. 5th edition. New York: Springer-Verlag. 348 p.

Wood, S.A., 1990a. The aqueous geochemistry of the rare-earth elements and yttrium. 1. Review of available low-temperature data for inorganic complexes and the inorganic REE speciation of natural waters. Chem. Geol. 82, 159-186.

Wood, S.A., 1990b. The aqueous geochemistry of the rare-earth elements and yttrium. 2. Theoretical predictions of speciation in hydrothermal solutions to 350° C at saturation water vapor pressure. Chem. Geol. 88, 99-125.

Appendix 1. Composition of amphiboles. Early type = hydrothermal amphibole, late type = regional metamorphic amphibole. Formulae calculated using the RECALC-program (Powell and Holland 1988).

Study area		Eksymäselkä					Lehtovaara								
	Sample	118-1					1036-3			053-11					
	Rock	Albite diabase					Albite diabase			Albite diabase					
	Type	early	early	late	late	late	late	late	late	early	early	early	early	early	early	early
	SiO2	50.57	49.04	38.55	39.99	38.27	39.67	43.20	53.65	52.20	54.25	52.53	52.25	53.11	54.63	54.06
	TiO2	0.18	0.20	0.28	1.74	0.27	0.31	0.81	0.07	0.13	0.06	0.05	0.11	0.05	0.03	0.00
	Al2O3	2.38	2.71	14.59	11.21	12.57	15.80	10.13	3.85	1.88	1.78	1.79	2.33	2.65	1.42	1.18
	FeO	19.48	20.86	26.24	25.39	28.24	22.27	20.68	14.56	9.85	10.78	11.41	12.88	10.54	10.56	9.91
	MnO	0.40	0.37	0.32	0.27	0.28	0.16	0.24	0.16	0.15	0.16	0.11	0.12	0.14	0.15	0.14
	MgO	10.46	10.25	3.92	4.80	3.08	6.55	7.96	14.07	17.66	17.83	16.59	16.10	16.31	17.17	18.18
	CaO	12.20	12.11	11.59	12.38	11.44	12.33	12.12	12.49	12.91	13.39	13.35	12.07	12.91	13.23	13.27
	Na2O	0.26	0.36	1.36	1.22	1.60	1.29	1.53	0.42	0.24	0.19	0.19	0.25	0.29	0.24	0.19
	K2O	0.12	0.20	0.77	0.74	1.05	0.52	0.19	0.11	0.02	0.07	0.09	0.11	0.15	0.05	0.06
	F	0.08	0.00	0.06	0.05	0.00	0.05	0.00	0.00	n.a.	n.a.	n.a.	n.a.	n.a.	n.a.	n.a.
	Cl	0.11	0.20	1.17	1.39	2.19	0.84	1.31	0.07	n.a.	n.a.	n.a.	n.a.	n.a.	n.a.	n.a.
	sum	96.24	96.30	98.85	99.18	98.99	99.79	98.17	99.45	95.04	98.51	96.11	96.22	96.15	97.48	96.99
Tet.	Si	7.63	7.47	6.02	6.23	6.12	5.99	6.59	7.60	7.63	7.67	7.65	7.62	7.68	7.78	7.73
	Al	0.37	0.49	1.98	1.77	1.88	2.02	1.41	0.40	0.32	0.30	0.31	0.38	0.32	0.22	0.20
Oct	Al	0.05	0.00	0.71	0.29	0.49	0.79	0.41	0.25	0.00	0.00	0.00	0.02	0.13	0.02	0.00
(M1-3)	Ti	0.02	0.02	0.03	0.20	0.03	0.04	0.09	0.01	0.01	0.01	0.01	0.01	0.01	0.00	0.00
	Fe3+	0.37	0.40	0.51	0.50	0.57	0.42	0.40	0.26	0.18	0.19	0.21	0.24	0.19	0.19	0.18
	Fe2+	2.09	2.26	2.91	2.81	3.21	2.39	2.24	1.47	1.02	1.08	1.18	1.34	1.08	1.07	1.01
	Mg	2.35	2.33	0.91	1.12	0.73	1.47	1.81	2.97	3.85	3.76	3.60	3.50	3.51	3.65	3.88
	Mn	0.05	0.05	0.04	0.04	0.04	0.02	0.03	0.02	0.02	0.02	0.01	0.02	0.02	0.02	0.02
M4	Ca	1.97	1.98	1.94	2.07	1.96	1.99	1.98	1.90	2.02	2.03	2.08	1.89	2.00	2.02	2.03
	Na	0.03	0.02	0.06	0.00	0.01	0.07	0.02	0.10	0.01	0.01	0.00	0.01	0.00	0.00	0.01
A	Na	0.05	0.09	0.35	0.37	0.48	0.31	0.43	0.01	0.05	0.04	0.05	0.06	0.08	0.07	0.04
	K	0.02	0.04	0.15	0.15	0.21	0.10	0.04	0.02	0.00	0.01	0.02	0.02	0.03	0.01	0.01

n.a. = not analysed.

Appendix 1. Continued.

Study area		Myllyvaara												Isolaki			
	Sample	056-13					056-14				059-13			030-4			
	Rock	Lamprophyre					Lamprophyre				Lamprophyre			Albite diabase			
	Type	late	late	late	late	late	early	early	early	early	early	early	early	early	early	late	late
	SiO2	52.47	55.06	53.67	53.82	54.45	54.77	54.60	53.29	55.56	52.93	51.65	52.42	55.31	54.23	54.89	54.15
	TiO2	0.66	0.57	0.49	0.76	0.75	0.04	0.09	0.03	0.02	0.08	0.16	0.12	0.04	0.11	0.02	0.22
	Al2O3	2.13	1.73	2.04	1.93	2.06	0.92	1.09	1.32	1.35	2.80	3.71	2.88	0.51	0.70	1.00	2.03
	FeO	10.45	8.47	7.26	8.13	8.94	10.91	9.57	12.03	9.25	12.32	12.81	11.00	8.88	10.56	9.58	10.07
	MnO	0.09	0.07	0.05	0.07	0.08	0.17	0.03	0.12	0.06	0.09	0.09	0.06	0.22	0.18	0.26	0.12
	MgO	18.04	18.89	17.86	18.94	18.68	17.90	18.14	16.71	19.15	16.15	16.07	16.45	18.64	17.52	18.22	19.18
	CaO	11.63	12.00	12.07	10.35	10.79	12.89	12.44	11.12	12.97	12.47	12.89	12.65	13.83	13.32	12.69	13.64
	Na2O	0.92	0.82	0.90	1.11	1.00	0.36	0.36	0.28	0.30	0.27	0.33	0.35	0.02	0.14	0.20	0.25
	K2O	0.23	0.36	0.24	0.35	0.36	0.13	0.11	0.12	0.08	0.18	0.23	0.15	0.02	0.04	0.05	0.03
	F	n.a.	n.a.	n.a.	n.a.	n.a.	0.08	0.00	0.11	0.23	n.a.	n.a.	n.a.	0.00	0.00	0.00	0.00
	Cl	n.a.	n.a.	n.a.	n.a.	n.a.	0.01	0.01	0.01	0.02	n.a.	n.a.	n.a.	0.00	0.05	0.01	0.13
	sum	96.62	97.97	94.58	95.46	97.11	98.18	96.44	95.14	98.99	97.29	97.94	96.08	97.47	96.85	96.92	99.82
Tet.	Si	7.56	7.73	7.77	7.73	7.71	7.77	7.82	7.81	7.76	7.61	7.43	7.60	7.83	7.79	7.82	7.56
	Al	0.36	0.27	0.23	0.27	0.29	0.15	0.18	0.20	0.22	0.39	0.57	0.40	0.08	0.12	0.17	0.33
Oct	Al	0.00	0.02	0.12	0.05	0.06	0.00	0.00	0.03	0.00	0.09	0.06	0.10	0.00	0.00	0.00	0.00
(M1-3)	Ti	0.07	0.06	0.05	0.08	0.08	0.00	0.01	0.00	0.00	0.01	0.02	0.01	0.00	0.01	0.00	0.02
	Fe3+	0.19	0.15	0.13	0.15	0.16	0.19	0.17	0.22	0.16	0.22	0.23	0.20	0.16	0.19	0.17	0.18
	Fe2+	1.07	0.85	0.75	0.83	0.90	1.10	0.97	1.25	0.92	1.26	1.31	1.13	0.89	1.08	0.97	1.00
	Mg	3.88	3.95	3.85	4.05	3.94	3.79	3.87	3.65	3.99	3.46	3.44	3.56	3.94	3.75	3.87	3.99
	Mn	0.01	0.01	0.01	0.01	0.01	0.02	0.00	0.02	0.01	0.01	0.01	0.01	0.03	0.02	0.03	0.01
M4	Ca	1.80	1.81	1.87	1.59	1.64	1.96	1.91	1.75	1.94	1.92	1.99	1.97	2.10	2.05	1.94	2.04
	Na	0.04	0.16	0.13	0.24	0.22	0.02	0.07	0.08	0.01	0.04	0.02	0.03	0.00	0.01	0.05	0.04
A	Na	0.21	0.06	0.13	0.07	0.05	0.08	0.03	0.00	0.07	0.04	0.08	0.06	0.01	0.03	0.01	0.03
	K	0.04	0.07	0.04	0.06	0.07	0.02	0.02	0.02	0.01	0.03	0.04	0.03	0.00	0.01	0.01	0.01

n.a. = not analysed.

Appendix 1. Continued.

Study area		Honkavaara													
	Sample	1044-2		1044-2		1044-16									
	Rock	Albite diabase		Fels. volc. rock		Albite diabase									
	Type	early	early	early	early	late	late	late	late	late	late	late	late	late	late
	SiO2	55.09	55.72	54.86	55.76	46.22	47.57	43.65	44.66	39.53	38.71	38.26	40.21	41.63	38.40
	TiO2	0.01	0.00	0.00	0.00	0.90	0.93	0.46	0.95	0.32	0.19	0.30	0.17	0.16	0.34
	Al2O3	0.83	0.62	1.28	0.82	5.61	5.46	8.60	6.89	11.64	14.44	14.74	14.68	14.97	14.95
	FeO	10.01	8.97	8.22	9.26	21.06	20.00	17.54	17.83	24.99	23.84	23.21	22.50	22.96	22.60
	MnO	0.08	0.08	0.04	0.13	0.26	0.32	0.04	0.18	0.12	0.10	0.12	0.19	0.21	0.11
	MgO	18.40	19.48	19.51	19.17	9.82	10.06	11.26	11.90	6.31	6.39	5.46	6.62	6.16	6.28
	CaO	13.59	13.36	13.08	12.37	11.05	11.45	12.42	11.43	11.27	11.94	11.10	11.97	10.84	10.94
	Na2O	0.18	0.12	0.16	0.13	0.81	0.83	0.91	0.83	1.31	1.61	1.69	1.67	1.74	1.74
	K2O	0.01	0.04	0.04	0.02	0.47	0.35	0.43	0.51	1.60	0.96	0.97	0.73	0.63	0.71
	F	0.19	0.15	0.23	0.19	n.a.	n.a.	n.a.	n.a.	n.a.	n.a.	n.a.	n.a.	n.a.	n.a.
	Cl	0.01	0.01	0.02	0.00	n.a.	n.a.	n.a.	n.a.	n.a.	n.a.	n.a.	n.a.	n.a.	n.a.
	sum	98.40	98.55	97.44	97.85	96.20	96.97	95.31	95.18	97.09	98.18	95.85	98.74	99.30	96.07
Tet.	Si	7.78	7.81	7.76	7.85	7.07	7.16	6.68	6.84	6.21	5.97	6.02	6.09	6.23	5.99
	Al	0.14	0.10	0.21	0.14	0.93	0.84	1.32	1.16	1.79	2.04	1.98	1.91	1.77	2.01
Oct	Al	0.00	0.00	0.00	0.00	0.08	0.13	0.23	0.08	0.36	0.59	0.75	0.71	0.87	0.74
(M1-3)	Ti	0.00	0.00	0.00	0.00	0.10	0.11	0.05	0.11	0.04	0.02	0.04	0.02	0.02	0.04
	Fe3+	0.18	0.16	0.15	0.16	0.40	0.38	0.34	0.34	0.49	0.46	0.46	0.43	0.43	0.44
	Fe2+	1.01	0.89	0.83	0.93	2.89	2.14	1.91	1.94	2.79	2.61	2.59	2.42	2.44	2.51
	Mg	3.87	4.07	4.11	4.02	2.24	2.26	2.57	2.72	1.48	1.47	1.28	1.50	1.37	1.46
	Mn	0.01	0.01	0.01	0.02	0.03	0.04	0.01	0.02	0.02	0.01	0.02	0.02	0.03	0.02
M4	Ca	2.06	2.01	1.98	1.87	1.81	1.85	2.04	1.88	1.90	1.97	1.87	1.94	1.74	1.83
	Na	0.01	0.02	0.01	0.02	0.08	0.14	0.04	0.08	0.10	0.10	0.02	0.05	0.12	0.12
A	Na	0.04	0.01	0.03	0.01	0.16	0.10	0.23	0.17	0.30	0.39	0.50	0.44	0.38	0.41
	K	0.00	0.01	0.01	0.00	0.09	0.07	0.08	0.10	0.32	0.19	0.20	0.14	0.12	0.14

n.a. = not analysed.

Appendix 1. Continued.

Study area		Sivakkavaara					Palovaara	
	Sample	035-13			106-1		2-9,00	
	Rock	Albite diabase			Lamprophyre		Ultramafic lava	
	Type	early	late	late	early	early	early	late
	SiO2	54.33	43.09	43.83	54.02	54.16	53.39	53.26
	TiO2	0.02	1.25	1.06	0.00	0.00	0.08	0.04
	Al2O3	0.57	8.49	8.23	1.45	1.47	1.90	1.89
	FeO	13.56	25.62	23.91	9.91	11.18	10.59	14.68
	MnO	0.36	0.29	0.36	0.23	0.27	0.21	0.22
	MgO	16.18	6.68	7.92	16.63	17.53	17.78	16.46
	CaO	13.02	11.45	11.42	13.00	13.41	12.46	12.71
	Na2O	0.18	1.32	1.12	0.24	0.15	0.19	0.12
	K2O	0.09	0.95	1.12	0.06	0.08	0.05	0.05
	F	0.20	0.00	0.00	0.06	0.24	0.01	0.00
	Cl	0.81	1.14	1.72	0.00	0.00	0.02	0.00
	sum	99.32	100.28	100.69	95.60	98.49	96.68	99.43
Tet.	Si	7.79	6.59	6.66	7.83	7.70	7.67	7.58
	Al	0.10	1.41	1.34	0.17	0.25	0.32	0.17
Oct	Al	0.00	0.12	0.13	0.08	0.00	0.00	0.00
(M1-3)	Ti	0.00	0.14	0.12	0.00	0.00	0.01	0.00
	Fe3+	0.24	0.49	0.46	0.18	0.20	0.19	0.26
	Fe2+	1.38	2.78	2.58	1.02	1.13	1.08	1.49
	Mg	3.46	1.52	1.79	3.59	3.71	3.81	3.29
	Mn	0.04	0.04	0.05	0.03	0.03	0.03	0.03
M4	Ca	2.00	1.88	1.86	2.02	2.04	1.92	1.94
	Na	0.02	0.07	0.06	0.00	0.01	0.02	0.03
A	Na	0.03	0.33	0.27	0.07	0.03	0.03	0.00
	K	0.02	0.19	0.22	0.01	0.02	0.01	0.01

n.a. = not analysed.

Appendix 2. Composition of chlorites. Formulae calculated using the RECALC-program (Powell and Holland 1988). Temperature Tc calculatd after Cathelineau (1988) and temperature Tk after Kranidiotis and MacLean (1987). No addition of 50° on the Tk temperatures of "Al-undersaturated" ultramafics was made.

	Eksymäselkä															
Sample	40-13						118-1		033-9				036-2			
Rock	albite diabase						albite diabase		ultramafic differentiate of albite diabase				Fe-tholeiitic lava			
Type	early						early		early				early			
SiO2	25.50	26.01	25.93	26.24	26.13	25.35	24.15	24.69	28.83	28.46	29.73	28.91	27.07	26.28	27.11	27.41
TiO2	0.07	0.11	0.04	0.08	0.07	0.07	0.00	0.05	0.08	0.02	0.06	0.02	0.03	0.07	0.03	0.00
Al2O3	21.23	21.07	21.98	22.09	22.03	21.07	20.48	20.11	18.61	18.50	18.08	19.49	21.38	21.44	20.29	21.32
FeO	23.55	24.43	24.40	24.65	24.46	24.22	31.93	32.24	15.97	15.12	16.05	15.54	20.17	20.44	20.03	20.16
MnO	0.16	0.20	0.24	0.19	0.21	0.15	0.31	0.29	0.08	0.07	0.08	0.06	0.10	0.05	0.02	0.06
MgO	16.76	15.46	17.16	17.28	16.86	17.34	11.77	11.96	23.01	22.92	23.05	22.62	21.18	20.56	20.70	21.04
CaO	0.06	0.02	0.04	0.02	0.05	0.03	0.03	0.00	0.05	0.06	0.04	0.01	0.01	0.01	0.02	0.05
Na2O	0.01	0.02	0.04	0.05	0.03	0.02	0.11	0.08	0.00	0.01	0.00	0.01	0.05	0.01	0.00	0.02
K2O	0.01	0.13	0.01	0.09	0.05	0.05	0.04	0.01	0.09	0.00	0.08	0.03	0.01	0.05	0.01	0.04
F	0.09	0.00	0.06	0.13	0.08	0.04	0.00	0.03	n.a.	n.a.	n.a.	n.a.	0.11	0.15	0.38	0.00
Cl	0.08	0.15	0.07	0.09	0.07	0.09	0.11	0.09	n.a.	n.a.	n.a.	n.a.	0.02	0.02	0.05	0.05
sum	87.35	87.45	89.84	90.69	89.89	88.30	88.82	89.43	86.72	85.16	87.17	86.69	90.00	88.91	88.21	90.10
Si	5.29	5.40	5.24	5.25	5.27	5.22	5.15	5.23	5.79	5.79	5.93	5.78	5.34	5.27	5.46	5.40
Al[iv]	2.71	2.60	2.76	2.75	2.73	2.78	2.84	2.77	2.22	2.21	2.07	2.22	2.66	2.73	2.54	2.60
Al[vi]	2.48	2.57	2.47	2.47	2.52	2.34	2.31	2.26	2.19	2.23	2.18	2.37	2.32	2.33	2.28	2.35
Ti	0.01	0.02	0.01	0.01	0.01	0.01	0.00	0.01	0.01	0.00	0.01	0.00	0.00	0.01	0.00	0.00
Fe3+	0.61	0.64	0.62	0.62	0.62	0.63	0.85	0.86	0.40	0.39	0.40	0.39	0.50	0.51	0.51	0.50
Fe2+	3.46	3.61	3.50	3.51	3.51	3.55	4.84	4.86	2.28	2.19	2.27	2.21	2.83	2.91	2.87	2.82
Mg	5.18	4.79	5.17	5.16	5.07	5.32	3.74	3.78	6.88	6.95	6.85	6.74	6.23	6.14	6.21	6.18
Mn	0.03	0.04	0.04	0.03	0.04	0.03	0.06	0.05	0.01	0.01	0.01	0.01	0.02	0.01	0.00	0.01
Ca	0.01	0.00	0.01	0.00	0.01	0.01	0.01	0.00	0.01	0.01	0.01	0.00	0.00	0.00	0.00	0.01
Na	0.00	0.01	0.02	0.02	0.01	0.01	0.05	0.03	0.00	0.00	0.00	0.00	0.02	0.00	0.00	0.01
K	0.00	0.03	0.00	0.02	0.01	0.01	0.01	0.00	0.02	0.00	0.02	0.01	0.00	0.01	0.00	0.01
Tc/°C	374	357	382	381	378	386	395	384	295	294	271	295	366	378	347	357
Tk/°C	349	339	354	353	351	356	373	366	284	282	268	284	336	344	324	330

n.a. = not analysed

Appendix 2. Continued.

	Eksymäselkä		Myllyvaara												
Sample	040-55		036-3		056-30			057-24		059-1			059-5		
Rock	ultramafic differentiate of diabase		Siltstone		Siltstone			Siltstone		Quartzite			lamprophyre		
Type	early		carb->albite		carb->chlorite			carb->chlorite		late			late		
SiO2	30.65	31.59	30.12	29.95	29.72	29.47	29.48	30.08	30.29	28.50	29.30	27.54	28.73	29.49	29.34	29.28
TiO2	0.10	0.01	0.00	0.04	0.02	0.04	0.02	0.01	0.06	0.00	0.02	0.06	0.04	0.13	0.09	0.01
Al2O3	17.57	15.43	21.46	21.86	20.90	21.42	20.90	21.79	20.68	18.91	20.14	20.59	20.44	19.96	19.57	20.43
FeO	9.49	9.02	5.92	7.36	7.89	8.63	7.48	6.04	5.70	13.89	13.23	14.45	13.45	13.04	12.42	13.89
MnO	0.07	0.05	0.01	0.04	0.03	0.00	0.00	0.00	0.01	0.04	0.02	0.03	0.02	0.04	0.01	0.06
MgO	26.85	27.23	29.25	27.37	28.14	25.96	28.35	28.94	30.15	25.56	24.58	23.66	23.62	25.82	25.30	25.81
CaO	0.04	0.00	0.01	0.03	0.00	0.04	0.03	0.00	0.00	0.03	0.02	0.02	0.03	0.08	0.05	0.03
Na2O	0.02	0.01	0.03	0.17	0.00	0.01	0.01	0.00	0.00	0.03	0.00	0.03	0.02	0.03	0.02	0.03
K2O	0.05	0.03	0.00	0.01	0.00	0.00	0.01	0.05	0.02	0.05	0.04	0.03	0.02	0.00	0.01	0.02
F	n.a.	n.a.	0.00	0.21	0.00	0.23	0.06	0.11	0.32	0.40	0.24	0.35	0.17	0.17	0.09	0.22
Cl	n.a.	n.a.	0.01	0.03	0.01	0.03	0.00	0.02	0.01	0.02	0.00	0.00	0.03	0.03	0.01	0.03
sum	84.84	83.37	86.80	86.83	86.70	85.57	86.28	86.91	86.91	87.00	87.35	86.40	86.37	88.59	86.81	89.56
Si	6.08	6.35	5.73	5.73	5.72	5.76	5.69	5.72	5.76	5.65	5.74	5.51	5.70	5.70	5.77	5.62
Al[iv]	1.92	1.65	2.27	2.27	2.28	2.24	2.31	2.28	2.24	2.35	2.26	2.49	2.30	2.30	2.23	2.38
Al[vi]	2.18	2.01	2.54	2.67	2.46	2.69	2.45	2.60	2.39	2.08	2.40	2.37	2.49	2.25	2.31	2.25
Ti	0.01	0.00	0.00	0.01	0.00	0.01	0.00	0.00	0.02	0.00	0.00	0.02	0.01	0.02	0.01	0.00
Fe3+	0.24	0.23	0.14	0.18	0.19	0.21	0.18	0.14	0.14	0.35	0.33	0.36	0.33	0.32	0.31	0.33
Fe2+	1.34	1.29	0.80	1.00	1.08	1.20	1.03	0.82	0.77	1.96	1.84	2.06	1.90	1.79	1.74	1.90
Mg	7.94	8.16	8.29	7.81	8.07	7.56	8.16	8.20	8.54	7.56	7.18	7.06	6.99	7.44	7.41	7.39
Mn	0.02	0.01	0.00	0.01	0.01	0.00	0.00	0.00	0.00	0.01	0.00	0.01	0.00	0.01	0.00	0.01
Ca	0.01	0.00	0.00	0.00	0.00	0.00	0.00	0.00	0.00	0.00	0.00	0.00	0.01	0.02	0.01	0.01
Na	0.01	0.00	0.01	0.03	0.00	0.00	0.00	0.00	0.00	0.01	0.00	0.01	0.01	0.01	0.01	0.01
K	0.01	0.01	0.00	0.00	0.00	0.00	0.00	0.01	0.00	0.01	0.01	0.00	0.01	0.00	0.00	0.00
Tc/°C	247	204	304	304	305	299	310	305	299	316	302	339	308	308	297	321
Tk/°C	241	211	271	274	276	274	278	272	267	293	284	310	289	287	279	296

n.a. = not analysed

Appendix 2. Continued.

	Lehtovaara							Honkavaara								
Sample	053-11			054-1			1036-3	036-4				40-39		1044-17		
Rock	albite diabase			albite diabase			albite diabase	albite diabase				albite diabase		felsic volcanic rock		
Type	early			carb->chlorite			early	early				early		carb->chlorite		
SiO2	26.13	26.79	26.37	25.66	24.87	26.31	25.90	24.91	26.13	26.66	26.54	29.58	29.22	27.67	28.72	28.05
TiO2	0.10	0.09	0.06	0.08	0.05	0.03	0.02	0.05	0.10	0.06	0.03	0.03	0.04	0.05	0.05	0.07
Al2O3	22.47	22.51	21.51	23.08	22.11	22.81	22.45	21.99	21.75	21.71	21.68	18.72	18.90	21.25	20.38	20.24
FeO	18.57	17.87	17.78	18.68	18.24	17.73	24.58	17.11	17.34	16.55	16.75	16.46	16.68	13.35	13.66	13.74
MnO	0.17	0.15	0.16	0.08	0.08	0.03	0.19	0.07	0.02	0.04	0.00	0.04	0.06	0.04	0.02	0.00
MgO	21.31	21.01	21.71	21.56	19.57	20.29	16.74	20.73	21.56	21.94	21.46	24.26	24.48	25.13	24.25	24.73
CaO	0.06	0.04	0.12	0.17	0.27	0.05	0.06	0.03	0.01	0.01	0.00	0.02	0.02	0.13	0.13	0.12
Na2O	0.03	0.00	0.04	0.04	0.01	0.01	0.04	0.03	0.04	0.08	0.00	0.01	0.02	0.08	0.04	0.03
K2O	0.02	0.02	0.04	0.01	0.09	0.00	0.02	0.18	0.05	0.01	0.04	0.00	0.00	0.03	0.06	0.04
F	0.13	0.02	0.07	0.00	0.00	0.00	0.01	0.16	0.24	0.15	0.05	0.43	0.33	0.22	0.00	0.16
Cl	0.04	0.03	0.04	0.03	0.04	0.05	0.02	0.04	0.02	0.02	0.03	0.06	0.04	0.04	0.03	0.02
sum	88.86	88.48	87.79	89.36	85.29	87.26	90.00	85.10	87.00	87.06	86.50	89.12	89.42	87.73	87.31	87.02
Si	5.19	5.32	5.29	5.08	5.16	5.29	5.22	5.16	5.28	5.35	5.36	5.78	5.70	5.43	5.65	5.55
Al[iv]	2.80	2.68	2.71	2.92	2.84	2.71	2.78	2.84	2.72	2.65	2.64	2.22	2.30	2.57	2.34	2.44
Al[vi]	2.46	2.58	2.38	2.46	2.57	2.70	2.56	2.52	2.45	2.49	2.53	2.09	2.05	2.34	2.38	2.28
Ti	0.01	0.01	0.01	0.02	0.02	0.01	0.00	0.01	0.02	0.01	0.00	0.00	0.01	0.01	0.01	0.01
Fe3+	0.46	0.44	0.45	0.46	0.47	0.45	0.62	0.44	0.44	0.42	0.42	0.40	0.41	0.33	0.34	0.34
Fe2+	2.62	2.52	2.54	2.63	2.69	2.53	3.52	2.52	2.49	2.36	2.41	2.29	2.31	1.86	1.91	1.93
Mg	6.31	6.21	6.49	6.36	6.05	6.08	5.03	6.39	6.49	6.56	6.46	7.06	7.12	7.35	7.12	7.30
Mn	0.03	0.03	0.03	0.01	0.01	0.01	0.03	0.01	0.00	0.01	0.00	0.01	0.01	0.01	0.00	0.00
Ca	0.01	0.01	0.02	0.02	0.03	0.01	0.01	0.01	0.00	0.00	0.00	0.00	0.00	0.03	0.03	0.02
Na	0.01	0.00	0.02	0.01	0.00	0.00	0.02	0.01	0.02	0.03	0.00	0.00	0.01	0.03	0.02	0.01
K	0.01	0.01	0.01	0.00	0.01	0.00	0.01	0.05	0.01	0.00	0.01	0.00	0.00	0.01	0.02	0.01
Tc/°C	389	370	374	408	395	374	386	395	376	365	363	295	308	352	315	331
Tk/°C	349	336	339	362	355	340	357	353	339	331	330	283	292	316	293	303

n.a. = not analysed

Appendix 2. Continued.

	Sivakkavaara												
Sample	035-13		035-26						100-1				106-1
Rock	albite diabase		mafic tuffite						lamprophyre				lampro-phyre
Type	early		early						carb->chlorite				early
SiO2	27.02	27.31	29.14	29.02	30.22	30.08	27.66	28.53	27.52	27.72	27.60	27.43	27.75
TiO2	0.05	0.06	0.03	0.02	0.02	0.03	0.03	0.04	0.05	0.05	0.05	0.05	0.01
Al2O3	21.79	21.51	20.08	21.77	19.10	18.26	20.37	17.92	23.31	22.95	21.31	22.57	21.69
FeO	20.70	20.66	12.61	12.92	11.09	11.98	12.47	10.65	17.23	17.32	16.36	17.45	14.92
MnO	0.27	0.18	0.07	0.09	0.08	0.02	0.07	0.11	0.11	0.09	0.03	0.10	0.16
MgO	20.06	20.42	24.20	25.06	26.15	26.19	25.62	26.06	22.56	22.50	23.05	22.78	22.27
CaO	0.04	0.04	0.05	0.01	0.02	0.01	0.01	0.01	0.06	0.05	0.03	0.02	0.00
Na2O	0.07	0.06	0.00	0.00	0.00	0.00	0.02	0.00	0.02	0.04	0.03	0.01	0.02
K2O	0.04	0.05	0.01	0.02	0.01	0.01	0.01	0.01	0.00	0.01	0.02	0.04	0.02
F	0.00	0.00	n.a.	n.a.	n.a.	n.a.	n.a.	n.a.	0.00	0.00	0.25	0.14	0.22
Cl	0.05	0.07	n.a.	n.a.	n.a.	n.a.	n.a.	n.a.	0.03	0.03	0.03	0.02	0.05
sum	90.04	90.29	86.19	88.91	86.69	86.58	86.26	83.33	90.86	90.73	88.48	90.45	86.84
Si	5.34	5.38	5.77	5.58	5.91	5.92	5.50	5.82	5.29	5.34	5.44	5.31	5.52
Al[iv]	2.66	2.62	2.23	2.42	2.10	2.08	2.50	2.18	2.71	2.66	2.56	2.69	2.48
Al[vi]	2.43	2.38	2.46	2.52	2.30	2.15	2.27	2.12	2.58	2.55	2.39	2.46	2.62
Ti	0.02	0.02	0.00	0.00	0.00	0.00	0.00	0.01	0.02	0.02	0.02	0.02	0.00
Fe3+	0.51	0.51	0.31	0.31	0.27	0.30	0.31	0.27	0.42	0.42	0.40	0.42	0.37
Fe2+	2.91	2.90	1.78	1.77	1.54	1.68	1.76	1.54	2.36	2.37	2.29	2.40	2.11
Mg	5.91	6.00	7.14	7.18	7.62	7.68	7.59	7.92	6.46	6.46	6.77	6.57	6.61
Mn	0.05	0.03	0.01	0.01	0.01	0.00	0.01	0.02	0.02	0.01	0.01	0.02	0.03
Ca	0.00	0.00	0.01	0.00	0.00	0.00	0.00	0.00	0.01	0.01	0.00	0.00	0.00
Na	0.01	0.01	0.00	0.00	0.00	0.00	0.01	0.00	0.00	0.01	0.01	0.00	0.01
K	0.01	0.01	0.00	0.00	0.00	0.00	0.01	0.00	0.00	0.00	0.00	0.01	0.01
Tc/°C	366	360	297	328	276	273	341	289	374	366	350	371	337
Tk/°C	338	333	280	300	263	262	307	271	337	332	320	335	311

n.a. = not analysed

Appendix 2. Continued.

	Palovaara											Isolaki				
Sample	2-9.00		2-100.30				3-82.00					030-4		030-11		
Rock	ultramafic lava		albite diabase				intermediate tuffite					ultramafic differentiate of diabase		albite diabase		
Type	early		early				early					early		early		
SiO2	27.80	27.57	25.91	26.06	26.92	26.62	26.02	26.43	26.49	26.27	26.61	30.45	29.69	26.60	25.64	26.93
TiO2	0.01	0.09	0.04	0.01	0.02	0.00	0.04	0.06	0.02	0.08	0.01	0.08	0.05	0.10	0.04	0.04
Al2O3	19.78	19.62	20.19	19.54	18.93	19.74	20.65	20.65	21.40	21.79	21.80	17.44	17.08	21.69	22.02	21.40
FeO	20.83	20.85	27.86	28.00	27.78	27.37	21.30	20.92	22.93	21.33	22.84	16.55	16.79	19.69	19.60	19.50
MnO	0.13	0.14	0.08	0.05	0.07	0.09	0.08	0.07	0.06	0.06	0.06	0.10	0.15	0.19	0.15	0.14
MgO	20.35	19.19	16.67	16.28	16.54	16.84	19.66	20.06	18.44	19.43	18.50	24.17	24.32	20.40	19.91	20.10
CaO	0.00	0.01	0.02	0.01	0.00	0.03	0.02	0.04	0.02	0.00	0.02	0.04	0.06	0.07	0.05	0.05
Na2O	0.00	0.04	0.05	0.07	0.06	0.03	0.05	0.04	0.07	0.02	0.05	0.02	0.00	0.05	0.05	0.03
K2O	0.03	0.04	0.01	0.08	0.04	0.00	0.02	0.01	0.03	0.00	0.07	0.02	0.00	0.01	0.01	0.04
F	0.00	0.00	0.03	0.00	0.18	0.15	0.06	0.27	0.24	0.37	0.17	0.18	0.00	0.10	0.00	0.19
Cl	0.05	0.03	0.02	0.07	0.03	0.03	0.04	0.04	0.03	0.06	0.04	0.03	0.02	0.05	0.04	0.07
sum	88.93	87.55	90.83	90.10	90.36	90.72	87.84	88.28	89.46	88.98	89.96	88.99	88.15	88.80	87.47	88.23
Si	5.57	5.61	5.27	5.35	5.50	5.40	5.31	5.35	5.33	5.28	5.32	5.97	5.89	5.32	5.21	5.41
Al[iv]	2.43	2.39	2.73	2.65	2.50	2.60	2.69	2.65	2.67	2.72	2.68	2.04	2.11	2.68	2.79	2.59
Al[vi]	2.24	2.32	2.12	2.09	2.06	2.12	2.28	2.28	2.41	2.44	2.46	1.99	1.88	2.43	2.48	2.47
Ti	0.00	0.01	0.01	0.00	0.00	0.00	0.01	0.01	0.00	0.01	0.00	0.01	0.01	0.02	0.01	0.01
Fe3+	0.52	0.53	0.71	0.72	0.71	0.70	0.55	0.53	0.58	0.54	0.57	0.41	0.42	0.49	0.50	0.49
Fe2+	2.97	3.02	4.03	4.09	4.03	3.95	3.09	3.01	3.28	3.05	3.25	2.30	2.37	2.80	2.83	2.78
Mg	6.08	5.82	5.05	4.98	5.03	5.09	5.98	6.05	5.53	5.82	5.51	7.06	7.19	6.08	6.03	6.01
Mn	0.02	0.02	0.01	0.01	0.01	0.02	0.01	0.01	0.01	0.01	0.01	0.02	0.03	0.03	0.03	0.02
Ca	0.00	0.00	0.00	0.00	0.00	0.01	0.00	0.01	0.00	0.00	0.00	0.01	0.01	0.01	0.01	0.01
Na	0.00	0.02	0.02	0.03	0.02	0.01	0.02	0.02	0.03	0.01	0.02	0.01	0.00	0.02	0.02	0.01
K	0.01	0.01	0.00	0.02	0.01	0.00	0.01	0.00	0.01	0.00	0.02	0.00	0.00	0.00	0.00	0.01
Tc/°C	329	323	378	365	341	357	371	365	368	376	370	266	278	370	387	355
Tk/°C	313	310	354	346	330	340	342	337	342	345	343	264	272	339	351	329

n.a. = not analysed

Appendix 3. Compositions of calcite - dolomite/ankerite pairs used in carbonate geothermometry. Dolomite and ankerite formulae calculated based on 2 cations, calcite formulae on 1 cation.Temperature calculated after Essene and Anovitz (1987).

	Eksymäselkä							Sivakkavaara						Honkavaara	
Sample	33-9				041-44			042-46		042-61				036-5	
Rock	Albite diabase				Albite diabase			Albite diabase		Rhyolite				Albite diabase	
Mineral	dol	cal	dol	cal	dol	dol	cal	cal	cal	cal	dol	dol	cal	cal	dol
FeO	6.31	0.84	6.92	0.65	4.32	4.33	0.11	0.97	0.90	1.19	9.62	9.46	1.33	0.38	6.56
MnO	0.42	0.58	0.58	0.35	0.21	0.12	0.04	0.16	0.24	0.68	1.39	1.16	0.57	0.19	0.40
MgO	16.70	0.79	16.90	0.77	20.40	20.60	0.68	1.07	1.08	0.82	15.69	16.88	0.90	0.65	19.51
CaO	30.50	52.50	29.90	53.00	28.40	28.50	55.90	57.77	57.46	56.02	32.14	30.25	57.20	56.40	32.10
FeCO3	0.17	0.01	0.18	0.01	0.11	0.11	0.00	0.01	0.01	0.02	0.24	0.24	0.02	0.01	0.16
MnCO3	0.01	0.01	0.02	0.01	0.01	0.00	0.00	0.00	0.00	0.01	0.04	0.03	0.01	0.00	0.01
MgCO3	0.79	0.02	0.79	0.02	0.94	0.94	0.02	0.02	0.03	0.02	0.70	0.76	0.02	0.02	0.84
CaCO3	1.03	0.96	1.01	0.97	0.94	0.94	0.98	0.96	0.96	0.96	1.03	0.98	0.95	0.98	0.99
T/°C		384		371			314	425	426	389			406	306	

	Lehtovaara													
Sample	052-5				053-7				053-13					
Rock	Albite diabase				Albite diabase				Albite diabase					
Mineral	dol	dol	cal	cal	cal	dol	cal	dol	cal	dol	cal	dol	cal	dol
FeO	8.02	8.20	1.46	1.17	1.44	7.09	1.13	7.31	1.19	4.83	1.23	4.18	1.26	6.82
MnO	0.51	0.47	0.34	0.31	0.29	0.43	0.31	0.41	0.18	0.21	0.27	0.14	0.19	0.12
MgO	17.50	17.60	1.10	1.02	1.42	17.69	1.10	16.65	1.41	19.56	1.44	20.43	1.19	17.70
CaO	28.80	28.50	52.90	50.60	54.12	29.52	51.72	30.63	55.93	30.31	56.77	29.98	52.94	28.72
FeCO3	0.21	0.21	0.02	0.02	0.02	0.18	0.02	0.19	0.02	0.12	0.02	0.11	0.02	0.18
MnCO3	0.01	0.01	0.00	0.00	0.00	0.01	0.00	0.01	0.00	0.01	0.00	0.00	0.00	0.00
MgCO3	0.81	0.82	0.03	0.03	0.03	0.82	0.03	0.77	0.03	0.89	0.03	0.92	0.03	0.84
CaCO3	0.96	0.95	0.95	0.95	0.94	0.98	0.95	1.02	0.95	0.99	0.95	0.97	0.95	0.98
T/°C			463	450	501		457		486		488		470	

	Lehtovaara					
Sample	054-1					
Rock	Albite diabase					
Mineral	cal	dol	cal	dol	cal	dol
FeO	1.16	7.02	0.93	7.69	1.20	7.93
MnO	0.23	0.22	0.28	0.20	0.23	0.18
MgO	1.15	19.37	0.65	17.13	0.83	18.59
CaO	54.63	30.53	54.46	30.99	52.37	28.76
FeCO3	0.02	0.17	0.01	0.20	0.02	0.20
MnCO3	0.00	0.01	0.00	0.01	0.00	0.00
MgCO3	0.03	0.85	0.02	0.78	0.02	0.85
CaCO3	0.95	0.97	0.97	1.02	0.96	0.94
T/°C	455		342		408	

cal = calcite: dol = dolomite

Tätä julkaisua myy

GEOLOGIAN
TUTKIMUSKESKUS (GTK)
Julkaisumyynti
02150 Espoo

☎ (90) 46 931

Teleksi: 123185 geolo sf
Telekopio: (90) 462 205

GTK, Väli-Suomen
aluetoimisto
Kirjasto
PL 1237
70211 Kuopio

☎ (971) 205 111

Telekopio: (971) 205 215

GTK, Pohjois-Suomen
aluetoimisto
Kirjasto
PL 77
96101 Rovaniemi

☎ (960) 297 219

Teleksi: 37295 geolo sf
Telekopio: (960) 297 289

Denna publikation säljes av

GEOLOGISKA
FORSKNINGSCENTRALEN (GFC)
Publikationsförsäljning
02150 Esbo

☎ (90) 46 931

Telex: 123185 geolo sf
Telefax: (90) 462 205

GFC, Distriktsbyrån för
Mellersta Finland
Biblioteket
PB 1237
70211 Kuopio

☎ (971) 205 111

Telefax: (971) 205 215

GFC, Distriktsbyrån för
Norra Finland
Biblioteket
PB 77
96101 Rovaniemi

☎ (960) 297 219

Telex: 37295 geolo sf
Telefax: (960) 297 289

This publication can be
obtained from
GEOLOGICAL SURVEY
OF FINLAND (GSF)
Publication sales
FIN-02150 Espoo, Finland

☎ +358 0 46 931

Telex: 123185 geolo sf
Telefax: +358 0 462 205

GSF, Regional office of
Mid-Finland
Library
P.O. Box 1237
FIN-70211 Kuopio, Finland

☎ +358 71 205 111

Telefax: +358 71 205 215

GSF, Regional office of
Northern Finland
Library
P.O. Box 77
FIN-96101 Rovaniemi, Finland

☎ +358 60 297 219

Telex: 37295 geolo sf
Telefax: +358 60 297 289

ISBN 951-690-537-4
ISSN 0367-522X